Queen Mary
University of London

The innate immune kinase IKKε as a novel regulator of PSAT1 and serine metabolism

William Edward Jones

A PhD thesis submitted in partial fulfilment of the
requirements of the Degree of Doctor of Philosophy

Principal Supervisor: Dr Katiuscia Bianchi
Secondary Supervisor: Dr Tyson Sharp

Barts Cancer Institute
Barts and the London School of Medicine and Dentistry
Queen Mary University of London

May 02, 2018

Statement of Originality

I, William Edward Jones, confirm that the research included within this thesis is my own work and that where it has been carried out in collaboration with, or supported by others, that this is duly acknowledged below, and my contribution indicated. Previously published material is also acknowledged below.

I attest that I have exercised reasonable care to ensure that the work is original and does not, to the best of my knowledge, break any UK law, infringe any third party's copyright or other Intellectual Property Right, or contain any confidential material.

I accept that the College has the right to use plagiarism detection software to check the electronic version of the thesis.

I confirm that this thesis has not been previously submitted for the award of a degree by this or any other university.

Signature: 

Date: 2nd May 2018

Details of collaboration and publications:

- The work presented throughout this thesis is currently under peer review at The EMBO Journal in advance of publication.

- Work presented in this thesis was selected for presentation in poster form at Cell Symposia: Hallmarks of Cancer 2016 in Ghent, Belgium

Contents

- Collaborations:

    - Labelled metabolite analysis was performed in collaboration with Dr Ruoyan Xu (Barts Cancer Institute, London, UK) who prepared the samples, and Dr Christian Frezza and Dr Sofia De Costa (MRC Cancer Unit, Cambridge, UK) who performed mass spectrometry analysis and provided the heat-maps of significantly modified results presented in Figures 3.5 and 3.6. This author contributed to the subsequent analysis of these results.

    - Phosphoproteomic analysis was performed in collaboration with Dr Ewa Wilcz-Villega (Barts Cancer Institute, London, UK) who prepared the samples, and Dr Pedro Cutillas and Dr Vinothini Rajeeve (Barts Cancer Institute, London, UK) who performed mass spectrometry analysis and the KEGGs pathway analysis of the results. This author contributed to the subsequent analysis of these results.

    - The *in vitro* kinase assay was performed in collaboration with Dr Pedro Cutillas and Dr Vinothini Rajeeve. This author prepared the samples, and Dr Cutillas and Dr Rajeeve performed the mass spectrometry analysis.

    - The promoter analysis investigating the presence of transcription factor binding sites in the promoter regions of *PHGDH*, *PSAT1* and *PSPH* genes was performed in collaboration with Professor Claude Chelala and Dr Ai Nagano of the bioinformatics team at Barts Cancer Institute, London, UK. This author contributed to the analysis of these results.

    - The investigations into the effect of siRNA-mediated suppression of ATF4 in breast cancer cell lines were performed with the support of Miss Sheila Olendo Barasa, a masters degree student under this authors supervision in the lab. Miss Barasa performed two replica for the experiments presented in Figure 5.8.

    - The data describing analysis of oxygen consumption rate was kindly provided by Dr Ruoyan Xu.

    - Analysis of mitochondrial membrane potential by TMRM staining was performed in collaboration with Professor Gyorgy Szabadkai (University College London, London, UK) who imaged mitochondrial staining following preparation of cells by Dr Ruoyan Xu and this author.

Acknowledgements

My first and foremost thanks must go to my supervisor, Katiuscia, who made what I can only assume was a significant gamble and took on a relatively unproven young student, giving him the opportunity to learn and thrive amongst a fantastic group of people. Thank you for your patience with all the failed westerns, for helping me to become a capable and confident scientist, for offering me the freedom to drive my own project and work in a dynamic and exciting field, but ultimately, for taking a chance on a nervous young undergraduate student who wore a tie for his preliminary Skype interview.

My thanks also go to both Ruoyan and Ewa. The Bianchi lab membership has fluctuated over 3 and a half years, as masters and undergraduate students have come and gone, but our core group of 3 has remained. Thank you both for your perpetual willingness to help. Your endless endurance against my steady flow of questions and requests for assistance has not gone unappreciated and it has been a genuine pleasure working alongside you both.

I would also like to thank both Tyson, my secondary supervisor and our centre lead, for his support and guidance and, of course, all the collaborators on this project, who have provided crucial assistance at key points in the work presented within. Thank you to Christian Frezza and Sofia De Costa for the labelled metabolite analysis, to Pedro Cutillas and Vinothini Rajeeve for the various mass spectrometry work, to Claude Chelala and Ai Nagano for the promoter analysis, to Gyorgy Szabadkai for the TMRM staining and to Tencho Tenev for unparalleled assistance with cloning. My gratitude must also go to the Medical Research Council for their funding, without which I could not have performed this work in the first place.

To the members of the KiSS group, both past and present, thank you for making the Barts Cancer Institute 3rd floor sauna a thoroughly enjoyable place to work. I hope you will continue to cope without mum around. Particular thanks must go to the members of the McClelland lab, of whom I am absolutely, definitely not a member. Nadeem, Naoka, Alice and Tineke, you all saved me from the eternal threat of solitary lunches and provided much-needed social distractions whenever it was most required. I hope the newest members of your lab Laura and Sarah will enjoy their time with you as much as I did, and I sincerely hope that our paths will continue to cross in the future.

For their consistent love and care I must thank my family, particularly Mum and Dad. Your invaluable wisdom on work, life, the universe and everything have seen me through the ups and downs of my first quarter century and a seemingly eternal education. I certainly cannot express the full extent of my gratitude with so few words. I love you both.

Lastly, but most importantly, my thanks go to my fiancée Charlotte. This thesis, which I am sure you will find long, dull and tedious, exists because of the love you have given me. To put it simply, I would not have achieved everything I have without your support and I owe you everything. As the end of this journey draws near, I am excited that our true adventure can finally begin.

Abstract

Induced and activated as part of the innate immune response, the first line of defence against bacterial or viral infections, Inhibitor of Kappa-B Kinase ε (IKKε) triggers NF-κB and IFNβ signalling. Whilst not expressed at basal levels in healthy cells and tissue, the kinase is overexpressed in roughly 30% of human breast cancer cases, driving oncogenesis through aberrant activation of NF-κB.

The impracticality of therapeutic targeting of NF-κB for cancer treatment has led to a requirement for greater understanding of IKKε's oncogenic potential to treat tumours driven by the kinase. Considering that IKKε alters cellular metabolism in dendritic cells, promoting aerobic glycolysis akin to the metabolic phenotype observed in cancer, it was hypothesised that the kinase would play a similar role in breast cancer.

Using a Flp-In 293 model of IKKε induction and suppressing IKKε expression in a panel of breast cancer cell lines using siRNA, IKKε-dependent changes in cellular metabolism were characterised using labelled metabolite analysis. IKKε was found to induce serine biosynthesis, an important pathway in breast cancer development that supports glutamine-fuelling of the TCA cycle and contributes to one carbon metabolism to maintain redox balance. Promotion of serine biosynthesis occurred via a dual mechanism. Firstly, PSAT1, the second enzyme of the pathway, was found to be phosphorylated in an IKKε-dependent manner, promoting protein stabilisation. Secondly, an IKKε-dependent transcriptional upregulation of all three serine biosynthesis enzymes, *PHGDH*, *PSAT1* and *PSPH*, was observed, induced by the inhibition of mitochondrial activity and the subsequent induction of ATF4-mediated mitochondria-to-nucleus retrograde signalling.

These data demonstrate a previously uncharacterised mechanism of metabolic regulation by IKKε and highlight new potential therapeutic targets for the treatment of IKKε-driven breast cancer in the form of the enzymes of the serine biosynthesis pathway.

Contents

Contents

List of Figures

List of Tables

Abbreviations List

+	positive
^{12}C	carbon-12
^{13}C	carbon-13
^{14}N	nitrogen-14
^{15}N	nitrogen-15
2-HG	2-hydroxyglutarate
3'-UTR	3 prime untranslated region
5CIC	5-chlorocytosine
α-KG	alpha-ketoglutarate
ABC-like DLBCL	activated B-cell like diffuse large B-cell lymphoma
Acetyl-CoA	acetyl coenzyme A
ADP	adenosine diphosphate
AP-1	activator protein 1
ARD	ankyrin repeat domain
ATF4	activating transcription factor 4
ATP	adenosine triphosphate
BAFF	B-cell activating factor
BSA	bovine serum albumin
C/EBP	ccaat-enhancer-binding protein
CAC	colitis-associated cancer
CCND1	cyclin D1-encoding gene
CHUK	IKKα-encoding gene
cIAP	cellular inhibitor of apoptosis protein
CK2	casein kinase 2
CPW	cells per well
DAMP	damage-associated molecular pattern
DCA	dichloroacetate
DCIS	ductal carcinoma *in situ*
DMEM	Dulbecco's modified Eagle's medium

DMSO	dimethyl sulfoxide
DNA	deoxyribonucleic acid
dsRNA	double stranded RNA
DSS	dextran sulfate sodium
ECL	enhanced chemiluminescence
EDTA	ethylenediaminetetraacetic acid
EGF	epidermal growth factor
EGFR	epidermal growth factor receptor
EMT	epithelial mesenchymal transition
EOC	epithelial ovarian cancer
EP300	E1A-associated protein p300
ER	estrogen receptor
ERE	estrogen response elements
ETC	electron transport chain
FBS	foetal bovine serum
FCCP	Carbonyl cyanide 4-(trifluoromethoxy)phenylhydrazone
FDA	Food and Drug Administration
FGF	fibroblast growth factor
FH	fumarate hydratase
FOXO3a	forkhead box O3
GAF	gamma activated factor
GAPDH	glyceraldehyde-3-phosphate dehydrogenase
GAS	gamma activated sequence
GFP	green fluorescent protein
GFPT1	glucosamine-fructose-6-phosphoate aminotransferase
GLS	glutaminase
GLUT	glucose transporter
GSK3β	glycogen synthase kinase 3 beta
H3K4me3	tri-methylation of histone H3 lysine 4
H3T11	histone H3 threonine 11
HA-tag	human influenza haemagglutinin-tag

HCC	hepatocellular carcinoma
HDAC	histone deacetylase
HEK	human embryonic kidney
HER2	human epidermal growth factor receptor 2
HF	high-fidelity
HGF	hepatocyte growth factor
HIF1	hypoxia inducible factor 1
HPLC	high-pressure liquid chromatography
HRP	horseradish peroxidase
HSC	haematopoietic stem cells
hTERT	human telomerase reverse transcriptase
IBiD	IRF3 binding domain
IDH	isocitrate dehydrogenase
IFN	interferon
IFNAR	IFNα/β receptor
IGF	insulin-like growth factor
IκB	inhibitor of kappa-B
IKBKB	IKKβ-encoding gene
IKBKE	IKKε-encoding gene
IKK	inhibitor of kappa-B kinase
IL-1	interleukin-1
IL-10	interleukin-10
IRF	IFN regulatory factor
ISG	IFN-stimulated gene
ISGF3	IFN-stimulated gene factor 3
ISRE	IFN-stimulated response element
JAK	Janus family of protein kinases
JNK	c-Jun N-terminal kinases
JOSD2	Josephin Domain-containing 2
K63	lysine 63
KD-m	kinase domain mutant
KEGGS	Kyoto encyclopaedia of genes and genomes

KGF	keratinocyte growth factor
LC-MS	liquid chromatography-mass spectrometry
LDH	lactate dehydrogenase
LPS	lipopolysaccharide
LT	large SV40 T antigen
LT-β	lymphotoxin-beta
MAPK	mitogen activated protein kinase
MAVS	mitochondrial antiviral-signaling protein
MEF	mouse embryonic fibroblast
MHC	major histocompatibility complex
miRNA	microRNA
MMP	matrix metalloproteinase
mRNA	messenger RNA
mTOR	mechanistic target of rapamycin
$Na_2H_2P_2O_7$	disodium diphosphate
Na_3VO_4	sodium orthovanadate
NAD	nicotinamide adenine dinucleotide
NAD^+	oxidised NAD
NADH	reduced NAD
NaF	sodium fluoride
NAK	NF-κB-activating kinase
NAP1	nucleosome assembly protein 1
NBD	NEMO-binding domain
NEMO	NF-κB essential modulator
NF-κB	nuclear factor kappa-B
NH_4HCO_3	ammonium bicarbonate
NIK	NF-κB-inducing kinase
NNT	nicotinamide nucleotide transhydrogenase
NRF2	nuclear factor erythroid-2-related factor 2
NSCLC	non-small cell lung cancer
NTC	Notch transcriptional complex

OCR	oxygen consumption rate
ORF	open reading frame
OXPHOS	oxidative phosphorylation
PAMP	pathogen-associated molecular pattern
PBS	phosphate buffered saline
PCR	polymerase chain reaction
PDAC	pancreatic ductal adenocarcinoma
PDB	protein data bank
PDGF	platelet-derived growth factor
PDHA1	pyruvate dehydrogenase E1 component subunit alpha
PDHC	pyruvate dehydrogenase complex
PDK	pyruvate dehydrogenase kinase
PEP	phosphoenolpyruvate
PFK1	phosphofructokinase 1
PFKFB3	6-phosphofructo-2-kinase/fructose-2,6-bisphosphatase
PGAM	phosphoglycerate mutase
PGC-1β	PPAR-γ coactivator-1 beta
PGK	phosphoglycerate kinase
PHD	prolyl hydroxylase
PHGDH	phosphoglycerate dehydrogenase
PI3K	phosphoinositide 3-kinase
PKCζ	protein kinase C zeta
PKL	pyruvate kinase liver isoform
PKM1	pyruvate kinase muscle type-1 isoform
PKM2	pyruvate kinase muscle type-2 isoform
PKR	pyruvate kinase red blood cell isoform
PLK1	polo-like kinase 1
PPAR-γ	peroxisome proliferator-activated receptor-gamma
PPP	pentose phosphate pathway
PRR	pattern recognition receptor
PSAT1	phosphoserine aminotransferase 1
PSPH	phosphoserine phosphatase
qRT-PCR	quantitative real-time polymerase chain reaction

RANK	receptor activator of NF-κB
RANKL	receptor activator of NF-κB ligand
RELA	p65-encoding gene
RHD	Rel homology domain
RIPK1	receptor-interacting serine/threonine-protein kinase 1
RISC	RNA-induced silencing complex
RNA	ribonucleic acid
ROS	reactive oxygen species
RPMI-1640	Roswell Park Memorial Institute 1640
S>A	serine 331 to alanine point mutation
S>E	serine 331 to glutamic acid point mutation
S6K	S6 kinase
SAICAR	succinylaminoimidazolecarboxamide ribose-5'-phosphate
SAM	S-adenosylmethionine
SBP	serine biosynthesis pathway
SCC	squamous cell carcinoma
SCO2	synthesis of cytochrome c oxidase 2
SDH	succinate dehydrogenase
SDS-PAGE	sodium dodecyl sulfate – polyacrylamide gel electrophoresis
Ser +	serine + (serine - medium reconstituted with serine)
Ser -	serine -
SESAME	serine-responsive SAM-containing metabolic enzyme
SGC	Structural Genomics Consortium
SHMT	serine hydroxymethyltransferase
shRNA	short hairpin RNA
SINTBAD	similar to NAP1 TBK1 adaptor
siRNA	small interfering RNA
SMRT	silencing mediator for retinoic acid and thyroid hormone receptor
SNAP-23	synaptosomal-associated protein 23
SP1	specificity protein 1
ST	small SV40 T antigen
ST7L	suppressor of tumourigenicity 7 protein-like
STAT	signal transducer and activator of transcription

TAD	transactivation domain
TAE	tris acetate EDTA
TANK	TRAF family member-associated NF-κB activator
TBK1	tank-binding kinase 1
TCA	tricarboxylic acid
TET	ten-eleven translocation
Tet Op	tetracycline operator
TetR	tetracycline repressor
TGFβ	transforming growth factor beta
THF	tetrahydrofolate
TIGAR	TP53-inducible glycolysis and apoptosis regulator
TIR	toll-interleukin receptor
TLR	toll-like receptor
TMRM	tetramethylrhodamine, methyl ester
TNFα	tumour necrosis factor alpha
TNFR	TNFα receptor
TRADD	TNFR type 1-associated DEATH domain protein
TRAF	TNFR-associated factor
TRIF	TIR-domain-containing adapter-inducing interferon beta
TSC	tuberous sclerosis
tTA	tetracycline trans-activator
UAP1	UDP-N-acetylhexosamine pyrophosphorylase
UCP1	uncoupling protein 1
ULD	ubiquitin-like domain
VEGF	vascular endothelial growth factor
VHL	von-Hippel-Lindau
wt	wild-type
YAP1	yes associated protein 1

Chapter 1

Introduction

1.1 Inflammation and immunity

The activation of cellular immunity and the induction of an inflammatory response signify the key aspects of an organism's response to infection or injury of endogenous tissue. The induction of inflammation represents the afflicted organism's initial attempts to clear the insulting stimulus and eventually promote the repair of damaged tissue. There are two main types of inflammatory response, namely acute and chronic, classified by the duration of the response and its ability to be resolved. Acute inflammation is the classical inflammatory response induced by an infection or tissue injury and is mediated by host cell recognition of pathogen-associated molecular patterns (PAMPs) or damage-associated molecular patterns (DAMPs) by a special receptor type, pattern-recognition receptors (PRRs), found either intracellularly or on the membranes of tissue resident immune cells or on cells of the damaged/infected tissue themselves[1].

Innate immunity

Signalling via the PRRs induces the activation of innate immunity, the first line of defence against invading pathogens, which acts to recruit immune cells such as macrophages and neutrophils to the site of infection or injury via the production of an acute inflammatory response[2]. The initial activation of PRRs induces the production of pro-inflammatory lipid mediators such as prostaglandins, which control blood flow and vessel dilation in the vasculature surrounding the inflammatory site; cytokines like interleukin 1β (IL-1β) and tumour necrosis factor α (TNFα), which activate immune cells like macrophages and neutrophils locally; and chemokines like CCL2, which recruit additional myeloid cells to the inflammatory site, aided by the release of cytokines that activate endothelial cells to increase vascular permeability and allow easier immune cell infiltration. These endothelial factors also trigger vasodilation of the vasculature, leading to the characteristic redness of inflamed tissue[3,4]. Recruited neutrophils are activated by interferon γ (IFNγ) that is produced from T-helper cells at the inflammatory site and subsequently attempt to kill the invading pathogen through secretion of toxic reactive oxygen species (ROS) and reactive nitrogen species[4] and by phagocytosis. Cytokines produced by the innate immune response also signal to activate the complement system, which leads to an enzymatic cascade that promotes the opsonisation of cells, in which antigens belonging to the invading pathogen are "tagged" for recognition by phagocytes, enhancing phagocytosis and immune clearance[5].

If the infecting pathogen is successfully killed the acute inflammatory response shifts into the next phase, in which inflammation is resolved and tissue repair begins. Due to the indiscriminate nature of the cytotoxic compounds that are produced to kill infecting agents, substantial collateral damage can occur during an inflammatory response. An off switch is therefore crucial to ensure that the host tissue is protected from further damage than is necessary. Pro-inflammatory signals are replaced by anti-inflammatory ones such as interleukin 10 (IL-10), which is produced from regulatory T-cells and inhibits the production of pro-inflammatory cytokines[3]. A group of molecules called lipoxins are also induced. Lipoxins inhibit the recruitment of neutrophils to the inflammatory site and reduce vessel permeability. As neutrophil recruitment ceases, the resolution phase begins in earnest and clearance of cellular debris and infiltrated immune cells is induced. As neutrophils stop arriving at the inflammatory site, those already there begin to undergo apoptosis due to their short life span[6]. Macrophages, which mature from lipoxin-recruited monocytes, then phagocytose the apoptotic neutrophils to clear them from the site, before being drained from the tissue themselves via the lymphatic vessel system, with macrophage levels in the tissue ultimately returning to pre-infection levels[6,7]. Repair signals are also induced to promote the regeneration of damaged tissues.

In the context of wound healing, an acute inflammatory response primarily promotes the repair of damaged tissue. The process remains relatively similar to that which occurs in the response to invading pathogens, beginning with the stimulation of DAMPs and the release of chemokines from resident immune cells or activated platelets and facilitate the recruitment of neutrophils to the wound site, followed by monocytes that mature into macrophages[8]. In the absence of an infecting pathogen, it has been proposed that the cytotoxic agents released by neutrophils may be detrimental to rapid wound healing and do more harm than good[9], but the neutrophil population at an injury site can have some benefit to the reparative process, acting as a source of early-stage pro-inflammatory cytokines like TNFα, IL-1α and IL-1β, which can induce expression of matrix metalloproteinases (MMPs) and keratinocyte growth factor (KGF) in fibroblasts to initiate repair[10]. The macrophages take the lead in the wound healing inflammatory process however, as the driving force behind the clearance of neutrophils from the wound site, but also as a source of many different growth factors and cytokines, including transforming growth factor β (TGFβ), platelet-derived growth factor (PDGF), insulin-like growth factor (IGF) and TNFα, which are essential for inducing the signalling pathways that control tissue repair. Macrophages are also the source of factors which stimulate re-epithelialisation of the cells at the wound edge and revascularisation post-repair, such as fibroblast growth factor (FGF) and vascular endothelial growth factor (VEGF) respectively[9,10].

Adaptive and trained Immunity

In the event an infecting agent is not neutralised by the activation of an innate immune response and the resultant inflammation, the immune system switches to a more targeted approach with the induction of the adaptive immune response. Dendritic cells, recruited to the site of infection as part of the innate immune response, are antigen-presenting cells which digest antigens from invading microorganisms. Antigen fragments are then displayed via major histocompatibility complex (MHC) proteins on the surface of the dendritic cells[11]. T-cells are activated by dendritic cells presenting such antigen fragments, stimulating T-cell differentiation to either cytotoxic T-cells (CD8+) or T-helper cells (CD4+)[12]. Cytotoxic T cells act to destroy infected cells and T-helper cells activate B-cells, which differentiate into antibody producing cells. B-cell produced antibodies target antigens on invading pathogens to target them for immune cell-related destruction. Following clearance of the pathogen, memory B-cells remain in circulation, ready to rapidly produce the same antibodies upon reinfection of the pathogen[11].

Whilst the accepted understanding of innate immunity versus adaptive immunity has long involved the idea that innate responses are non-specific and lack a memory-driven aspect, it is worth mentioning that recent work has begun to demonstrate that innate immunity does in fact possess an ability to adapt to stimuli and retain a memory. “Trained Immunity” is the term used to define the memory of the innate immune response and allows the mounting of a non-specific, yet adaptive response to immune challenges. In plants, histone modification at the gene promoters of defence genes in response to initial infection has been shown to “prime” genes for an amplified response in the event of a recurrent infection[13]. Evidence of trained immunity in mammals has also been observed. Infection of a mouse model with a non-lethal dose of *Candida albicans* has been found to protect mice against infection with a secondary lethal dose up to seven days post-initial infection[14]. It was found that exposure of monocytes to β-glucan, a component of the *C. albicans* cell wall, activated a programme of histone methylation and induced changes in cellular metabolism that promoted enhanced cytokine production from monocytes upon secondary stimulation of the innate immune response[14,15]. Whilst this concept of “trained immunity” is in its infancy, increasing evidence in multiple models demonstrates that the understanding of memory in innate immunity is rapidly evolving and the classical model of an un-adaptable response requires some revision. Given the focus of this thesis, discussing this subject in detail is beyond the scope of this introduction, but the concept has been extensively reviewed by Netea *et al*[16,17].

When a stimulus which induces an inflammatory response cannot be cleared, or recurs repeatedly over an extended period, chronic inflammation arises due to the inability for acute inflammation to be resolved. This essentially results in the inflammatory process continuing indefinitely. Chronic inflammation has been linked to many different diseases, including rheumatoid arthritis, coeliac disease and colitis, all of which arise due to ongoing or repeated cycles of inflammation. Importantly, the continued cycle of tissue damage and repair and the dysregulation of growth inducing signalling that arises from chronic inflammation also makes the condition a significant risk factor for another major disease: cancer.

1.1.1 Inflammation in cancer

As far back as 1863, it was recognised that tumour development and inflammation go hand in hand. Rudolf Virchow recognised that tissue injury resulted in inflammation of the injury site and subsequent proliferation of tissue for repair purposes and inflammatory diseases or conditions have repeatedly been recognised to increase the risk of developing various types of cancer[18]. A good example of this is the link between obesity, which is known to cause low-grade chronic inflammation, and multiple different cancer types[19]. In the intervening years better understanding of the tumour microenvironment has validated Virchow's initial observation and the link between inflammation and the development of cancers is now widely accepted, with inflammation of the tumour microenvironment fully recognised as a growth supporting feature of tumours[20].

In certain cancer types, oncogenes like Myc and Ras have been shown to directly induce inflammatory states via the production of cytokines like IL-1β, IL-8 and IL-6 that can support cancer progression[21-24] and along the same lines, Myc and Ras have been reported to co-operate in the tumour microenvironment in a mouse model of lung cancer, promoting the development of an inflammatory stroma and supporting tumour progression[25]. More ubiquitously however, it is now accepted that the microenvironment of most, if not all, tumours is heavily infiltrated by cells of the immune system[26]. It has become clear that inflammation facilitates the acquisition of properties necessary for tumour progression. Hanahan and Weinberg have described the common features of the majority of cancers, describing them as the "hallmarks of cancer". These features are uncontrolled proliferation, resistance to growth suppression, resistance to cellular death signals, unlimited replicative potential, invasive and metastatic properties, the ability to induce angiogenesis, the ability to evade immune destruction and finally, dysregulated cellular metabolism[20]. With those characteristics in mind, it is easy to see how inflammation, which stimulates cell growth and tissue repair, can drive cancer development in afflicted cells.

Akin to chronic inflammation, the heavy immune cell infiltrate in the tumour microenvironment produces the same growth factors, cytokines and signalling molecules as it does away from a tumour. Macrophages, which infiltrate the tumour site in large populations, are perhaps the most important player in this regard. They help the tumour acquire the ability to proliferate continuously by secreting growth factors, like epidermal growth factor (EGF). They can help the tumour evade the immune system, by secreting immunosuppressive cytokines like IL-10. They facilitate invasion and metastasis by promoting the production of MMPs which help to degrade the extracellular matrix. Macrophages even support the neovascularisation of the tumour, secreting pro-angiogenic factors like VEGF[27].

Furthermore, in addition to the numerous cytokines and growth factors that are provided by inflammation, the process also promotes genome instability that is favourable for tumour development. If a genome is more unstable, a mutation that favours cell growth and survival, is more likely to be selected for. Over time, this can potentially lead to accumulation of enough mutations, or just the right mutation, for malignant transformation. Therefore, inflammation can promote cancer progression by making conditions in the tumour favourable for such mutations to arise. Not only is the constant cycle of tissue damage and regeneration a favourable condition for spontaneous mutagenesis[28], but inflammation can also promote genome instability through the production of various mutagenic factors. The activation of immune cells, neutrophils in particular, often goes hand in hand with the production of reactive oxygen or nitrogen species which can have deoxyribonucleic acid (DNA) damaging effects and play an important part in carcinogenesis[29]. Inflammation derived ROS have even been suggested to be capable of activating the carcinogenic properties of certain environmental agents, demonstrating how the process can contribute to cancer development even through exogenous mechanisms[30]. In addition to this, neutrophils are responsible for the production of multiple other mutagenic compounds. They can use an enzyme called myeloperoxidase to oxidise uracil nucleotides to 5 -chlorouracil or 5-bromouracil, both of which can be mutagenic if incorporated into the DNA sequence[31]. Neutrophils also generate hypochlorous acid from myeloperoxidase which, when secreted, can be mutagenic. Hypochlorous acid has been shown to be mutagenic by leading to the generation and accumulation of 5-chlorocytosine (5CIC) lesions in the genome of exposed cells. 5CIC has intrinsic mutagenic properties and induces C to T transitions, which reportedly occur at high frequency in cancer genomes[32]. Furthermore, the ability of hypochlorous acid to generate DNA damage and induce mutagenesis has been demonstrated in lung epithelial cells at physiologically relevant conditions, suggesting its natural secretion in

inflammation in the lung could be sufficient promote mutagenesis that could lead to tumour formation[33].

Outside of the secretion of growth factors and the genome instability which arises from inflammation, a major part of the pro-tumourigenic effect of inflammation is the production of TNFα from infiltrating immune cells such as macrophages and neutrophils. TNFα can directly support cancer progression through the stimulation and activation of a pathway which enhances cell proliferation, inhibits apoptosis and induces the expression of genes that promote angiogenesis, invasion and metastasis. Indeed, TNFα binds to the TNFα receptor (TNFR) on the surface of cancer cells to induce a signalling cascade which culminates in the activation of the NF-κB pathway.

1.2 The NF-κB pathway

Activated by many different signalling molecules, including TNFα, the NF-κB pathway is one of the central regulators of the inflammatory response within the cell and has been extensively reviewed since its discovery over 30 years ago (reviews include Gilmore, 2006[34], Karin, 2009[35] and Hayden and Ghosh, 2012[36]). Activation of the NF-κB pathway induces a transcriptional program that involves the production of immunity and inflammatory mediators and signals that regulate tissue regeneration and cell death. NF-κB signalling itself is initiated by the activation of 5 distinct proteins which hetero- or homodimerise to create functional transcriptional regulators which bind to the promoters of NF-κB target genes. These 5 transcription factors are p65 (RelA), RelB, cRel, p105/p50 and p100/p52 and are all defined by a shared protein sequence known as the Rel homology domain (RHD), which mediates the dimerisation of subunits and their DNA binding[36]. p65, RelB and cRel all possess C-terminal transactivation domains (TADs)[34], allowing them to drive gene transcription. Although p50 and p52 lack such TADs, they can still promote transcription through heterodimer formation with other NF-κB subunits. Before they can do so however, they need to be processed from their inactive precursor forms, p105 and p100 respectively. p105 and p100 precursors both contain long C-terminal ankyrin repeat domains (ARDs) instead of TADs, which inhibit their function[37]. When activated, the longer precursors are ubiquitinated and the ARDs are degraded, leaving behind the mature active NF-κB subunits[38] which can then dimerise with other TAD-containing NF-κB subunits to activate pathway signalling.

As active dimers, NF-κB subunits translocate to the nucleus where they induce the NF-κB transcriptional program. Importantly, not all dimers are formed under the same circumstances and not all dimers activate the same genes. NF-κB dimers bind 9-10 base pair sites on target DNA sequences known as κB sites[34] and different dimer conformations will bind a different set of κB sites depending on which type of signal induces the pathway. Generally, an NF-κB response can be induced via two distinct mechanisms; the canonical pathway, or the non-canonical pathway.

1.2.1 Canonical NF-κB activation

The canonical pathway of NF-κB activation typically involves cellular stimulation with pro-inflammatory signals, leading to the activation of cytokine receptors such as the TNFR or toll-like receptors (TLRs)[39]. This triggers the activation of specific signalling cascades depending on the inciting stimuli. In the context of TNFα-mediated activation of NF-κB, TNFα binds to the TNFR

on the cell surface and triggers the binding of tumour necrosis factor receptor type 1-associated DEATH domain protein (TRADD) to the intracellular domain of the receptor. TRADD binding provides a platform for the recruitment of adaptor protein TNFR-associated factor 2 (TRAF2) and subsequently, TRAF2 associates with cellular inhibitor of apoptosis protein (cIAP) 1, cIAP2 and receptor-interacting serine/threonine-protein kinase 1 (RIPK1). cIAP1 and cIAP2 are ubiquitin ligases that ubiquitinate RIPK1 with lysine 63 (K63)-linked ubiquitin chains, facilitating the recruitment and activation of the inhibitor of kappa-B kinase (IKK) complex[40].

NF-κB subunits are typically sequestered in the cytoplasm by inhibitor of kappa-B (IκB) proteins, which prevent their nuclear translocation. To date, several IκB proteins have been described, including IκBα, IκBβ, IκBε and IκBζ, all of which feature NF-κB inhibiting ARDs[36]. Recruitment and activation of IKK's leads to phosphorylation and degradation of IκB proteins (discussed in-depth below in 1.2.3) which releases active NF-κB subunits from their sequestration. Active NF-κB dimers, usually containing either p65 or cRel with p50[39], are formed and undergo nuclear translocation where they can transcriptionally induce the expression of genes associated with inflammation, cell proliferation and inhibition of apoptosis (Figure 1.1).

1.2.2 Non-canonical NF-κB activation

The non-canonical aspect of NF-κB activation does not involve such extensive signalling cascades and instead, revolves primarily around the NF-κB-inducing kinase (NIK) and the processing and activation of p100/p52 (reviewed by Sun, 2011[41]).

In response to signalling mediated by a subset of TNF ligands, such as lymphotoxin-β (LT-β) or B-cell activating factor (BAFF), NIK is activated and induces the processing of p100[42]. Under basal conditions, TRAF3 associates with NIK, targeting it for proteasomal degradation[43], but stimulation of the LT-β receptor (LT-βR) leads to the recruitment of TRAF2 which, with the help of cIAPs, induces degradation of TRAF3 to stabilise NIK[44]. NIK then activates one of the IKKs[45] (see 1.2.3.1), which phosphorylates p100 to target it for ubiquitination, in turn leading to proteasome-mediated degradation of the ARD of p100 and leaving behind the mature active p52 subunit. p52, dimerised with RelB, then translocates to the nucleus where it activates NF-κB target genes involved in secondary lymphoid organogenesis, T-cell differentiation and B-cell maturation (reviewed by Sun, 2012[46]) (Figure 1.1).

The non-canonical NF-κB pathway therefore primarily differentiates from the canonical by the involvement and function of the so-called IKKs. Whilst both pathways involve their activation, the canonical pathway activates IKKs to target and degrade IκB proteins, whereas the non-

canonical pathway activates IKKs to directly target NF-κB subunits. The IKKs and their roles both in and out of NF-κB signalling are discussed below.

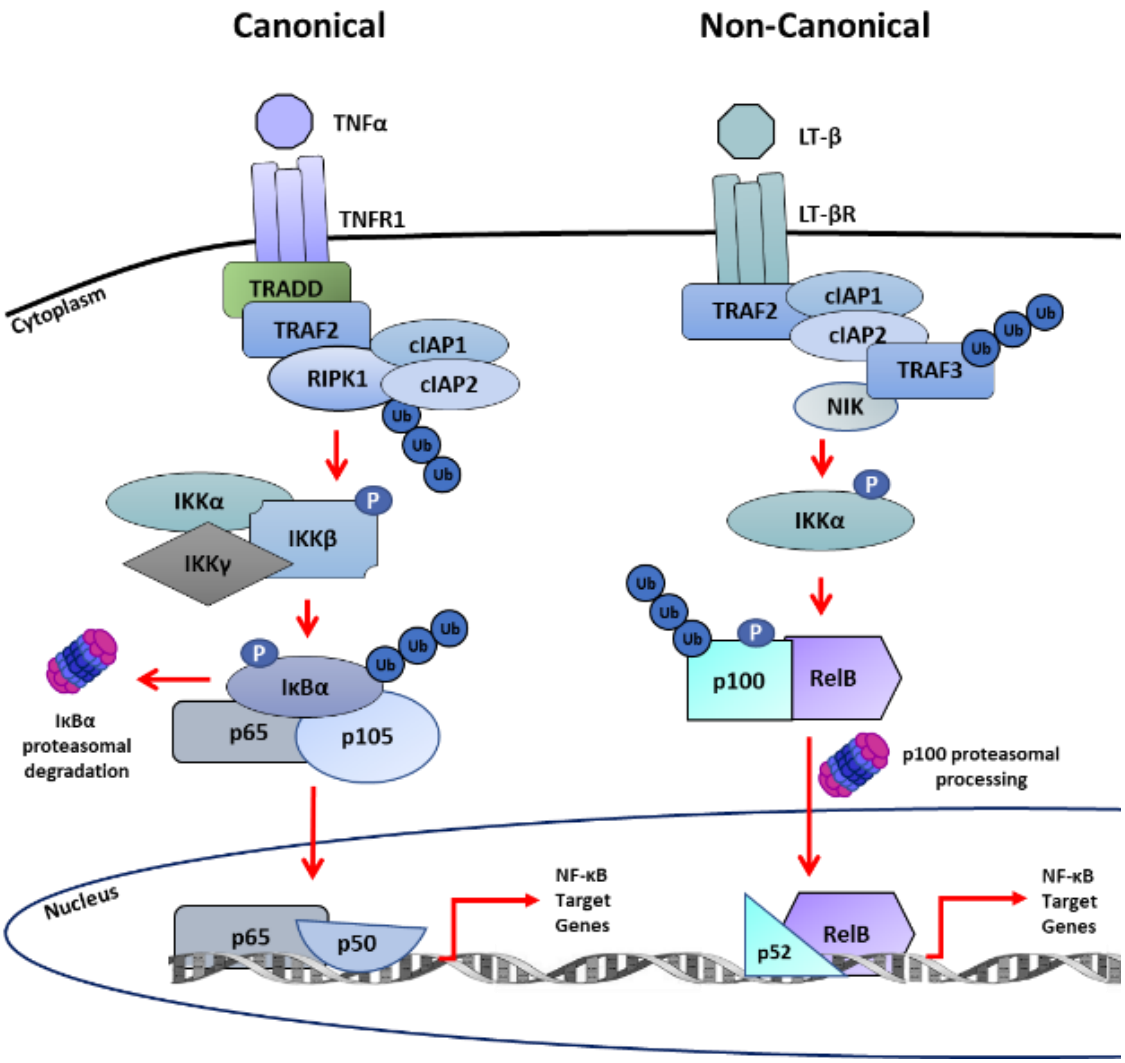

Figure 1.1 – The canonical and non-canonical mechanisms of NF-κB activation. The canonical NF-κB pathway is induced by activation of cytokine receptors in response to pro-inflammatory signals like TNFα, triggering recruitment of TRADD proteins to the intracellular domain of the cytokine receptor. TRADD recruitment facilitates association with TRAF2 and subsequently, cIAP1/2 and RIPK1. Ubiquitination of RIPK1 by cIAP1/2 promotes recruitment, phosphorylation and activation of the IKK complex, which phosphorylate IκB proteins, targeting them for ubiquitin-mediated proteasomal degradation, thereby releasing active NF-κB dimers. The non-canonical pathway is activated by specific TNF ligands like LT-β. Activation of ligand receptors triggers TRAF2 recruitment which associates with cIAP1/2 to ubiquitinate TRAF3 and induce its degradation. Release of NIK from TRAF3-mediated suppression allows it to phosphorylate and activate IKKα. In turn, IKKα phosphorylates NF-κB subunit p100, inducing ubiquitin-mediated degradation of the p100 ARD, producing the mature p52 subunit which, associated with RelB, translocates to the nucleus to trigger NF-κB transcriptional activity.

1.2.3 Inhibitor of Kappa-B kinases

As previously covered, NF-κB subunits are typically sequestered in the cytoplasm by IκB proteins, only released upon stimulation of the pathway by a wide variety of factors including TNFα. Upon activation of upstream signalling, IκBα is phosphorylated at 2 serine residues; Ser32 and Ser36[47,48], which subsequently leads to its ubiquitination at lysine residues Lys21 and Lys22, resulting in proteasomal degradation of the protein[49,50]. Degradation of IκBα releases the sequestered NF-κB subunits, allowing them to freely translocate to the nucleus and activate their transcriptional programmes. The Inhibitor of Kappa-B Kinase (IKK) family of kinases are the central regulators of NF-κB activation. This family, consisting of four kinases and one regulatory protein, is responsible for the phosphorylation of IκBα in response to activating stimuli. Structurally, the 4 kinases are relatively similar, all 4 containing a kinase domain for basic function and leucine zipper and helix-loop helix sequences that can facilitate dimer formation between IKK's[51]. IKKβ, IKKε and TBK1 also contain ubiquitin-like domains (ULDs) that are indispensable for their respective kinase activities[52,53] (Figure 1.2). Despite considerable structural similarities however, all 4 kinases have unique roles, which will be discussed below.

1.2.3.1 Canonical IKK's and the IKK complex

IKKα (or IKK1) was originally identified as "conserved helix-loop-helix ubiquitous kinase" (CHUK) in 1995[54,55] and was recognised as one of two integral components of an IκB kinase complex (IKK complex) in 1997, alongside IKKβ (or IKK2)[56-60]. IKKα and IKKβ are each capable of phosphorylating both Ser32 and Ser36 residues on IκBα[61] and both kinases are necessary for full activity of the IKK complex[60]. A third and final component of the IKK complex is regulatory subunit IKKγ (or NF-κB essential modulator – NEMO)[62,63]. IKKγ function, and the subsequent activation of NF-κB, depends on K-63-linked ubiquitination of IKKγ by multiple proteins including cIAP1 and TRAF6[64-67]. Upon its activation, IKKγ binds to a NEMO-binding domain (NBD) in IKKβ and regulates IKK complex activity[62]. Notably, although IKKγ is not itself a kinase, it is essential for NF-κB activation. Indeed, activation of the NF-κB response can be inhibited by blocking the ubiquitination of IKKγ or its interaction with IKKβ[65,66,68]. Upon stimulation of the TNFα receptor, the canonical NF-κB signalling cascade promotes the formation of the IKK complex, which phosphorylates IκBα to induce activation of NF-κB transcriptional activity (Figure 1.1).

Despite sharing 52% sequence similarity[59], IKKα and IKKβ do not share all functionality. Instead, they have unique roles to play, both in and out of NF-κB regulation. Firstly, their functions differ between the canonical and non-canonical pathways of NF-κB activation. IKKβ is heavily involved

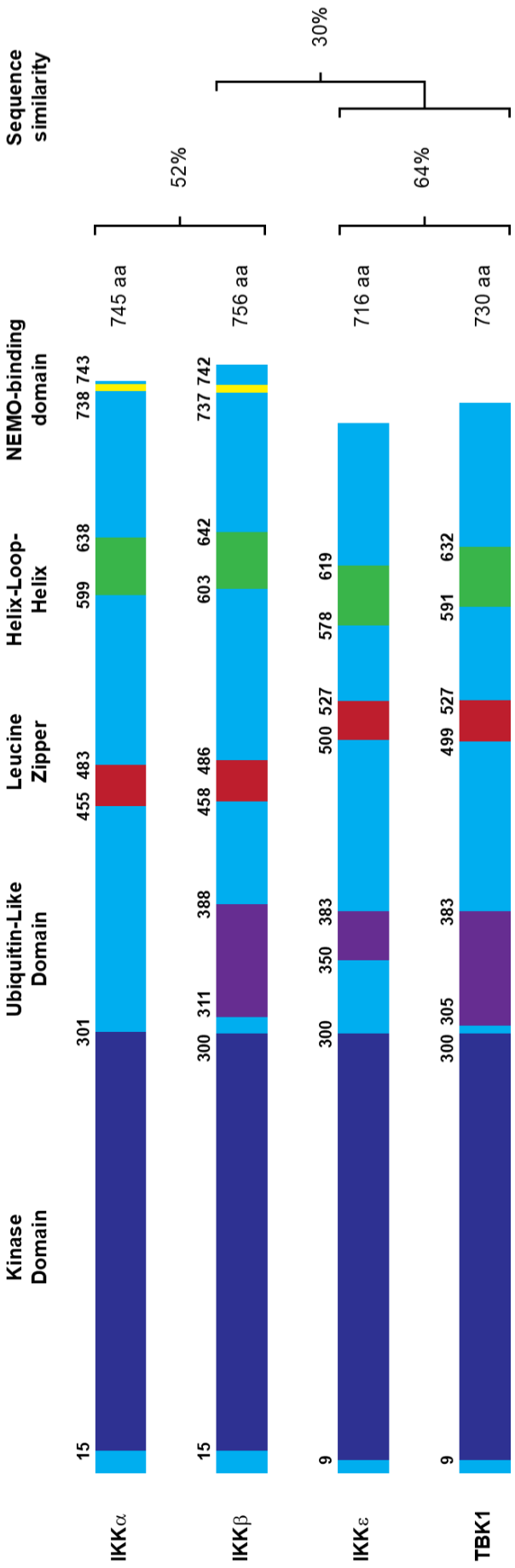

Figure 1.2 – Domain structures of the IKK's – A schematic representation of the protein domains found in the four IKK's. Each of the kinases share considerable sequence similarity. All contain a kinase domain to facilitate their primary functions and leucine zipper and helix-loop helix domains to aid dimer formation with other IKK's. IKKα and IKKβ also contain a NEMO-binding domain that allows interaction of the kinases with regulatory subunit IKKγ in the formation of the IKK complex. IKKβ, IKKε and TBK1 all contain a ubiquitin-like domain as well, which is essential for kinase activity. Adapted from Shen and Hahn, 2011[36].

in the canonical mechanism and is the main phosphorylating kinase for IκBα. Experiments performed with mice lacking the *CHUK* gene (encoding IKKα) provide evidence for its redundancy in canonical activation of the NF-κB pathway. It was demonstrated that *CHUK* -/- mice exhibit no impairment of IκBα degradation or induction of NF-κB signalling in response to cytokine stimuli. Although *CHUK* -/- mice do display other significant developmental problems, this highlights the redundancy of the kinase in induction of canonical NF-κB activation[69,70]. On the other hand, experiments performed with mice lacking the *IKBKB* gene (encoding IKKβ) show significant apoptosis in the liver, resulting in death before full gestation. Furthermore, *IKBKB* -/- cells are almost entirely defective in the activation of cytokine-induced NF-κB signalling demonstrating that, whilst IKKα is redundant in canonical NF-κB activation, IKKβ is indispensable in this process[71]. Comparatively, IKKβ is redundant in the activation of the non-canonical NF-κB pathway, where IKKα is the primary kinase involved, activated by stabilised NIK to phosphorylate and induce the processing of p100[45] (Figure 1.1).

NF-κB independent roles of canonical IKK's

As well as their contrasting roles in activating different branches of NF-κB signalling, the canonical IKK's also have important NF-κB independent roles to play. One such example is an important developmental role for IKKα in the skin. In mice, it has been demonstrated that the kinase is essential for proper embryonic skin development and, as mentioned above, *CHUK* -/- mice exhibit substantial developmental problems, such as impaired limb outgrowth, "shiny, taut and sticky skin" and a significantly thicker epidermis that cannot properly differentiate[72]. This demonstrates a key function for IKKα in promoting the proper differentiation of skin cells, particularly keratinocytes, during embryonic development, and although *CHUK* -/- mice can develop to term, they are perinatally lethal, dying shortly after birth[69,70,72]. Interestingly, as well as being independent of NF-κB activation, IKKα-mediated control of proliferation and differentiation of the epidermis is also entirely independent of IKKα kinase activity[73]. Instead, IKKα acts within the nucleus. A nuclear localisation sequence within IKKα's kinase domain regulates its entry into the nucleus[74] where it begins the differentiation process by inducing withdrawal from the cell cycle. Nuclear IKKα acts as a scaffolding protein, interacting with Smad2 and Smad3 transcription factors to induce *Ovol1* and *Mad2* expression, which leads to inhibition of Myc-dependent proliferation and facilitates keratinocyte differentiation[75]

IKKβ is involved in the early phases of an allergic response. When mast cells are stimulated by IgE, IKKβ is recruited to membrane lipid rafts where it phosphorylates a protein called synaptosomal-associated protein 23 (SNAP-23). Phosphorylation of SNAP-23 promotes

degranulation of the mast cell to allow the mounting of an appropriate allergic response and accordingly, the suppression of IKKβ in mast cells is reported to inhibit degranulation and reduce the anaphylactic response[76].

Both IKKα and IKKβ also play a role in preventing RIPK1-dependent cell death. TNF receptor activation induces various signalling activities that regulate cell death. Primarily, these are anti-apoptotic signals activated by NF-κB in response to TNF receptor activation, but TNF also activates RIPK1 which, rather than inhibiting cell death, can enhance it through induction of caspase-mediated apoptosis or induction of necroptosis. IKKα and IKKβ can protect cells from RIPK1 induced cell death by directly phosphorylating RIPK1 and inhibiting it, ensuring that the balance of survival/death signals induced by TNF signalling is firmly tipped into survival in inflammatory conditions[77]

1.2.3.2 Non-canonical IKK's

More recently described are the so-called "non-canonical IKK's". An inducible IKK, IKKε (or IKK-i)[78], was identified as a member of a wholly separate IκB kinase complex to what had previously been described[79]. The final IKK identified was TANK-binding kinase 1 (TBK1) (or NAK), shown to activate NF-κB as a part of a complex with TRAF2 and TANK[80] and through activation of the "canonical" IKK complex via directly activating IKKβ[81]. Since their characterisation, a clearer understanding of the roles of these "non-canonical" IKK's in the activation of NF-κB has emerged. Although capable of phosphorylating IκBα, IKKε or TBK1 on their own are only able to phosphorylate the Ser36 residue of the protein[79,81] which, alone, is insufficient to induce degradation[48]. This makes the kinases distinct from IKKα and IKKβ, both of which can phosphorylate both required residues, and suggests a minimal role for the "non-canonical" IKK's in the classical mechanism of NF-κB activation. Instead, the roles for IKKε and TBK1 in NF-κB regulation appear to be more in support of the activity of the canonical IKK's, fine-tuning the basal and induced activation of NF-κB transcription. Both IKKε and TBK1 can directly phosphorylate NF-κB subunits to regulate their activation independently of IκB degradation. The cRel subunit is directly phosphorylated by both IKKε and TBK1, facilitating its dissociation from IκBα independently of IκBα phosphorylation and allowing its nuclear translocation[82]. IKKε can also directly phosphorylate the p65 (RelA) NF-κB subunit at serine residues Ser468 and Ser536 to regulate NF-κB activity. Indeed, phosphorylation of Ser468 serves to enhance p65 transcriptional activity via modulation of transactivation potential upon release of the transcription factor from IκBα[83].

Since their discovery, it has become clear that although the IKK's show strong sequence homology with each other (IKKβ is 52% similar to IKKα[59], TBK1 and IKKε show 64% similarity and are both 30% similar to IKKβ[78,80,84]) and certainly share some functional similarity, the division of the IKK family into discrete "canonical" and "non-canonical" groups goes beyond their roles in NF-κB. Instead, classification can now be based upon well-defined and distinct primary functions. Whilst all IKK's are involved, to a greater or lesser extent, in the regulation of NF-κB, the non-canonical IKK's play unique and important roles in innate immunity and the activation of the interferon antiviral response.

Non-canonical IKK's and the innate immune response

Upon stimulation of the toll-like receptors (TLRs) by viral or bacterial products (such as double stranded RNA (dsRNA) or lipopolysaccharide (LPS) respectively) a signalling cascade is activated that culminates in the induction and secretion of type 1 interferon, interferon-β (IFNβ) (reviewed by Chau, 2008[85]). This pathway is dependent on both IKKε and TBK1[86-88], which directly phosphorylate interferon regulatory factor 3 (IRF3) at the serine residue Ser396[87] and IRF7 at serine residues Ser477 and Ser479[89], inducing their activation through dimerisation and nuclear translocation[87,90-92] wherein they bind to specific DNA sequences on a set of genes known as IFN-stimulated response elements (ISREs) in the promoters of target genes (reviewed by Honda and Taniguchi[93]). One key genetic target is interferon-β (IFNβ)[94], which is induced and secreted from signalling cells when IRF3 is activated. IFNβ then signals via the type 1 IFNα/β receptor (IFNAR) in an autocrine and paracrine manner, resulting in dimerisation of the 2 IFNAR subunits (IFNAR1 and IFNAR2). The interaction of IFNβ with IFNAR activates Janus family of protein kinases (JAK) Tyk2 and JAK1, resulting in the phosphorylation of signal transducer and activator of transcription (STAT) 1 and STAT2 and full activation of the JAK/STAT signalling cascade[95-97]. This signalling cascade culminates with the formation of a protein complex known as the IFN-stimulated gene factor 3 (ISGF3) complex, which is comprised of a STAT1/STAT2 heterodimer interacting with IRF9. The ISGF3 complex then binds to ISREs in the promoters of IFN-stimulated genes such as Ifit3 and OAS1 to produce the antiviral effects of the pathway[98,99] (Figure 1.3).

Whilst IKKε and TBK1 share common targets for phosphorylation and can both activate the IFN response, it is important to note that their activities do not entirely overlap. Despite IKKε only being inducible compared to TBK1's constitutive expression, IKKε does not act solely for redundancy or for the enhancement of an initial TBK1-mediated response. Experiments performed in TBK1-, IKKε- or TBK1/IKKε- deficient mouse embryonic fibroblasts (MEFs) show that, although *TBK1* -/- MEFs exhibit impaired IFNβ and interferon stimulated gene (ISG)

induction and *IKBKE* (IKKε-encoding gene) -/- MEFs do not, combined *TBK1/IKBKE* -/- MEFs show completely abolished activation of the interferon response, indicating that IKKε does have a unique function which, whilst comparatively minor, cannot be compensated for by TBK1[88].

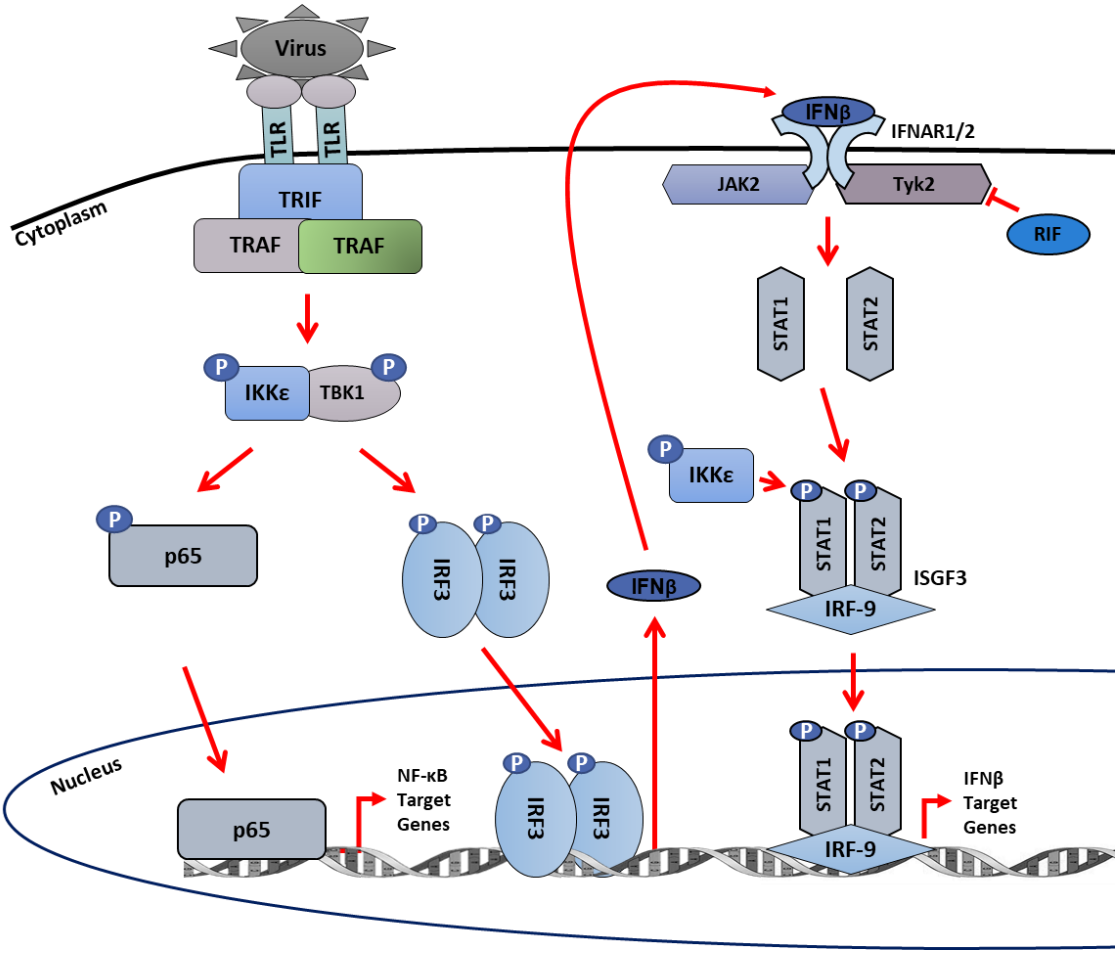

Figure 1.3 – IKKε and TBK1-mediated NF-κB and interferon signalling. In response to activation of the toll-like receptors, adaptor molecule toll-interleukin receptor (TIR)-domain-containing adapter-inducing interferon β (TRIF) is recruited to the TIR domain of the TLRs and acts as a platform for TRAF3 and TRAF6 recruitment. This induces the activation of IKKε and TBK1. Whilst neither kinase is capable of phosphorylating both IκBα serine residues necessary for degradation and therefore cannot induce the canonical NF-κB signalling pathway, they are able to directly phosphorylate specific NF-κB subunits including p65 and cRel, inducing their activation and nuclear translocation independently of IκB degradation. The primary function of IKKε and TBK1 involves the phosphorylation of IRF3, inducing its dimerisation and subsequent nuclear translocation. This induces the expression and secretion of IFNβ, which binds to the interferon receptor on the cell surface to activate the JAK/STAT signalling cascade, culminating in the formation of the ISGF3 complex, containing STAT1, STAT2 and IRF9. IKKε can also directly promote the formation of this complex via direct phosphorylation of STAT1. The ISGF3 complex translocates to the nucleus to activate transcription of IFNβ target genes and drive the innate immune response.

An explanation for this might come from the fact that IKKε plays a secondary role in IFN signalling, downstream of IRF3 and the IFNAR. IKKε directly phosphorylates STAT1 at serine residue Ser708, an event which dramatically increases ISGF3 binding to ISREs in ISGs. It is

thought that this phosphorylation facilitates a tighter, more stable interaction between STAT1 and STAT2 in the ISGF3 complex which, in turn, allows binding of the ISGF3 to shorter ISREs in target gene promoters. In agreement with this, there are a subset of IKKε-dependent ISG's (including *ADAR1*, an RNA targeting adenosine deaminase that can target viral dsRNA) that cannot be induced without expression of IKKε, even if JAK/STAT signalling is activated by TBK1 or via other means[99].

By the same mechanism, IKKε regulates the balance between type 1 and type 2 interferon responses. Whereas the type 1 response culminates with the formation of the ISGF3 complex, STAT1 does not always form a STAT1-STAT2 heterodimer ready for incorporation into the ISGF3. In response to type 2 IFN signalling (IFNγ), STAT1 can homodimerise to form the gamma-activated factor (GAF) complex[100], which binds to a different subset of genes, containing gamma activated sequences (GAS) in their promoter regions[101]. The same Ser708 phosphorylation of STAT1 by IKKε that promotes its incorporation into the ISGF3 also inhibits STAT1 homodimerisation. IKKε therefore inhibits GAF formation and promotes a type 1 IFN response over a type 2 response[102].

Non-canonical IKK's in metabolism

Interestingly, a role in various metabolic activities is emerging as a key part of the activities of the non-canonical IKK's. IKKε has been linked with the development of obesity in mice, where feeding of animals with a high-fat diet was found to increase expression of the kinase in white adipose tissue and the liver. It was found that, compared to wild type mice, mice lacking IKKε expression exhibited a reduction in diet-induced weight gain and an increase in energy expenditure, attributable to a significant increase in expression of uncoupling protein 1 (UCP1), which promotes energy usage through thermogenesis[103]. Alongside reduced weight gain, loss of the kinase in mice was also found to reduce chronic diet-induced hepatic steatosis (accumulation of fat in the liver) and obesity-induced chronic inflammation whilst preventing development of insulin resistance in response to a high-fat diet, indicating that IKKε might play an important role in the establishment of metabolic diseases such as diabetes[103]. Accordingly, anti-inflammatory drug amlexanox, approved for treatment of asthma, allergic rhinitis and aphthous ulcers, was found to be an inhibitor of IKKε and TBK1 and was shown to promote weight loss and energy expenditure in mice on high-fat diets, as well as restore insulin sensitivity and reverse hepatic steatosis[104].

Within the context of immune cells, IKKε and TBK1 have also been recently linked to the regulation of intracellular metabolism. In 2010, it was shown that TLR-activated dendritic cells

rapidly changed their metabolism, significantly increasing their glycolytic rate[105] and in 2014, it was demonstrated that this increase in glycolysis was induced by IKKε and TBK1, which promoted the association of glycolysis enzyme hexokinase II with the mitochondria. This association allowed the glycolytic enzyme to rapidly use mitochondrial adenosine triphosphate (ATP), thereby massively increasing the speed of glycolysis to support the production of fatty acids necessary for the expansion of the endoplasmic reticulum and Golgi apparatus in dendritic cell activation[106]. This demonstrated that, in addition to their involvement in innate immunity, the non-canonical IKK's have the ability to regulate overall cellular metabolic state.

1.3 IKK's in cancer

Given its role in wound healing and tissue repair, as well as the fact that the NF-κB response plays important roles in the regulation of cell growth and proliferation, it is unsurprising that aberrant activation of the NF-κB pathway is a long-established mechanism of cancer development. In fact, NF-κB activation facilitates the acquisition of certain cancer hallmarks[20] (reviewed by Dolcet *et al.*[107] and Xia *et al.*[108]). For instance, NF-κB signalling can regulate the balance between pro- and anti-apoptotic signals to promote a pro-survival phenotype through the induction of anti-apoptotic Bcl proteins[109,110] or proteins like cFLIP, a homologue and competitive inhibitor of caspase-8[111,112]. Activation of the pathway can also promote proliferation through regulation of cell cycle genes like cyclin D1[113] and by inducing the production of various factors and cytokines necessary to support growth, such as angiogenic factors like VEGF[114,115]. Indeed, the components of the NF-κB signalling pathway are frequently dysregulated in cancer. Haematopoietic tumours often exhibit genetic changes that result in hyperactivation of NF-κB subunits. Inhibitory mutations in the *NFKBIA* gene, which encodes the IκBα protein, have been reported in Hodgkin lymphoma patients[116-118], and amplification and rearrangements of the *REL* gene, encoding the NF-κB subunit cRel, are common in various lymphoid malignancies (reviewed by Courtois and Gilmore[119]). Whilst mutations that directly activate NF-κB are much rarer in solid tumours, some have been reported. IκBα is, again, a target of such mutations. For example, the *NFKBIA* gene is subject to deletion in glioblastoma[120]. Furthermore, genetic gain of function mutations in upstream signalling molecules like K-Ras, EGF Receptor (EGFR) and HER2 can lead to enhanced NF-κB activation in a variety of cancers[121]. The predominant way that NF-κB is dysregulated in human cancer however, is from changes that occur in the tumour microenvironment, as inflammation and infiltration of immune cells signal to activate NF-κB signalling via activation of the IKK's.

1.3.1 Canonical IKK's in cancer

IKKα and IKKβ activity have been implicated in a variety of cancers since the discovery of their respective functions.

IKKα

Notch-1, a member of the Notch family of receptors which are heavily involved in regulating the balance between cellular proliferation and differentiation, has been found to interact with IKKα to promote different types of cancer. In cervical cancer, Notch-1 promotes cancer cell survival through the NF-κB pathway, interacting with IKKα to enhance IKK activity upon stimulation of

NF-κB signalling. It also interacts with IKKα in basal conditions to facilitate nuclear translocation of the kinase and promote its association with chromatin. Here IKKα can enhance NF-κB activity and contribute to NF-κB-mediated transcription by phosphorylating histone H3 at serine residue Ser10, a site associated with positive regulation of gene expression[122,123], as well as phosphorylating p65 and NF-κB repressor silencing mediator for retinoic acid and thyroid hormone receptor (SMRT) to promote p65 transcriptional activity[124,125]. In estrogen receptor (ER) positive (+) breast cancer, Notch-1 interacts with IKKα to form a "Notch transcriptional complex" (NTC) and translocate ERα to the nucleus in the absence of estrogen. This facilitates ERα recruitment to estrogen response elements (EREs) in the genome and, upon p300 recruitment, the transactivation of ERα-target genes that drive proliferation in cancer[126].

In ovarian cancer, IKKα is the target of microRNA (miRNA) miR-23a. Previously associated with oncogenesis in colorectal cancer[127], laryngeal carcinoma[128] and other types of cancer, miR-23a is also upregulated in epithelial ovarian cancer, where it has been reported to directly upregulate IKKα expression whilst simultaneously suppressing suppressor of tumourigenicity 7 protein-like (ST7L) via binding to its 3 prime untranslated region (3'-UTR). STL7 supresses tumour growth by inhibiting the Wnt/Mitogen-activated protein kinase (MAPK) pathway to prevent cell cycle progression and epithelial-mesenchymal transition (EMT). Upregulation of IKKα by miR-23a enhances NF-κB pathway activation to promote cell growth and invasion which, when combined with the parallel regulation of STL7, leads to increased cancer development[129].

IKKα also plays a large role in the progression of later stage prostate cancer. Generally speaking, highly invasive PC3 prostate cancer cells show increased NF-κB activity compared to a less invasive PC3 line, attributable to an increase in IκBα phosphorylation and accordingly, expression of an IκBα super-repressor, containing an S32/36A mutation that prevents it's IKK-dependent phosphorylation and subsequent ubiquitin-mediated proteasomal degradation, reduced this highly invasive phenotype, demonstrating involvement of NF-κB activation in oncogenesis[130]. Importantly however, IKKα also promotes prostate cancer via NF-κB independent mechanisms. Maspin, a serine protease inhibitor, has been shown to reduce tumour metastasis by enhancing cell adhesion to the extracellular matrix, thereby preventing migration of tumour cells[131,132]. When immune cells infiltrate the tumour microenvironment, receptor activator of NF-κB ligand (RANKL) expressed on their cell membranes binds to RANK on the prostate cancer cells. This activates IKKα and facilitates its translocation to the nucleus, where it is recruited to the promoter of the Maspin gene and represses its transcription, thereby promoting disease progression. In accordance with this, levels of active, nuclear IKKα in human

prostate cancer correlate with metastatic progression[133] and suppression of IKKα expression reduces pancreatic cancer PC3 cell line migration and invasion[134].

Intriguingly, IKKα appears to have an inhibitory role in squamous cell carcinoma. As previously mentioned, IKKα plays an important role in the differentiation of skin cells during embryonic development and is crucial for switching off the growth of the epidermal layer. This indicates that should the kinase's role in differentiation become dysregulated, skin cells would begin to uncontrollably proliferate and tumours would begin to form. Accordingly, reduced expression of IKKα has been observed in squamous cell carcinomas, with missense mutations reported in exon 15 of the *CHUK* gene[135] and epigenetic modifications in the *CHUK* promoter reported to silence gene expression in oral squamous cell carcinoma (SCC)[136]. Indeed, loss of IKKα expression has been shown to promote the development of skin cancers and SCC in particular[137]. In agreement with this, an inverse correlation between IKKα expression and disease aggression is observed in human SCC[135]. As indicated by the findings of disrupted skin development in *CHUK* -/- mice, the kinase acts as a tumour suppressor in SCC by enhancing the terminal differentiation of the epidermal layer through inhibition of Myc-dependent proliferation (see 1.2.3.1), thereby preventing the tumour development and progression of the disease to a metastatic phenotype.

IKKβ

IKKβ has also been implicated in various cancers. In the intestine, inflammation-driven colitis-associated cancer (CAC) was found to be dependent on IKKβ-mediated NF-κB activation in a mouse model. Deletion of *IKBKB* in the enterocytes of said model led to a dramatic reduction in tumour incidence due to enhanced apoptosis in the early stages of tumourigenesis, indicating that the kinase is important for tumour initiation. Furthermore, *IKBKB* deletion in the macrophages which infiltrate the tumour site caused a decrease in tumour growth, but had no effect on apoptosis of the tumour cells, indicating that, in myeloid cells, IKKβ is crucial for the production of inflammatory factors that support CAC tumour progression[138].

Interestingly, IKKβ's role in CAC development is more controversial in the context of mesenchymal cells. Two studies, published at the same time in the same journal, proposed two alternate hypotheses. The first proposed IKKβ as a tumour promoting kinase, showing that loss of kinase expression in these stromal cells reduced colitis in response to inflammatory factor dextran sulphate sodium (DSS) and subsequently had a preventative effect on of tumour initiation[139]. It was shown that expression of IKKβ in the mesenchymal cells was important for proper infiltration of inflammatory cells and production of cytokines in the intestine and that without IKKβ activity, the inflammation that drives CAC initiation cannot occur. The second study

presented findings that suggested IKKβ activity in cancer associated mesenchymal cells has tumour suppressive properties instead, reporting that loss of IKKβ in fibroblasts led to an increase in the size of CAC tumours, attributable to an increase in proliferation of epithelial cells and a decrease in tumour cell apoptosis[140]. It was shown that loss of kinase expression led to a reduction in *Smad7* expression and a corresponding increase in TGFβ signalling, which ultimately increased the secretion of hepatocyte growth factor (HGF) from the fibroblasts and increased tumour cell proliferation. Whilst both studies used Cre based systems to knockout *IKBKB* in the mesenchymal cells, the first used a constitutive ColVIcre knockout, whereas the second used a tamoxifen inducible Col1a2creER system which targeted a much larger mesenchymal cell population than the ColVIcre system. It was therefore suggested that IKKβ's pro- or anti-tumourigenic effect in fibroblasts is highly dependent on the level of expression within the whole population or on its expression in uncharacterised sub-populations[139]. It was also noted that the ColVIcre knockout of *IKBKB* primarily affected tumour incidence and the early stages of CAC, whereas the Col1a2creER knockout had little impact at that stage, suggesting that the kinase might play different roles in the fibroblasts at different time points, enhancing inflammation and promoting tumour development in early stage CAC, but preventing progression at later stages. Whatever the explanation for this discrepancy, IKKβ clearly plays a highly intricate role in CAC, with well-defined pro-tumourigenic function in epithelial and myeloid cells and a more complex role in the stroma.

Similar to IKKα, IKKβ has also been shown to be regulated by miRNA's in ovarian cancer. miR-199a has a direct inhibitory effect on the expression of IKKβ. Concurrently, one study found that a subset of epithelial ovarian cancer (EOC) cells which showed low levels of miR-199a had correspondingly high levels of IKKβ, allowing induction of the NF-κB pathway and increased survival in response to chemotherapy drug paclitaxel, low levels of apoptosis in the face of TNFα stimulation and secretion of pro-tumour cytokines. Comparatively, a subset of EOC cells with high levels of miR-199a had much lower levels of IKKβ, struggled to produce an NF-κB response when treated with paclitaxel and, upon treatment with TNFα, exhibited significantly higher levels of apoptosis. This indicated that IKKβ expression regulates chemosensitivity and tumour aggression in ovarian cancer[141].

IKKβ is also a target of miRNA's in non-small cell lung cancer (NSCLC), where miR-503 has been shown to repress disease progression through the suppression of the oncogenic phosphoinositide 3-kinase (PI3K) p85 subunit and IKKβ. In NSCLC, expression of miR-503 correlates positively with patient survival and the tumour suppressive abilities of miR-503 were found to be tightly linked to the reduction of PI3K p85 and IKKβ expression. Ectopic expression

of the two kinases partially negated the tumour suppressive effects of the miRNA[142], which suggests an important role for the IκB kinase, and PI3K, in the development of NSCLC.

Outside of its NF-κB related activities, IKKβ has also been linked to tumourigenesis through regulation of the mechanistic target of rapamycin (mTOR) pathway. The tuberous sclerosis (TSC) 1/TSC2 complex inhibits mTOR signalling, but IKKβ activates the pathway by restricting activity of the TSC1/TSC2 complex through direct inhibitory phosphorylation of TSC1 at serine residues Ser487 and Ser511. IKKβ-mediated inhibition of the TSC1/TSC2 complex therefore indirectly activates the mTOR pathway, which results in the secretion of VEGF and the subsequent promotion of angiogenesis to support tumour development. In patient samples, IKKβ phosphorylation (indicative of activity) correlated strongly with phosphorylation of TSC1 and Kaplan-Meier analysis demonstrated association of phosphorylation of TSC1 with poor survival outcome[143].

Joint roles of IKKα and IKKβ

The two canonical IKK's also work in tandem in some cancers. In head and neck cancer, IKKα and IKKβ are both overexpressed and phosphorylated, and both kinases contribute to nuclear activation of the canonical and alternative NF-κB transcription factors. Whilst knockdown of either IKKα or IKKβ individually reduced NF-κB activation, combined knockdown of both kinases had a synergistically inhibitory effect on NF-κB activity and on cell proliferation and migration[144]. In the same cancer setting, dual knockdown of both IKK's suppressed a broad gene expression program that involved genes associated with the EGFR-activator protein 1 (EGFR-AP-1) pathway. The EGFR-AP-1 pathway specifically regulates cell proliferation and migration, indicating that the two IKK's also contribute to head and neck cancer via the activation of such growth factor pathways[144]. In liver cancer, high expression of IKKα and IKKβ has been shown to contribute to malignancy. Human hepatocellular carcinoma (HCC) tumour samples exhibited high levels of both kinases, along with high levels of c-FLIP and cyclin D1 and reduced levels of Maspin[145]. As previously mentioned, c-FLIP is an anti-apoptotic protein that can be induced by NF-κB activation[111,112] and reduction in Maspin levels is a phenotype observed in IKKα-driven prostate cancer that promotes metastatic progression[133]. This indicates that in certain liver cancers, both NF-κB-dependent and NF-κB-independent functions of IKK's are active and contributing to survival and development of the tumour. Accordingly, in HCC cell lines suppression of both IKKα and IKKβ has been shown to increase apoptosis and, in a subcutaneous injection mouse model using HCC cell lines, siRNA-mediated suppression of both IKKα and IKKβ reduced tumour

growth[145]. Together, these studies demonstrate how both kinases can work together to enhance tumourigenesis and disease progression in multiple cancer types.

1.3.1.1 Therapeutic targeting of canonical IKK's in cancer

Given the role that NF-κB plays in cancer and the importance of the IKK's in the variety of cancers discussed above, both in and out of the context of NF-κB activation, it is unsurprising that there has been much interest in developing IKK inhibitors. Indeed, some of the aforementioned studies have demonstrated the efficacy of using such inhibitors to treat breast cancer[143]. Even in some circumstances where a particular IKK inhibitor has had little antiproliferative or pro-apoptotic effect, treatment with the IKK inhibitors has been shown to improve response to other therapeutic agents such as doxorubicin[146]. Much of the effort to develop inhibitors has focused on the development of small molecule inhibitors of the kinases, with most focusing on inhibition of IKKβ due to its central role in canonical NF-κB activation.

One such example is IKKβ inhibitor BMS-345541, which has been shown to sensitise breast cancer cells to ionising radiation by inhibiting the cells ability to repair double-strand breaks via homologous recombination. This results in an increased DNA damage response, increased cell death *in vitro* and reduced tumour growth in a xenograft mouse model in response to ionising radiation[147]. Efficacy has also been demonstrated in melanoma, where the same inhibitor reduced proliferation of human melanoma cells *in vitro* and in an *in vivo* xenograft mouse model[148].

Another example of an IKKβ inhibitor is PS1145. The effectiveness of PS1145 has been tested in prostate cancer cells, where it was shown to effectively reduce NF-κB activity and induce apoptosis while simultaneously sensitising cells to TNFα-induced apoptosis. The drug was also shown to reduce proliferation and invasion of prostate cancer cells *in vitro*[149]. Interestingly, when studied in leukaemia, PS1145 was found to not only inhibit cell proliferation, but also restore sensitivity to imatinib in resistant cell lines[150].

CHS 828 is another inhibitor with IKK inhibiting properties[151]. However, whilst this compound showed promising effects in lung and breast cancer cell lines *in vitro* and even in *in vivo* lung and breast cancer xenograft mouse models[152], attempts to translate this efficacy to a range of solid tumours in the clinic have yielded disappointing results[153].

More disappointing is the fact that most of these IKK inhibitors are still in the preclinical stage, so the true efficacy of these compounds in patients remains to be seen. Some promise has been shown in the use of IKKγ mimetic peptides (NEMO peptides) however. NBD peptide inhibits the

formation of the canonical IKK complex and has been demonstrated to be effective in inhibiting the growth of pancreatic cancer both *in vitro* and in an *in vivo* xenograft model, whilst also sensitising cells to gemcitabine[154]. Efficacy has also been shown in a phase I clinical trial of activated B-cell like diffuse large B-cell lymphoma (ABC-like DLBCL), although this was in a canine cohort, not human[155].

However, even if more effective inhibitors are described, the primary aim of inhibition of canonical IKK activity is still to block NF-κB activation. Whilst it would be expected that NF-κB inhibition would be an effective therapeutic strategy in many cancers, the inhibition of NF-κB activation and downstream signalling causes significant negative effects that may ultimately limit the therapeutic efficacy of NF-κB inhibitors in the clinic, suggesting that targeting NF-κB through the inhibition of the canonical IKKs might not be a particularly effective strategy for cancer treatment (see 1.3.3.1).

1.3.2 Non-canonical IKK's in cancer

1.3.2.1 TBK1 in cancer

In the years since its identification, TBK1 has frequently been closely associated with lung cancer pathogenesis, by a variety of mechanisms. Firstly, TBK1 kinase activity has been shown to be induced by Ras signalling[156]. With mutations resulting in constitutively active, oncogenic K-Ras being very common in lung cancer, it is therefore unsurprising that TBK1 would play an active role. Indeed, it has been identified that TBK1, through its ability to activate NF-κB, functions as a key effector of mutant K-Ras-driven oncogenesis. The kinase has been reported as essential for the induction of anti-apoptotic signals from Bcl proteins that arise from the activation of NF-κB signalling downstream of mutated K-Ras, and it has been shown that suppression of TBK1 in K-Ras-dependent human lung cancer cells led to a significant down-regulation in an NF-κB gene signature and increased apoptosis, indicating that TBK1 expression and activity is a crucial player in K-Ras-driven cancer, without which, cells cannot tolerate mutated K-Ras and will die[157]. Secondly, and independently of NF-κB activity, the direct phosphorylation of AKT by TBK1 has been shown to contribute to oncogenic transformation in the lung. Accordingly, inhibition of TBK1 in certain lung cancer cell lines has been found to impair AKT signalling. Activation of AKT by TBK1 can lead to the inhibition of apoptosis or the promotion of cell growth, thereby contributing to tumour development[158]. In addition to this, TBK1 has been shown to support the activation of AKT/mTORC1, not only through the phosphorylation of AKT, but also through interaction with mTORC1 subunit Raptor and phosphorylation of mTORC1 effector S6 kinase

(S6K)[159]. TBK1 therefore tightly regulates the mTOR pathway, with involvement at multiple stages both early, with phosphorylation of AKT, and late, with phosphorylation of S6K, indicating that activation of mTOR signalling may represent a large piece of TBK1's oncogenic potential.

A recent phosphoproteomic study also shed light on other mechanisms by which TBK1 contributes to lung cancer, recognising a subset of lung cancer cells which were highly sensitive to TBK1 knockdown. Notably, these cells showed no changes in the basal levels of AKT phosphorylation when TBK1 was suppressed, suggesting the activation of AKT is inessential for pro-survival signalling mediated by the kinase. Furthermore, TBK1 knockdown impaired cell viability in cells where NF-κB and IRF3 signalling was constitutively active, indicating that known TBK1-mediated signalling is also not always required for its ability to promote tumour development in the lung[160]. Instead, polo-like kinase 1 (PLK1), a kinase involved in the G2/M transition of the cell cycle and previously established to be synthetically lethal in K-Ras mutant tumours[161], was identified as a direct substrate of TBK1 indicating that the IκB-related kinase plays a role in the regulation of mitosis[160]. Activated during the G2/M transition phase of mitosis, TBK1 phosphorylates PLK1 to drive cell cycle progression. TBK1 was also found to indirectly induce phosphorylation of metadherin, a protein which enhances angiogenesis and correlates with poor prognosis in early-stage lung cancer. Cell sensitivity to pharmacological inhibition of PLK1 and suppression of metadherin both correlated strongly with cell sensitivity to TBK1 knockdown, implicating both PLK1 and metadherin as key effectors of TBK1's role in lung cancer growth[160].

Whilst TBK1 regulates a complex network of signalling in lung cancer, it has also been connected to other cancer types. One example is pancreatic cancer. Somewhat paradoxically, autophagy, the controlled intracellular degradation of cytoplasmic components, has been shown to be pro-tumourigenic in K-Ras-driven pancreatic tumours, due to the fact that it helps maintain mitochondrial integrity and oxidative metabolism[162] whilst detoxifying reactive oxygen species[163]. TBK1 has previously been shown to induce autophagy[164,165] and correspondingly, impairment of the process has been reported in pancreatic cancer upon the inhibition of TBK1. Intriguingly, the same study also demonstrated that TBK1 activity is limited by autophagy[166] suggesting the existence of a tightly-controlled negative feedback loop. Indeed, as it is evident that TBK1 is closely involved in the regulation of controlled levels of autophagy within K-Ras-driven pancreatic tumours, it has been suggested that oncogenic K-Ras induces TBK1 activity to promote autophagy to a level at which it is beneficial for tumour growth. In turn, autophagy can limit the activation of TBK1, thereby preventing autophagy levels from tipping over the balance into the point where it is no longer beneficial[166].

In human epidermal growth factor receptor 2 (HER2) positive (+) breast tumours, an shRNA kinome screen identified TBK1 as a potential therapeutic target. Both knockdown and pharmacological inhibition of the kinase suppressed the growth of HER2+ breast cancer cells, and pharmacological TBK1 inhibition was synergistic with HER2 targeting drug lapatinib in *in vivo* models. Consistently with its roles in other cancers, TBK1's role in HER2+ breast cancer appears to be more in favour of driving the progression of the cell cycle rather than inhibition of apoptosis. Inhibition of TBK1 induced cellular senescence in HER2+ breast cancer cells but treatment failed to induce apoptosis, perhaps explaining the synergistic effect of TBK1 inhibition and lapatinib. TBK1 inhibition causes cells to arrest, then lapatinib induces apoptosis[167]. Interestingly, TBK1-mediated regulation of the cell cycle in this context is not regulated via the phosphorylation of PLK1 as it is in lung cancer[160]. Instead it is the activation of NF-κB signalling that explains TBK1's pro-tumourigenic effect in this tumour type[167].

Finally, TBK1 has been reported to be involved in the regulation of dormancy and drug resistance in advanced prostate cancer. Prostate cancer cells are known to metastasise to the haematopoietic stem cell (HSC) niche in the bone marrow[168] and TBK1 levels in prostate cancer cells are increased following the binding of those cells to osteoblasts in the HSC niche, suggesting a role the kinase might play a role in late stage disease progression. Intriguingly, in prostate cancer cells in this context, TBK1 inhibits mTOR signalling, rather than promoting it as it does in other settings. This has the effect of inducing dormancy in the cells, which confers drug resistance to the population and facilitates the development of a prostate cancer stem-like cells[169].

1.3.2.2 IKKε in cancer

Like other IKK's, IKKε has been implicated in a variety of cancer types and has been reported to drive tumourigenesis via a variety of mechanisms.

Recent years have uncovered important roles for IKKε in glioma's. The kinase has been shown to be overexpressed in both human glioma cell lines and patient tissue specimens, where it promotes resistance to apoptosis via the NF-κB-mediated induction of anti-apoptotic proteins[170]. Knockdown of the kinase in glioma cell lines also resulted in reduced proliferative rates and a reduction in migration and invasion, indicating IKKε also enhances tumour development by promoting growth, not just by inhibiting cell death[171]. Whilst this pro-proliferation/pro-invasion activity is also mediated by activation of NF-κB signalling, other mechanisms of IKKε-induced tumourigenesis in gliomas have been reported. Yes-associated protein 1 (YAP1) is a transcription factor that activates the expression of pro-proliferative genes

and suppresses apoptotic genes. Its transcriptional activity is typically repressed as part of the Hippo pathway, a signalling pathway that regulates organ size by controlling the cellular balance between proliferation and apoptosis. Given the pathways tight control over such processes, it is understandable that it is frequently a target of dysregulation in human cancers (reviewed by Harvey *et al.*[172]). In human glioma cell lines IKKε stabilises YAP1 protein and transports it to the nucleus to enhance its transcriptional activity. In turn YAP1, as well as inducing its pro-proliferative transcriptional program, suppresses the expression of microRNA's miR-let-7b and miR-let-7i[173], which have previously been shown to inhibit IKKε expression in glioblastoma, suppressing invasion and migration as a result[174]. Inhibition of miR-let-7b and miR-let-7i by YAP1 therefore sustains expression of IKKε, which can continue to enhance YAP1 activity in a positive feedback loop. IKKε therefore promotes the growth of gliomas through both pro-proliferative NF-κB and YAP1 transcriptional programs and anti-apoptotic NF-κB signalling.

IKKε is also involved in colorectal cancer, where it has been shown to inhibit β-catenin signalling[175]. Whilst β-catenin is frequently mutated in various cancers and its activation is well known to be oncogenic, as it promotes the EMT, it has been proposed that hyper-activation of β-catenin signalling can in fact have a negative effect on proliferation. For example, in melanoma, β-catenin expression has been shown to be linked with decreased proliferation and the upregulation of genes associated with melanocyte differentiation[176]. IKKε has been shown to directly interact with β-catenin and phosphorylate it at multiple serine residues to inhibit its signalling activity, and in colorectal cancer cells inhibition of the kinase enhances β-catenin transcriptional activity and inhibits proliferation. It has therefore been suggested that IKKε contributes to the development of colorectal cancer by phosphorylating β-catenin to limit its activation, keeping signalling activity below the threshold where it becomes anti-proliferative[175].

In lung cancer, IKKε has been shown to inhibit forkhead box O3 (FOXO3a)[177], a known tumour suppressor that is capable of inducing apoptosis[178] and promoting quiescence[179]. The kinase directly phosphorylates FOXO3a at serine residue Ser644, leading to inhibition of FOXO3a transcriptional activity, sequestration of the transcription factor in the cytoplasm and induction of protein degradation, thereby preventing FOXO3a induced apoptosis. Overexpression of IKKε has been shown to correlate with phosphorylation of FOXO3a in human lung tumours, indicating that the kinase contributes to tumourigenesis in the lung through regulation of FOXO3a transcriptional activity[177].

The kinase also supports lung cancers by promoting the development of drug resistance. Transcription factor STAT3 is frequently activated by environmental carcinogens like nicotine[180]

and, in NSCLC, activation of STAT3 in response to nicotine has been reported to induce IKKε expression. The transcription factor binds directly to STAT3 response elements in the *IKBKE* promoter (encoding IKKε) to induce kinase expression, which supports tumour development by conferring resistance to chemotherapeutic agents such as cisplatin, gemcitabine and doxorubicin, reducing levels of apoptosis in NSCLC cells upon treatment with such agents[181].

In terms of later stage cancer progression, IKKε has also been reported to promote lung cancer metastasis. Experiments performed using murine lung carcinoma cells (M27) have shown that IKKε can transcriptionally regulate the expression of MMP3 via regulation of NF-κB and AKT signalling[182]. MMP's are a group of enzymes that help degrade proteins of the extracellular matrix and are frequently dysregulated in many different cancers due to their ability to help cancer cells metastasise (reviewed by Gialeli *et al.*[183] and Shay *et al.*[184]). For example, increased MMP3 expression in M27 cells has been shown to promote lung colonisation. The IKKε-mediated upregulation of MMP3 therefore represents a mechanism by which the kinase facilitates metastatic tumour growth in the lung. Similarly, in gastric cancer, high levels of IKKε expression correlate with worse patient prognosis and suppression of the kinase has been shown to inhibit tumour progression and metastasis in a xenograft mouse model using gastric cancer cells[185]. Together, these studies demonstrate a clear role for the kinase in the metastasis of various cancers.

IKKε is therefore linked to a wide variety of different cancer types. On top of those mentioned above, it has also been implicated in ovarian cancer, where it is overexpressed and contributes to cisplatin resistance[186] and invasion and metastasis[187], in pancreatic cancer, where its expression correlates with poor patient prognosis[188] and it enhances glycolytic metabolism to support tumour growth[189], in renal clear cell carcinoma, where its expression again correlates with prognosis[190] and in melanoma, where it promotes proliferation via activation of NF-κB, AKT and MAPK signalling[191]. The main cancer type where IKKε is oncogenic however, is breast cancer, where the role of the kinase has recently been closely investigated.

1.3.3 IKKε in breast cancer

The first indication that IKKε was involved in the development of breast cancer came in 2005, when it was reported that expression of the kinase was significantly higher in a range of breast cancer cell lines than it was in untransformed MCF-10 breast epithelial cells and was expressed in patient tumour samples. Expression of IKKε was reported to strongly correlate with the expression of casein kinase 2 (CK2)[192], a kinase which has been heavily linked to cancer in the past due to the anti-apoptotic effects of its activity and its role in cell cycle progression (reviewed

by Trembley *et al.*[193]). CK2 was shown to induce IKKε which, in turn, enhanced degradation of IκBα and activation of NF-κB to promote cell growth. In agreement with this, inhibition of IKKε kinase activity reduced colony formation in a soft agar assay, indicating that the kinase played a part in driving cell proliferation and assisted anchorage independent growth in breast cancer[192].

A subsequent study demonstrated that IKKε regulated basal, constitutive activation of NF-κB in breast cancer cells. As previously mentioned, IKKε can phosphorylate NF-κB family member p65 directly at serine residues Ser468 and Ser536 (see 1.2.3.2). Phosphorylation of p65 at Ser536 has been detected in a variety of cancer cells, including a selection of breast cancer cell lines. Whilst IKKε was dispensable for cytokine-induced phosphorylation of p65, it's expression in cancer maintained p65 phosphorylation at a level high enough to facilitate some basal NF-κB transcriptional activity and maintain induction of NF-κB-mediated pro-proliferative signals[194]. Therein a mechanism by which expression of IKKε in cancer maintains a constant background activation of NF-κB to promote tumour formation was proposed.

These early connections between IKKε and breast cancer were then expanded upon when, in 2007, Boehm *et al.* formally identified the kinase as a fully-fledged breast cancer oncogene[195]. Hahn *et al.* had previously characterised a mechanism of cellular transformation by which they could generate *bona fide* human cancer cells. They showed that human embryonic kidney (HEK) epithelial cells expressing human telomerase reverse transcriptase (*hTERT*) and large and small SV40 T antigens (LT and ST respectively) could be tipped over into tumourigenic status by the expression of oncogenic, constitutively active H-Ras^{V12} [196]. Boehm *et al.* set out to investigate which downstream effectors of H-Ras^{V12} would contribute to cellular transformation in this model, termed herein as HA1E cells. Initially finding that a combination of constitutively active MAPK and PI3K signalling would substitute for H-Ras^{V12}, they became interested in kinases that could induce PI3K signalling. Expressing a mutated, constitutively active MEK^{DD} to activate MAPK signalling, they screened for kinases that could replace constitutively active AKT in the activation of PI3K, eventually concluding that IKKε was sufficient to substitute for PI3K signalling and render HA1E cells expressing MEK^{DD} (HA1E-M cells) tumourigenic. Subsequently, the IKKε gene, *IKBKE*, was found to be the subject of a genetic copy number gain or amplification at chromosomal region 1q32 in 16% of breast cancer cell lines and 30% of human breast tumours, leading to overexpression of the kinase. Copy number gain was also found in 4/10 ductal carcinoma *in situ* (DCIS) tumours analysed, which indicated that the amplification of the kinase was an early event in breast tumour development and may contribute to early stage growth. Suppressing IKKε expression in *IKBKE* amplified breast cancer cell lines led to a reduction in proliferation and cell viability, demonstrating the essential role of the kinase in cells where it is amplified. Importantly,

expression of an IκBα super-repressor, which cannot be phosphorylated and degraded, in HA1E-M cells blocked the transforming effect of IKKε, demonstrating that aberrant activation of NF-κB was the driving force behind the kinases oncogenic potential. Furthermore, expression of IKKε in breast cancer cell lines was linked with expression of NF-κB-induced MMP9 and Bcl2, suggesting enhancement of invasive properties and inhibition of apoptosis in cell lines expressing the kinase. Notably, the primary function of the kinase, in the phosphorylation of IRF3 and the activation of innate immunity, was determined to be redundant for transformation[195]. As previously discussed, IKKε has also been reported to directly activate NF-κB subunits like cRel[82], inducing their nuclear translocation independently of IκBα phosphorylation (See 1.2.3.2). Accordingly, Boehm *et al.* demonstrated that expression of IKKε in breast cancer patient tissues correlated with the expression and nuclear localisation of cRel[195].

IKKε can also contribute to the canonical activation of NF-κB in breast cancer. Activation of canonical IKK's and subsequent NF-κB induction involves ubiquitination of various signalling components including IKKγ and several upstream factors. CYLD, a tumour suppressor and deubiquitinase enzyme, has been shown to inhibit NF-κB activation by removing the conjugated ubiquitin from said components. IKKε has been shown to phosphorylate CYLD at serine residue Ser418, a modification which restrains CYLD deubiquitinase activity and thereby inhibits the tumour suppressor[197]. Phosphorylation of CYLD by IKKε therefore promotes the activation of NF-κB signalling and may provide an explanation for how the kinase induces degradation of IκBα in spite of the fact that IKKε itself can only phosphorylate one of the two required serine residues to do so[79]. These studies therefore demonstrate how IKKε can activate NF-κB in breast cancer to drive disease progression, both by contributing to the degradation of IκBα and by directly activating NF-κB subunits to drive breast cancer development.

1.3.3.1 Downsides of targeting NF-κB in cancer therapy

30% of human breast cancer cases is a substantial fraction for IKKε to be involved in and, with no clear association with particular breast cancer subtypes[195], the kinase is therefore an attractive therapeutic target for a large group of patients.

For the treatment of IKKε-driven breast cancer, IKKε inhibitors have previously been described. 3 separate IKKε/TBK1 dual inhibitors, designated SR8185, 200A and 200B, have been shown to suppress the proliferation of breast cancer, prostate and oral cancer cells *in vitro*. 200A was also shown to induce apoptosis in the same cells *in vitro* and suppressed the growth of tumours in a xenograft mouse model, demonstrating the effectiveness of IKKε/TBK1 inhibition for cancer

therapy[198]. However, like the canonical IKK inhibitors, these IKKε/TBK1 inhibitors remain at a preclinical stage, so have not yet been tested for efficacy in patients.

One more promising compound is a drug called amlexanox. Already approved for clinical use by the US Food and Drug Administration (FDA) in America, amlexanox is an anti-inflammatory compound, typically used for the treatment of recurring mouth ulcers and, in Japan, has been used to treat other inflammatory conditions such as asthma or rhinitis. Amlexanox was shown to selectively inhibit both non-canonical IKK's[104] and has been demonstrated to induce cell cycle arrest and apoptosis in glioma cells and suppress glioblastoma growth in xenograft models[199]. However, even though, in this circumstance, amlexanox was shown to exert anti-tumour effects by inhibiting IKKε-mediated activation of the Hippo pathway, the drug has still been shown to inhibit the activation of the NF-κB pathway[200], and therein lies the problem with targeting the IKK's directly.

Despite the high frequency occurrence of NF-κB dysregulation in cancers, it is not a particularly useful therapeutic target. In fact, inhibition of the NF-κB pathway presents several significant complications. Given the high number of cellular processes in which NF-κB signalling is involved, inhibition is likely to result in many undesirable effects, including immunosuppression.

Additionally, NF-κB signalling on the whole is remarkably complex and includes various feedback mechanisms that can just as easily restrict inflammation as promote it. Indeed, NF-κB inhibition has surprisingly been reported to increase the production of pro-inflammatory cytokine IL-1β from neutrophils and macrophages. IL-1β precursor pro-IL-1β is produced in response to NF-κB signalling, but simultaneously, NF-κB induces expression of serine protease inhibitors in neutrophils, which inhibit the processing of pro-IL-1β to IL-1β. Accordingly, suppression of NF-κB subunit p65 or inhibition of NF-κB via pharmacological inhibition of IKKβ in a mouse model was shown to substantially upregulate plasma IL-1β levels due to increased pro-IL-1β processing and secretion[201]. NF-κB has also been reported to upregulate p62, a protein which binds to proteins and organelles to target them for autophagy-mediated degradation. In macrophages, IL-1β processing is controlled by the "inflammasome", a protein complex that contains caspase 1 and processes pro-IL-1β to its mature secretable form. Signals from the mitochondria in primed macrophages can activate the inflammasome, but p62, upregulated by NF-κB activation in macrophages, can bind to polyubiquitinated mitochondria, degrading them via mitophagy. This cuts off the inflammasome activating signals, thereby reducing IL-1β processing and secretion[202] and again, demonstrating how inhibition of NF-κB can promote inflammation. Such mechanisms have been suggested to have developed as an NF-κB independent inflammatory

mechanism to ensure appropriate host defence and protective inflammation could be raised in response to pathogens that were capable of inhibiting NF-κB signalling[201]. Importantly, these mechanisms suggest that the long-term inhibition of NF-κB necessary for tumour treatment may serve to promote an inflammatory environment that could potentially enhance tumour formation.

Furthermore, NF-κB has been suggested to play tumour suppressive roles in certain contexts. In epidermal cells, expression of an IκBα super repressor protein and subsequent inhibition of NF-κB activity was shown to induce hyperplasia, which could be blocked by expression of NF-κB subunits[203]. In endothelial cells, NF-κB reportedly maintains vessel structural integrity, as cells expressing the IκBα super repressor showed increased angiogenic potential and the vessels formed from those cells demonstrated disrupted tight junction formation, leading to increased vessel permeability that is favourable for tumour metastasis[204]. In liver parenchymal cells, deletion of regulatory subunit IKKγ, which is necessary for canonical NF-κB activation, led to development of steatohepatitis and spontaneous development of hepatocellular carcinoma in a mouse model, indicating a tumour suppressive role for NF-κB in the development of liver cancers[205]. Considering these context specific roles, it is clear that inhibition of NF-κB signalling, whilst initially beneficial, might lead to further complications further down the line including, in extreme circumstances, giving rise to further tumour development.

As briefly discussed earlier (see 1.3.1.1), to date there has been little success with the development of NF-κB inhibitors, with most attempts stuck firmly in the pre-clinical stages of development. One relatively successful compound is bortezomib, a proteasome inhibitor which can prevent NF-κB activation by inhibiting the degradation of IκB proteins, thereby maintaining the cytoplasmic sequestration of NF-κB subunits[206]. However, whilst bortezomib has shown some efficacy in haematological cancers and has been approved for clinical use in multiple myeloma and lymphoma patients[207], it has been found to be ineffective in solid tumours. Indeed, this story is true of many other compounds. It is likely these disappointing results are down to the fact that such inhibitors are very broad therapeutics, failing to target NF-κB specifically and having very generalised effects in patients. Accordingly, targeted inhibitors have shown more signs of promise (reviewed by Godwin *et al.*[208]). NBD peptide, which specifically targets NF-κB activation by inhibiting the formation of the canonical IKK complex by binding with IKKγ (or NEMO) to prevent its interaction with IKKβ, was mentioned previously. This peptide has been shown to reduce cytokine inducible NF-κB-dependent gene expression[68] and some efficacy has been demonstrated in head and neck squamous cell carcinoma, melanoma and pancreatic ductal adenocarcinoma (PDAC) where it inhibited constitutive NF-κB activation, reduced

proliferation and migration and induced apoptosis[154,209,210]. Furthermore, NBD peptide has been shown to be efficacious in a phase I clinical trial of ABC-like DLBCL in canines[155].

Despite this, these targeted inhibitors still work to inhibit NF-κB activation and therefore, still risk the negative effects described above, meaning the benefits of using such compounds to inhibit the pathway for cancer treatment need to be carefully weighed against the drawbacks. In the meantime, keeping in mind the context of treating IKKε-driven breast cancers, the question remains as to whether therapeutic intervention that avoids targeting NF-κB signalling would be possible. To understand the answer to that question, a better understanding of the full scope of IKKε's oncogenic potential is required. As discussed previously (see 1.3.2.2), IKKε has been shown to play NF-κB independent roles in the development of various tumour types, and that is no different in breast cancer.

1.3.3.2 NF-κB independent mechanisms of IKKε-driven oncogenesis in breast cancer

Despite Boehm *et al.*'s findings that IKKε-mediated transformation was dependent on NF-κB activity, recent findings have highlighted a selection of other mechanisms by which the kinase can support breast tumour development.

As previously mentioned, IKKε can promote lung tumour development by phosphorylating and inhibiting tumour suppressor FOXO3a at serine residue Ser644, resulting in decreased levels of apoptosis (see 1.3.2.2). The same phosphorylation also occurs in breast cancer and, as in the lung, IKKε expression has been found to correlate with phosphorylation of FOXO3a in breast tumours. This indicates that the kinase contributes to breast cancer development by inhibiting FOXO3a-induced apoptosis in addition to promoting NF-κB-mediated anti-apoptotic signals[177].

IKKε has also been shown to promote the expression of an alternate variant of ERα in breast cancers that are typically classified as ER negative (ER-). ERα-36 is a truncated version of the receptor that is primarily cytoplasmic or contained to the cell membrane, having little nuclear activity[211]. IKKε directly interacts with the shortened receptor, inducing its expression in ER- breast cancer cells. ERα-36 expression leads to the activation of MAPK signalling and induction of cyclin D1 and c-Myc to promote ERα-36-mediated cell growth in ER- breast cancers[212].

Additionally, whilst Boehm *et al.* described IKKε's role in innate immunity as dispensable for cellular transformation, a subset of triple negative breast cancer cell lines where IKKε activated the type 1 interferon pathway and JAK/STAT signalling was identified in 2014. In this study IKKε-mediated JAK/STAT signalling generated a cytokine network which supported the development of the tumour[213]. These "immunomodulatory" breast cancer cells demonstrated increased

secretion of pro-tumourigenic cytokines CCL5 and IL-6, which stimulated cell growth. It was shown that simultaneous inhibition of IKKε and JAK signalling abrogated the increased CCL5 and IL-6 secretion and reduced proliferation, suggesting therapeutic targeting of the IRF3 branch of IKKε signalling might be a valid option for patients with IKKε-driven breast cancer after all.

Furthermore, it remains to be seen whether any of the NF-κB-independent mechanisms by which IKKε promotes tumourigenesis in other cancer types might be at play in a breast cancer setting. IKKε has been shown to enhance proliferation of gliomas by stabilising YAP1[173], which has itself been previously linked to breast cancer, albeit in a somewhat contrasting manner. In some instances, it has been shown to be overexpressed and pro-tumourigenic in breast cancer, promoting proliferation in cell lines and xenograft tumour formation in a mouse model[214]. In other breast cancer circumstances, YAP1 has been reported to be tumour suppressive, as expression was found to be decreased or completely absent in tumour tissues and suppression of YAP1 was shown to increase migration and invasion in cells and in a xenograft mouse model[215]. Irrespectively of which side of the fence YAP1 is ultimately shown to fall in breast cancer, it is not outside the realms of possibility that if IKKε is promoting glioma formation via stabilisation of YAP1, it might also promote breast tumour development in the same way. Similarly, IKKε induces MMP3 in lung carcinomas, which helps invasion and metastasis[182]. MMP3 is overexpressed in many different types of cancers, including breast, and its elevated expression is predictive for poor patient outcome in breast tumours[216]. It remains to be seen whether IKKε also upregulates MMP3 in breast cancer, but it could easily represent another mechanism by which the kinase can support the later stage progression of tumours in the breast.

One area of particularly notable interest is the emerging understanding that IKKε appears capable of regulating intracellular metabolism. The role of IKKε in promoting an essential increase in glycolytic rate in dendritic cells to support their activation has been previously discussed (see 1.2.3.2). Whilst this was the first indication that IKKε could regulate cellular metabolic states, the kinase has subsequently been linked with cellular metabolism in pancreatic cancer, where it was shown to induce a Myc-mediated upregulation in glucose metabolism to support the rapid proliferation of the cancer cells[189].

Given the ubiquitous nature of metabolic reprogramming in human cancers it is now increasingly recognised as a key part of tumour formation and a hallmark of cancer[20]. The increasing evidence that IKKε is emerging as a central regulator of metabolism in both immune and cancer settings is therefore very exciting, and the question of whether IKKε regulates metabolism in other cancers where it is oncogenic, including breast cancer, is a question worth investigating.

1.4 Cancer metabolism

1.4.1 Aerobic vs. anaerobic respiration

Respiration describes the process by which the nutrients taken up by a cell are converted into energy. The aim of the process is to break down nutrients into useable biological material, so that energy held within the nutrients can be stored for future use, or so that the compounds can be converted into materials useful for cell growth and proliferation. The most common nutrient taken up by cells is sugar in the form of glucose, but while this nutrient uptake is largely the same between different cell types, the way in which the nutrients are used within cells is highly context-dependent.

When a source of oxygen is present and readily available, the metabolism of the majority of differentiated cells is described as “aerobic”. In aerobic respiration, glucose is used in a process called glycolysis, which involves a sequence of biochemical reactions that convert glucose, step-wise, into pyruvate within the cell (Figure 1.4). The glucose-derived pyruvate then enters the mitochondria, where it undergoes decarboxylation by the pyruvate dehydrogenase complex to produce a compound called acetyl coenzyme A (acetyl-CoA). Acetyl-CoA is then used as a source of acetyl groups to fuel the tricarboxylic acid (TCA) cycle within the mitochondria. As well as producing various biosynthetic intermediates, a crucial aerobic product of the TCA cycle is the reduced form of nicotinamide adenine dinucleotide (NAD), aka NADH, which is subsequently used to fuel oxidative phosphorylation (OXPHOS) by donating electron to an intermembrane complex in the inner mitochondrial membrane. These electrons are then passed along a series of similar intermembrane protein complexes before being ultimately donated to oxygen, reducing it to water. The passing of electrons from complex to complex produces energy which is used to pump protons, also donated by NADH, across the inner mitochondrial membrane into the intermembrane space. This generates and maintains a proton gradient, which ensures there is a pool of H^+ protons to fuel the phosphorylation of adenosine diphosphate (ADP) to adenosine triphosphate (ATP) via the transportation of the protons back into the cristae through the ATP synthase enzyme complex (Figure 1.5). ATP acts as an intracellular energy store and the production of ATP via oxidative phosphorylation, fuelled by the electron transport chain (ETC), is a highly efficient process, producing a net total of 32 moles of ATP for every mole of glucose that is taken into the cell.

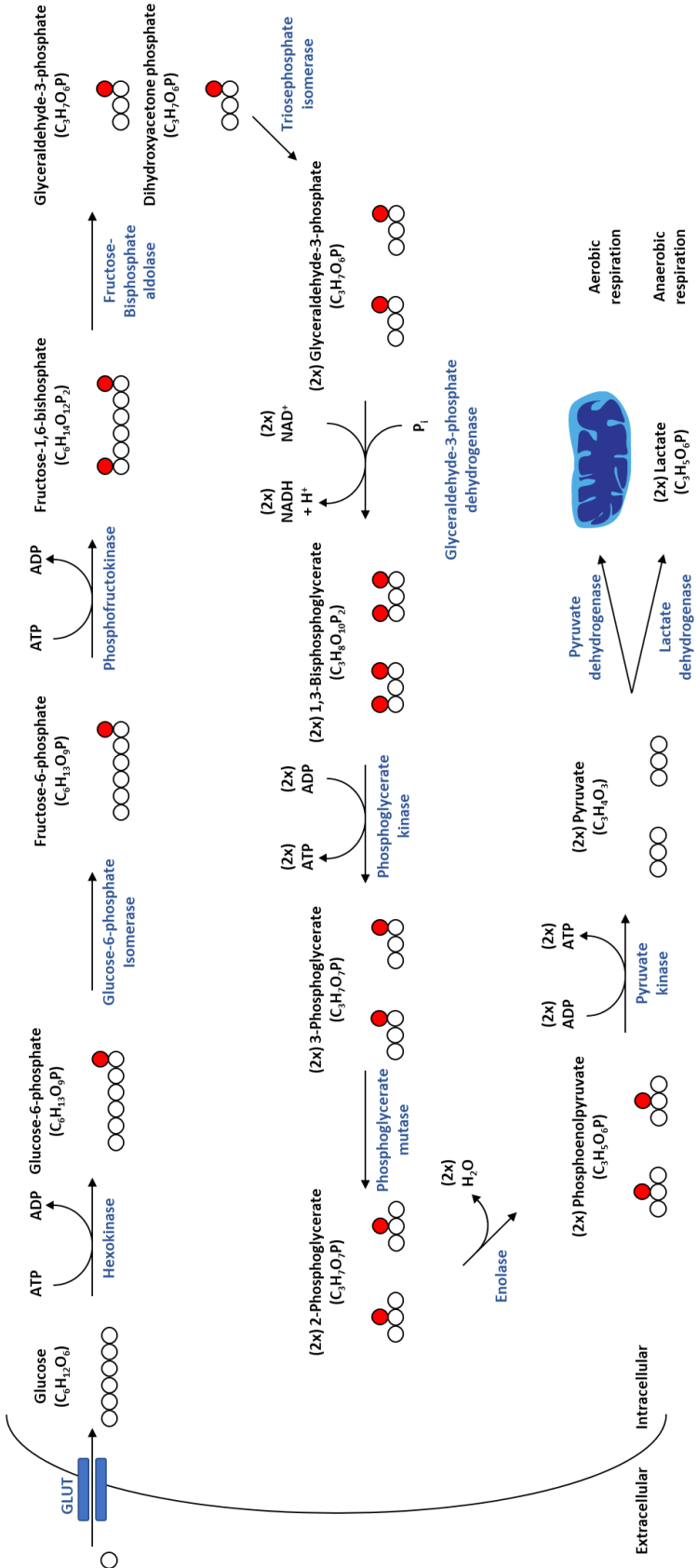

Figure 1.4 – Overview of glycolysis – A schematic representation of the sequential reactions that occur in the glycolytic process. Glucose is transported into cells via glucose transporter proteins (GLUTs) and ten biochemical reactions oversee the conversion of one glucose molecule into two pyruvate molecules ready for use in downstream metabolic processes. The glycolytic pathway yields a net gain of two molecules of ATP, as one molecule is used in the conversion of glucose to glucose-6-phosphate by hexokinase and one molecule is used in the conversion of fructose-6-phosphate to fructose-1,6-bisphosphate by phosphofructokinase, but then, as the 6-carbon molecule is divided into two 3-carbon molecules, two ATP molecules are generated in the conversion of two 1,3-bisphosphoglycerates to two 3-phosphoglycerates by phosphoglycerate kinase and two molecules are produced in the conversion of two phosphoenolpyruvates to two pyruvates, giving four molecules produced in total and a net gain of two. This net positive increase in ATP levels provides the basis for why ATP can still be generated in anaerobic conditions. Pyruvate produced from glucose can be used in the mitochondria to fuel the TCA cycle and subsequently OXPHOS, or it can be converted to lactate by lactate dehydrogenase. Carbon atoms are represented by white circles and red circles represent phosphate groups.

In the absence of oxygen, the ETC lacks a terminal electron acceptor and therefore cannot function, meaning mitochondrial production of ATP ceases. Instead, hypoxic conditions trigger a switch in the metabolic activities of cells. Instead glycolysis being used to fuel the TCA cycle and subsequently drive OXPHOS, hypoxic cells exhibit "glycolytic" metabolism. Glycolytic cells display a significantly increased rate of glycolysis and, instead of producing acetyl-CoA, convert glucose-derived pyruvate to lactate via lactate dehydrogenase (LDH). This switch is primarily mediated by hypoxia inducible factor 1 (HIF1), a transcription factor complex crucial for the intracellular response to changes in oxygen availability[217].

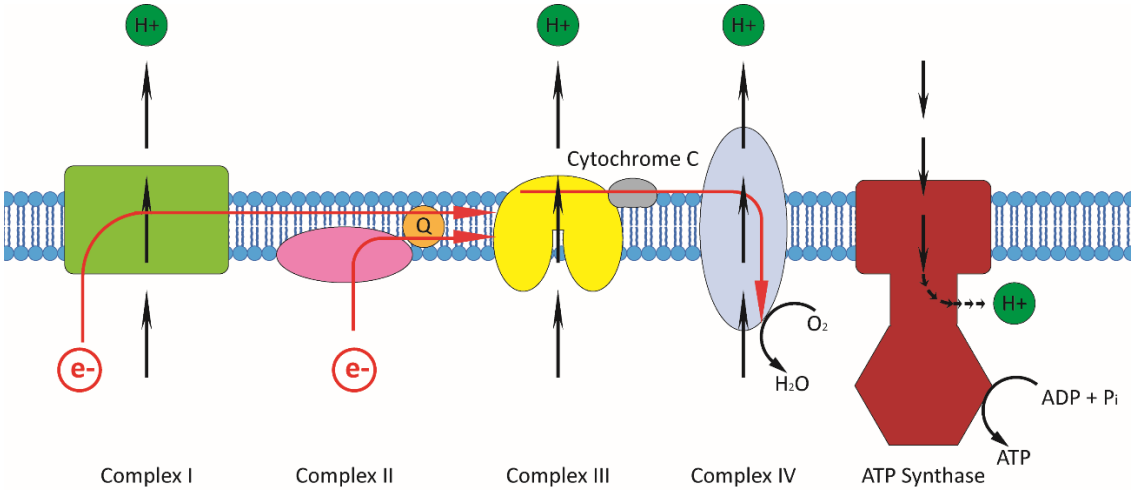

Figure 1.5 – The electron transport chain. NADH produced in the TCA cycle fuels the ETC to drive OXPHOS through the donation of electrons and protons to the inner mitochondrial membrane. The passing of electrons along a series of inter-membrane protein complexes provides the energy necessary to pump protons through those complexes and into the inter-membrane space of the mitochondria. The maintenance of a proton gradient ensures that the protons will pass back into the cristae of the mitochondria via the enzyme complex ATP synthase, providing the energy necessary for the complex to phosphorylate ADP and generating one molecule of energy storage unit ATP. The electrons that are passed along the membrane are donated to terminal electron acceptor oxygen, hence the term oxidative phosphorylation and the requirement of oxygen for mitochondrial respiration.

HIF1 and the balance between aerobic and anaerobic respiration

HIF1 is a heterodimer complex comprised of the constitutively expressed HIF1β and the post-translationally regulated HIF1α. The alpha subunit is degraded in the presence of oxygen due to the action of oxygen-dependent prolyl hydroxylases (PHDs), which target HIF1α for ubiquitination by the von-Hippel-Lindau (VHL) protein and subsequent degradation by the proteasome. When cellular oxygen availability is low, the PHDs cannot modify the HIF1α subunit which is therefore no longer degraded. Stabilised HIF1α dimerises with HIF1β, facilitating nuclear translocation and induction of HIF1 target gene expression[218-220].

HIF1 induces the anaerobic metabolic state by upregulating glucose transporters like glucose transporter 1 (GLUT1) to increase glucose uptake[221,222], by upregulating LDH to increase lactate production and by inhibiting the mitochondrial uptake of glucose derived carbon through the upregulation of pyruvate dehydrogenase kinase (PDK), which phosphorylates and inhibits pyruvate dehydrogenase to limit the conversion of pyruvate to acetyl-CoA[223,224]. This increase in glycolytic rate and production of lactate is the key characteristic of "anaerobic respiration", which is significantly less efficient than OXPHOS, producing a net gain of just 2 moles of ATP, generated during the main glycolytic process[225]. Importantly though, as the rate of glycolysis is increased by the increase in glucose uptake, the rate of ATP production is much faster which allows cells to salvage some overall ATP production despite the lack of oxygen (Figure 1.6).

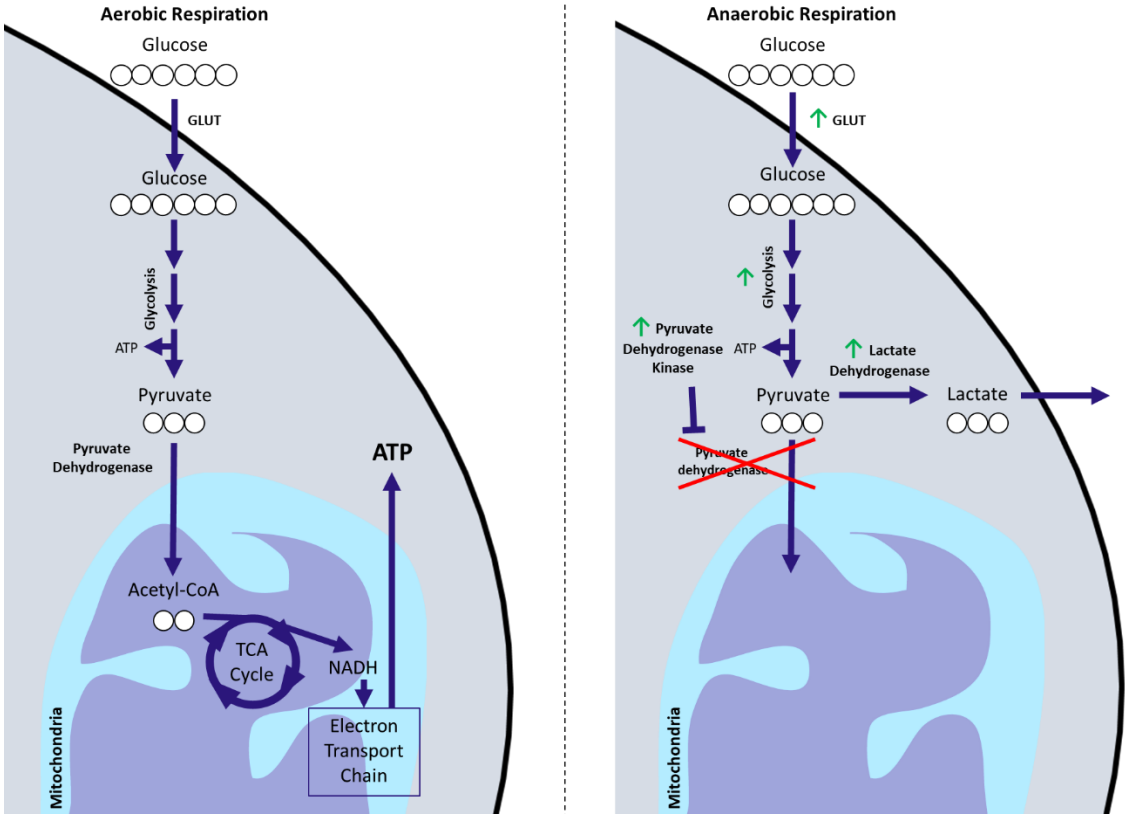

Figure 1.6 – Aerobic vs anaerobic respiration. When oxygen is available, normal differentiated cells will metabolise glucose to pyruvate and then convert that pyruvate to acetyl-CoA, which can enter the mitochondria and combine with oxaloacetate in the TCA cycle to regenerate citrate to allow continuation of the cycle. NADH is produced in the cycle which is used to drive the ETC and OXPHOS, producing large amounts of ATP. This is efficient respiration, producing a net gain of about 32 moles of ATP for each mole of glucose consumed. When cells are starved of oxygen, the ETC cannot function and the cells enter a state of anaerobic respiration. Transcription factors like HIF1 drive the cellular adaptation to hypoxia, by diverting metabolic flux away from the mitochondria. Glucose uptake, glycolytic rate and lactate production is elevated, and glucose-derived carbon entry into the mitochondria is inhibited through upregulation of pyruvate dehydrogenase kinase, which inhibits pyruvate dehydrogenase to prevent acetyl-CoA production. This ensures cells increase their glycolytic rate to maximise production of ATP in hypoxic conditions.

1.4.2 The altered metabolic state of tumours

Whilst most differentiated cells only convert pyruvate to lactate in the absence of oxygen, rapidly proliferating cells will exhibit "glycolytic metabolism" and preferentially convert glucose-derived pyruvate to lactate, irrespective of oxygen availability. Indeed, cancer cells, which are inherently rapidly proliferative, often, if not always, display this metabolic phenotype in both normoxic and hypoxic conditions, exhibiting substantially increased glucose uptake and lactate secretion compared to normal differentiated cells. This glycolytic metabolic state, irrespective of oxygen availability, is known as "aerobic glycolysis".

The observation that cancer cells displayed an altered metabolic state was initially made nearly 100 years ago in 1924 by German physiologist Otto Warburg[226]. Warburg hypothesised that the reason why cancer cells converted pyruvate to lactate was due to defective mitochondria, proposing that mitochondrial dysfunction was an inciting factor in cancer. More recent work, and a better understanding of the metabolic state of tumours, has disproven Warburg's hypothesis by demonstrating that cancer cells do in fact exhibit a working TCA cycle[227,228] and even, in some cancers, intact and functional OXPHOS[229,230]. However, the aerobic glycolysis phenotype, elevated glycolytic rate and the increased conversion of glucose to lactate, is still seen as a key hallmark of human cancers and is important for the development of tumours[20].

As mentioned previously, aerobic glycolysis is far less efficient in terms of ATP production than classical aerobic respiration via OXPHOS. Therefore, it may seem paradoxical that rapidly proliferating cells and cancer cells would preferentially choose a less efficient form of energy production. It appears counter-intuitive, especially when one would consider rapid proliferation to have higher energy demands than quiescence or senescence. However, sustained aerobic glycolysis confers proliferative advantages to cells that go beyond energy production. In order to proliferate and generate new cells, certain molecules are required. Lipids are required for membrane production, nucleic acids for DNA replication, amino acids for protein production, these are the building blocks necessary for creating new cells and rapid proliferation brings a high demand for these "anabolic molecules". Aerobic glycolysis is often accompanied by shifts in the fluxes of other intracellular metabolic pathways, mediated by oncogenic activity or otherwise, that promote a significant increase in the production of essential anabolic molecules. As more glucose is taken up by cells and less pyruvate is taken into the mitochondria, the result is an accumulation of glycolytic intermediates available to be diverted into these other metabolic pathways for generation of anabolic molecules, allowing cells to meet the high anabolic demand and facilitate the continuation of proliferation (Figure 1.7).

Altered pathway dynamics in aerobic glycolysis

One example of this anabolic shift is the enhanced activity of the pentose phosphate pathway (PPP) in many cancers. The PPP is a metabolic pathway that branches out from the main glycolysis pathway and is fuelled by the glucose-6-phosphate produced in the first glycolytic reaction when glucose is phosphorylated by hexokinase. The PPP is one of the body's main sources of reducing agents, producing large amounts of NADPH. NADPH is necessary for generating reduced glutathione, a key ROS scavenger within the body, and can also be used in biosynthesis reactions including fatty acid synthesis. The pathway also generates ribose-5-phosphate and other pentose-phosphates essential for the production of nucleotides[231]. Accordingly, the pathway is often aberrantly activated in cancers. Common loss of function mutations in tumour suppressor p53 or gain of function mutations in K-RAS have both been shown to enhance PPP activity in cancers[232,233] and an increase in glucose uptake due to aerobic glycolysis results in greater glucose-6-phosphate availability to fuel the PPP in cancer.

Another example is the altered role that the TCA cycle plays in cancer. When not being used to fuel OXPHOS the TCA cycle essentially becomes a biosynthetic hub for anabolic molecule production, producing basic components necessary for the synthesis of lipids, proteins and nucleotides. The diversion of glucose-derived carbon away from entry into the mitochondria means that replenishment of TCA cycle intermediates must be driven by an alternative fuel. In most cancers that fuel is glutamine, and accordingly, many cancers exhibit glutamine addiction[234-236] and overexpress glutamine transporters, resulting in elevated glutamine uptake[235,237,238]. Glutamine can be converted to glutamate by the enzyme glutaminase (GLS) and subsequently to TCA cycle intermediate α-ketoglutarate (α-KG) by any of a number of aminotransferases. Glutamine-derived α-KG can directly fuel the cycle in the absence of glucose-derived acetyl-CoA. In agreement with this, ^{13}C-labelled glutamine-based flux analysis, tracking the incorporation of glutamine-derived carbon into metabolites, has confirmed the incorporation of glutamine-derived carbon into the TCA cycle in cancer[227,236]. The continued replenishment of TCA cycle intermediates, even in the absence of glucose-derived carbon entry, allows the cancer cells to continue to take advantage of the biosynthetic products of the TCA cycle. For example, oxaloacetate can be used to generate aspartate, which in turn is converted to arginosuccinate and subsequently to arginine in the urea cycle. Arginine is an amino acid on which rapidly proliferating cells, and many cancers, depend to produce nucleotides, proteins, polyamines and more[239]. Citrate is also an important TCA cycle intermediate for anabolic molecule production, as it can be shuttled to the cytoplasm where it is cleaved to acetyl-CoA to fuel fatty acid synthesis.

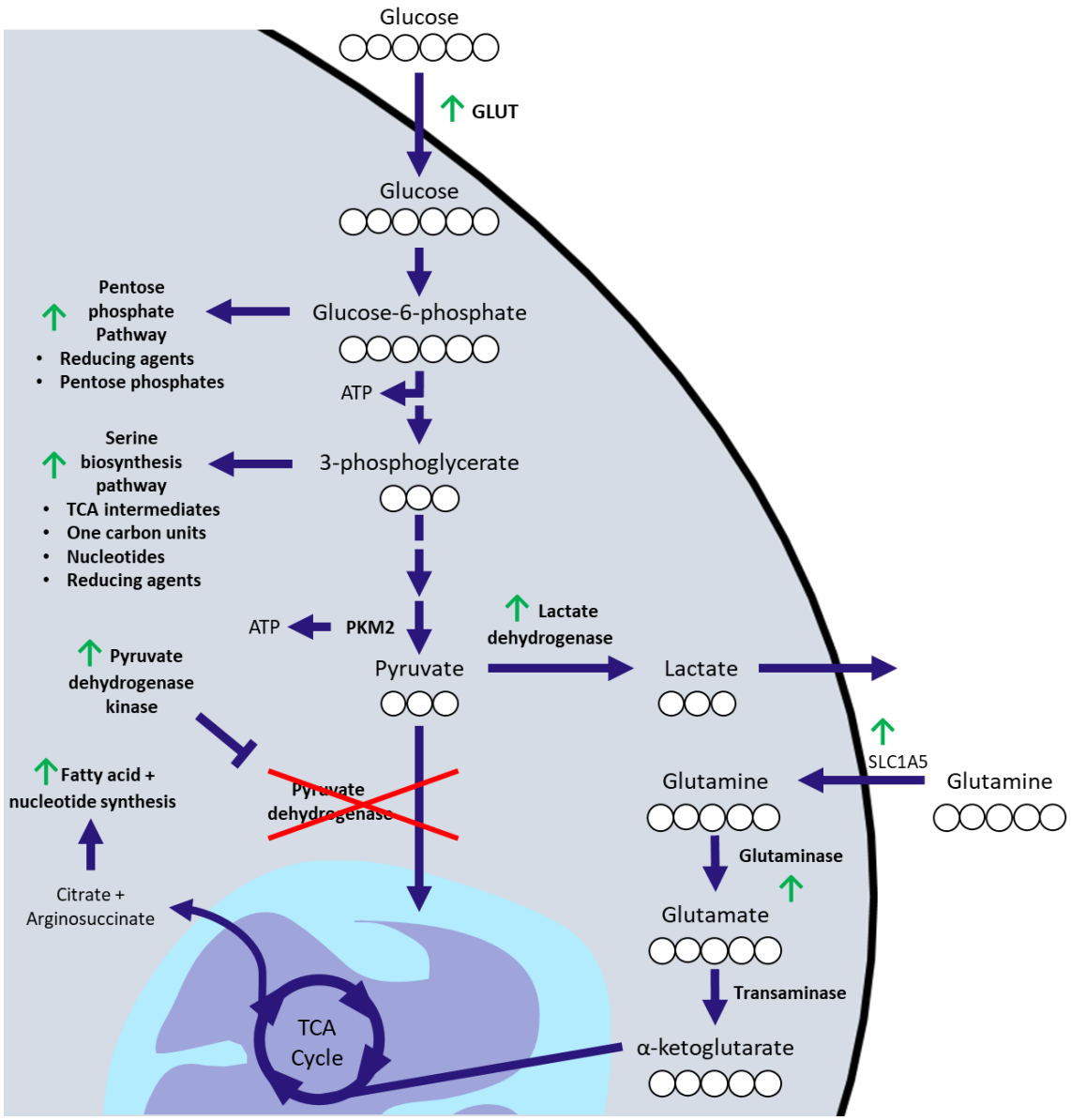

Figure 1.7 – Altered tumour metabolism. A schematic overview of some of the key changes that occur in the intracellular metabolic network of tumour cells. Similar to anaerobic respiration, tumour cells preferentially exhibit glycolytic metabolism and repress mitochondrial respiration. The benefit of this is that the increased glycolytic flux allows for increased diversion of glucose-derived carbon into biosynthetic pathways like the pentose phosphate pathway or the serine biosynthesis pathway, which allows cells to produce large amounts of anabolic molecules like nucleotides and fatty acids to support new cell growth and allows cells to maintain redox balance to avoid oxidative toxicities. Cancer cells also utilise glutamine-derived carbon to continue to replenish TCA cycle metabolites in the absence of glucose-derived carbon uptake, ensuring the biosynthetic reactions in the cycle can continue. Glucose and glutamine-derived carbon atoms are represented as white circles.

Citrate generation within a glutamine-fuelled TCA cycle is not always as straight forward as the TCA cycle progressing from α-KG to completion as normal, as lack of glucose-derived carbon mitochondrial uptake can mean a lack of acetyl-CoA that can be combined with oxaloacetate to regenerate citrate. Instead, generation of citrate from α-KG can require the cycle to run in reverse, in a process called reductive carboxylation. In this process, α-KG is oxidised to succinate,

generating a reducing agent in the form of NADH. The NADH is converted to NADPH by an enzyme called nicotinamide nucleotide transhydrogenase (NNT) and then fuels the conversion of α-KG to isocitrate by the action of the isocitrate dehydrogenase (IDH) isoform 2 (IDH2). Isocitrate can then be converted back to citrate for anabolic use[240,241].

One carbon metabolism represents another pathway that is enhanced in aerobically glycolytic conditions. This broad term describes the combined folate and methionine cycles which generate one carbon units within cells that are necessary for nucleotide synthesis and DNA methylation events. One-carbon metabolism also generates NADPH, which can be used for the reduction of glutathione to maintain intracellular redox balance. Enhanced folate and methionine cycle activity therefore allows cancer cells to generate more nucleotides to support their rapid proliferation and protect against ROS generation to prevent cell death (reviewed by Yang and Vousden, 2016[242] and Newman and Maddocks, 2017[243]). As with the PPP, aerobically glycolytic conditions support enhanced one carbon flux as accumulation of glycolytic intermediates allows diversion of more glucose-derived carbon into the one-carbon cycles via a branching biosynthesis pathway that generates the amino acids serine and glycine. The contribution of the "serine biosynthesis pathway" to one carbon metabolism and cancer will be discussed below (see 1.4.4.1 and 1.4.4.2).

1.4.3 Oncogene-driven metabolic alterations

With altered metabolism playing such an important role in supporting the development of tumours, it is understandable that many different oncogenes have been shown to induce metabolic changes or, from another perspective, that many proteins which induce metabolic changes have been classified as oncogenes, or effectors of oncogenic signalling. A selection of such key regulators is discussed below.

1.4.3.1 HIF1α

Activation of the aforementioned hypoxia-inducible factor 1 (HIF1) in hypoxic conditions is a key mechanism behind how cells switch between aerobic and anaerobic respiration and, unsurprisingly, many tumours feature dysregulated HIF1 activation. Overexpression of the alpha subunit is common in many cancers, in a manner often predictive of poor patient outcome[244-246]. HIF1α is stabilised in cancers in a variety of ways, facilitating its dimerisation with HIF1β and activation of HIF transcriptional activity. A common way involves the expansion of a tumour beyond the range of oxygen perfusion from the existing vasculature. This results in the centre of the tumour becoming hypoxic. The lack of oxygen results in stabilisation of HIF1α and

subsequent HIF1 transcriptional activity promotes the revascularisation of the tumour by inducing expression of VEGF, which simulates endothelial cell growth and vessel formation[247,248].

As well as stimulation of angiogenesis, HIF1 target genes also promote the adaptation of cancer cells to the hypoxic environment by promoting the aerobic glycolysis phenotype, thereby reducing the dependency of cells on oxygen to respire. As mentioned earlier, this action comes through the regulation of glycolysis at multiple nodes. Firstly, HIF1 increases the amount of fuel available for glycolysis, increasing glucose uptake by enhancing expression of glucose transporters. The best reported upregulation is of GLUT1[222], but HIF1 has been linked with upregulation of other GLUT's in cancer as well. For example, in glioma HIF1 expression correlates with GLUT3[249]. HIF1 also promotes aerobic glycolysis by diverting carbon flux away from the mitochondria and toward lactate production through upregulation of pyruvate dehydrogenase kinase and lactate dehydrogenase respectively[223,224], effectively preventing the mitochondrial use of glucose-derived carbon. Additionally, HIF1 has been reported to actively contribute to the increased rate of glycolysis by upregulating the expression of glycolytic enzymes hexokinase II[250], fructose-bisphosphate aldolase, phosphoglycerate kinase (PGK) and pyruvate kinase M (PKM)[251]. HIF1 also induces the expression of a kinase called 6-phosphofructo-2-kinase/fructose-2,6-bisphosphatase (PFKFB3)[252,253]. Glycolytic enzyme phosphofructokinase 1 (PFK1) is a key enzyme in the glycolytic process, catalysing the irreversible conversion of fructose-6-phosphate into fructose-1,6-bisphosphate whilst consuming 1 mole of ATP in the process. PFK1 is itself allosterically activated by fructose-2,6-bisphosphate, and PFKFB3 is a bifunctional enzyme which promotes both the synthesis and degradation of fructose-2,6-bisphosphate, thereby tightly regulating PFK1 activity. Therefore, induction of PFKFB3 and glycolytic enzymes like hexokinase II by HIF1 allows hypoxia-mediated regulation of glycolytic rate which, combined with regulation of glucose uptake and mitochondrial uptake of glucose-derived carbon, gives HIF1 extensive control over the aerobic glycolysis phenotype.

HIF1 activation in tumours is not solely dependent on hypoxic conditions however, as many tumours exhibit "pseudohypoxia", or the stabilisation of HIF1α even in the presence of oxygen. Pseudohypoxia can be induced by a number of factors, including loss of function mutations in the gene encoding VHL protein[254] or activation of the PI3K/AKT/mTOR pathway which leads to an mTOR-mediated increase in the rate of HIF1α synthesis, allowing stable expression of HIF1α above what is degraded[255]. Pseudohypoxia can therefore arise through loss of function mutations in PI3K inhibitor PTEN[256] or gain of function mutations in mTOR-associated receptor tyrosine kinases such as HER2[255], both of which are common in cancers. One other example of a mechanism by which pseudohypoxia can be induced is through the common mutation of

succinate dehydrogenase (SDH) in cancers. SDH catalyses the conversion of succinate to fumarate in the TCA cycle, and loss of function mutations or downregulation of expression of SDH is common in cancers[257,258]. This results in an accumulation of succinate which, in the context of HIF1 activation, inhibits PHDs in the cytosol to prevent the degradation of HIF1α in normoxic conditions[259].

1.4.3.2 Myc

The Myc family of transcription factors, specifically the c-Myc protein, have been extensively linked to cancer, and recent studies have demonstrated that aberrant activation of c-Myc transcriptional activity is heavily involved in the regulation of cellular metabolism in many human cancers.

Originally identified as a mammalian cell homolog of v-Myc, a retroviral oncogene, in Burkitt lymphoma patients (where it is the target of common chromosomal translocations)[260], c-Myc is transcriptionally activated by various signalling pathways that regulate cell growth and proliferation, and acts as a convergence point for pathways like Wnt/β-catenin and ERK/MAPK signalling in the downstream induction of genes that promote proliferation. Accordingly, Myc dysregulation is a common event in cancer development. In haematological malignancies, it is frequently subject to chromosomal translocations which lead to enhanced activation, and studies examining genetic amplification in human cancers have repeatedly identified it as one of the most frequently amplified genes across a variety of cancer types[261-263].

As understanding of c-Myc's role in cancer has developed, it has become evident that the transcription factor tightly regulates cellular metabolism in a myriad of ways. Firstly, the oncogene has been shown to promote enhanced glycolysis, as activation of Myc induces expression of glucose transporter GLUT1; glycolytic enzymes like hexokinase II, PFK1, glyceraldehyde-3-phosphate dehydrogenase (GAPDH), PGK and enolase[264,265]; and LDH[266]. This enhances glucose uptake, glycolysis and lactate production respectively to promote aerobic glycolysis.

As well as regulating glucose metabolism though, Myc appears to play an important role in glutamine metabolism in tumours. The importance of glutamine to tumours was discussed earlier (see 1.4.2), but briefly, the uptake of glutamine allows cancer cells to continue to fuel a truncated version of the TCA cycle in the absence of glucose-derived carbon uptake. Myc supports this by enhancing glutamine metabolism. The oncogene has been reported to transcriptionally upregulate the expression of glutamine transporters and glutaminase to

promote glutamine uptake and the conversion of glutamine to glutamate respectively. The oncogene has been shown to bind directly to the promoter regions of genes encoding glutamine transporters in order to upregulate them[235] and experiments performed using tamoxifen-inducible c-Myc-expressing MEFs have demonstrated that expression of the oncogene leads to an increase in *GLS* mRNA levels and glutaminase enzymatic activity[235]. Furthermore, liver tumours induced specifically by *MYC* in a mouse model have been shown to exhibit significantly increased *GLS* mRNA levels compared to normal tissues[265]. Interestingly, c-Myc has also been shown to regulate glutaminase expression indirectly in a Burkitt lymphoma cell line, through transcriptional repression of miRNA's miR-23a and miR-23b, both of which target the 3' UTR of *GLS* mRNA, demonstrating how the oncogene can regulate glutaminase expression through both direct and indirect means.

Notably, Myc appears to regulate the expression of multiple glutaminase isoforms. *GLS1* and *GLS2* encode tissue-specific glutaminase isoforms (*GLS1* encodes kidney-type isoforms and *GLS2* encodes liver-type[267], however alternate splice variants of each type have been detected in a range of tissues[268]). Fellow Myc family member N-Myc has been shown to directly bind to intron 1 of the *GLS2* gene and directly induce promoter activation[269]. A binding site for c-Myc in the same intron has been predicted[268], indicating that the *GLS2* promoter could also be activated by c-Myc as well as N-Myc.

Together, the studies mentioned above demonstrate how c-Myc promotes glutamine metabolism by enhancing uptake and processing of glutamine within cancer cells. However, increased glutamine metabolism may provide a potential therapeutic exploit for treatment of tumours. It has been demonstrated that the enhancement of glutamine metabolism by c-Myc triggers glutamine dependency within cancer cells. Indeed, cells which express c-Myc have been shown to undergo apoptosis when deprived of glutamine, in a manner that can be rescued by delivery of TCA intermediates[234,235]. Not only does this demonstrate the importance of cancer cells continuing to fuel the TCA cycle in the absence of glucose-derived carbon uptake, it highlights how blocking the entry of glutamine-derived carbon into the TCA cycle might represent an effective therapeutic strategy in cancers which exhibit aerobically glycolytic metabolism.

1.4.3.3 Pyruvate Kinase

Arguably one of the most central regulators of cancer metabolism is glycolytic enzyme pyruvate kinase, which catalyses the conversion of Phosphoenolpyruvate (PEP) to Pyruvate, producing one molecule of ATP in the process (Figure 1.4). Four distinct isoforms of the kinase exist from

two separate genes. Alternative splicing of the *PKLR* gene generates the PKL or PKR isoforms, expressed in the liver or the red blood cells respectively[270], whereas alternative *PKM* splicing gives rise to either the muscle type-1 (PKM1) isoform, which is predominantly expressed in most adult tissues, or the muscle type-2 (PKM2) isoform, which is usually only expressed during embryonic development[271,272].

Most cancers exclusively express the M2 isoform[271]. It can be transcriptionally upregulated by HIF1 activity and c-Myc has been shown to regulate *PKM* alternative splicing to inhibit the generation of the M1 isoform and thus promote M2 expression[273,274]. Aberrant activation of EGFR, which is commonly observed in tumours, has also been demonstrated to induce PKM2 expression in a range of breast cancer cell line, via the activation of canonical NF-κB signalling[275]. PKM2 also exists in discrete forms which dictate the activity of the kinase. In a tetrameric form PKM2 is highly active, whereas in a monomeric or a dimeric form it exhibits very low activity. The enzyme is known to be allosterically regulated by fructose-1,6-bisphosphate, succinylaminoimidazolecarboxamide ribose-5'-phosphate (SAICAR) and serine which dynamically controls the state of PKM2 activity in response to glucose availability and different requirements for glucose utilisation[276-278]. Intriguingly however, the predominant state is one of inactivity. This means that cancers preferentially express a variant of pyruvate kinase whose basal activity is lower than that of normal tissues. Whilst this seems to go against the idea of a rapid aerobic glycolysis phenotype, the restriction of glycolytic flow is in fact beneficial for proliferation.

The reduction in pyruvate kinase activity triggers a build-up of upstream glycolytic intermediates as a consequence of reduced conversion of PEP to pyruvate. This actively promotes the anabolic phenotype of tumour metabolism, as build-up of glycolytic intermediates significantly increases the pool of glucose-derived carbon that is available for use in the biosynthetic pathways that branch from glycolysis such as the PPP, hexosamine biosynthesis pathway, or the serine biosynthesis pathway, thereby enhancing the production of anabolic molecules in order to support the rapid proliferation of tumours. Indeed, the importance of PKM2 for continued proliferation of cancer cells and the maintenance of aerobic glycolysis has been demonstrated in many cancer models. Examples include human lung cancer cells and xenograft mouse models, where suppression of PKM2 reduced cell proliferation, and expression of PKM1 was shown to increase OXPHOS and suppress tumour formation in mice compared to PKM2 expression[271]; ovarian cancer cell lines, where PKM2 suppression inhibited proliferation and invasion, and induced apoptosis[279]; and colorectal cancer cells, where suppression of PKM2 reduced lactate production, proliferation and invasion, and increased apoptosis[280].

It is important to note however, that the preferentially inactive state of PKM2 does not completely abolish pyruvate production in cancer cells. Instead, the expression of PKM2 allows cells to respond to the changing demands of proliferation, letting them adapt to ever-changing nutrient availability on the fly. In aerobic glycolysis, glucose-derived carbon is either used to produce pyruvate (and subsequently lactate) facilitating ATP production, or it is used in biosynthesis. Expression of allosterically regulated PKM2 allows cells to recognise when one requirement is greater than the other. As mentioned earlier, serine is capable of activating PKM2 and does so when its intracellular concentration is high enough. This provides the cell with a mechanism by which it can respond to biosynthetic needs. If enough glucose-derived carbon is being diverted into biosynthesis, intracellular serine production will be elevated and serine concentration will rise. In turn, PKM2 will be activated allowing a balance between the use of glucose-derived carbon in biosynthesis and in glycolysis. In circumstances where glucose availability is low, the amount of glucose-derived carbon being diverted into biosynthesis will drop and accordingly, so will serine concentration. PKM2 will subsequently inactivate and the progression of glycolysis will be blocked. This will result in build-up of glycolytic intermediates and the maximal biosynthetic use of glucose until such a time when nutrient availability increases, or biosynthetic demands are met[277]. Essentially, dynamic regulation of PKM2 facilitates the carefully controlled balance between energy production and biosynthesis that arises from aerobic glycolysis.

Aside from this dynamic regulation, there is evidence to suggest that inactive PKM2 can enhance aerobic glycolysis in other ways as well. Firstly, it has been suggested that PKM2 inactivity allows the glycolytic pathway to escape inhibitory feedback loops that normally restrict the rate of glycolysis within cells. Key glycolytic enzymes like PFK1 are subject to end-product inhibition by ATP[281], which helps to slow the rate of glycolysis when ATP concentrations are high. Because conversion of PEP to pyruvate by pyruvate kinase produces ATP, the classical glycolysis pathway can contribute to cellular ATP concentration and, considering the speed at which glycolysis occurs in tumours, could be sufficient to induce such inhibition. PKM2's lack of activity thereby prevents glycolytic production of ATP, allowing the upstream reactions to continue unhindered. In accordance with this model, an alternative end to the glycolytic process has been proposed in the presence of inactive PKM2, whereby the phosphate group of PEP, which would usually be transferred to ADP to make ATP by pyruvate kinase, is instead transferred to a catalytic residue on phosphoglycerate mutase (PGAM) (Figure 1.8). This mechanism has been demonstrated in both lung cancer cells and prostate and breast carcinoma tissue from mice and represents a mechanism by which cancer cells expressing PKM2 can generate pyruvate in glycolysis

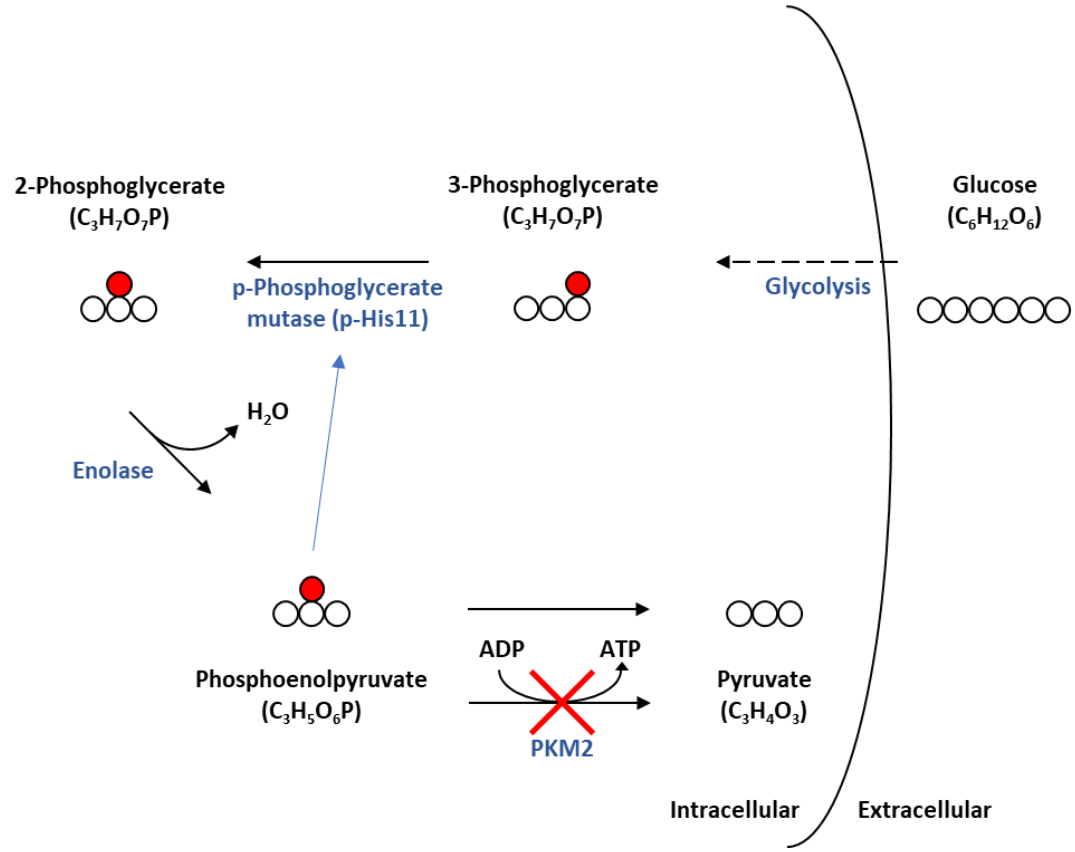

Figure 1.8 – The alternative glycolytic pathway. In order to avoid ATP-mediated end product inhibition of glycolytic flux, an alternative culmination of the glycolytic sequence has been proposed[260]. As PKM2 is an inactive version of pyruvate kinase, it cannot remove the phosphate group from PEP and therefore cannot produce ATP. Instead, the phosphate-group from PEP has been shown to be donated to the PGAM enzyme at physiological concentrations, phosphorylating PGAM histidine residue His11 when PKM2 is expressed. This allows the production of pyruvate without concurrent ATP synthesis and therefore, completion of glycolysis with no net ATP gain, which can allow cancer cells to maintain rapid glycolytic rates without end-product inhibition due to accumulation of ATP. White circles represent carbon atoms and red circles represent phosphate groups on glycolytic intermediates.

independently of ATP production, thereby uncoupling glycolysis from ATP-mediated end product inhibition and allowing glycolysis to progress unhindered[282].

Secondly, the inactive monomer or dimer form of PKM2 is capable of nuclear translocation, whereas the tetrameric form is not. Interestingly, nuclear PKM2 has been linked with both HIF1-mediated regulation of aerobic glycolysis and c-Myc-associated tumourigenesis. Dimeric PKM2 has been shown to interact with nuclear HIF1α and, in doing so, promote the binding of HIF1 to the promoters of HIF-responsive genes, including the glycolytic genes which it regulates[283,284]. Interestingly, treatment of NSCLC cell lines with activators of PKM2, which promote the formation of stable PKM2 tetramers, reduced cell proliferation under hypoxic conditions and triggered a reduction in lactate production whilst simultaneously increasing oxygen consumption rate, both of which are characteristic changes indicative of a metabolic switch from

aerobic glycolysis to OXPHOS. Furthermore, activation of PKM2 was shown to reduce tumour growth in an NSCLC xenograft mouse model[285]. This highlights two things. Firstly, the importance of PKM2 inactivity for the maintenance of aerobic glycolysis and promotion of tumour formation and secondly, that the HIF1-mediated response to hypoxia, and its ability to promote aerobic glycolysis, is dependent on inactive PKM2. This therefore further emphasises the benefits that can be provided to cells preferentially expressing an inactive form of the kinase.

Nuclear PKM2 has also been associated with phosphorylation of histone H3 at threonine 11 (H3T11). Phosphorylation of the histone at this site has been linked with cancer in the past. In prostate cancer, increased H3T11 phosphorylation correlated with a higher Gleason score and therefore, worse prognosis[286], and levels of H3T11 phosphorylation have been shown to correlate with malignancy grade and prognosis in gliomas[287]. Nuclear PKM2 has been reported to directly bind to and phosphorylate H3T11, possibly in combination with serine biosynthesis enzymes (see 1.4.4.1) and S-adenosylmethionine (SAM) synthetases as part of a serine-responsive SAM-containing metabolic enzyme (SESAME) complex, although this complex has, so far, only been characterised in yeast[287,288]. Phosphorylation of H3T11 induces the dissociation of histone deacetylase 3 (HDAC3) from the promoter regions of *CCND1* and *MYC* genes, encoding cyclin D1 and c-Myc respectively. Since histone deacetylases repress gene transcription, disassociation of deacetylases from gene promoters can conversely induce gene expression and accordingly, phosphorylation of H3T11 by PKM2 has been shown to induce cyclin D1 and c-Myc expression, thereby promoting tumour cell proliferation[287].

PKM2 has also been shown to promote tumourigenesis via other non-metabolic mechanisms, including protecting cells from oxidative stress and ROS-induced apoptosis through direct phosphorylation and stabilisation of Bcl2[289], and promoting the phosphorylation and nuclear translocation of STAT3 to promote EMT and migration in colorectal cancer[290]. PKM2 therefore plays an important role in tumourigenesis, both by promotion of the aerobic glycolysis metabolic phenotype and by other non-metabolism related mechanisms.

1.4.4 Metabolites as supporters of cancer development

Many different oncogenes and tumour suppressors have repeatedly been shown to be involved in the regulation of the aerobic glycolysis phenotype. In addition to those discussed above, oncogenic PI3K/AKT/mTOR signalling actively promotes aerobic glycolysis through the upregulation of glucose transporters[291] and stabilisation of HIF[292], and loss of tumour suppressor p53 is associated with increased expression of glucose transporters[293] and reduced expression of cytochrome c oxidase 2, which is necessary for OXPHOS complex formation[294]. What is also

becoming clearer as our understanding of cancer metabolism develops is how metabolite alterations that arise from aerobically glycolytic conditions can themselves support the development of cancer outside of anabolic benefits.

A good example of this is the previously mentioned succinate and its ability to stabilise HIF1α in normoxic conditions, resulting in pseudohypoxia and induction of all the pro-tumourigenic HIF1 target genes. Succinate levels are frequently elevated in cancer as a consequence of SDH inactivation or dysfunction but can also be elevated by altered tumour metabolism as a consequence of increased glutamine metabolism and feeding of the TCA cycle with glutamine-derived carbon[295]. Accumulated succinate can induce HIF1α stabilisation via inhibition of PHDs[259] and, in turn, promote HIF1-mediated angiogenesis, invasion and metastasis to support tumour development.

Another example comes from the role that metabolites can play in the regulation of the epigenome in cancer. Recent years have seen an increase in the understanding of the cross-talk that occurs between metabolism and the epigenetic regulation of gene expression. Indeed, PKM2's aforementioned ability to modulate gene expression via phosphorylation of H3T11 and subsequent modulation of histone acetylation stands as a prime example of that cross-talk. Importantly though, recent studies have shown that metabolites themselves can effect changes in gene expression through epigenetic regulation. Gain of function mutations in the gene encoding TCA cycle enzyme IDH are common in gliomas and leukaemia[296-298] and confer cells with the ability to convert α-KG into oncometabolite 2-hydroxyglutarate (2-HG)[299]. 2-HG competitively inhibits a class of enzymes called α-KG-dependent dioxygenases. This dioxygenase enzyme class includes enzymes that regulate the methylation status of the genome, such as histone demethylases and ten-eleven translocation (TET) hydroxylases, which convert 5-methylcytosine that is used for DNA methylation to 5-hydroxmethylcytosine[300]. The inhibition of these enzymes by 2-HG therefore facilitates increased DNA methylation. Indeed, the production of 2-HG in glioma and leukaemia has been shown to induce a state of global DNA hypermethylation, which establishes a gene expression programme that supports cancer development in a manner which is at least partially attributable to reductions in cellular differentiation. Reduced cellular differentiation therefore promotes a more proliferative stem-like state for the cancer cells[301,302].

Similarly, other TCA cycle metabolites, like fumarate and succinate, have also been shown to be competitive inhibitors of histone demethylases and TET hydroxylases and can promote histone and DNA hypermethylation in cancers when accumulated. Accordingly, siRNA-mediated

suppression of fumarate hydratase (FH) or SDH *in vivo*, modelling common loss of function mutations in cancers, has been shown to induce histone methylation and upregulate the expression of genes associated with the regulation of differentiation in a mouse model[303].

Modulation of cellular metabolism is therefore integral to tumour development for several reasons. Increasing the production of anabolic molecules allows cells to meet the high biosynthetic demands of rapidly proliferating cells, but modulation of intracellular metabolite levels can also support cancer development in ways independent of classic metabolic roles, by enhancing the transcriptional activity of an oncogene or by tuning the global gene expression programme to a state that encourages tumourigenesis. It is therefore easy to understand why cancers exhibit these drastically altered metabolic states. From a therapeutic standpoint, the benefits of this are clear. There are specific metabolic pathways that exhibit increased activity in many cancers that can facilitate all of these pro-tumourigenic activities combined and therefore represent possible critical nodes of altered metabolism in tumours which potentiate multiple growth benefits. Identification of these key pathways can therefore highlight several attractive therapeutic targets, the inhibition of which could significantly destabilise tumour metabolism and prevent disease progression. One of the best examples of such a pathway is the serine biosynthesis pathway.

1.4.4.1 Serine biosynthesis and catabolism

Responsible for the *de novo* production of non-essential amino acid serine inside the cell, the serine biosynthesis pathway (SBP) is comprised of three biochemical reactions that sequentially convert glycolytic intermediate 3-phosphogylcerate into serine (Figure 1.9). The first enzyme of the pathway, phosphoglycerate dehydrogenase (PHGDH) diverts glucose-derived carbon away from the main glycolytic process, oxidising 3-phosphoglycerate to produce phosphohydroxypyruvate and reducing agent NADH. The second reaction is a transamination reaction, catalysed by phosphoserine aminotransferase 1 (PSAT1), which transfers an amino group from glutamine-derived glutamate to phosphohydroxypyruvate, converting it to phosphoserine as well as converting glutamate to α-KG in the process. The third and final step involves hydrolysis of phosphoserine and removal of the phosphate group. This step is catalysed by phosphoserine phosphatase (PSPH) and leaves fully synthesised serine.

Serine can then be catabolised to produce glycine via the action of the serine hydroxymethyltransferase (SHMT) enzyme. SHMT catalyses the transfer of a methyl group from serine to tetrahydrofolate (THF). This produces methylene-tetrahydrofolate, which is used in one-carbon metabolism, and serine-derived glycine. Unlike the other reactions of the pathway,

this is a reversible reaction, meaning serine and glycine are readily interconvertible. Indeed, serine can also be synthesised within the cell from glycine. However, this yields little benefit for cells other than serine production, whereas the forward progression of serine biosynthesis from glucose and the subsequent production of glycine from serine support the rapid proliferation of cancer cells in various ways.

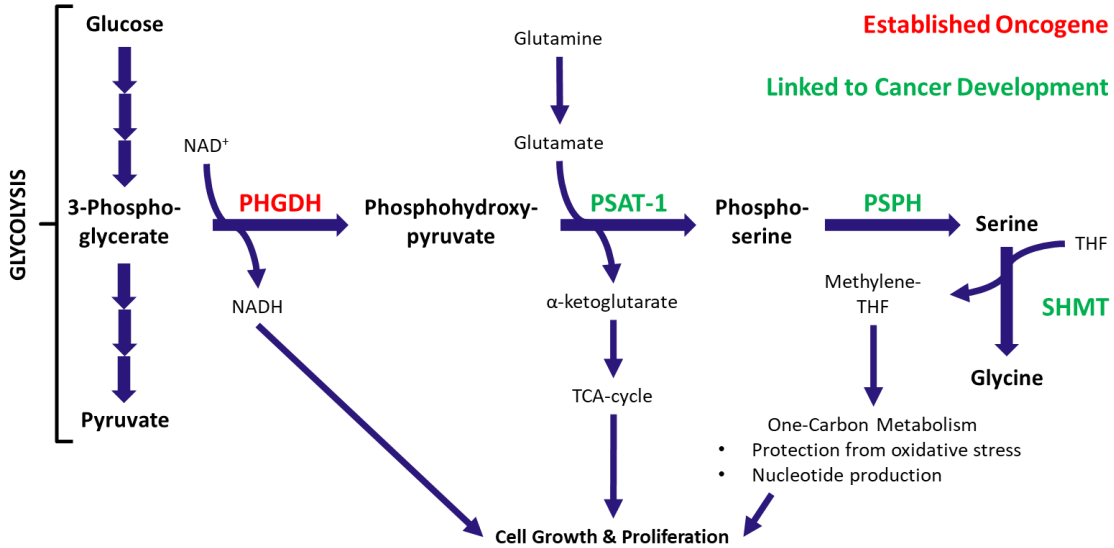

Figure 1.9 – The serine biosynthesis pathway and catabolism to glycine. Serine and glycine production within tumour cells represents a key metabolic pathway for support of rapid proliferation. Serine and glycine production benefits cells in terms of protein production, but the by-products of the pathway are crucial for supporting anabolic metabolism and maintaining redox balance. The second enzyme of the pathway is catalysed by PSAT1, an aminotransferase that can facilitate the conversion of glutamate to α-KG, thereby allowing the use of glutamine-derived carbon in the anabolic reactions of the TCA cycle. The catabolism of serine to glycine involves the donation of carbon atoms to the one-carbon pool, which supports rapidly proliferating cells through the production of nucleotides and reducing agents essential for maintaining cellular redox states at non-toxic levels. Indicative of the importance of the pathway for cancer, PHGDH is an established oncogene and all the other enzymes have been implicated in various cancers as well.

1.4.4.2 The serine biosynthesis pathway in cancer

In 2011, near simultaneous publications identified PHGDH as an oncogene, reporting copy number gain of the genetic locus wherein the *PHGDH* gene resides. This copy number gain resulted in amplification of the gene, overexpression of the PHGDH enzyme and increased serine production as a result in melanoma and breast cancer. It was demonstrated that suppression of PHGDH, or other serine biosynthesis enzymes PSAT1 and PSPH, in cell lines where *PHGDH* was amplified resulted in suppression of proliferation, and suppression of PHGDH in a breast cancer xenograft mouse model reduced tumour formation. Furthermore, ectopic expression of PHGDH in MCF-10A breast epithelial cells promoted lumen filling and loss of cellular polarity in a 3D

spheroid formation assay, indicating the enzyme promoted cancer like properties and enhanced anchorage-independent growth[304,305]. Increased PHGDH expression has also been reported in pancreatic tumours, where it has been shown to correlate with patient prognosis. Higher PHGDH expression correlated with greater tumour size, metastasis and worse staging in pancreatic cancer patients. Accordingly, suppression of PHGDH reduced proliferation, migration and invasion of pancreatic cancer cells[306]. PHGDH was also shown to correlate with poor prognosis in a subset of lung adenocarcinomas. In this subset, cells exhibited a higher glycolytic rate and elevated serine biosynthesis, and suppression of the enzyme induced cell death demonstrating dependency on the pathway for cell survival. These cells also displayed higher levels of reduced glutathione and PHGDH suppression induced DNA damage, demonstrating a pro-tumourigenic role for the enzyme in protection against oxidative stress and DNA damage[307]. In multiple myeloma PHGDH expression and increased SBP activity has also been shown to promote resistance to bortezomib due to an increased anti-oxidant capacity[308].

Other enzymes of the pathway have been associated with tumour development as well. PSAT1 has been implicated in colon cancer, where overexpression of the enzyme increased colon cancer cell proliferation and xenograft formation in a mouse model. PSAT1 was also demonstrated to induce chemoresistance in colon cancer cells, reducing apoptosis in response to therapy. Correspondingly, expression level of PSAT1 in patient tumours negatively correlated with tumour regression in response to therapy[309]. In NSCLC, PSAT1 has been implicated in regulation of the cell cycle. Overexpression of PSAT1 in NSCLC has been shown to promote cyclin D1 expression and cell cycle progression through a glycogen synthase kinase 3 β (GSK3β)/β-catenin signalling axis[310]. Furthermore, overexpression of the PSAT1 also correlates with poor prognosis in breast, nasopharyngeal and oesophageal squamous cell carcinoma[311-313]. The enzymes of the SBP have additionally been associated with later stage disease progression. In a breast cancer context, PHGDH and PSAT1 were overexpressed in a metastatic breast cancer cell line compared to a less metastatic variant, and suppression of PSAT1 reduced cell proliferation in the metastatic cell line, suggesting a potential role for the pathway in more aggressive metastatic tumours[314].

Although less well studied, recent work has begun to implicate PSPH in cancer as well. It has been reported that aberrant expression of the enzyme correlates with poor outcome in HCC patients[315] and, in colorectal cancer tissues, overexpressed PSPH has been shown to promote resistance to 5-fluorouracil therapy[316] and act a prognostic marker, correlating with invasion and metastasis in patient samples[317]. Although not a mainline serine biosynthesis enzyme, SHMT has also been associated with cancer development, including in ovarian cancer where the enzyme

has been reported to promote tumour growth and migration through the induction of pro-oncogenic inflammatory cytokines IL-6 and IL-8[318]; breast cancer, where the expression of the enzyme negatively correlated with patient prognosis[319]; and neuroblastoma, where the enzyme was reported to protect against redox imbalance in hypoxia and its expression again correlated with poor patient outcome[320].

The repeated overexpression of the SBP enzymes and enhanced SBP activity in so many cancer types indicates the importance of the pathway for tumour growth and development. A big reason for this importance is likely down to the fact that enhanced *de novo* production of serine and glycine from glucose-derived carbon yields several benefits for proliferating cells. Obviously, production of serine and glycine is beneficial to cells in terms of protein production. Moreover, increased serine levels can have unexpected benefits for cancers, as the amino acid has been shown to induce osteoclastogenesis to stimulate bone resorption, which can contribute to the metastasis of primary breast tumours to bone[314]. However, most serine and glycine used by cells is just taken up from the extracellular environment when it is readily available. Instead, the main benefit of increased SBP activity comes from increased flux through the biochemical reactions that both produce serine and catabolise it to glycine.

Serine and glutamine anaplerosis

As previously mentioned, many cancers exhibit glutamine addiction and feature elevated glutamine uptake and glutaminolysis. The benefit of this phenotype is that cancer cells can continue to fuel the TCA cycle in the absence of glucose-derived carbon usage, thereby facilitating the continuation of the biosynthetic reactions that occur within the cycle (see 1.4.2). The PSAT1-catalysed SBP reaction can support this phenotype, as the catabolism of glutamine requires its conversion to glutamate by glutaminase and the subsequent removal of an amino group from glutamate to generate α-KG ready for use in the TCA cycle. PSAT1 is an aminotransferase enzyme and can therefore transfer the amino group from glutamate to phosphohydroxypyruvate. In the process, this reaction progresses serine biosynthesis but also converts glutamate to α-KG, facilitating the usage of glutamine-derived carbon in the TCA cycle. Indeed, when PHGDH's oncogenic potential in breast cancer was discovered, it was noted that a substantial portion of α-KG in PHGDH amplified breast cancer cells was derived from serine biosynthesis. It was also recognised that reduced breast cancer cell proliferation resulting from PHGDH suppression was not necessarily attributable to reductions in serine production, since serine was readily available in the medium, but rather to the reduction in PSAT1-mediated α-KG production. Concurrently, suppression of both PHGDH and PSAT1 was shown to significantly

reduce incorporation of glutamine-derived carbon into the TCA cycle[305]. Enhanced activity of the SBP is therefore a major contributor to maintaining TCA cycle anaplerosis in aerobic glycolysis and is a key supporter of glutamine metabolism.

Serine and redox balance

The other major growth benefits of the SBP come from the catabolism of serine to glycine. The importance of one-carbon metabolism in aerobic glycolysis and cancer growth has been previously mentioned (see 1.4.2) and the breakdown of serine to glycine is a major contributor to the one carbon pool. Catalysed by SHMT, the one carbon unit that is removed from serine to generate glycine is donated to THF, generating methylene-THF. From this point on, serine-derived carbon has entered the folate cycle and can support cancer development through nucleotide production and the generation of critical reducing agent NADPH. The NADPH produced within the folate cycle following the conversion of methylene-THF to 10-formyl-THF, is used to produce reduced glutathione, which is an essential ROS scavenger and crucial for protecting against oxidative stress. Enhanced SBP flux can therefore benefit cancer cells by maintaining intracellular redox balance and protecting against ROS-mediated toxicity[320]. By extension, this also explains why cancers with enhanced SBP activity or serine biosynthesis enzyme expression have been shown to exhibit resistance to therapeutics which cause oxidative damage[307,308,316].

Serine and epigenetic regulation

The donation of one carbon units from serine to one carbon metabolism also contributes to oncogenic epigenetic regulation via the methionine cycle. After cycling around the folate cycle, the one carbon unit from serine is eventually transferred into the methionine cycle, where it is combined with homocysteine to regenerate methionine. Methionine is then converted to SAM with the addition of an adenosine nucleoside. SAM can then stimulate DNA methyltransferase reactions and inhibit the activity of DNA demethylases, thereby promoting DNA hypermethylation and the epigenetic regulation of gene expression[321]. This allows cells to maintain regulation of DNA methylation even in the event of methionine starvation.

Notably however, serine still contributes to the regulation of DNA methylation in a methionine rich environment. If serine-derived one carbon units are not used to generate methionine, they are still used, along with serine derived glycine, for purine synthesis and *de novo* ATP production, which is used in the conversion of methionine to SAM. This therefore demonstrates that serine catabolism to glycine is a crucial step for regulation of DNA methylation in all conditions[322].

It is important not to understate the importance of serine's catabolism to glycine in the maintenance of cancer cell proliferation. Further demonstrating that the pathway, not the product, is the crucial aspect of upregulated SBP activity in cancer, it has been shown that serine starvation, but not glycine starvation, has an inhibitory effect on the proliferation of breast cancer cells due to a reduction in nucleotide synthesis. This is important as it demonstrates that, although serine can be generated from glycine, the serine itself is redundant. Instead, it is the donation of serine-derived carbon to the one carbon cycle that is the essential factor for maintenance of cell growth[323].

The enzymes of the SBP are also involved in the epigenetic regulation of gene expression. As previously mentioned, it has been demonstrated that yeast homologs of the serine biosynthesis enzymes PHGDH and SHMT can form a multi-subunit protein complex with the yeast homolog of PKM2 (Pyk1) and the SAM synthetases. This protein complex is known as SESAME and facilitates Pyk1-mediated phosphorylation of histone H3T11[288], which is an important event for epigenetic regulation of pro-tumourigenic genes like *CCND1* (cyclin D1) and *MYC* (c-Myc) (see 1.4.3.3).

The SBP therefore contributes to cancer in a wide variety of ways and accordingly, various mechanisms that upregulate expression of PHGDH, PSAT1 and PSPH in cancer have been described. Oncogenic c-Myc signalling has been shown to induce serine biosynthesis enzyme expression in HCC[315] and in lung cancer, the SBP has been shown to be regulated by the transcription factor nuclear factor erythroid-2-related factor 2 (NRF2). NRF2 was reported to induce PHGDH, PSAT1 and SHMT expression via the transcription factor activating transcription factor 4 (ATF4), in order to support glutathione production and nucleotide synthesis[324]. The pathway has also been shown to be regulated by p73, which indirectly activates serine biosynthesis through regulation of glutaminase 2 to promote glutathione production[325]. Importantly however, there is still more to understand about the regulation of these enzymes in cancer, and even more to uncover about how, if at all, these enzymes are regulated at a post-translational level. PHGDH protein level has been shown to be subject to ubiquitin-mediated proteasomal degradation and deubiquitinating enzyme Josephin Domain-containing 2 (JOSD2) has been reported to regulate PHGDH's protein stability in this regard[307]. PHGDH activity has also been linked to phosphorylation of two threonine residues, Thr57 and Thr78, by protein kinase C ζ (PKCζ)[326]. Other than this, nothing is known about the post-translational regulation of the serine biosynthesis enzymes, which needs to be addressed in order to effectively target this hugely important metabolic pathway.

1.5 Project aims

Whilst IKKε has been identified as an oncogene in about 30% of human breast cancer cases, its characterised mechanism of oncogenesis in breast tissue is via aberrant activation of NF-κB signalling. The impracticalities of therapeutic inhibition of the NF-κB pathway mean there is a desperate need to develop our understanding of how IKKε overexpression in breast tissue can lead to cancer development so that a substantial subset of breast cancer patients might be more effectively treated. Some progress has been made into identifying NF-κB-independent mechanisms of IKKε activity in tumour formation but generally, little is known about how else the kinase can contribute to disease progression in the breast.

Recent studies have identified a role for IKKε in the rewiring of cellular metabolism. The kinase has been shown to promote a metabolic phenotype resembling aerobic glycolysis in dendritic cells during their activation in the immune response. More recently, IKKε was demonstrated to induce aerobic glycolysis in cancer in pancreatic ductal adenocarcinoma (PDAC). As changes in intracellular metabolism in cancer cells are increasingly recognised as critical events in tumour formation, the indication that IKKε has a part to play in metabolic rewiring opens up new areas of exploration for investigating the full scope of the kinases oncogenic potential. The entry point for this project was in data described at the beginning of chapter 3, which details the finding that IKKε promotes an aerobic glycolysis like phenotype in a breast cancer cell line setting. This project subsequently set out to explore the mechanism of IKKε-mediated metabolic regulation in breast cancer, with the hope of identifying new therapeutic targets that might be exploitable for the treatment of IKKε-driven tumours.

The specific aims of this project were therefore;

1) To outline the mechanism by which IKKε regulates cellular metabolism in breast cancer

2) To identify novel IKKε phosphotargets involved in IKKε-driven metabolic rewiring

3) To determine what contribution, if any, established IKKε signalling pathways make to the altered metabolic phenotype induced by the kinase

Chapter 2

Materials and Methods

2.1 Cell culture

2.1.1 Culture medium

Cells were routinely cultured in either Dulbecco's modified Eagle's medium (DMEM) - high glucose, containing 4.5 g/L glucose, 0.584 g/L L-glutamine and 0.11 g/L sodium pyruvate (Sigma Aldrich - #D6429), or Roswell Park Memorial Institute 1640 medium (RPMI-1640), containing 2.0 g/L glucose and 0.3 g/L L-glutamine (Sigma Aldrich - #R8758).

For siRNA oligo transfections, Opti-MEM® reduced serum medium, containing L-glutamine, Phenol Red and 2.4 g/L sodium bicarbonate, was used (Gibco, Life Technologies – #31985062).

Serine-free medium experiments were performed using custom DMEM or RPMI-1640 medium which were both formulated without glucose, glutamate, glutamine, glycine, serine and sodium pyruvate by the Custom Media Production units at either the Institute of Cancer Research, London, UK or the Francis Crick Institute, London, UK. When used, custom DMEM was supplemented with 4.5 g/L glucose and custom RPMI was supplemented with 2.0 g/L glucose to match their respective concentrations in commercial DMEM #D6429 and RPMI-1640 #R8758. In addition to glucose, custom DMEM was supplemented with 0.11 g/L sodium pyruvate, custom RPMI was supplemented with 0.02 g/L glutamate and both types of media were supplemented with 0.3 g/L glutamine and 0.01 g/L glycine. Serine was also supplemented at a concentration of 0.03 g/L in control conditions.

All medium was supplemented with 10% (v/v) foetal bovine serum (FBS) (Gibco, Life Technologies - #10500) (Serine-free medium was supplemented with Dialyzed FBS (Gibco, Life Technologies - #26400044)), 1% (v/v) penicillin-streptomycin (Sigma Aldrich - #P4333) and 0.2% Normocin™ (InvivoGen - #ant-nr-1) prior to use, and stored at 4°C.

2.1.2 Cell lines

All Flp-In 293 cells were maintained in DMEM – high glucose medium. Parental Flp-In 293 cells were a gift from Professor Pascal Meier and Tencho Tenev (Institute of Cancer Research, London, UK). Generation of inducible Flp-In 293 cells is described in 2.2. Stable inducible Flp-In 293 cell lines were selected for using hygromycin (Merck Millipore - #400051-1MU) at a concentration of 300 µg/ml.

The panel of breast cancer cell lines was cultured in appropriate medium as described in Table 2.1 and were kindly provided by William Hahn (Dana-Farber Cancer Institute, Boston, US), Professor David Sabatini (Whitehead Institute for Biomedical Research, Massachusetts, US), or Professor Peter Schmid and Dr Alice Shia (Barts Cancer Institute, London, UK) as indicated.

Table 2.1 – Cell lines used within this project.

Cell Line	Cell Type	Culture Medium	Original Source
Flp-In 293 (Parental or Dox-inducible)	Embryonic kidney	DMEM + 10% FBS + P/S	Prof. Pascal Meier (ICR)
HA1E-M	Embryonic kidney	DMEM + 10% FBS + P/S	Prof. William Hahn (Dana-Farber)
HA1E-M F-IKKε	Embryonic Kidney	DMEM + 10% FBS + P/S	Prof. William Hahn (Dana-Farber)
Cal120	Breast cancer (Basal)	DMEM + 10% FBS + P/S	Prof. Peter Schmid (BCI)
HCC1143	Breast Cancer (Basal)	RPMI-1640 + 10% FBS + P/S	Prof. Peter Schmid (BCI)
MCF7	Breast Cancer (Luminal-A)	RPMI-1640 + 10% FBS	Prof. Peter Schmid (BCI)
MDA-MB-231	Breast Cancer (Basal)	RPMI-1640 + 10% FBS	Prof. David Sabatini (Whitehead)
MDA-MB-453 (Parental or Dox-inducible PSAT1)	Breast Cancer (Basal)	RPMI-1640 + 10% FBS	Prof. Peter Schmid (BCI)
MDA-MB-468	Breast Cancer (Basal)	RPMI-1640 + 10% FBS	Prof. David Sabatini (Whitehead)
SUM44	Breast Cancer (Luminal-A)	DMEM + 10% FBS + 1 mM E2	Prof. Peter Schmid (BCI)
T47D	Breast Cancer (Luminal-A)	RPMI-1640 + 10% FBS	Prof. Peter Schmid (BCI)
ZR-75-1	Breast Cancer (Luminal-A)	RPMI-1640 + 10% FBS	Prof. Peter Schmid (BCI)

2.1.3 Maintenance of 2D cell cultures

Cells were cultured in a 2D monolayer in 75 cm^2 flasks (Corning) and cultures were maintained through incubation at a temperature of 37°C with atmospheric conditions of 5% CO_2 in a Binder incubator.

Cells were passaged upon reaching 80-90% confluency. Medium was removed from the flask using an aspirator and the cell monolayer was washed with 10 ml of sterile autoclaved phosphate buffered saline (PBS). PBS was then aspirated and 5 ml of 0.05% v/v Trypsin ethylenediaminetetraacetic acid (EDTA) (Sigma Aldrich - #T4299) was added to cells to detach the monolayer from the flask surface. For Flp-In 293 cells Trypsin EDTA was aspirated immediately to avoid cell loss. For breast cancer cell lines, flasks were incubated with Trypsin for up to 5 minutes at 37°C, 5% CO_2 in the culture incubator. Flasks were agitated to fully detach all adherent cells, after which fresh medium was added to resuspend cells and inactivate residual trypsin. The cell suspension was mixed thoroughly by pipetting to ensure complete cell separation and generation of as true a single cell suspension as possible. Medium was added to a volume necessary for the required passaging ratio, and 1 ml of the cell suspension was added to a new flask, i.e. if cells were passaged at a 1:10 ratio, the cells were suspended in a volume of 10 ml and 1 ml was taken out. Medium in the new flask was topped up to a volume of 15 ml and mixed gently to ensure even distribution of cells across the flask surface. The new cell flask was then labelled appropriately with the name of the cell line, the date of passage and the passage number, then returned to the incubator.

2.1.4 Freezing and thawing

An 80-90% confluent 75 cm^2 flask of cells was processed as in 2.1.3 till trypsin detachment. Following detachment of adherent cells from the flask surface, cells were resuspended in 4 ml FBS. 0.9 ml of the resulting cell suspension was then aliquoted into 2 ml capacity cryovials (Corning) containing 0.1 ml dimethyl sulfoxide (DMSO – Sigma Aldrich - #D5879-500ML), achieving a final concentration of 10% v/v DMSO in FBS. Cryovials were then frozen at -80°C and later transferred to liquid nitrogen for storage at -185°C long term.

When thawed, cells were removed from liquid nitrogen and transported on dry ice to maintain freezing during transportation. Cells were thawed in a 37°C water bath and cell suspension was subsequently added to 24 ml of the appropriate culture medium in a 75 cm^2 flask to substantially dilute the DMSO in the cell suspension. The flask was placed in a 37°C incubator to allow cells to

attach to the flask surface and medium was changed the following day, further diluting the DMSO to negligible amounts and removing cells that had died during the freezing and thawing cycle. Following thawing, cells were passaged at least once prior to experimental use, to allow re-acclimatisation.

2.1.5 Cell plating

An 80-90% confluent 75 cm^2 flask of cells were processed as in 2.13 till cell resuspension in culture medium and generation of single cell suspension. 10 µl of cell suspension was mixed thoroughly with 10 µl of Trypan Blue Solution, 0.4% (Gibco, Life Technologies - #15250-061) for exclusion of dead cells in counting. 10 µl of cell/Trypan Blue mixture was added to a counting slide (Bio-Rad - #1450015) so that cell numbers in the suspension could be counted using a TC20® Automated Cell Counter (Bio-Rad - #1450102). Cells/ml counts were taken in duplicate and an average was calculated to more accurately represent cell numbers within a suspension. The volume of cell suspension required for the desired number of cells was calculated and added to a 10 cm^2 dish (Corning), or a 6-well or 96-well plate (Corning). For experiments involving either no treatment of cells or basic drug treatments, cells were plated at densities described in Table 2.2. For all IncuCyte experiments, or for experiments that required siRNA-mediated suppression of mRNA prior to drug treatments, cells were plated at densities described in Table 2.3.

Table 2.2 – Cell plating density for drug treatment of cell lines in 6-well plates or 10 cm dishes.

	Plating density (Cells per well (CPW))	
	6-well	**10 cm**
Flp-In 293 (Various)	400,000	5,000,000
ZR-75-1	600,000	-
T47D	500,000	-
MDA-MB-453	600,000	-
MDA-MB-468	400,000	-
MDA-MB-231	400,000	-
MCF7	400,000	-
Cal120	500,000	-
HCC1143	600,000	-
SUM44	600,000	-

Table 2.3 – Cell plating density for IncuCyte experiments, or experiments involving siRNA transfection of cell lines in 6-well or 96-well plates or 10 cm dishes.

	Plating density (Cells per well (CPW))		
Cell Line	**6-well**	**96-well**	**10 cm**
Flp-In 293 (Various)	150,000	5,000	2,000,000
ZR-75-1	300,000	10,000	-
T47D	200,000	7,500	-
MDA-MB-453	300,000	10,000	-
MDA-MB-468	200,000	4,000	-
MDA-MB-231	150,000	4,000	-
MCF7	125,000	3,000	-
Cal120	150,000	5,000	-
HCC1143	125,000	3,000	-
SUM44	300,000	10,000	-

2.1.6 Drug treatments

Doxycycline was used to induce expression of HA-tagged GFP, IKKε wild-type (wt) and kinase dead mutant (KD-m) and PSAT1 wt and S>A or S>E mutant variants in corresponding Flp-In 293 cell lines and PSAT1 wt and S>A or S>E mutants in MDA-MB-453 PSAT1 cell lines. Doxycycline was kindly provided by Susana Godinho (originally sourced from Sigma Aldrich - #D9891).

α-IFNAR blocking antibody (Merck Millipore - #MAB1155) was used to inhibit the activation of the IFNAR upon induction of HA-IKKε in Flp-In 293 cells, thereby preventing activation of the JAK/STAT signalling cascade and IKKε-mediated IFNβ signalling.

Dichloroacetate (DCA) (Sigma Aldrich - #347795) is a pyruvate dehydrogenase kinase (PDK) inhibitor and was used to activate the pyruvate dehydrogenase complex in the presence of HA-IKKε induction in Flp-In 293 cells.

All compounds were stored at -20°C and diluted in water, so no vehicle control was required in non-treated cells when used.

2.1.7 siRNA transfection

Cells were transfected with siRNA oligos detailed in Table 2.4 to suppress the expression of specific proteins. AllStars Negative Control siRNA (Qiagen - #SI03650318) was used for non-targeting transfections to control for the transfection process.

For western blotting and quantitative real-time PCR (qRT-PCR) experiments involving siRNA suppression of protein expression, Flp-In 293 cells or breast cancer cell lines were plated in a 6-well plate. For IncuCyte experiments involving siRNA transfection, cells were plated in a 96-well plate. For suppression of endogenous PSAT1 in HA-pulldown assays, cells were plated in a 10 cm dish. Plating densities for siRNA experiments are indicated in Table 2.4. After incubation of plated cells for 24 hours at 37°C to allow cells to attach to the growth surface, siRNA was transfected in a total volume of 700 µl in a 6-well plate, 100 µl in a 96-well plate and 4 ml in a 10 cm dish.

For one well of a 6-well, 1.75 µl of 20 µM control non-targeting siRNA oligo, or 0.875 µl of each oligo in a pool of 4 10 µM targeting oligos (or 3.5 µl for single oligo transfection) was added to 200 µl Opti-MEM® reduced serum transfection medium in an autoclaved 1.5 ml microcentrifuge tube. This mixture was briefly vortexed, following which 2 µl DharmaFECT 4 transfection reagent (Dharmacon - #T200402) was added and the mixture was vortexed once again. The transfection mixture was incubated at room temperature for 10 minutes, after which 200 µl of the mixture was added dropwise to 500 µl of medium in each well of a 6-well plate, giving a final siRNA concentration of 50 nM in 700 µl. 16 hours later, the transfection medium was aspirated and replaced with 2 ml of fresh DMEM or RPMI-1640 as required. Cells were incubated for 72 hours prior to harvesting. In the case of siRNA-mediated suppression of endogenous PSAT1, a pool of 3 10 µM siRNA oligos targeting the non-coding sequence of the *PSAT1* mRNA was used, with 1.17 µl of each oligo transfected per well.

For one well of a 96-well plate, 0.25 µl of 20 µM control non-targeting siRNA oligo, or 0.125 µl of each oligo in a pool of 4 10 µM targeting oligos was added to 20 µl Opti-MEM® reduced serum transfection medium in an autoclaved 1.5 ml microcentrifuge tube and the mixture was subsequently vortexed. 0.2 µl DharmaFECT 4 transfection reagent was then added followed by a second brief vortex and incubation of the mixture at room temperature for 10 minutes. 80 µl of culture medium was then added to give a total volume of 100 µl and a final siRNA concentration of 50 nM. Existing culture medium in the plate well was then aspirated and replaced with the transfection mixture. The plate was incubated at 37°C for 16 hours, following which the transfection medium was replaced with 200 µl fresh culture medium leaving the plate ready for growth analysis on the IncuCyte. For IncuCyte experiments involving the suppression of endogenous PSAT1, a pool of 3 10 µM non-coding sequence targeting siRNA oligos was used and 0.17 µl of each oligo was transfected per well.

For a 10 cm dish, 10.1 µl of 20 µM control non-targeting siRNA oligo, or 6.8 µl of each oligo in a pool of 3 10 µM *PSAT1*-targeting oligos was added to 1.16 ml Opti-MEM® reduced serum transfection medium in a 15 ml Falcon® tube (corning). The mixture was vortexed and 11.6 µl DharmaFECT 4 transfection reagent was then added. Following further vortexing and 10 minutes incubation, the siRNA mixture was added dropwise to 2.9 ml of medium in the dish. From here, experiments progressed as in a 6-well plate.

Table 2.4 – Qiagen FlexiTube GeneSolution siRNA oligos used for protein knockdown. *PSAT1 oligo Hs_PSAT1_10 was not used in transfections specifically targeting the non-coding sequence of *PSAT1* mRNA. †ATF4 oligo Hs_ATF4_5 was the single oligo used for *ATF4* knockdown prior to use of an oligo pool.

Target	Oligo product name	Catalogue Number	Oligo target sequence
IKBKE (IKKε)	Hs_IKBKE_6	SI02622319	acggcggaacaaggagatcat
	Hs_IKBKE_7	SI02622326	ccgcatcatcgaacggctaaa
	Hs_IKBKE_8	SI02655317	aagaagcatccagcagattca
	Hs_IKBKE_9	SI02655324	caagatgaacttcatctacaa
PSAT1	Hs_PSAT1_10*	SI03019709	aaggaattattagactacaaa
	Hs_PSAT1_12	SI03222142	gtgcattatagcattccatta
	Hs_PSAT1_14	SI04265625	ccaggcgaagggcaaactgta
	Hs_PSAT1_15	SI04272212	tagatcgatctttatgctgtt
ATF4	Hs_ATF4_5†	SI03019345	cagcgttgctgtaaccgacaa
	Hs_ATF4_8	SI03218404	gaggatagtcaggagcgtcaa
	Hs_ATF4_9	SI04236337	aagcctaggtctcttagatga
	Hs_ATF4_10	SI04261614	aggagataggaagccagacta
IRF3	Hs_IRF3_4	SI02626526	cagcctcgagtttgagagcta
RELA (p65)	Hs_RELA_5	SI00301672	aagatcaatggctacacagga

2.1.8 Cell harvesting

Following the culmination of cell treatment, medium was aspirated from the cells and cells were washed with ice cold PBS. PBS was subsequently aspirated, leaving empty wells. Plates or dishes were then sealed using parafilm and stored at -80°C till sample processing.

2.2 Generation of PSAT1 mutant cell lines

To investigate phosphorylation of the enzyme, PSAT1 serine residue Ser331 was mutated using point mutagenesis. To mimic unphosphorylated serine, Ser331 was mutated to an alanine residue by changing 1 nucleotide in the DNA sequence. To mimic phosphorylated serine, Ser331 was mutated to a glutamic acid residue by changing 2 nucleotides in the DNA sequence.

2.2.1 Point mutagenesis primers

Primers were designed to modify the *PSAT1* DNA sequence at nucleotides relevant to the Ser331 residue within the protein sequence. All primers were manufactured by Sigma Aldrich. Modified nucleotides are indicated in red.

PSAT1 S>A mutagenesis primers:

Forward – 5'-gaactcaatatgttg**g**ccttgaaagggc-3'

Reverse – 5'-gccctttcaagg**c**caacatattgag-3'

PSAT1 S>E mutagenesis primers:

Forward – 5'-gaactcaatatgttg**ga**cttgaaagggc-3'

Reverse – 5'-gccctttcaag**tc**caacatattgag-3'

2.2.2 *PSAT1* point mutagenesis

2.2.2.1 PCR Mutagenesis

PSAT1 cDNA Open Reading Frame (ORF) Clone in the *pGEM-T* vector (Sino Biological - #HG14187-G) was used for point mutagenesis PCR.

Mutagenesis PCR was performed using Phusion® High-Fidelity DNA Polymerase (New England Biolabs - #M0530). The PCR was performed in a 50 µl volume in an autoclaved Fisherbrand™ 0.2 ml Flat-Cap PCR tube (Fisher Scientific - #12174102) as per the manufacturer's recommended instructions with 1 ng of template *pGEM-T PSAT1* cDNA (Table 2.5). Reaction mixtures were

briefly vortexed, centrifuged and placed on a C1000 Touch™ Thermocycler (Bio-Rad). Mutagenesis PCR was performed with the protocol described in Table 2.6.

Table 2.5 – Composition of 50 µl Phusion® High-Fidelity DNA Polymerase PCR reaction for *PSAT1* mutagenesis.

Component	In 50 µl
5x Phusion® HF Buffer	10 µl
10 mM dNTP mix	1 µl
10 µM Forward Primer	2.5 µl
10 µM Reverse Primer	2.5 µl
DMSO	1.5 µl
Phusion® High-Fidelity DNA Polymerase	0.5 µl
Template *PSAT1* cDNA	1 ng
Nuclease-free water (Invitrogen - #AM9915G)	Volume to 50 µl total

Table 2.6 – Thermocycler program for *PSAT1* mutagenesis PCR.

Temperature	Time	
98°C	30 seconds	
98°C	10 seconds	17 x
51°C	30 seconds	
72°C	3 minutes	
72°C	10 minutes	
4°C	∞	

2.2.2.2 DpnI digestion

DpnI restriction enzyme (New England Biolabs - #R0176S) was used to digest the wild-type *pGEM-T PSAT1* plasmid in the S>A and S>E PCR mutagenesis products to ensure the purity of the mutated *pGEM-T PSAT1 S>A* or *pGEM-T PSAT1 S>E* plasmids. DpnI cleaves methylated sites, which are present on the wild-type plasmid but are not maintained during PCR amplification. DpnI digestion therefore only cleaves the template plasmid to leave a pure PCR product.

A 60 µl reaction mixture for DpnI digestion was prepared in an autoclaved Fisherbrand™ 0.2 ml Flat-Cap PCR tube as described in Table 2.7 using the PCR product from 2.2.2.1, then incubated in a thermocycler at 37°C for 1 hour to allow DpnI-dependent cleavage and at 80°C for 20 minutes to inactivate the enzyme.

Table 2.7 – Composition of 60 µl DpnI digestion reaction for digestion of template *pGEM-T PSAT1* plasmid.

Component	In 60 µl
PCR product	50 µl
DpnI restriction enzyme	2 µl
10x CutSmart® Buffer (Included with DpnI)	6 µl
Nuclease-free water	2 µl

2.2.2.3 Bacterial transformation

The *pGEM-T* vector contains an ampicillin resistance gene, which allows cells expressing the vector to survive in the presence of the antibiotic. Therefore, in order to validate successful PCR of entire *pGEM-T PSAT1* plasmid and eventually confirm mutagenesis, the PCR product was used to transform Alpha-Select Gold Efficiency competent cells (Bioline - #BIO-85027). Transformed cells expressing a full plasmid were then selected by their ability to grow on LB-agar plates containing 100 µg/ml ampicillin.

Alpha-Select Gold Efficiency competent cells were thawed on ice. 5 µl of mutagenesis PCR product was mixed with 45 µl of cells in an autoclaved 1.5 ml microcentrifuge tube. The DNA/cell mixture was incubated on ice for 30 minutes, then heat-shocked via incubation at 42°C in a water bath for 1 minute. Following heat-shock the cells were returned to ice for 5 minutes, after which 950 µl of autoclaved LB broth was added to the cells. The cells were thoroughly mixed by pipetting, then incubated at 37°C for 1 hour in a shaking incubator at 200 RPM. Cells were subsequently pipetted onto the surface of a pre-warmed LB-agar plate containing 100 µg/ml ampicillin and spread across the agar surface with a cell spreader. Plates were then incubated at 37°C for 24 hours. Cells containing an ampicillin resistance gene, due to successful PCR and transformation with the *pGEM-T PSAT1* plasmid, formed colonies in the presence of ampicillin, whereas untransformed cells failed to grow.

2.2.2.4 Mini-prep

A mini-prep was performed to amplify *pGEM-T PSAT1 S>A* and *pGEM-T PSAT1 S>E* plasmid DNA from the transformed bacterial cells. Several colonies from the transformation plates were picked and separate colonies were each transferred to 3 ml of LB-broth containing 100 µg/ml ampicillin in a 30 ml universal tube. The bacteria were cultured overnight at 37°C in a shaking incubator at 200 RPM, allowing amplification of transformed cells and the contained plasmid.

DNA from the cultured bacterial cells was then extracted using the QIAprep Spin Miniprep Kit (Qiagen - #27104).

Bacterial cells were pelleted by centrifugation at 7000 g for 3 minutes, resuspended in 250 µl of Buffer P1 and transferred to an autoclaved 1.5 ml microcentrifuge tube. Cells were then lysed with the addition of 250 µl Buffer P2, followed by thorough mixing through inversion of the tube until the solution turned blue due to the presence of pH indicator LyseBlue reagent in Buffer P1. Cells were left lysing at room temperature for up to 5 minutes. Following lysis, 350 µl of Buffer N3 was added to neutralise the pH, and the LyseBlue-containing mixture turned colourless accordingly. Cells were then centrifuged at 18,000 g for 10 minutes and the supernatant was transferred to a QIAprep spin column. Centrifugation of the spin column, at 18,000 g for 1 minute allowed DNA to bind to the membrane within the column. Flow through from the centrifugation was collected in a 2 ml collection tube and subsequently discarded. 500 µl of Buffer PB was added to the spin column to wash the membrane. The column was again centrifuged at 18,000 g for 1 minute, after which the flow through was discarded. 750 µl of Buffer PE was then added to further wash the spin column membrane. The spin column was centrifuged at 18,000 g for 1 minute and flow through was again discarded. The spin column was immediately centrifuged again at 18,000 g for 1 minute, allowing the membrane to dry and facilitating removal of residual wash buffer. The QIAprep spin column was then transferred to an autoclaved 1.5 ml microcentrifuge tube and 50 µl of Buffer EB was added directly to the column membrane. The column was the incubated at room temperature for 1 minute. Finally, the spin column was centrifuged a final time at 18,000 g for 1 minute, eluting the DNA from the column membrane and collecting it in the 1.5 ml microcentrifuge tube.

2.2.2.5 Quantification of DNA

Following miniprep extraction of plasmid DNA from the bacterial cells, DNA concentration was quantified using a Nanodrop-2000 spectrophotometer (ThermoFisher Scientific - #ND-2000).

The absorbance of light at a 260 nm wavelength of 1.5 µl of Buffer EB was measured to quantify background absorbance in the DNA samples. The absorbance of 1.5 µl of each DNA extraction was then quantified. The ng/µl concentration of DNA in each sample was automatically calculated by the Nanodrop using the Beer-Lambert Law, which describes the linear correlation between absorbance and concentration.

2.2.2.6 *PSAT1* PCR

To confirm the presence of *PSAT1* within the *pGEM-T* plasmid, a PCR reaction was used to amplify the gene from the plasmids extracted from each bacterial colony. The primers for *PSAT1* amplification were the same primers that would later be used for amplification of *PSAT1* in preparation for cloning of the gene into the pcDNA5.5 vector (see 2.2.3). PCR was performed using Q5® High-Fidelity DNA Polymerase (New England Biolabs - #M0491S).

A 25 µl reaction mixture was prepared in an autoclaved Fisherbrand™ 0.2 ml Flat-Cap PCR tube as per the manufacturer's recommended instructions with 0.5 ng of *pGEM-T PSAT1* plasmid DNA (Table 2.8). The reaction mixture was briefly vortexed and centrifuged, then placed on a thermocycler to run the PCR with conditions described in Table 2.9

Table 2.8 – Composition of 25 µl Q5® High-Fidelity DNA Polymerase PCR reaction for *PSAT1* amplification.

Component	In 25 µl
5x Q5 Reaction Buffer	5 µl
10 mM dNTP mix	0.5 µl
10 µM Forward Primer	1.25 µl
10 µM Reverse Primer	1.25 µl
Q5 High-Fidelity DNA Polymerase	0.25 µl
Template *PSAT1* cDNA	0.5 ng
Nuclease-free water	Volume to 25 µl total

Table 2.9 – Thermocycler program for PCR amplification of *PSAT1.*

Temperature	Time	
98°C	30 seconds	
98°C	10 seconds	29 x
60°C	30 seconds	
72°C	45 seconds	
72°C	2 minutes	
4°C	∞	

The PCR product from each colony was then analysed on a 1% w/v agarose gel. 0.5 g of agarose was dissolved in 50 ml of 1x Tris Acetate EDTA (TAE) diluted from 50x concentrated stock that was prepared by Dr Ruoyan Xu (242 g of Tris Base (Sigma Aldrich - #D5879), 57.1 ml of Glacial

Acetic Acid (Honeywell - #33209) and 25 ml of 200 mM EDTA pH 8.0 (Severn Biotech - #20-5300-01) made up to a total volume of 1 L with distilled water). Microwaving in 30 second intervals followed by mixing was used to heat the TAE buffer and facilitate dissolving of agarose. The agarose/TAE solution was allowed to cool sufficiently to add 1 µl of GelRed® Nucleic Acid Gel Stain (Biotium - #41003). GelRed® intercalates with nucleic acids and fluoresces under exposure to UV light, thereby allowing visualisation of DNA within the gel. The agarose/TAE solution was then poured into a gel mould and allowed to cool enough to set, ready for 2D gel electrophoresis. The PCR product was mixed with Gel Loading Dye, Purple (6x) no SDS (New England Biolabs - #B7025S) diluting the loading dye to 1x concentration. The PCR product/loading dye mixture was loaded to the 1% w/v agarose gel alongside 5 µl of 1 kb DNA ladder (New England Biolabs – #N3232S). The gel was run in 1x TAE at 80V till adequate separation was achieved. Amplification of *PSAT1* was assessed by visualisation of the DNA within the gel using an Amersham Imager 600UV chemidoc system (GE Healthcare - #29083463).

2.2.2.7 Sequencing

Following the confirmation of *PSAT1* presence in the plasmid DNA extracted from bacteria, *pGEM-T PSAT1 S>A* and *pGEM-T PSAT1 S>E* plasmid DNA samples were sent for sequencing to confirm successful mutagenesis of the gene sequence. 20 µl of 100 ng/µl dilutions of each plasmid was prepared in autoclaved 1.5 ml microcentrifuge tubes. The plasmids were sent for Sanger sequencing by GATC Biotech using pre-paid SUPREMERUN Tube barcodes (GATC Biotech – #B50100100). 2 samples per plasmid were sent for sequencing to sequence both forward and reverse strands of *PSAT1* within the *pGEM-T* multiple cloning region. The forward and reverse strands were sequenced using the GATC Biotech in-house M13-FP and M13-RP sequencing primers respectively. Sequencing results were analysed using DNADynamo Sequence Analysis Software (BlueTractorSoftware Ltd)

2.2.3 Cloning of *PSAT1* into the *pcDNA5.5* vector

For generation of Flp-In 293 cells expressing HA-tagged PSAT1 wt or mutant variants, *PSAT1 wt*, *PSAT1 S>A* or *PSAT1 S>E* DNA from the *pGEM-T* vector was cloned into a modified version of the *pcDNA5* vector which contains 2x human influenza haemagglutinin (HA-) and 2x Strep-tag sequences that are added to the N-terminus of coded proteins to generate tagged proteins. The vector was also mutated to allow use of the EcoRI restriction site in its multiple cloning region.

This modified vector was generated and kindly provided by Tencho Tenev (Institute of Cancer Research, London, UK) and is herein termed *pcDNA5.5*.

PSAT1 DNA was amplified from the *pGEM-T* vector via PCR. For eventual cloning into *pcDNA5.5*, amplification primers were designed to insert KpnI and EcoRI restriction sites at the start and end of the *PSAT1* DNA sequence respectively. The KpnI restriction site is indicated in green and the EcoRI restriction site is indicated in blue. Arrows indicate the exact cutting site within the sequence.

PSAT1 pcDNA5.5 primers:

Forward (KpnI) – 5'-ttggtac$^{\blacktriangledown}$cagccatggacgcccccaggcag-3'

Reverse (EcoRI) – 5'-gatggatatctgcag$^{\blacktriangledown}$aattctagctgatgcatctcc-3'

PSAT1 PCR was performed using the *pGEM-T PSAT1 wt*, *pGEM-T PSAT1 S>A* and *pGEM-T PSAT1 S>E* plasmids as template DNA, using Q5® High-Fidelity DNA Polymerase as described in 2.2.2.6. This generated *PSAT1 wt*, *PSAT1 S>A* and *PSAT1 S>E* PCR products containing KpnI and EcoRI restriction sites. The *PSAT1* PCR products and *pcDNA5.5* vector were then digested with KpnI-High-Fidelity (HF®) (New England Biolabs - #R3142S) and EcoRI-HF® (New England Biolabs - #R3101S) restriction enzymes ready for ligation. Separate digestions for the *PSAT1* PCR product and the *pcDNA5.5* vector were prepared in autoclaved Fisherbrand™ 0.2 ml Flat-Cap PCR tubes as described in Table 2.10.

Table 2.10 – Composition of reaction mixtures for digestion of *PSAT1* PCR product and *pcDNA5.5* vector.

PCR Product Digestion		**pcDNA5.5 Digestion**	
Component	**In 50 µl**	**Component**	**In 20 µl**
PSAT1 PCR product	40 µl	*pcDNA5.5* Vector	5 µl
CutSmart® Buffer	5 µl	CutSmart® Buffer	2 µl
KpnI-HF®	2 µl	KpnI-HF®	2 µl
EcoRI-HF®	2 µl	EcoRI-HF®	2 µl
Nuclease-free water	1 µl	Nuclease-free water	9 µl

The digestion reaction mixtures were vortexed and centrifuged briefly and placed on a thermocycler for digestion. Reaction mixtures were incubated at 37°C for 2 hours to facilitate restriction enzyme cutting, then incubated at 65°C for 20 minutes to inactivate KpnI and EcoRI.

Following digestion, the digested vector was run on a 1% w/v agarose gel as described in 2.2.2.6. The resultant plasmid backbone and cleavage products were then visualised within the gel using a UV transilluminator. The section of the gel containing the plasmid backbone was then cut out using a scalpel and stored in a pre-weighed, autoclaved 1.5 ml microcentrifuge tube. The combined weight of the gel section and the tube was noted and used to calculate the weight of the gel section. The digested plasmid backbone was then extracted from the agarose gel using the QIAquick Gel Extraction Kit (Qiagen - #28704) as per the manufacturer's instructions. Using a conversion rate where 100 mg of gel is equivalent to roughly 100 µl volume, 3 volumes of Buffer QG was added to 1 volume of gel. The gel was then incubated at 50°C in a heat block for up to 10 minutes, with periodic vortexing, allowing the section to completely dissolve. 1 gel volume of isopropanol was added, and the solution was transferred to a QIAquick spin column. The spin column was centrifuged at 18,000 g for 1 minute to allow DNA to bind to the column membrane. The flow through was collected in a 2 ml collection tube and discarded. 750 µl of Buffer PE was added to the spin column to wash the membrane. The column was centrifuged again at 18,000 g for 1 minute and the flow through was discarded. The empty spin column was immediately centrifuged again at 18,000 g for 1 minute to remove residual washing buffer. The spin column was then transferred to an autoclaved 1.5 ml microcentrifuge. To elute the extracted DNA, 50 µl of Buffer EB was added directly to the membrane within the spin column and allowed to soak through for 1 minute. The column was centrifuged once more at 18,000 g for 1 minute and DNA was collected in the 1.5 ml microcentrifuge.

Ultimately, the digested *PSAT1* PCR products and *pcDNA5.5* backbone were ligated to generate *pcDNA5.5 HA-PSAT1 wt*, *pcDNA5.5 HA-PSAT1 S>A* and *pcDNA5.5 HA-PSAT1 S>E* plasmids. Ligation was performed in a total volume of 10 µl using 80 ng of DNA, with the *pcDNA5.5* vector and *PSAT1* insert used at a molar ratio of 4:1 vector to insert. T4 DNA Ligase (New England Biolabs - #M0202S) was used to catalyse the ligation and a 10 µl reaction mixture was prepared in an autoclaved Fisherbrand™ 0.2 ml Flat-Cap PCR tube as per the manufacturers recommended instructions (Table 2.11). The 10 µl reaction mixture was then incubated at 16°C overnight on a thermocycler to facilitate ligation.

As with *pGEM-T*, the *pcDNA5.5* vector contains an ampicillin resistance gene. Therefore, successful ligation was confirmed by transforming competent bacterial cells as described in

2.2.2.3 and growing transformed bacterial colonies overnight on LB-agar plates containing 100 µg/ml ampicillin. Colonies were then mini-prepped as described in 2.2.2.4 to amplify and extract *pcDNA5.5 HA-PSAT1 wt*, *pcDNA5.5 HA-PSAT1 S>A* and *pcDNA5.5 HA-PSAT1 S>E* plasmid DNA ready for cellular transfection.

Table 2.11 – Composition of 10 µl T4 DNA Ligase reaction.

Component	In 10 µl
T4 DNA Ligase Buffer (10x)	1 µl
Vector DNA (4 kb)	40 ng
PSAT1 DNA (1 kb)	40 ng
T4 DNA Ligase	1 µl
Nuclease-free water	Volume to 10 µl

The resulting *pcDNA5.5 PSAT1 wt*, *pcDNA5.5 PSAT1 S>A* and *pcDNA5.5 PSAT1 S>E* plasmids were also sent for Sanger sequencing as in 2.2.2.7, using GATC Biotech's in-house CMV-Forward and BGH-Reverse sequencing primers to sequence the forward and reverse strands of the gene insert site respectively, as an additional confirmation for successful ligation.

2.2.4 Flp-In 293 HA-PSAT1 cell line generation

The Flp-In™ T-REx™ system allows the generation of stable cell lines expressing single copies of gene inserts at a pre-integrated FRT site in the host cell genome. The *pcDNA5.5* vector also contains an FRT site. When the *pcDNA5.5* vector is co-transfected with the *pOG44* vector, which expresses FLP recombinase under a constitutive *CMV* gene promoter, homologous recombination between FRT sites in the *pcDNA5.5* vector and in the host cell genome integrates the *pcDNA5.5* gene insert into the host cell genome. Flp-In 293 T-REx cells are a variant of the human embryonic kidney (HEK)-293 cell line, containing an FRT site and a constitutively expressed tetracycline repressor (TetR) protein. TetR protein dimers bind to tetracycline operator (*Tet Op*) sequences in the promoter region that controls the expression of genes in the FRT site and represses gene expression. Doxycycline, when present, can bind to the TetR protein dimers and trigger a conformational change that inhibits binding to the *Tet Op* sequences, thereby de-repressing gene expression. Flp-In 293 T-REx cells were therefore used to generate cell lines expressing doxycycline inducible *HA-PSAT1 wt*, *HA-PSAT1 S>A* and *HA-PSAT1 S>E* genes.

Flp-In 293 T-REx cells were plated at a density of 125,000 cells per well in 6-well plates and transfected the following day with a combination of *pOG44* and one of the three *pcDNA5.5 HA-PSAT1* plasmids. 3.3 µg of DNA was transfected in total, with *pOG44* and the *pcDNA5.5 HA-PSAT1* plasmid being transfected in a ratio of 9 *pOG44*: 1 *pcDNA5.5 HA-PSAT1* (i.e. 2790 ng *pOG44*: 330 ng *pcDNA5.5 HA-PSAT1*). For the transfection of Flp-In 293 T-REx cells, 150 µl Opti-MEM® reduced serum transfection medium, 3.3 µg of DNA and 9.9 µl of FuGENE® HD Transfection Reagent (Promega - #E2311) were mixed together in an autoclaved 1.5 ml microcentrifuge tube and incubated at room temperature for 10 minutes. The transfection mixture was then added dropwise to the plated cells in 2 ml of medium. In addition to combined transfection of *pOG44* and *pcDNA5.5 HA-PSAT1* plasmids, transfection of each plasmid individually (2790 ng *pOG44* or 330 ng of *pcDNA5.5 HA-PSAT1*) was also performed to control for proper recombination in the presence of both plasmids. Recombination of the *HA-PSAT1* gene insert from the *pcDNA5.5* vector provides Flp-In 293 cells with a hygromycin resistance gene. Therefore, to select for cells in which homologous recombination had occurred, transfected cells were incubated at 37°C for 48 hours and transfection medium was then replaced with fresh medium containing 300 µg/ml hygromycin.

2.2.5 Cloning of *PSAT1* into the *pTRIPZ* vector

In order to generate MDA-MB-453 breast cancer cell lines expressing inducible PSAT1 wt, PSAT1 S>A and PSAT1 S>E proteins, *PSAT1 wt*, *PSAT1 S>A* or *PSAT1 S>E* cDNA was cloned from the *pcDNA5.5* vector into the lentiviral *pTRIPZ* vector, using methods described in detail in 2.2.3. PCR was performed from the *pcDNA5.5* vectors using primers that inserted AgeI and EcoRI restriction sites at the beginning and end of the *PSAT1* DNA sequence respectively, facilitating compatible ligation with the *pTRIPZ* vector following digestion of both insert and vector with AgeI-HF® (New England Biolabs - #R3552S) and EcoRI-HF®. The AgeI and EcoRI primer sequences used are indicated below. The AgeI restriction site is indicated in green and the EcoRI restriction site is indicated in blue. The specific cutting sites within the sequence are indicated by arrows.

PSAT1 pTRIPZ primers:

Forward (AgeI) – 5’-ata$^{\blacktriangledown}$ccggtaccatggacgcccccag-3’

Reverse (EcoRI) – 5’-tgcgcg$^{\blacktriangledown}$aattctcatagctgatgcatctcc-3’

As with cloning of the *PSAT1 wt*, *PSAT1 S>A* and *PSAT1 S>E* genes into the *pcDNA5.5* vector, successful ligation was confirmed via Sanger sequencing with GATC Biotech, sequencing the *pTRIPZ PSAT1 wt*, *pTRIPZ PSAT1 S>A* and *pTRIPZ PSAT1 S>E* plasmids as described in 2.2.2.7. The mutagenesis primers described in 2.2.1 were used as sequencing primers to read from the middle of the *PSAT1* sequence outwards, checking for alignment with the *pTRIPZ* vector sequence at the beginning and end of the gene. Alignment with the *pTRIPZ* sequence at the start and end of the *PSAT1* gene confirmed the gene was contained within the *pTRIPZ* vector and ligation was successful.

2.2.6 MDA-MB-453 PSAT1 cell line generation

2.2.6.1 Lentiviral generation

For transduction of *pTRIPZ PSAT1* vectors into the MDA-MB-453 breast cancer cell lines, a strategy of lentiviral infection was used. To generate lentiviruses carrying each *pTRIPZ PSAT1* vector, as well as a control *pGIPZ* vector which constitutively expresses GFP, Flp-In 293 T-REx cells were grown in 25 cm^2 flasks to around 60-70% confluency, at which point they were transfected with a virus generation transfection mixture. 2.2 µg *psPAX* and 0.9 µg of *pMD2.G*, the plasmids encoding the components necessary to assemble the virus, were mixed via vortexing along with 2.9 µg of the *pTRIPZ PSAT1* vector in 600 µl of Opti-MEM® reduced serum transfection medium. Transfection was performed using Effectene Transfection Reagent (Qiagen - #301425) so, after mixing the DNA plasmids in the Opti-MEM® reduced serum transfection medium, 15 µl of Effectene Enhancer Buffer was added to the mixture, which was then vortexed once again. Finally, 21 µl of Effectene Transfection Reagent was added to the mixture which was vortexed once more to mix thoroughly. The transfection mixture was then incubated at room temperature for 5 minutes and added directly into the 25 cm^2 flask of Flp-In 293 T-REx cells in 6 ml of medium.

Cells were incubated at 37°C for 10 hours to allow transfection of the virus-generating plasmids and the *pTRIPZ PSAT1* vector. Transfection medium was then changed to 10 ml of fresh medium, in which assembled virus was collected for 48 hours (after 24 hours, cells generating the *pGIPZ* virus were checked for green fluorescence to assess successful transfection of DNA and viral assembly). Virus containing medium was collected from the flasks and filtered through a Millex-HP 45 µm pore-size syringe filter unit (Merck Millipore - #SLHP033RS). Filtered viral medium was then stored at -80°C till use.

2.2.6.2 Lentiviral infection of MDA-MB-453 cells

MDA-MB-453 cells were plated in a 6-well plate at a density of 300,000 cells per well and incubated at 37°C for 24 hours. Hexadimethrine bromide (commercially named Polybrene – Sigma Aldrich - #H9268), which increases the efficiency of virus infection in receiving cells, was diluted to 8 μg/ml in lentiviral medium. 1 ml of lentiviral medium per well was then added to the MDA-MB-453 cells and cells were incubated for 72 hours, facilitating infection of the breast cancer cells by the virus. Green fluorescence of MDA-MB-453 cells infected with the *pGIPZ* virus was used to assess the efficiency of infection. *pTRIPZ* contains a puromycin resistance gene so, after 72 hours of incubation of MDA-MB-453 cells with the lentiviral medium, the lentiviral medium was removed from the cells and replaced with medium containing 3 μg/ml puromycin to select for cells where *pTRIPZ PSAT1* transduction was successful. The resulting post-selection cells were passaged into 25 cm^2 flasks and subsequently into 75 cm^2 flasks when sufficiently confluent, ready for experimental use.

All virally contaminated materials, including medium, pipette tips, plates and filters were decontaminated in 1% w/v Virkon (1x 5 g Rely+On™ Virkon™ tablet (DuPont) dissolved in 500 ml of water) for at least 24 hours to kill any residual virus prior to disposal.

2.3 HA-GFP and HA-IKKε cell line generation

Flp-In 293 cells expressing inducible HA-tagged GFP and IKKε wt or KD-m proteins were generated by Dr Ruoyan Xu, using techniques described in detail in 2.2. Similar to the generation of PSAT1 mutant variants, an IKKε kinase dead mutant was generated using point mutagenesis PCR to mutate the *IKBKE* gene sequence encoding lysine residue Lys38 on the IKKε protein to an alanine residue. This was done by changing 2 nucleotides in the DNA sequence. As with *PSAT1* mutagenesis, *IKBKE* mutagenesis primers were manufactured by Sigma Aldrich.

IKBKE K>A mutagenesis primers:

Forward – 5'-gagctggttgctgtggcggtcttcaacactac-3'

Reverse – 5'-gtagtgttgaagaccgccacagcaaccagc-3'

2.4 IncuCyte Growth Analysis

Cells were plated in either a 96-well or 6-well plate at densities described in Table 2.3. In 96-well plates, cells were plated in triplicate for each condition. For experiments involving siRNA treatments, cells were transfected 24 hours after plating as described in 2.1.7, washed 16 hours later and placed on the IncuCyte Zoom system (Essen BioScience). For drug treatments, cells were treated 24 hours after plating and placed immediately on the IncuCyte Zoom system.

Cells were cultured within the IncuCyte Zoom system for up to 7 days at 37°C with 5% CO_2. Brightfield images at 100X magnification were captured in at least 6 hourly intervals and from at least 4 independent locations within the wells, depending on the well size.

Cell confluency in each image was quantified using an imaging mask programmed to recognise cells within the image. An average of the cell confluency from the images in each well was taken to calculate cell confluency per well. Delta confluency over 72 hours was calculated by subtracting confluency at 0 hours from confluency at 72 hours and was used as a readout to compare relative cell growth. Full details of the imaging masks used for analysis of each cell line are included as supplementary materials (see Table 7.1).

2.5 Western Blotting

2.5.1 Pre-mixed buffers and Reagents

Pre-prepared 1 M Tris HCl (pH 7.4) and 1 M $MgCl_2$ solutions (both from Severn Biotech) were used in the preparation of Triton 1% lysis buffer for extraction of proteins from cells. Both solutions were stored at room temperature.

20% w/v Sodium Dodecyl Sulfate solution (Sigma Aldrich - #05030-500ML-F) was used in the preparation of 6x loading dye for gel loading. The 20% solution was stored at room temperature and would occasionally precipitate when ambient temperature dropped. In this circumstance, the solution was warmed to 40°C in a water bath and incubated for 15 minutes to facilitate re-solubilisation.

NuPAGE™ MOPS SDS Running Buffer 20x solution (50mM MOPS, 50 mM Tris Base, 0.1% SDS, 1 mM SDS, pH 7.7) (Life Technologies - #NP000102) was used for SDS-PAGE protein separation. The solution was diluted to 1x concentration in distilled water. The 20x solution was stored at room temperature and the 1x dilution was freshly prepared when required.

Tris Glycine 10x solution (250 mM Tris, 1.92 M Glycine) (Severn Biotech - #20-6300-100) was used for the preparation of wet transfer buffer. The solution was diluted to 1x in distilled water when required. The 10x solution was stored at room temperature.

Tris Buffered Saline (TBS) 10x solution (1.37 M Sodium Chloride, 200 mM Tris) (Severn Biotech - #20-7301-10) was used for the preparation of TBS-T used for preparing immunoblot membrane blocking solution, antibody solutions and for washing membranes in between antibody incubations. The 10x solution was stored at room temperature.

2.5.2 Cell lysis

Cell culture plates frozen at -80°C were removed from the freezer and placed on ice. 150 µl of Triton 1% lysis buffer (Table 2.12) was added to each well and wells were scraped using a cell scraper to suspend cells in the lysis buffer. The cell suspension was then transferred to a 1.5 ml microcentrifuge tube and centrifuged at 13,000 g for 15 minutes at 4°C, pelleting unwanted cellular debris at the bottom of the microcentrifuge tube. The resulting cell lysate supernatant was transferred to a fresh microcentrifuge tube and stored at -80°C when not in use.

Table 2.12 – Recipe for Triton 1% lysis buffer. Lysis buffer was stored at 4°C when not in use.

Component	Concentration
Tris HCl (pH 7.4)	20 mM
NaCl	135 mM
$MgCl_2$	1.5 mM
Glycerol ≥ 99% (Sigma Aldrich - #G5516-1L)	10% v/v
Triton™ X-100 (Sigma Aldrich - #T8787-100ML)	1% v/v
cOmplete™ Mini Protease Inhibitor Cocktail (Roche - #11836153001)	1 tablet

2.5.3 Protein quantification using DC protein assay (Bio-Rad)

To measure the concentration of the protein content of cell lysates, the Bio-Rad DC protein assay was used, utilising a colourimetric reaction to determine unknown concentrations from a curve plotted using standards of known concentrations. The assay was performed as per the kit manufacturer's instructions. Briefly, using an 8 µl total volume per well of a 96-well plate, a standard curve was generated using a bovine serum albumin standard (BSA (Sigma Aldrich - #A2153) dissolved in Triton 1% lysis buffer, stored at -20°C and thawed on ice when required) of a known concentration of 1 mg/ml. Wells containing 1 mg/ml, 0.5 mg/ml, 0.25 mg/ml and 0.125 mg/ml were prepared in triplicate and diluted using water (i.e. 8 µl BSA = 1 mg/ml, 4 µl BSA + 4 µl water = 0.5 mg/ml, 2 µl BSA + 6 µl water = 0.25 mg/ml, 1 µl BSA + 7 µl water = 0.125 mg/ml). For each unknown sample, 2 µl of cell lysate was added to a well of a 96-well plate in triplicate and the volume was topped up to 8 µl using water. 3 lysis buffer control wells were also prepared using 2 µl of lysis buffer and 6 µl water to control for background absorbance in the lysis buffer in the unknown samples (Figure 2.1).

With 8 µl total volume in each well, the reagents for the colourimetric reaction were prepared and added. Reagent S' was prepared freshly as required, mixing DC Protein Assay Reagent A (Bio-Rad - #500-0113) with DC Protein Assay Reagent S (Bio-Rad - #500-0115) at a ratio of 1 ml Reagent A : 20 µl Reagent S. Reagent S' was vortexed briefly to thoroughly mix and 25 µl was added to each reaction well. Subsequently 200 µl of DC Protein Assay Reagent B (Bio-Rad - #500-0114) was added to each reaction well. The quantification plate was then incubated at room temperature for at least 20 minutes to allow the colourimetric reaction to occur to completion. The absorbance of light at an excitation wavelength of 630 nm was then measured for each well using a Victor^3 Multilabel Counter plate reader (Perkin Elmer - #1420-050).

Lysis Buffer (2 µl) + H_2O (6 µl)	1 mg/ml BSA (1 µl) + H_2O (7 µl)	1 mg/ml BSA (2 µl) + H_2O (6 µl)	1 mg/ml BSA (4 µl) + H_2O (4 µl)	1 mg/ml BSA (8 µl)							
Lysis Buffer (2 µl) + H_2O (6 µl)	1 mg/ml BSA (1 µl) + H_2O (7 µl)	1 mg/ml BSA (2 µl) + H_2O (6 µl)	1 mg/ml BSA (4 µl) + H_2O (4 µl)	1 mg/ml BSA (8 µl)							
Lysis Buffer (2 µl) + H_2O (6 µl)	1 mg/ml BSA (1 µl) + H_2O (7 µl)	1 mg/ml BSA (2 µl) + H_2O (6 µl)	1 mg/ml BSA (4 µl) + H_2O (4 µl)	1 mg/ml BSA (8 µl)							
Sample 1 (2 µl) + H_2O (6 µl)	Sample 2 (2 µl) + H_2O (6 µl)	Sample 3 (2 µl) + H_2O (6 µl)	Sample 4 (2 µl) + H_2O (6 µl)	Sample 5 (2 µl) + H_2O (6 µl)	Sample 6 (2 µl) + H_2O (6 µl)	Sample 7 (2 µl) + H_2O (6 µl)	Sample 8 (2 µl) + H_2O (6 µl)	Sample 9 (2 µl) + H_2O (6 µl)	Sample 10 (2 µl) + H_2O (6 µl)	Sample 11 (2 µl) + H_2O (6 µl)	Sample 12 (2 µl) + H_2O (6 µl)
Sample 1 (2 µl) + H_2O (6 µl)	Sample 2 (2 µl) + H_2O (6 µl)	Sample 3 (2 µl) + H_2O (6 µl)	Sample 4 (2 µl) + H_2O (6 µl)	Sample 5 (2 µl) + H_2O (6 µl)	Sample 6 (2 µl) + H_2O (6 µl)	Sample 7 (2 µl) + H_2O (6 µl)	Sample 8 (2 µl) + H_2O (6 µl)	Sample 9 (2 µl) + H_2O (6 µl)	Sample 10 (2 µl) + H_2O (6 µl)	Sample 11 (2 µl) + H_2O (6 µl)	Sample 12 (2 µl) + H_2O (6 µl)
Sample 1 (2 µl) + H_2O (6 µl)	Sample 2 (2 µl) + H_2O (6 µl)	Sample 3 (2 µl) + H_2O (6 µl)	Sample 4 (2 µl) + H_2O (6 µl)	Sample 5 (2 µl) + H_2O (6 µl)	Sample 6 (2 µl) + H_2O (6 µl)	Sample 7 (2 µl) + H_2O (6 µl)	Sample 8 (2 µl) + H_2O (6 µl)	Sample 9 (2 µl) + H_2O (6 µl)	Sample 10 (2 µl) + H_2O (6 µl)	Sample 11 (2 µl) + H_2O (6 µl)	Sample 12 (2 µl) + H_2O (6 µl)

Figure 2.1 – Example layout for a 96-well protein concentration quantification plate. A standard curve is generated using 1 mg/ml BSA dissolved in Triton 1% lysis buffer at a concentration of 1 mg/ml, 0.5 mg/ml, 0.25 mg/ml and 0.125 mg/ml and a Triton 1% lysis buffer blank for background control as indicated. 2 µl of each sample of unknown concentration is diluted in 6 µl H_2O as indicated. All samples are assayed in triplicate and 25 µl of DC Protein Assay Reagent S' was added to each well, followed by 200 µl of DC Protein Assay Reagent B. Absorbance of light at a wavelength of 630 nm was measured for each well and the concentration of unknown samples was calculated using the standard curve.

Microsoft Excel was used to plot a standard curve from the average absorbance values of the triplicate BSA samples and generate the curve equation. The average absorbance values for unknown samples were fed into the equation to calculate the concentrations of the cell lysates.

2.5.4 Preparation of cell lysates for SDS-PAGE

To facilitate comparison of relative protein expression upon completion of the western blotting protocol, cell lysates must be analysed in equal amounts. Therefore, being kept on ice at all times, cell lysates were diluted to an equal concentration of 1 µg/µl where possible, or to an equal concentration with the most dilute lysate in instances where lysate concentration was too low to normalise to 1 µg/µl. 6x concentrated loading dye (Table 2.13) was subsequently added to a final concentration of 1x in the lysates. Lysates were then incubated at 95°C for 10 minutes in a heat block to ensure full denaturation of proteins, after which, brief centrifugation ensured collection of full lysate at the bottom of the microcentrifuge. Lysates were then either placed on ice once again, ready for gel loading, or stored at -80°C for use at a later time.

Table 2.13 – Recipe for 6x concentrated loading dye.

Component	Concentration
Glycerol ≥ 99%	40% v/v
β-mercaptoethanol (Sigma Aldrich - #M3148-25ML)	30% v/v
20% w/v Sodium dodecyl sulfate (SDS) solution	6% v/v
Bromophenol blue (Sigma Aldrich - #B8026-5G)	-

2.5.5 SDS-PAGE

Sodium dodecyl sulfate – polyacrylamide gel electrophoresis (SDS-PAGE) was used to separate lysate proteins based on size. 18 µl of each sample lysate (containing 15 µg protein in 15 µl lysate and 3 µl of 6x loading dye) was loaded per well of a 10-well, 12-well or 20-well precast NuPAGE™ Novex™ 4-12% Bis-Tris Midi Protein Gels (Life Technologies – #NP0321BOX (10-well), #NP0322BOX (12-well), #WG1402BOX (20-well)), which had been inserted into either an XCell SureLock™ Mini-Cell (for 10- and 12-well gels, Invitrogen - #EI0001) or an XCell SureLock™ Midi-Cell (for 20-well gels, Invitrogen - #WR0100) prior to sample loading. In addition to loading the lysate samples, one well to the left of the samples was loaded with 8 µl PageRuler™ Plus Prestained Protein Ladder (ThermoFisher Scientific - #26619) and one well to the right of the samples with 4 µl of ladder. This allowed visualisation of protein molecular weights in the gel and orientation of the gel and membrane at later points. Following sample loading, the gel tank was filled with NuPAGE™ MOPS SDS Running Buffer (20x) diluted to 1x in distilled water. 120V was then run through the gel for 2 hours to resolve the proteins.

2.5.6 Transfer to PVDF membrane

Following separation of the proteins via SDS-PAGE, proteins were transferred to 0.45 µm pore-size PVDF membrane (Merck Millipore - #IPVH00010) using either semi-dry or wet transfer techniques.

2.5.6.1 Semi-dry transfer

Semi-dry transfer was performed using a TE77 PWR Semi-Dry Transfer Unit (GE Healthcare - #11001342). Completed SDS-PAGE gels were removed from the electrophoresis tank and incubated in Kat (-) buffer (Table 2.13) for 20 minutes. PVDF membrane cut to the necessary size of the gel used was briefly incubated in methanol to activate the membrane and allow proper

binding of proteins. 2 pieces of Grade 17 Chr Cellulose Chromatography paper (GE Healthcare - #3017-915) were soaked in Kat (+) buffer (Table 2.14) and placed onto the anode base of the transfer unit. The PVDF membrane was washed in Kat (-) buffer to remove excess methanol and placed on top of the blotting paper. Following incubation, the completed gel was carefully laid on top of the membrane ensuring no air bubbles were present between the membrane and the gel. 2 further pieces of blotting paper were soaked in Kat- buffer and placed on top of the gel to complete the transfer "sandwich". A 5 ml pipette was then rolled across the surface of the transfer sandwich, with pressure applied to remove any potential bubbles between any of the layers. The transfer unit was closed and 20V was applied for 1 hour to allow migration of resolved proteins from the gel to the membrane in parallel, maintaining the protein separation throughout the process.

Table 2.14 – Recipe's for Kat (-) and Kat (+) buffers for semi-dry transfer.

Kat (-) Buffer		**Kat (+) Buffer**	
Component	**Concentration**	**Component**	**Concentration**
Tris Base	24.8 mM	Tris Base	302.1 mM
E-Aminocaproic Acid	40.4 mM	MetOH	20% v/v
(Sigma Aldrich – #A7824)		Distilled water	80% v/v
MetOH	20% v/v		
Distilled water	80% v/v		

2.5.6.2 Wet transfer

Wet transfer was performed using a TE62 Transfer Cooled Unit (GE Healthcare - #TE62), kept in the fridge at all times. The tank was filled with transfer buffer (Table 2.15), which was reused for multiple transfers and replaced when signs of inefficient transfer began to appear (i.e. low running voltage and retention of protein ladder within the gel following completion of transfer). As with semi-dry transfer, PVDF membrane was incubated briefly in methanol to activate it. Transfer cassettes were assembled in a plastic tray containing transfer buffer. 2 pieces of X50 chromatography paper (Fisher Scientific - #1156-7393), cut to the size of the cassette and soaked in the transfer buffer contained within the tray, were placed on top of a buffer-soaked sponge on the grey (positive) side of the cassette. The activated PVDF membrane was washed in the transfer buffer and placed on top of the blotting paper. Completed SDS-PAGE gels were removed from the electrophoresis tank, gently washed in transfer buffer and carefully laid on top of the membrane, again taking care to avoid the trapping of air bubbles between the membrane and

the gel. 2 more pieces of thin blotting paper were soaked in the transfer buffer and placed on top of the existing layers and a 5 ml pipette was rolled across the gel containing section of the transfer sandwich to push out any bubbles present between the layers. Another buffer-soaked sponge was laid on top of the transfer sandwich. The cassette was closed and submerged in the transfer tank, ensuring correct orientation of the cassette within the tank (grey/positive to anode and black/negative to cathode). The transfer was run for 2 hours using 1 Amp.

Table 2.15 – Recipe for Tris Glycine transfer buffer for wet transfer.

Component	Concentration
Tris Glycine (10x solution)	10% v/v
MetOH	20% v/v
Distilled water	70% v/v

2.5.7 Immunoblotting

Following completion of transfer, the membranes were subject to immunoblotting for visualisation of specific proteins of interest. Firstly, membranes were incubated in 5% w/v skimmed milk powder (Sigma Aldrich - #70166) in TBS-T (a 0.1% v/v TWEEN® 20 (Sigma Aldrich - #P1379) solution prepared in 1x TBS buffer) for 1 hour at room temperature on a rocking platform. Subsequently, membranes were cut into multiple pieces based on molecular weight to facilitate immunoblotting of multiple proteins from a single membrane. Membrane sections were then incubated in primary antibody diluted in 5% w/v skimmed milk powder in TBS-T overnight at 4°C either in a petri dish on a rocking platform, or in a 30 ml universal tube on a rolling mixer depending on membrane size. The following day, membrane sections were washed 3 times for 15 minutes a piece in TBS-T at room temperature to remove unbound antibody. Membranes were then incubated in horseradish peroxidase (HRP)-conjugated secondary antibody diluted in 5% w/v skimmed milk powder in TBS-T for 1 hour at room temperature. Full details of both primary and secondary antibodies used in this project are found in 2.5.7.1 and Table 2.16. Following secondary incubation, membrane sections were washed again for 15 minutes, 3 times over at room temperature in TBS-T to remove excess secondary antibody. After washing, the immunoblot was developed using an Amersham Imager 600UV chemidoc system (GE Healthcare - #29083463) or Fuji Medical X-Ray Film (Fujifilm - #47410 19289). For development using the chemidoc system, membranes were placed on the surface of a tray with a white plastic insert. Standard strength Pierce™ enhanced chemiluminescence (ECL) Western Blotting Substrate (ThermoFisher Scientific - #32106), high strength SuperSignal™ West Pico

PLUS Chemiluminescent Substrate (ThermoFisher Scientific – #34577) or maximum strength SuperSignal™ West Femto Maximum Sensitivity Substrate (ThermoFisher Scientific - #34094) was added to the membranes to induce the HRP-mediated chemiluminescent reaction. The tray with the membranes on was then inserted into the chemidoc system for detection of chemiluminescent signal. For development to X-Ray film, ECL substrate was added and membranes were placed between 2 sheets of clear plastic film inside an autoradiography cassette. In a dark room, X-Ray film was inserted in the cassette and exposed to the membranes for up to 15 minutes depending on signal strength. X-Ray films were subsequently developed using an SRX-101A table-top medical film processor (Konica Minolta) and scanned to digital .jpg format using a table-top scanner for figure preparation.

If membranes were re-probed with additional antibodies following the completion of the immunoblot, membranes were stripped by incubation in Restore™ PLUS Western Blot Stripping Buffer (ThermoFisher Scientific – #46430) for 10 minutes, followed by 5x 3-minute washes in PBS and 1 hour blocking at room temperature. Re-probing was then performed.

2.5.7.1 Antibodies

Primary antibodies specific to protein of interest and secondary HRP-conjugated antibodies were obtained from commercial sources and stored at either 4°C or -20°C as required. Primary antibodies were used initially at a dilution of 1:1000 which was then adjusted based on signal strength as necessary. Secondary antibodies were used at a dilution of either 1:2000 or 1:5000. Specific details of each antibody used are indicated in the Table 2.16.

2.5.8 Densitometry analysis western blot quantification

In order to quantify differences in protein expression between samples, relative protein band density was quantified using NIH's ImageJ software[327]. Firstly, relative protein band density of the vinculin loading control in each sample was quantified as a percentage of total protein band density for vinculin across all samples. Then, the same process was repeated for the protein of interest, quantifying the density of each individual protein band as a percentage of total protein band density for the protein of interest across all samples. Finally, the percentage density for the protein of interest was divided by the percentage density for the loading control for each sample, to generate relative values for each protein normalised to loading. Further normalisation of density values for proteins of interest was then performed for specific experiments and is indicated in such cases throughout the results chapters. All western blots were repeated in at least three biologically independent experiments unless otherwise stated.

Table 2.16 – Details of antibodies used for immunoblot protein detection. *antibody discontinued. †HRP linked.

Type	Target	Company	Cat. Number	Host	Storage	Dilution
Primary	Actin	Santa Cruz	sc1615	Goat	4°C	1:1000
Primary	ATF4	Cell Signaling	11815	Rabbit	-20°C	1:1000
Primary	HA-tag	Roche	11867423001	Rat	-20°C	1:4000
Primary	IKKε	Sigma Aldrich	I4907*	Rabbit	-20°C	1:1000
Primary	IRF3	Cell Signaling	11904	Rabbit	-20°C	1:1000
Primary	IRF3 pSer396	Cell Signaling	4947	Rabbit	-20°C	1:1000
Primary	NF-κB p65	Cell Signaling	8242	Rabbit	-20°C	1:1000
Primary	NF-κB p65 pSer468	Cell Signaling	3039	Rabbit	-20°C	1:1000
Primary	PHGDH	Sigma Aldrich	HPA021241	Rabbit	-20°C	1:4000
Primary	PSAT1	ThermoFisher Scientific	PA5-22124*	Rabbit	-20°C	1:1000
Primary	PSAT1	ProteinTech	20180-1AP	Rabbit	-20°C	1:1000
Primary	PSPH	ProteinTech	14513-1-AP	Rabbit	-20°C	1:1000
Primary	SHMT2	Cell Signaling	12762	Rabbit	-20°C	1:1000
Primary	STAT1	Cell Signaling	9172	Rabbit	-20°C	1:1000
Primary	STAT1 pTyr701	Cell Signaling	9167	Rabbit	-20°C	1:1000
Primary	TBK1	Cell Signaling	3013	Rabbit	-20°C	1:1000
Primary	Vinculin	ProteinTech	66305-1-Ig	Mouse	-20°C	1:1000
Secondary†	Goat IgG	Santa Cruz	sc2020	Donkey	4°C	1:2000
Secondary†	Mouse IgG	Cell Signaling	7076	Horse	-20°C	1:2000
Secondary†	Rabbit IgG	GE Healthcare	NA934-1ML	Donkey	4°C	1:2000
Secondary†	Rat IgG	Santa Cruz	sc2956	Chicken	4°C	1:2000

2.6 Labelled Metabolite Analysis

Samples were prepared for labelled metabolite analysis by Dr Ruoyan Xu and were subsequently sent to Dr Christian Frezza and Dr Sofia De Costa (MRC Cancer Unit, Cambridge, UK) for mass spectrometry detection of total and labelled metabolites. Flp-In 293 HA-GFP and Flp-In 293 HA-IKKε cells were treated with 50 ng/ml doxycycline. T47D breast cancer cells were transfected with either a single non-targeting control oligo or a pool of 4 IKKε-targeting siRNA oligos to a final concentration of 50 nM as described in 2.1.7. 2 hours post-doxycycline induction of Flp-In 293 cells or 48 hours post-transfection of T47D cells, cells were incubated with either U-$^{13}C_6$-D-glucose (Cambridge Isotope Laboratories - #CLM-1396-5) or $^{15}N_2$-L-glutamine (Cambridge Isotope Laboratories – #NLM-1328-0.25) for 14 hours to facilitate incorporation of labelled carbon or nitrogen into intracellular metabolites. Flp-In 293 HA-PSAT1 cells were transfected with a pool of 3 siRNA oligos targeting the non-coding sequence of PSAT1 mRNA to a final concentration of 50 nM as described in 2.1.7. 24 hours post-transfection, 50 ng/ml doxycycline was added to the cells to induce PSAT1 expression. 24 hours post-doxycycline induction (48 hours post-transfection) cells were incubated with $^{15}N_2$-glutamine for 24 hours to measure the intracellular synthesis of serine via incorporation of labelled nitrogen.

Following incubation with labelled glucose or glutamine, cells were washed 3 times in PBS and placed on methanol and dry ice for metabolite extraction. At a ratio of 1 ml buffer/10^6 cells, ice-cold metabolite extraction buffer (Table 2.17) was added to the cells which were then incubated for 15 minutes. After incubation, cells were placed on a rocking platform for 15 minutes at 4°C, then incubated for 1 hour at -20°C. The cell/buffer mixture was transferred to autoclaved 1.5 ml microcentrifuge tubes and centrifuged at 13,000 RPM for 15 minutes at 4°C, after which the supernatant was transferred into autosampler glass vials (ThermoFisher Scientific - #60180-600) and stored at -80°C prior to mass spectrometry analysis.

Table 2.17 – Recipe for metabolite extraction buffer for extraction of labelled and unlabelled metabolites for mass spectrometry analysis.

Component	Concentration
MetOH, LC-MS CHROMASOLV® Grade (Honeywell - #34966-1L)	50% v/v
Acetonitrile, for HPLC, gradient grade, ≥99.9% (Sigma Aldrich - #34851-1L)	30% v/v
Water, LC-MS CHROMASOLV® Grade (Honeywell - #39253-1L-R)	20% v/v
HEPES	100 ng/ml

For mass spectrometry detection of metabolites, samples were randomised and processed blindly to avoid bias. Each sample was subject to liquid chromatography-mass spectrometry (LC-MS) analysis using a Dionex U3000 UHPLC system (ThermoFisher Scientific) coupled to a Q Exactive™ Hybrid Quadrupole-Orbitrap™ mass spectrometer (ThermoFisher Scientific). For high-pressure liquid chromatography (HPLC), the Dionex U3000 UHPLC system was fitted with a SeQuant® ZIC®-pHILIC column (150 mm x 2.1 mm) (Merck Millipore - #150460) and a SeQuant® ZIC®-pHILIC guard column (20 mm x 2.1 mm) (Merck Millipore - #150438) and temperature was maintained at 45°C. The mobile phase used is described in Table 2.18 and the flow rate was set at 200 µl/min at a gradient previously described by Mackay *et al.*[328]. The mass spectrometer was operated in full MS and polarity switching mode and acquired spectra traces were analysed by Dr Christian Frezza and Dr Sofia De Costa using XCalibur™ Qual Browser and XCalibur™ Quan Browser software (ThermoFisher Scientific).

The raw data from all labelled metabolite analysis experiments are provided in the supplementary materials (see chapter 7), specifically on the provided CD.

Table 2.18 – Recipe's for Solvent A and Solvent B comprising the mobile phase for High-Pressure Liquid Chromatography separation of metabolites.

Solvent A		**Solvent B**	
Component	**Concentration**	**Component**	**Concentration**
Ammonium carbonate	20 mM	Acetonitrile	100%
Ammonium hydroxide	0.1% v/v		
Water	To 2 litres total volume		

2.7 Phosphoproteomic Analysis

The samples for phosphoproteomic analysis were prepared by Dr Ewa Wilcz-Villega. Mass spectrometry analysis was performed by Dr Pedro Cutillas and Dr Vinothini Rajeeve (Barts Cancer Institute, London, UK). 3 independent single cell clones of Flp-In 293 HA-GFP and Flp-In 293 HA-IKKε cells were treated with 100 ng/ml doxycycline for 16 hours. Cells were then washed twice in PBS containing sodium orthovanadate (Na_3VO_4) and sodium fluoride (NaF) phosphatase inhibitors (kindly provided by Dr Vinothini Rajeeve). 250 µl of phosphoproteomic lysis buffer (Table 2.19 - including phosphatase inhibitors, again kindly provided by Dr Vinothini Rajeeve) was added to each well. Cells were incubated with lysis buffer on ice for 5 minutes, then scraped using a cell scraper and collected in a 1.5 ml microcentrifuge tube. The samples were then centrifuged at 13,000 g for 10 minutes at 4°C to pellet cellular debris. The supernatant was subsequently transferred to fresh microcentrifuge tubes. The samples were then frozen on dry ice and handed over to Dr Vinothini Rajeeve for mass spectrometry analysis.

After cell lysates were thawed, protein content was digested using trypsin. Phosphopeptides were enriched using TiO_2 as previously described[329] and peptides were then analysed using LC-MS with an Orbitrap mass analyser. Peptides were identified from MS/MS spectra using the Mascot search engine[330] and were quantified using Pescal as previously described[331].

Table 2.19 – Recipe for phosphoproteomic lysis buffer.

Component	Concentration
Urea	8 M
HEPES	20 mM
Sodium Orthovanadate (Na_3VO_4)	1 mM
Sodium Fluoride (NaF)	1 mM
β-Glycerol phosphate	1 mM
Disodium diphosphate ($Na_2H_2P_2O_7$)	0.25 mM

2.8 qRT-PCR

2.8.1 RNA extraction

RNA was extracted from cells in 6-well plates stored at -80°C following application of experimental conditions in tissue culture. The RNeasy Mini Kit (Qiagen - #74104) was used to extract RNA from cells by following kit instructions. Cell culture plates were removed from the -80°C freezer and placed on ice for lysis. In each well of a 6-well plate, 350 µl of RLT buffer was added to lyse the cells. A cell scraper was used to collect cells and 350 µl of 70% v/v ethanol was added to precipitate nucleic acids. The lysates were mixed thoroughly by pipetting with a p1000 pipette and transferred to an RNeasy spin column. The spin column was centrifuged at 8,000 g for 15 seconds to allow the passing of cell lysate through the column, during which RNA in the lysate binds to the membrane within the column. The flow through, containing the majority of DNA, proteins and cellular debris was collected in a 2 ml collection tube and subsequently discarded. The membrane within the column was then stringently washed with the addition of 700 µl of RW1 buffer to the spin column, which was then centrifuged again at 8,000 g for 15 seconds. This removes biomolecules like carbohydrates and fatty acids bound non-specifically to the membrane within the column. The flow through was again discarded. Two more washes with buffer RPE, a much milder washing buffer than RW1 designed to remove salt traces present on the column membrane, were performed. 500 µl of RPE buffer was added to the column, followed by centrifugation at 8,000 g for 15 seconds and discarding of the flow through. A further 500 µl of RPE buffer was added to the column, which was centrifuged again at 8,000 g, but this time for 2 minutes. The RNeasy spin column was then placed in a new 2 ml collection tube and centrifuged at 13,000 g for 1 minute to dry the column and remove residual buffers soaked within the membrane. Finally, the RNeasy spin column was transferred to an autoclaved 1.5 ml microcentrifuge tube and 30 µl of nuclease-free water was pipetted directly onto the membrane within the column, releasing the membrane-bound RNA. Centrifugation for 1 minute at 8,000 g then collected the RNA in the microcentrifuge tube, which was kept on ice or stored at -80°C till use.

2.8.2 Quantification of RNA concentration

The concentration of RNA extracted using the RNeasy Mini Kit was quantified using a Nanodrop-2000 spectrophotometer as described in 2.2.2.5, using the absorbance of light at a 260 nm

wavelength of 1.5 µl of nuclease-free water to quantify background absorbance in the RNA samples. The absorbance of 1.5 µl of each RNA sample was then quantified and used to calculate the ng/µl concentration of RNA in each sample.

2.8.3 cDNA synthesis

cDNA was prepared from cellular RNA extracts in Fisherbrand™ 0.2 ml Flat-Cap PCR tubes, using the Omniscript® RT Kit (Qiagen - #205111). Per sample, RNA was diluted to 83.3 ng/µl in 12 µl of nuclease-free water, using a total of 1000 ng of RNA for cDNA synthesis. A 20 µl cDNA synthesis reaction was then prepared in an autoclaved 0.2 ml PCR tube as described in Table 2.20. The 20 µl reaction mixture was then thoroughly mixed by vortexing and briefly centrifuged in a table top centrifuge. The reaction was then incubated at 37°C for 1 hour to facilitate cDNA production. Generated cDNA was stored at -20°C till use.

Table 2.20 – Composition of 20 µl Omniscript® RT cDNA synthesis reaction for synthesis of cDNA from cellular RNA extracts.

Component	In 20 µl
Buffer RT (10x)	2 µl
dNTP Mix (5 mM)	2 µl
50 µM Oligo (dT) Primer (Invitrogen - #AMG5730G)	2 µl of 10 µM dilution, diluted prior to use in nuclease-free water
40 units/µl RNase Inhibitor (New England Biolabs - #M0307S)	1 µl of 10 units/µl dilution, diluted prior to use in 1x Buffer RT (diluted in nuclease-free water)
Omniscript RT	1 µl
RNA extract (83.3 ng/µl)	12 µl (1000 ng total)

2.8.4 PCR reaction

The qRT-PCR reaction was performed in a MicroAmp™ Optical 96-Well Reaction Plate (Applied Biosystems - #N8010560) using either the 7500 Real-Time PCR System (Applied Biosystems - #4351105) or the QuantStudio™ 5 Real-Time PCR System (Applied Biosystems - #A28569). cDNA samples were run in triplicate, along with a single no cDNA control for each mRNA probe used.

In each sample well, a 20 µl TaqMan™ reaction mixture was prepared as detailed in Table 2.21. The Optical 96-Well Reaction Plate was then sealed with a MicroAmp™ Optical Adhesive Film (Applied Biosystems - #360954) and centrifuged for 1 minute at 2000 g to collect the whole of the reaction mixture at the bottom of the plate well. The qRT-PCR reaction was then run using one of the PCR machines. The PCR programme used involved a 10-minute incubation at 95°C to activate the polymerase, followed by 40 cycles of 15 seconds incubation at 95°C and 1-minute incubation at 60°C to facilitate TaqMan™ probe primer annealing and DNA amplification. Full details of TaqMan™ Gene Expression probes used within this project are detailed in Table 2.22.

Relative gene expression was quantified by using the Ct values from the qRT-PCR run (the number of cycles necessary for fluorescence from gene probes to pass a pre-determined threshold). Ct values were used for ΔΔCt analysis to calculate gene expression relative to a control value arbitrarily defined as "1". Gene expression in treated samples was normalised to *ACTB* (β-Actin) mRNA level, to control for differences in plate loading.

Table 2.21 – Composition of 20 µl TaqMan™ PCR reaction for quantitative analysis of mRNA expression.

Component	In 20 µl
TaqMan™ Universal PCR Master Mix (2x)	10 µl
TaqMan™ Gene Expression Probe	1 µl
Nuclease-free water	8 µl
Sample cDNA (Or nuclease-free water in no cDNA control)	1 µl

Table 2.22 – Details of TaqMan™ Gene Expression Probes used for qRT-PCR analysis of mRNA expression.

mRNA Target	Product Name/Assay ID	Source Company	Catalogue Number	Reporter Dye	Quencher Dye
PHGDH	Hs00198333_m1	ThermoFisher Scientific	4331182	6-FAM™	NFQ-MGB
PSAT1	Hs00795278_mH	ThermoFisher Scientific	4331182	6-FAM™	NFQ-MGB
PSPH	Hs00190154_m1	ThermoFisher Scientific	4331182	6-FAM™	NFQ-MGB
ACTB (β-Actin)	Human ACTB (Beta Actin) Endogenous Control	Applied Biosystems	4310881E	VIC®	TAMRA™

2.9 HA-Pulldown assays

Flp-In 293 cells expressing HA-PSAT1 wt, S>A or S>E were plated in 10 cm dishes at densities described in Table 2.2 (or Table 2.3 for pull-down assays in which siRNA was used to suppress endogenous PSAT1). Following necessary treatment, cells were washed twice with 1 ml of ice cold PBS and frozen at -80°C till use.

Cells were lysed on ice for 30 minutes with 1 ml of Triton 1% lysis buffer, then centrifuged at 13,000 g for 30 minutes at 4°C. Protein concentration was quantified as described in 2.5.3 and 1 mg of protein was diluted in 1 ml of Triton 1% lysis buffer. The protein sample was then incubated with 20 µl Monoclonal Anti-HA-Agarose Beads (Sigma Aldrich - #A2095) in a 1.5 ml microcentrifuge tube on a rotator mixer for 1 hour at 4°C. Samples were centrifuged in a table top centrifuge at 4500 RPM for 30 seconds to pellet the Anti-HA-Agarose beads and the supernatant was aspirated. 1 ml of lysis buffer was added to wash the beads. This washing step was repeated 3 more times.

A glycine elution was then performed to detach bound protein from the beads. 90 µl of 0.2 M glycine pH 2.5 (Severn Biotech) was added to the bead pellet and the samples were incubated at room temperature for 30 minutes. A final centrifugation at 4500 RPM for 30 seconds in a table top centrifuge was performed and the 90 µl glycine elution was pipetted away from the beads and added to 10 µl of 1 M ammonium bicarbonate (NH_4HCO_3) pH 8.8 (Severn Biotech) in a fresh 1.5 ml microcentrifuge tube. 6x loading dye was diluted to 1x in the elution and western blotting was performed to analyse protein pulldown.

2.10 *in vitro* kinase assay

Flp-In 293 cells expressing HA-IKKε wt or HA-IKKε KD-m were plated in 10 cm dishes at densities described in Table 2.2. 24 hours post-plating, cells were treated with 100 ng/ml doxycycline for 16 hours to induce HA-tagged kinase expression. Following doxycycline treatment, cells were washed with ice cold PBS containing Na_3VO_4 and NaF phosphatase inhibitors and frozen at -80°C till use. Cells were thawed and lysed on ice for 30 minutes with Triton 1% lysis buffer supplemented with HALT™ Phosphatase Inhibitor Cocktail (ThermoFisher Scientific - #78428). Cell lysates were centrifuged for 30 minutes at 13,000 g and lysate protein concentration was quantified as described in 2.5.3. HA-IKKε was purified from 1 mg of protein lysates using an HA-Pulldown as described in 2.9 up to the washing steps. After 2 washes in lysis buffer, Anti-HA-Agarose beads were washed twice in kinase buffer (Table 2.23 - as with the phosphoproteomic analysis, all phosphatase inhibitors were kindly provided by Dr Vinothini Rajeeve).

Following washes, the beads were resuspended in 40 µl of kinase buffer. 5 µl of 1 picoMol/µl recombinant His-tagged PSAT1 (Creative Biomart - #PSAT1-1328H) was added to the bead suspension, along with 5 µl of 10 mM ATP (New England Biolabs - #P0756S) to trigger the phosphorylation reaction. The reaction was incubated at room temperature for 20 minutes, after which the reaction was halted by adding 24 mg of solid urea (to a final 8M concentration in 50 µl) and vortexing till the urea had completely dissolved. The samples were then stored at -80°C till mass spectrometry analysis by Dr Pedro Cutillas and Dr Vinothini Rajeeve as described in 2.7. Phosphorylation of recombinant PSAT1 was analysed by integrating the peak areas of extracted ion chromatograms of the phosphorylated and un-phosphorylated PSAT1 derived peptides.

Table 2.23 – Recipe for kinase buffer for *in vitro* kinase assay.

Component	Concentration
Tris HCl (pH 7.8)	25 mM
$MgCl_2$	10 mM
EGTA	0.5 mM
DTT	1 mM
Na_3VO_4	1 mM
$Na_2P_2H_2O_7$	2.5 mM
β-glycerophosphate	20 mM

2.11 Analysis of Mitochondrial Function

For evaluation of oxygen consumption rate (OCR) in doxycycline-treated Flp-In 293 HA-IKKε cells and IKKε-siRNA-transfected breast cancer cells, Dr Ruoyan Xu prepared cells as described below and measured OCR using either an Oroboros O2k-FluoRespirometer (Oroboros - #10002-02) (Flp-In 293 cells) or a Seahorse XFe96 Analyzer (Agilent) (breast cancer cells).

For Flp-In 293 cells, cells were plated in 6-well plates and subsequently treated with 50 ng/ml doxycycline for 16 hours. Following treatment, cells were resuspended in Seahorse XF Assay Medium (Agilent - #102365-100) containing 4.5 g/l glucose, 1 mM pyruvate and 25 mM HEPES and OCR was measured at 37 °C using an Oroboros O2k-FluoRespirometer.

For breast cancer cell lines, cells were plated in 6-well plates and 24 hours later, were transfected with *IKBKE*-targeting siRNA as described in 2.1.7. 24 hours post-transfection, cells were trypsinised and re-plated in Seahorse XF Assay Medium in a Seahorse XF96 cell culture microplate (Agilent - #101085-004). 48 hours later, OCR was measured using the Seahorse XFe96 Analyzer.

Measurement of mitochondrial membrane potential was performed in collaboration with Professor Gyorgy Szabadkai at (University College London, London, UK). Flp-In 293 HA-GFP and HA-IKKε cells were plated in 96-well Black Clear Thin Bottom tissue culture plates (BD Falcon - #353219) at a density of 4000 cells per well and incubated at 37°C for 24 hours before use. Experimental conditions were applied as described in specific experiments and prior to imaging, 1 µg/ml Hoechst 33342 (Sigma Aldrich) and 30 nM tetramethylrhodamine, methyl ester (TMRM) (Molecular Probes) was added to the cells for 30 minutes. TMRM was also present in the medium (DMEM w/o phenol red) throughout imaging. Images were acquired by Dr Szabadkai using the ImageXpress Micro XL (Molecular Devices) high content wide field digital imaging system using a Lumencor SOLA light engine illumination with ex377/50 nm and em446/60 nm filters for detection of Hoechst staining or ex562/40 nm and em624/40 nm filters for detection of TMRM staining and a 60x, S PlanFluor ELWD 0.70 NA air objective, using laser based autofocusing. 16 fields were acquired per each well and images were analysed with the granularity analysis module in the MetaXpress 6.2 software (Molecular Devices) which identified mitochondrial (TMRM +) and nuclear (Hoechst +) objects. Average TMRM intensity per cell was calculated and averaged for each well and the mean from each well was used as individual data for statistical comparison of TMRM staining intensity between conditions.

2.12 Statistical Analysis and Figure Preparation

All statistical tests were performed in either GraphPad Prism version 5.04 or version 7.03 for Windows (GraphPad Software) using data from at least 3 biologically independent experiments, unless otherwise stated in figure legends. Specific tests on an experiment by experiment basis are detailed in figure legends. GraphPad Prism was also used to prepare graphs and Adobe Illustrator version 16.0.3, purchased as part of the Adobe Creative Suite 6 software package (Adobe Systems), was used to generate western blot figures. The heat map presented in Figure 3.8 B was generated using R and RStudio software with the ggplot2 package[332-334]. Schematics were prepared using a combination of Adobe Illustrator and Microsoft® PowerPoint® 2016 (Microsoft).

Chapter 3

Results I

IKKε directly phosphorylates PSAT1 to promote protein stability

Disclaimer: Whilst such instances are clearly indicated previously in the materials and methods and again in the following text and figure legends, the samples sent for labelled metabolite analysis and phosphoproteomic analysis with collaborators (Dr Christian Frezza and Dr Sofia De Costa at the MRC Cancer Unit in Cambridge, UK and Dr Pedro Cutillas and Dr Vinothini Rajeeve at Barts Cancer Institute in London, UK respectively) were prepared for analysis by other members of the Bianchi Lab group. The samples for labelled metabolite analysis (data presented in Figures 3.5, 3.6 and 3.18) were prepared by Dr Ruoyan Xu and the samples for phosphoproteomic analysis (data presented in Figure 3.8 and Table 3.2) were prepared by Dr Ewa Wilcz-Villega. In both cases, the author assisted with the post-run analysis of this data and the data was included with the intention to provide context for the work performed in this study as key cornerstones in the basis of the project, not as an attempt to suggest the work was performed by the author.

3.1 IKKε expression models

3.1.1 The Flp-In 293 system

As evidence emerges of a link between IKKε and regulation of cellular metabolism[106,189], this project set out to examine that link in a breast cancer setting. In order to investigate the effects of initial upregulation of IKKε on cellular metabolism, a model of IKKε induction was utilised, to reflect the early changes that will occur when the kinase is first overexpressed in cancer. Untransformed human embryonic kidney (HEK) cell line Flp-In 293 was used to generate a cell line in which HA-tagged IKKε could be induced via treatment with doxycycline. The Flp-In 293 system can generate stable cell lines expressing gene inserts via homologous recombination, as FRT sites flanking a gene insert are recombined with FRT sites in the host cell genome (see 2.2.4). In each parental Flp-In 293 cell line there is only one FRT gene insert site in the host cell genome meaning genes can only be inserted at a single location. When generating multiple cell lines, this means different genes are always inserted at the same location in the genome and are always expressed equally under the control of the same promoter. This allows comparison of proteins based on protein function rather than expression level, which makes the Flp-In 293 system a particularly effective system for comparing the activity of mutant versions of the same protein.

Doxycycline-inducible HA-IKKε and, for control purposes, HA-green fluorescent protein (GFP) Flp-In 293 cell lines were generated by Dr Ruoyan Xu to evaluate the effect of kinase induction on cellular metabolism. Consistent with the fact that IKKε is an inducible kinase, typically not expressed in basal conditions in most tissues[78], IKKε expression was undetectable in Flp-In 293 HA-IKKε cells prior to doxycycline treatment, but treatment with doxycycline resulted in stable expression of HA-tagged IKKε (Figure 3.1 B). A Flp-In 293 cell line expressing a HA-tagged kinase-dead mutant variant of IKKε was developed simultaneously with the HA-GFP and HA-IKKε wild-type (wt) cells. Introduction of a K38A point mutation in the kinase domain of IKKε is well known to ablate kinase activity[79]. An HA-tagged IKKε K38A mutant was generated by Dr Ruoyan Xu using point mutagenesis and, akin to GFP and IKKε wt, was expressed under a doxycycline inducible promoter in Flp-In 293 cells. The discrete cell lines will be termed Flp-In 293 HA-GFP, Flp-in 293 HA-IKKε wt and Flp-In 293 HA-IKKε KD-m from here on (Figure 3.1 C). To validate lack of HA-IKKε KD-m kinase activity, HA-IKKε wt and HA-IKKε KD-m were induced in Flp-In 293 cells and phosphorylation of IRF3 at serine residue Ser396, a known IKKε substrate, was assessed via western blotting. IRF3 was phosphorylated in the presence of HA-IKKε wt, but expression of HA-IKKε KD-m failed to phosphorylate IRF3, confirming of a lack of kinase activity (Figure 3.1 D).

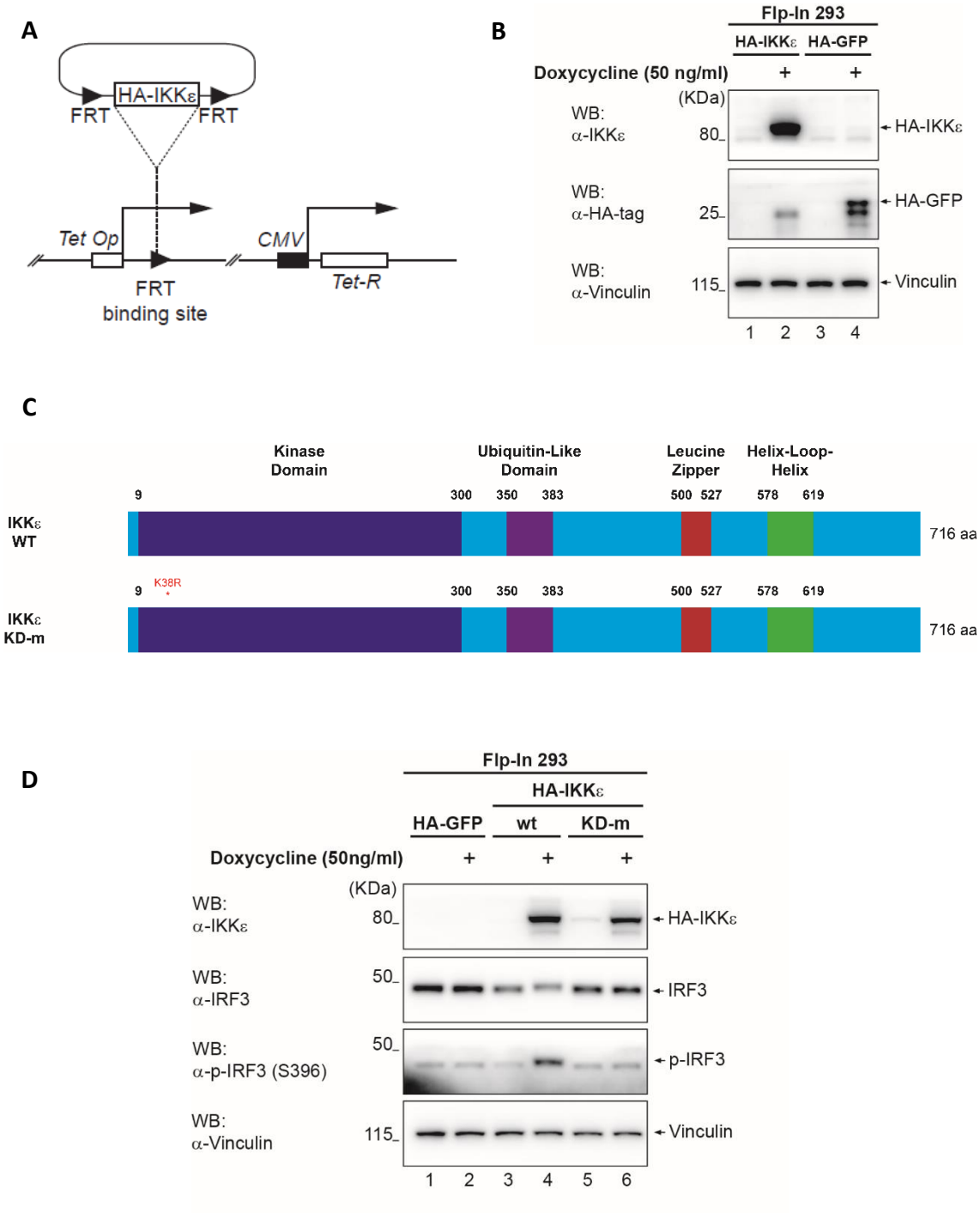

Figure 3.1 – Induction of HA-tagged IKKε expression in a Flp-In 293 cell model. (A) Schematic representation of the Flp-In system used in 293 HEK cells. HA-tagged IKKε within a *pcDNA5.5* vector is recombined into the host genome at FRT sites through the expression of FLP-recombinase on a secondary *pOG44* vector. The constitutively expressed *Tet-R* gene tetracycline repressor protein (TetR). TetR protein dimers bind the *Tet Op* sequence in the inducible gene promoter to repress transcription. Doxycycline binds TetR protein and prevents its binding to the *Tet Op* sequence, de-repressing transcription and driving HA-IKKε expression. **(B)** Western blot demonstrating induction of HA-IKKε or HA-GFP in Flp-In 293 cells. Indicated cell lines were treated with 50 ng/ml doxycycline for 16 hours, inducing expression of the kinase or GFP accordingly. Vinculin is shown as a loading control. **(C)** Schematic representation of the point mutation introduced into the IKKε sequence to ablate kinase domain function. **(D)** Western blot highlighting the lack of kinase activity in HA-IKKε KD-m. Indicated Flp-In 293 cell lines were treated with 50 ng/ml doxycycline for 16 hours to induce expression of their respective gene inserts. Phosphorylation of known substrate IRF3 by IKKε at serine residue Ser396 (S396) is abrogated by mutation of IKKε's kinase domain, demonstrating a lack of kinase activity. Vinculin is shown as a loading control.

3.1.2 Breast cancer cell line panel

To examine the effects of IKKε on cellular metabolism in breast cancer and in a setting where, in comparison to the Flp-In 293 system, kinase expression was long term and established, a panel of nine breast cancer cell lines were selected, all with varying degrees of IKKε expression and, since no correlation between oncogenic activity of the kinase and breast cancer subtype has been observed, from a range of disease subtypes (Table 3.1).

Table 3.1 – Breast cancer cell lines panel. Summary of the breast cancer cell lines used in this study, including the cancer type and subtype of the source disease.

Breast Cancer Cell Line	ZR-75-1	T-47D	MDA-MB-453	MDA-MB-468	MDA-MB-231	MCF7	Cal-120	HCC1143	SUM44
Cancer type	Invasive Ductal carcinoma	Invasive Ductal carcinoma	Metastatic carcinoma	Metastatic Adeno-carcinoma	Metastatic Adeno-carcinoma	Metastatic Adeno-carcinoma	Adeno-carcinoma	Ductal Carcinoma	Invasive Lobular Carcinoma
Subtype	Luminal-A (ER+)	Luminal-A	Basal (Triple Negative)	Basal (Triple Negative)	Basal (Triple Negative)	Luminal-A	Basal (Triple Negative)	Basal (Triple Negative)	Luminal A

To modulate IKKε expression in the breast cancer cells, cell lines were transfected with a pool of 4 small interfering RNA (siRNA) oligos targeting the *IKBKE* mRNA (which codes for IKKε). siRNA silences protein expression for a short period of time (typically less than 5 days) by targeting mRNA sequences for degradation via the RNA-Induced Silencing Complex (RISC). Assessing protein knockdown via western blot, it was confirmed that transfection of breast cancer cell lines with *IKBKE*-targeting siRNA suppressed kinase expression (Figure 3.2), facilitating comparison of cell line metabolic status before and after kinase knockdown. This therefore allowed characterisation of the effects of long term IKKε expression on cellular metabolism.

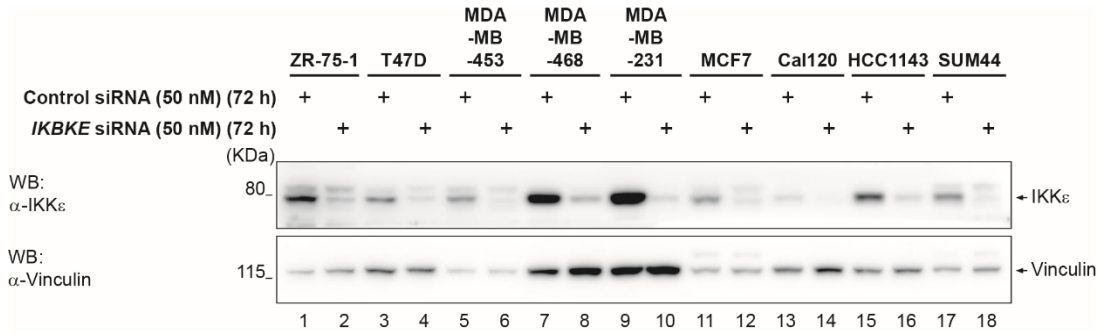

Figure 3.2 – siRNA-mediated suppression of IKKε expression in a panel of breast cancer cell lines. Western blot demonstrating effective knockdown of IKKε in breast cancer cell lines using siRNA. Indicated cell lines were transfected with a pool of 4 *IKBKE*-targeting siRNA oligos, to suppress IKKε, or a single non-targeting control oligo to a final concentration of 50 nM for 72 hours. Following transfection, the efficiency of IKKε protein level knockdown was assessed. Vinculin is shown as a loading control.

When oncogenic in a subset of breast cancer cells, IKKε has been shown to be required for maintenance of proliferative rates[195]. To determine the best cell line model for characterising metabolic changes, the effect of siRNA-mediated IKKε suppression on proliferation was evaluated to identify a cell line in which the kinase was essential for continued proliferation (Figure 3.3). Breast cancer cell growth upon siRNA-mediated knockdown of IKKε was assessed using the IncuCyte Zoom system, a live cell imaging system which incubates cells at optimal growth conditions to facilitate imaging over longer periods. By training the system to recognise cells, a mask can be applied to captured phase-contrast images (Figure 3.3 A and B) which can be used to determine cell confluency at defined time intervals. Tracking cell confluency over time at repeated time intervals therefore allows the generation of reliable growth curves and the measurement of proliferation. Tracking of cell proliferation upon siRNA-mediated suppression of IKKε in the breast cancer cell line panel revealed that kinase suppression significantly reduced proliferative rates of 3 out of the 8 cell lines tested; ZR-75-1, T47D and MCF7 (Figure 3.3 C-F). This is in partial agreement with existing literature, where suppression of IKKε via short hairpin RNA (shRNA) has been shown to reduce the proliferation of ZR-75-1 and MCF7[195]. However shRNA-mediated suppression of the kinase has also been shown to suppress proliferation of MDA-MB-231 and MDA-MB-468 cell lines[213], where no effect on proliferation was observed according to this data. This discrepancy is likely attributable to the different approaches taken to suppress IKKε expression and the inherent difference between stable suppression of the kinase with shRNA compared to transient suppression with siRNA. Different knockdown efficiency of the kinase could also easily have different effects on proliferation, though it is difficult to compare the efficiency of knockdown between shRNA and siRNA. The effect of siRNA knockdown of IKKε must therefore be compared with previous findings using shRNA with some caution. In the context of this project, this data demonstrates that ZR-75-1, T47D and MCF7 breast cancer cell lines exhibit a dependency on IKKε for maintenance of proliferation, suggesting that IKKε is strongly oncogenic in these models.

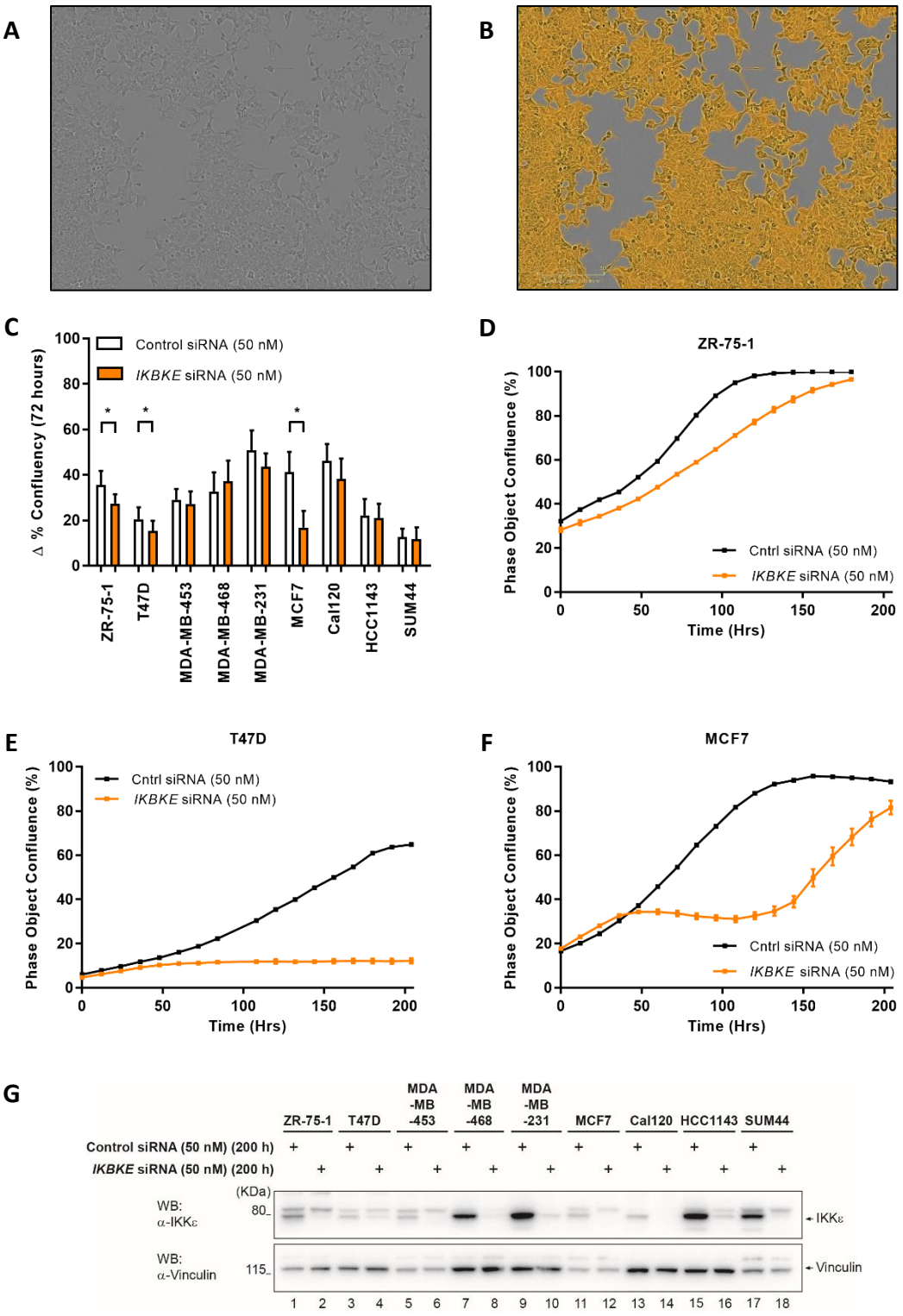

Figure 3.3 – IKKε suppression reduces proliferation in a subset of breast cancer cell lines. (A and B) Representative images of IncuCyte cell growth tracking. Phase contrast image is captured (A) then a cell mask is applied (B) using the IncuCyte Zoom 2016A software to track confluency. **(C)** siRNA-mediated suppression of IKKε reduced proliferation in ZR-75-1, T47D and MCF7 breast cancer cell lines. Proliferation of indicated cell lines was tracked using the IncuCyte over the days following transfection with a pool of 4 *IKBKE*-targeting siRNA oligos, to suppress IKKε, or a single non-targeting control oligo to a final concentration of 50 nM. Cells were washed of siRNA 16 hours post-transfection and placed on the IncuCyte for ongoing growth tracking. Delta confluency was calculated between 0 and 72 hours to identify significant changes in proliferation. n≥3 independent experiments, mean ± SEM, * $p<0.05$ as measured by two-tailed Student's t-test. **(D-F)** Representative IncuCyte growth curves for single experiments in ZR-75-1 (D), T47D (E) and MCF7 (F) cell lines. Mean ± SD. **(G)** Western blot of cells harvested at the end of IncuCyte growth tracking demonstrating maintenance of knockdown to the end of the experiment. Vinculin is shown as a loading control.

3.2 Characterisation of IKKε-dependent metabolic changes

In order to determine what changes in metabolic states were induced by modulation of IKKε expression, labelled metabolite analysis was performed with the kind help of Dr Christian Frezza and Dr Sofia De Costa at the MRC cancer unit in Cambridge, UK. Labelled metabolite analysis allows the tracking of the utilisation of glucose-derived carbon or glutamine-derived nitrogen throughout the intracellular metabolic pathways by feeding cells with labelled versions of glucose and glutamine. Carbon atoms typically have an atomic mass of 12 (^{12}C) and nitrogen atoms typically have a mass of 14 (^{14}N). By feeding cells with a version of glucose in which the 6 carbon atoms are replaced with ^{13}C, or with a version of glutamine in which the nitrogen atom is replaced with ^{15}N, carbon and nitrogen atoms which are heavier than usual by 1 unit of atomic mass are incorporated into the cellular metabolic network. As glucose and glutamine are subsequently metabolised within the cell, these heavier carbon and nitrogen atoms are incorporated into the resulting metabolites, increasing their molecular weights by a measurable degree proportional to the number of heavier carbon or nitrogen atoms they contain. Increases in metabolite mass can be detected by mass spectrometry and therefore, the heavier carbon/nitrogen atom can be tracked from its glucose/glutamine source to the end product, allowing mapping of the intracellular metabolic networks and characterisation of the utilisation of glucose carbon and glutamine nitrogen (Figure 3.4).

Labelled metabolite analysis was performed in Flp-In 293 HA-IKKε wt cells and compared to analysis performed in Flp-In 293 HA-GFP cells. For analysis of IKKε-dependent breast cancer cells, T47D was selected as the optimal model as, whilst siRNA knockdown also reduced proliferation of ZR-75-1 and MCF7 cell lines, ZR-75-1 and MCF7 both eventually overcame IKKε knockdown and continued proliferation, whereas T47D showed a much greater loss of proliferation upon knockdown of the kinase (Figure 3.3 D-F). As with the Flp-In 293 cell models, labelled metabolite analysis was performed in *IKBKE*-targeting siRNA-transfected T47D cells and in control, non-targeting siRNA-transfected cells. By comparing the results in Flp-In 293 cells and T47D cells before and after modulation of IKKε expression, it was possible to map key changes in intracellular metabolism which were induced or maintained by the kinase.

To characterise IKKε-dependent changes in cellular metabolism, Dr Ruoyan Xu treated Flp-In 293 HA-IKKε and HA-GFP cells with 50 ng/ml doxycycline for 16 hours and transfected T47D breast cancer cells with a pool of 4 *IKBKE*-targeting siRNA oligos, to suppress IKKε, or a single non-targeting control oligo for 72 hours. Following this, metabolites were extracted and mass spectrometry analysis of labelled and total metabolite abundance was performed by Dr Christian

Frezza and Dr Sofia De Costa and characterisation of IKKε-dependent metabolic changes was facilitated by plotting the Z-scores for each metabolite in each individual sample in a heat map. Raw data from these experiments are presented as supplementary material (see supplementary materials: Table 7.2.)

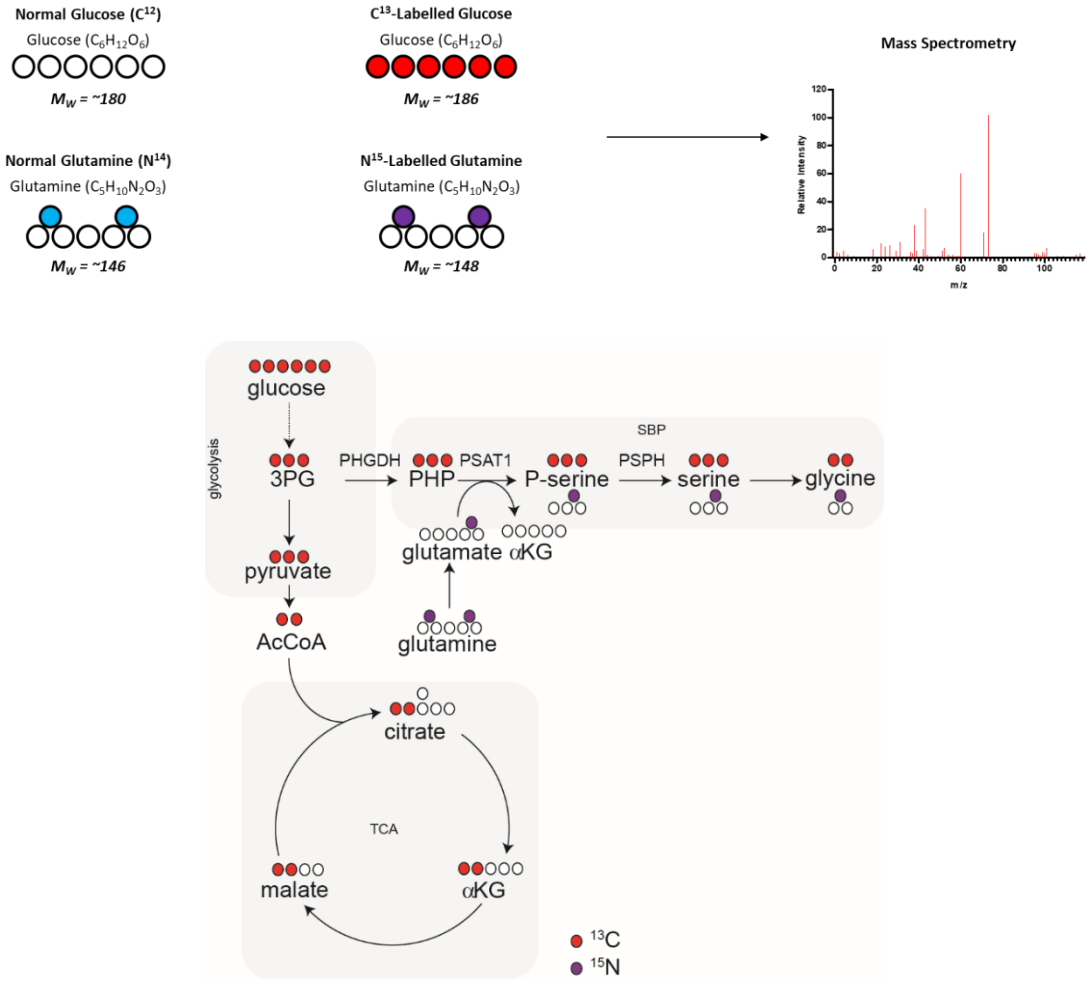

Figure 3.4 – Principal of labelled metabolite analysis. Cells are fed with a version of glucose containing ^{13}C carbon (as opposed to ^{12}C) or a version of glutamine containing or ^{15}N nitrogen (instead of ^{14}N). As the glucose and glutamine are metabolised within the cell, the heavier carbon and nitrogen atoms are incorporated into the structures of metabolites, generating a pool of metabolites with higher molecular weights than usual. This increase in molecular weight can be detected by mass spectrometry to track the utilisation of glucose-derived carbon and glutamine-derived nitrogen throughout the cell. Labelled (^{13}C) carbon is represented as red dots and labelled (^{15}N) nitrogen as purple dots to represent how labelled atoms are incorporated throughout the intracellular metabolic network.

In both the Flp-In 293 and T47D cell models, modulation of IKKε expression demonstrated significant metabolic effects. In the Flp-In 293 cells HA-IKKε-expressing cells exhibited significantly higher intracellular levels of various amino acids such as serine and glycine, a significant increase in intracellular glutamine levels and a significant decrease in the levels of

TCA metabolites such as citrate and malate compared to the levels detected in HA-GFP-expressing cells. Concurrently, suppression of IKKε expression in T47D breast cancer cells led to a significant decrease in intracellular levels of multiple amino acids such as, again, serine and glycine, a significant decrease in glutamine levels and lactate concentration and a significant increase in levels of TCA metabolites like citrate, malate and fumarate (Figure 3.5 A and Figure 3.6 A). Together, these data indicated that expression of IKKε upregulates and maintains intracellular concentrations of multiple amino acids and glutamine, whilst suppressing concentrations of TCA cycle intermediates.

Of all the amino acids which exhibited a significant increase in IKKε-expressing cells, the significant increase in intracellular serine and glycine levels stood out as particularly interesting, given the established importance of the SBP in breast cancer[304,305] (see 1.4.4.2). With this in mind, metabolite ion levels were examined in order to identify the source of the serine and glycine which was responsible for the increased intracellular concentrations observed. As each ^{13}C carbon atom is exactly 1 unit of atomic mass heavier than natural ^{12}C carbon (and ^{15}N nitrogen is exactly 1 unit heavier than natural ^{14}N), the molecular weight of a metabolite will be increased by 1 for every labelled atom that is incorporated into its structure. Therefore, increases in the molecular weight of metabolites in discrete intervals of 1 atomic unit allows determination of how many labelled atoms are incorporated into the metabolite structure. By understanding how many carbons and nitrogens are donated to a protein during biosynthesis, it is therefore possible to distinguish between metabolites that are synthesised within the cell and those which are merely taken up into the cell from the extracellular environment. In the context of serine and glycine, serine that is produced via *de novo* serine biosynthesis from glucose incorporates 3 glucose-derived carbons into its structure and glycine incorporates 2. Therefore, cells that have been supplied with ^{13}C-labelled glucose will produce a serine m+3 ion and a glycine m+2 ion. On the other hand, serine is also frequently obtained from the extracellular environment and this will not contain labelled carbon. Therefore, serine sourced from extracellular pools and glycine produced from such serine will only be detected at their regular molecular weights. Similarly, the amino group added to biosynthesised serine and carried over to glycine is obtained from glutamine. Therefore, it gains one nitrogen atom from glutamine in the process and an m+1 ion of serine and glycine will be produced in biosynthesised serine when cells are fed with ^{15}N-labelled glutamine (Figure 3.4).

Induction of IKKε in Flp-In 293 cells resulted in a significant upregulation in the levels of m+3 labelled serine and of ^{15}N-labelled serine in cells fed with ^{13}C-labelled glucose and ^{15}N-labelled glutamine respectively (Figure 3.5 B). Additionally, whilst serine m+3 levels could not be stably

detected in T47D cells, siRNA-mediated suppression of IKKε lead to a significant decrease in glycine m+2 ion levels in cells fed with ^{13}C-labelled glucose and a significant decrease in levels of ^{15}N-labelled glycine in cells fed with ^{15}N-labelled glutamine (Figure 3.6 B). An increase in serine m+3 and ^{15}N-serine levels in glucose and glutamine-labelled analysis indicates an increase in serine biosynthesis activity within Flp-In 293 cells expressing HA-IKKε. Similarly, a decrease in glycine m+2 and ^{15}N-glycine levels indicates a decrease in serine biosynthesis activity in *IKBKE* siRNA-transfected T47D cells. Together, these data demonstrate that IKKε expression enhances SBP activity in cells in which it is expressed.

As most cancers divert glucose-derived carbon away from mitochondrial entry and TCA cycle utilisation, it was also intriguing to observe an IKKε-induced reduction in the levels of TCA metabolites like citrate, malate and fumarate. Again, examination of changes in labelled metabolite ion levels revealed further details about this reduction. In Flp-In 293 cells, IKKε expression significantly reduced citrate and malate m+2 ion levels. Furthermore, suppression of the kinase in T47D breast cancer cells resulted in a significant upregulation of citrate and malate m+2 ion levels, confirming that the kinase inhibits the formation of these m+2 ions (Figure 3.5 C and Figure 3.6 C). When the TCA cycle is fuelled by glucose-derived carbon, each turn of the cycle involves the combining of oxaloacetate from the cycle with a molecule of glucose-derived acetyl-CoA to regenerate citrate. Acetyl-CoA contains 2 glucose-derived carbon atoms, meaning that each turn of the TCA cycle involves the incorporation of 2 glucose-derived carbon atoms to its metabolite pool. This means that feeding of cells with ^{13}C-labelled glucose will result in the generation of m+2 ions for the TCA cycle intermediates (Figure 3.4). Hence, an IKKε-mediated reduction in m+2 TCA metabolite ions indicates that expression of the kinase reduces the incorporation of glucose-derived carbon into the TCA cycle.

It is therefore evident that IKKε dramatically alters the state of the intracellular metabolic network. Labelled metabolite analysis data revealed IKKε-dependent increases in lactate, elevated biosynthetic activity in the form of increased serine biosynthesis and reduced incorporation of glucose-derived carbon in the TCA cycle. It is particularly interesting to note that this 3-pronged change in metabolic state is characteristic of the key metabolic changes that frequently occur in the aerobic glycolysis phenotype of tumours. Tumours with such a metabolic phenotype almost always exhibit increased glycolysis with diversion of glucose-derived carbon away from mitochondrial pathways, increased lactate production and increased biosynthetic pathway activities. Consequently, this data suggests that expression of IKKε is sufficient to promote and maintain an aerobic glycolysis-like phenotype in Flp-In 293 cells and human breast cancer cells.

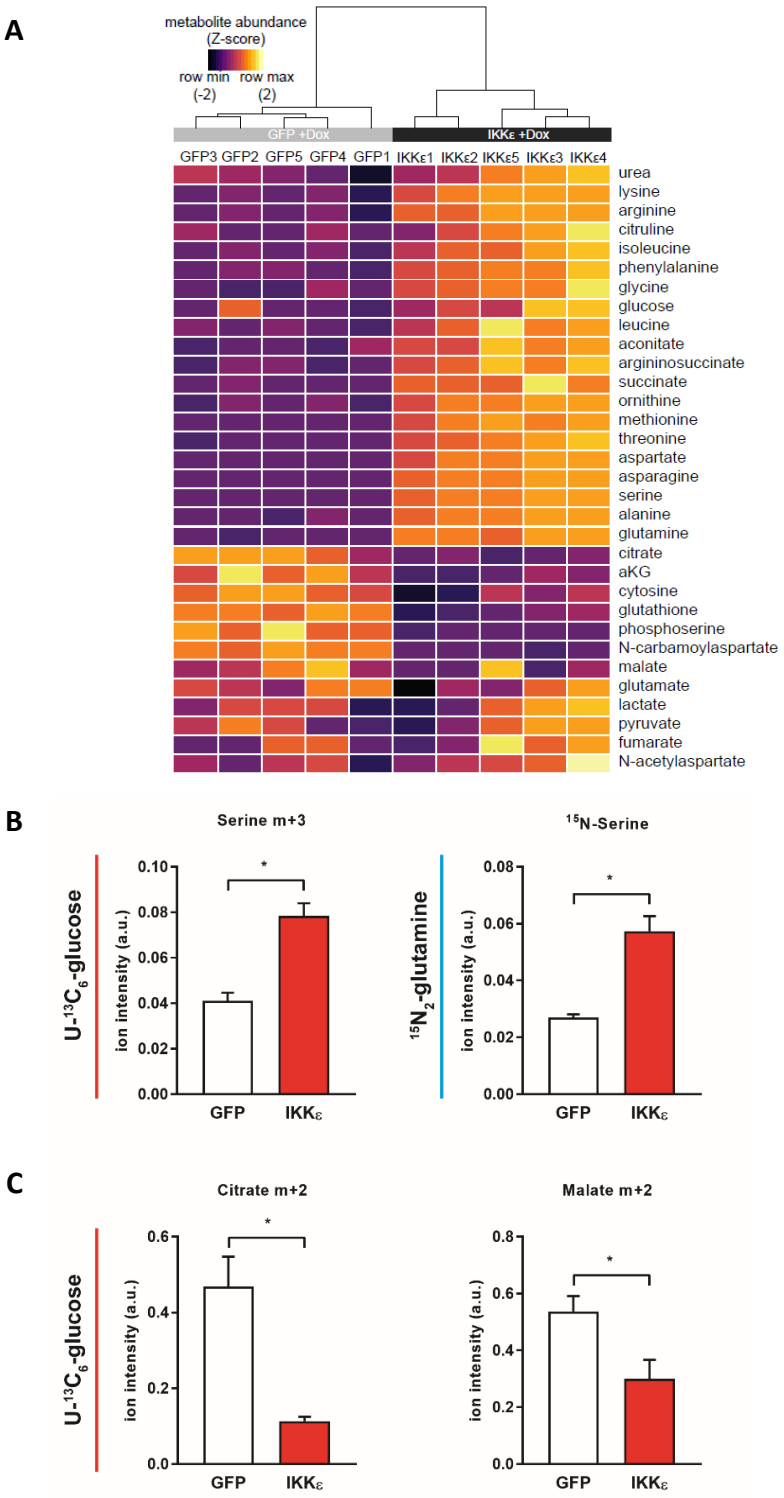

Figure 3.5 – IKKε induces an aerobic glycolysis-like phenotype in Flp-In 293 cells. Flp-In 293 HA-IKKε and HA-GFP cells were treated, by Dr Ruoyan Xu, with 50 ng/ml doxycycline for 16 hours, with simultaneous addition of ^{13}C-labelled glucose and ^{15}N-labelled glutamine tracer compounds for the final 14 hours. Intracellular metabolite abundance was measured using mass spectrometry, kindly performed by Dr Christian Frezza and Dr Sofia De Costa. **(A)** Heat map and hierarchical clustering produced by Dr Christian Frezza and Dr Sofia De Costa following analysis of significant changes in relative metabolite abundance in HA-IKKε-expressing Flp-In 293 cells compared to HA-GFP-expressing cells. **(B)** IKKε induces serine production from glucose (serine m+3 in ^{13}C-labelled glucose fed cells) and glutamine (^{15}N-serine in ^{15}N-labelled glutamine fed cells). **(C)** IKKε inhibits incorporation of glucose-derived carbon into the TCA cycle (citrate m+2 and malate m+2 in ^{13}C-labelled glucose fed cells). n=5 biological replicates, mean ± SEM, *p<0.05 as measured by two-tailed Student's t-test.

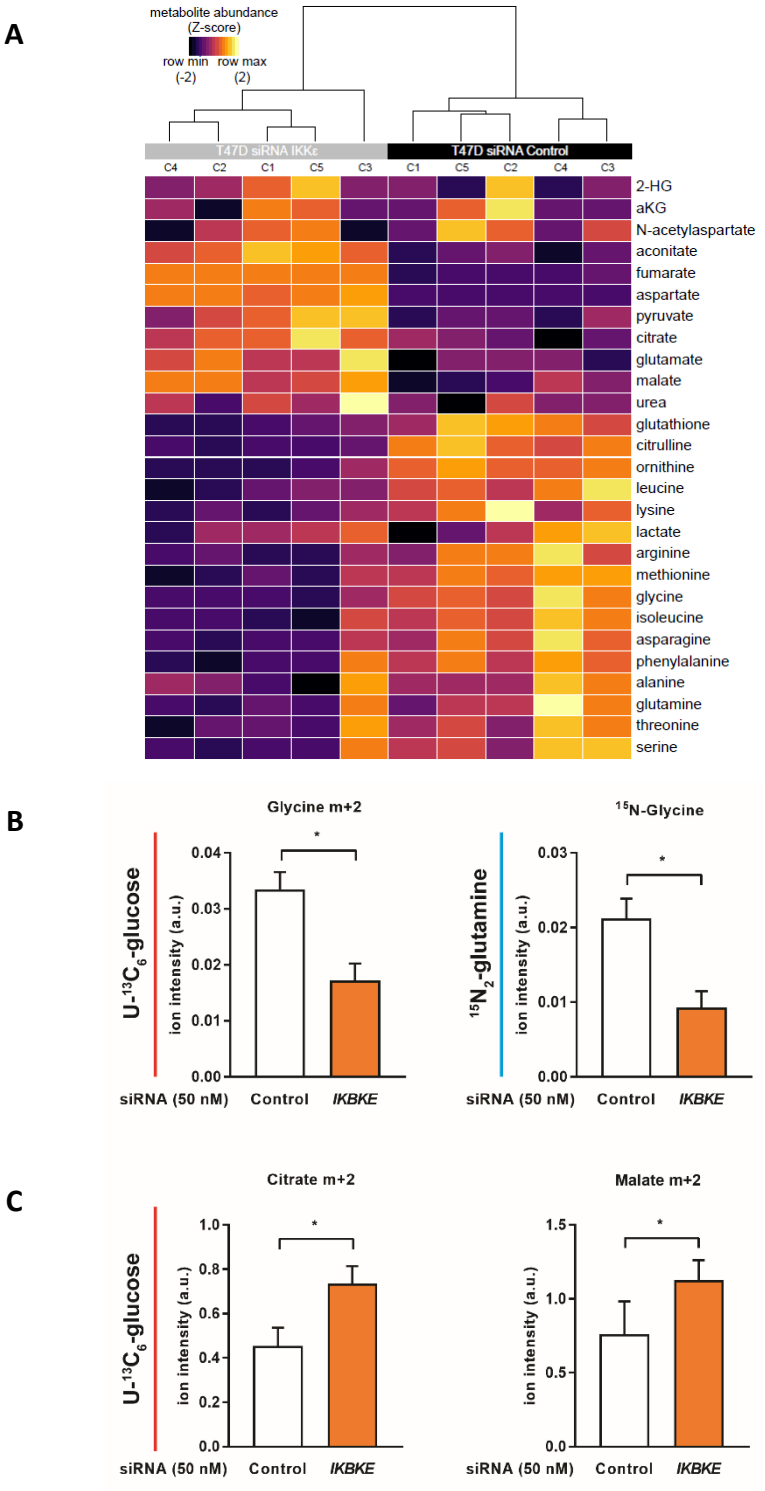

Figure 3.6 – IKKε maintains an aerobic glycolysis-like phenotype in T47D breast cancer cells. T74D breast cancer cells were transfected, by Dr Ruoyan Xu, with 4 siRNA oligos targeting *IKBKE* mRNA, to suppress IKKε, or a single non-targeting control oligo at 50 nM final concentration for 72 hours. Cells were fed with labelled glucose and glutamine tracer compounds for the final 14 hours. Intracellular abundance of metabolites was measured by mass spectrometry, performed by Dr Christian Frezza and Dr Sofia De Costa. **(A)** Heatmap and hierarchical clustering produced by Dr Christian Frezza and Dr Sofia De Costa following analysis of significantly changing metabolite abundance following siRNA-mediated IKKε suppression in T47D cells **(B)** IKKε silencing reduces serine and thus glycine production from glucose (glycine m+2 in cells fed with ^{13}C-labelled glucose) and glutamine (^{15}N-glycine in cells fed with ^{15}N-labelled glutamine). **(C)** IKKε silencing promotes incorporation of glucose-derived carbon into the TCA cycle (citrate m+2 and malate m+2 in cells fed with ^{13}C-labelled glucose). n≥4 biological replicates, mean ± SEM, *p<0.05 as measured by Student's t-test.

3.3 Identification of potential IKKε phosphotargets

In order to understand more about how IKKε was inducing changes in cellular metabolism in the Flp-In 293 and breast cancer cell models, possible effector targets were sought. Given its role as a kinase, a phosphoproteomic analysis was performed to identify proteins that exhibited significant changes in phosphorylation status upon modulation of IKKε expression. To identify protein phosphorylations which would be altered in a linear fashion relative to the expression level of the kinase, 3 independent single-cell clones of Flp-In 293 HA-IKKε cells, expressing HA-IKKε at varying degrees, were induced alongside 3 independent single-cell clones of Flp-In 293 HA-GFP cells. Protein phosphorylation status in Flp-In 292 HA-GFP cells was used as a control to define a basal level of IKKε-independent phosphorylation (Figure 3.7).

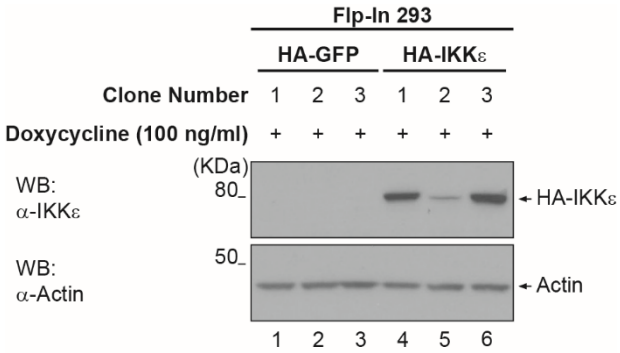

Figure 3.7 – Induction of HA-IKKε expression in 3 independent single-cell clones. Western blot demonstrating induction of HA-IKKε in 3 single-cell clones of Flp-In 293 HA-IKKε (wt) cells, following treatment of cells with 100 ng/ml doxycycline for 16 hours. 3 single-cell clones of Flp-In 293 HA-GFP cells were also treated with doxycycline as a control for IKKε expression. Actin is shown as a loading control.

Samples were prepared for the phosphoproteomic analysis by Dr Ewa Wilcz-Villega. Flp-In 293 HA-IKKε and HA-GFP single-cell clones were treated with doxycycline for 16 hours, after which cells were washed and lysed with a specialised lysis buffer containing multiple phosphatase inhibitors (Recipe: 8M Urea, 20 mM HEPES, 1 mM sodium orthovanadate (Na_3VO_4), 1 mM sodium fluoride (NaF), 1 mM β-Glycerol phosphate and 0.25 mM disodium diphosphate ($Na_2H_2P_2O_7$)) to maintain protein phosphorylation status within the lysate. Subsequently, protein phosphorylation was detected via mass spectrometry analysis in collaboration with Dr Pedro Cutillas and Dr Vinothini Rajeeve (Barts Cancer Institute, London, UK). Detected changes in protein phosphorylation were calculated as fold changes relative to the average phosphorylation of the protein in the 3 HA-GFP-expressing clones.

3.3.1 IKKε expression induces phosphorylation of serine biosynthesis enzyme PSAT1

To identify *bona fide* IKKε phosphorylation targets, proteins identified with significant changes in phosphorylation status were ranked from greatest increase in phosphorylation in the presence of IKKε, to greatest decrease (see supplementary materials: Table 7.3). Subsequently, pathway analysis was applied to group identified proteins based on their primary functions and identify potential phosphorylation targets that might explain the observed changes in cellular metabolism processes. To group the proteins in this way, identified proteins were analysed against the Kyoto encyclopaedia of genes and genomes (KEGGS) database and discrete cellular functions were ranked based on the number of differentially phosphorylated proteins identified. As expected based on IKKε's role in innate immunity, many of the pathways with the most proteins enriched for phosphorylation in the presence of IKKε are associated with the cellular response to infection, including pathways involved with antibiotic biosynthesis and pathways that respond to bacterial or viral infection. Reassuringly however, many metabolic pathways exhibited significant enrichment in protein phosphorylation. Such pathways included glycolysis, purine and carbon metabolism and most interestingly, given the increase in serine biosynthesis observed in IKKε-expressing cells, pathways involved in the biosynthesis of amino acids. Accordingly, changes in the IKKε-mediated phosphorylation of proteins associated with KEGGS pathway hsa01230: Biosynthesis of amino acids were represented as a heat map (Figure 3.8 B).

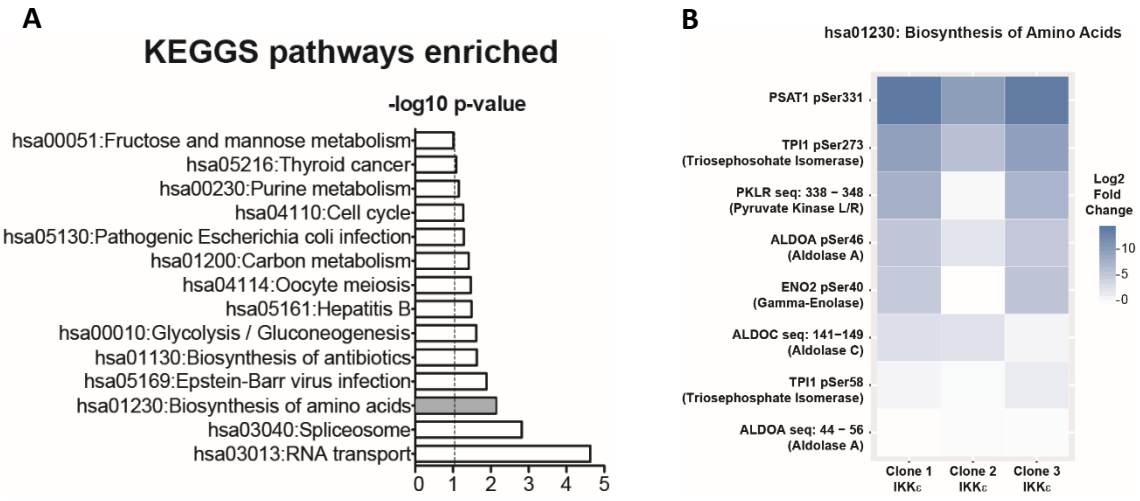

Figure 3.8 – KEGGS pathway enrichment analysis of phosphoproteomic data. (A) Identification of pathways enriched for phosphorylation of proteins in Flp-In 293 HA-IKKε cells compared to Flp-In 293 HA-GFP control cells identified a significant metabolic footprint in the phosphoproteome of IKKε-expressing cells, including significant enrichment of protein phosphorylation in biosynthetic processes involved in amino acid production. Enriched pathways from differentially phosphorylated proteins were determined by Dr Pedro Cutillas and Dr Vinothini Rajeeve, using David Bioinformatic resources[335]. **(B)** Heat map demonstrating the $\log_2$ fold changes in relative peptide abundance in 3 IKKε-expressing Flp-In 293 HA-IKKε single cell clones versus the average abundance in HA-GFP-expressing cells for peptides associated with KEGG pathway hsa01230: Biosynthesis of amino acids. Peptides are ranked by $\log_2$ fold change.

Closer examination of differentially phosphorylated peptides and identified phosphosites revealed a clear metabolic signature in Flp-In 293 HA-IKKε-expressing cells (Table 3.2). Multiple glycolytic enzymes were identified as more phosphorylated in the presence of IKKε including fructose-1,6-bisphosphate aldolase, which catalyses the conversion of fructose-1,6-bisphosphate to dihydroxyacetone phosphate and glyceraldehyde-3-phosphate; triosephosphate isomerase, which catalyses the conversion of dihydroxyacetone phosphate to glyceraldehyde-3-phosphate; and enolase, which catalyses the conversion of 2-phosphoglycerate to phosphoenolpyruvate (Figure 1.4). Glutamine-fructose-6-phosphate aminotransferase 1 (GFPT1), an enzyme which controls the flux of glucose-derived carbon into the hexosamine biosynthetic pathway was also identified as significantly more phosphorylated at Ser261 in IKKε-expressing cells. Ser 243 in a splice variant of GFPT1 is a key catalytic residue[336,337], which corresponds to Ser261 in the full-length protein. This therefore indicates that IKKε might induce GFPT1 activity through Ser261 phosphorylation, implicating the kinase in the regulation of hexosamine biosynthesis as well as serine.

Most interestingly however, considering the observed increase in serine biosynthesis in IKKε-expressing cells, was the identification of significantly increased PSAT1 phosphorylation at serine residue Ser331. PSAT1 catalyses the second step of the SBP. Again, no function for this Ser331 phosphosite has previously been described, but the observation that increased PSAT1 phosphorylation was occurring in the same context as increased serine biosynthesis led to the hypothesis that phosphorylation of enzyme at residue Ser331 might contribute to its activity and that IKKε might enhance serine biosynthesis through direct or indirect PSAT1 phosphorylation.

Table 3.2 – Selection of metabolic hits from phosphoproteomic analysis of HA-IKKε-expressing cells. Metabolism associated enzymes which were identified as significantly more or less phosphorylated at the indicated residues in HA-IKKε-expressing Flp-In 293 cells compared to HA-GFP controls. Phosphorylation of proteins in individual single-cell clones was expressed as a fold change (FC) vs the average basal phosphorylation across 3 HA-GFP-expressing single-cell clones. Information regarding phosphosite function was obtained from the PhosphoSitePlus® database[338]

Enzyme	Uniprot_ID	Metabolic role	p-Site	Function	Clone 1 IKKε FC	Clone 2 IKKε FC	Clone 3 IKKε FC
Acetyl CoA Carboxylase	ACACA_HUMAN	Fatty acid synthesis	Ser29	Unknown	-0.621988	0.093040754	-0.430474067
Fructose bisphosphate aldolase A	ALDOA_HUMAN	Glycolysis	Ser46	Unknown	5.2857515	2.041538354	5.016684377
Gamma enolase	ENOG_HUMAN	Glycolysis	Ser40	Unknown	4.765828412	-1.01621914	5.481481966
Glutamine-fructose-6-phosphate aminotransferase 1 (GFPT1)	GFPT1_HUMAN	Hexosamine synthesis	Ser261	Activity Induction	0.56334683	0.560639173	0.59498462
Phosphoserine aminotransferase 1 (PSAT1)	SERC_HUMAN	Serine synthesis	Ser331	Unknown	14.17208856	9.847138787	13.98893907
Pyruvate dehydrogenase E1 component subunit alpha (PDHA1)	ODPA_HUMAN	Acetyl CoA synthesis	Ser232	Activity Inhibition	0.92593026	0.022229478	0.968623429
Triosephosphate Isomerase	TPIS_HUMAN	Glycolysis	Ser58	Unknown	0.540049027	-0.18066612	1.356722214
Triosephosphate Isomerase	TPIS_HUMAN	Glycolysis	Ser273	Unknown	9.480225515	5.854468698	9.555515476

3.4 PSAT1 serine residue Ser 331 is phosphorylated in an IKKε-dependent manner

The observation that PSAT1 Ser331 was significantly more phosphorylated in the presence of IKKε led to the question of whether or not the kinase was itself directly phosphorylating the enzyme. When comparing the established IKKε recognition motif[197] with the amino acid sequence surrounding the identified PSAT1 phosphosite, overlap between 3 out of the 4 optimal residues was observed (Figure 3.9 A). This strongly indicated that the Ser331 residue on PSAT1 could be a phospho-target of IKKε, directly phosphorylated by the kinase. To test this hypothesis, an *in vitro* kinase assay was performed using recombinant PSAT1 and either HA-IKKε wt or HA-IKKε KD-m purified from Flp-In 293 cells via HA-pulldown. Flp-In 293 HA-IKKε wt and HA-IKKε KD-m cell lines were treated with doxycycline for 16 hours and lysates were incubated with anti-HA antibody-conjugated agarose beads to bind and purify HA-IKKε from the total lysate. Purified kinase was then combined with recombinant PSAT1 and ATP to facilitate a phosphorylation reaction *in vitro.* Phosphorylation of recombinant PSAT1 was subsequently detected via mass spectrometry analysis kindly performed by Dr Pedro Cutillas and Dr Vinothini Rajeeve.

Targeted analysis was performed to specifically search within the assay samples for peptides matching the profile of phosphorylated Ser331 PSAT1. Phosphorylation of the enzyme was detected in the *in vitro* kinase assay in the presence of HA-IKKε, but not in assay samples using HA-purified lysates where the kinase had not been induced, confirming IKKε-dependent phosphorylation of the enzyme. Somewhat discouragingly, phosphorylation was detected in samples containing HA-IKKε KD-m as well as HA-IKKε wt (Figure 3.9 B). To understand why the kinase dead mutant IKKε was inducing phosphorylation, the mutant's kinase activity was checked. Mass spectrometry analysis revealed the wt kinase was phosphorylated at several sites, whereas no phosphorylation of the KD-m mutant was detected (Figure 3.9 C). Active IKKε typically exhibits phosphorylation of serine residue Ser172 on its own sequence, attributable to kinase activity-mediated auto-phosphorylation[78] and whilst no Ser172 phosphorylation was detected with either kinase, a complete lack of any detectable phosphorylation on HA-IKKε KD-m indicates its lack of activity. Furthermore, western blot evaluation of HA-IKKε Ser172 phosphorylation demonstrated a complete absence of auto-phosphorylation with the kinase dead IKKε. HA-IKKε KD-m also exhibited an inability to phosphorylate known IKKε substrates such as IRF3 and p65 (Figure 3.9 D) confirming a lack of kinase activity. These data therefore demonstrated that phosphorylation of PSAT1 in the HA-IKKε KD-m samples was down to another explanation than residual kinase activity in the kinase-dead mutant.

The washing conditions used for the HA-pulldown were not particularly stringent (see 2.9 and 2.10) so it was hypothesised that protein-protein interactions might have been maintained throughout the pulldown allowing the presence of proteins other than IKKε to be purified from the cell lysates, meaning other proteins might have then been present in the *in vitro* kinase assay reaction. It was therefore hypothesised that the presence of a secondary kinase in the reaction might have been responsible for the observed PSAT1 phosphorylation in the HA-IKKε KD-m samples. To test this hypothesis, the mass spectrometry analysis was consulted to search for other kinases that were present in the assay and a total of 18 kinases other than IKKε were found to be detected in some, or all, of the other assay samples (Table 3.3). To determine whether one of these other kinases was a likely candidate for explaining the phosphorylation detected with HA-IKKε KD-m, the list of 18 kinases was filtered to highlight kinases that were detected in all of the samples were PSAT1 phosphorylation was detected. This left just 6 kinases from the initial 18. A secondary filter was then applied, ruling out kinases which were detected in the lysis buffer blank. No organic material should have been present in this sample and therefore any kinase detection was likely to be a false positive. Just one kinase was left from the 18 after applying this secondary filter: TBK1. This was particularly interesting, as TBK1 is a fellow IKK family member and is known to share several phospho-targets with IKKε, including IRF3 and p65. It was therefore hypothesised that if IKKε could phosphorylate PSAT1, then TBK1 might be responsible for the phosphorylation observed in the samples containing HA-IKKε KD-m. Whilst it is possible that all PSAT1 phosphorylation observed could be a result of secondary kinase activity, it is important to note that the observed phosphorylation is, at the very least, IKKε-dependent. Even though other kinases, TBK1 included, were present in the samples where PSAT1 phosphorylation was detected, the same kinases were also present in samples where PSAT1 phosphorylation was not detected. Indeed, phosphorylation was only detected in samples where HA-IKKε was present, demonstrating a dependency on the kinase. It is possible that TBK1 can phosphorylate PSAT1, but it seemingly requires IKKε to do so, possibly as a TBK1/IKKε heterodimer.

In order to attempt to distinguish which kinase in particular can phosphorylate PSAT1, an *in vitro* kinase assay was performed using recombinant PSAT1 with recombinant IKKε and recombinant TBK1, either alone or in combination. Unfortunately, no PSAT1 phosphorylation was detected in any of these samples and when using the mass spectrometry results to search for evidence of IKKε and TBK1 auto-phosphorylation, there was no indication of any kinase activation, suggesting that the lack of PSAT1 phosphorylation was attributable to kinase inactivity during the assay. Therefore, the furthest conclusion that can be drawn from this data is that PSAT1 Ser331 phosphorylation does occur in an IKKε-dependent manner. However, it remains to be

determined whether IKKε itself, or an IKKε containing complex with a secondary kinase, such as TBK1, is responsible for the actual phosphorylation event.

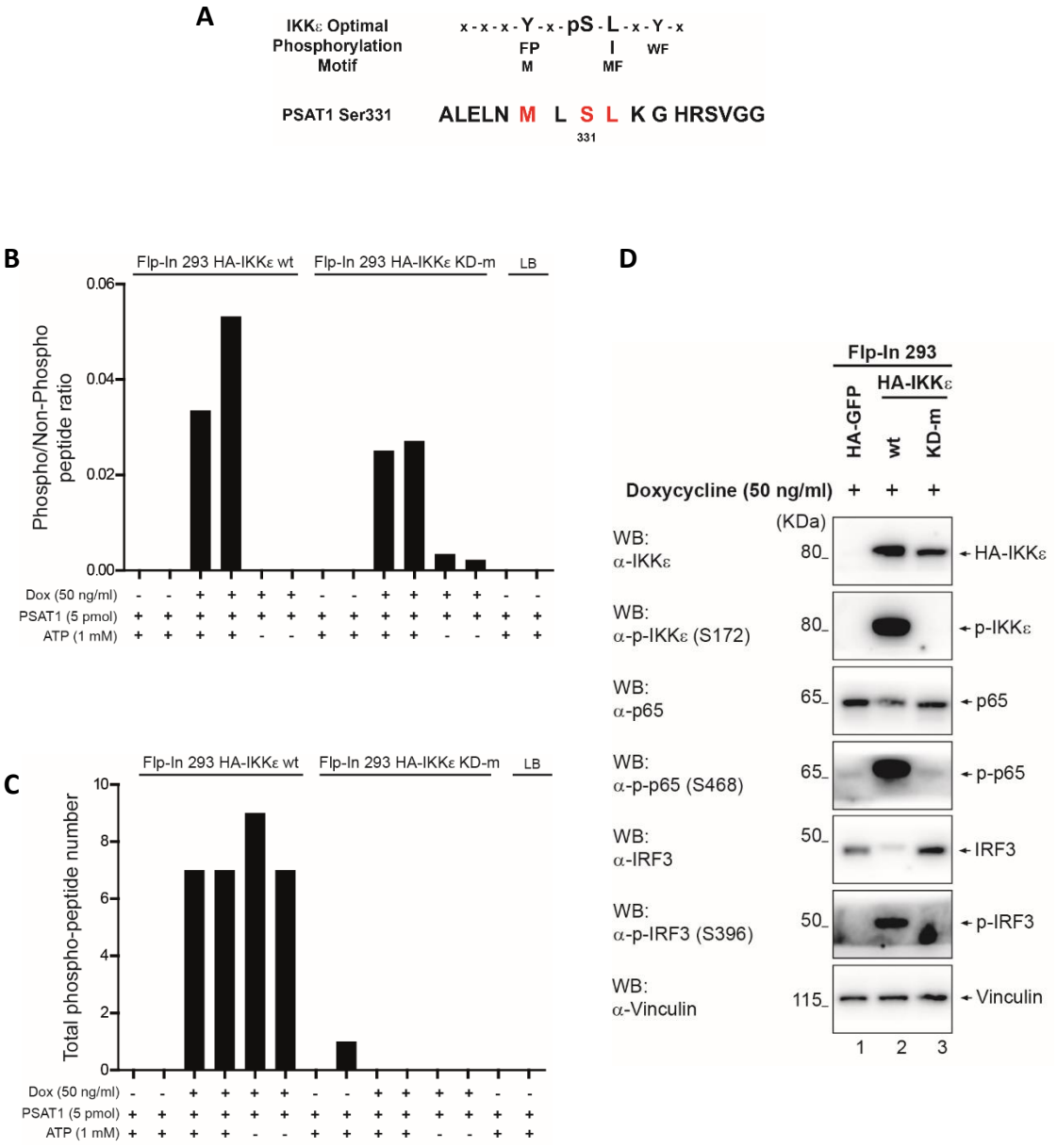

Figure 3.9 – PSAT1 is phosphorylated in an *in vitro* kinase assay in an IKKε-dependent manner. (A) IKKε's optimal phosphorylation motif, as described by Hutti *et al.* 2006[197], overlaps with the amino acid sequence surrounding PSAT1 Ser331 at 3 out of 4 preferred residues suggesting likely direct phosphorylation by the kinase. **(B)** An *in vitro* kinase assay was performed using HA-tag purified IKKε wt or KD-m mutant with recombinant PSAT1. Lysates from Flp-In 293 HA-IKKε wt or Flp-In 293 HA-IKKε KD-m cells + or – 16 hours of 100 ng/ml doxycycline treatment were subject to HA-pulldown to purify HA-IKKε. Resulting lysates were combined with recombinant PSAT1 and ATP as indicated. Blank lysis buffer was used as a control and samples were run in duplicate on the mass spectrometer by Dr Pedro Cutillas and Dr Vinothini Rajeeve. PSAT1 Ser331 phosphorylation was detected in samples containing HA-IKKε only, indicating kinase-dependent phosphorylation of the enzyme. **(C)** Phosphorylation of IKKε, indicating kinase activity, was only present on HA-IKKε wt. **(D)** Western blot analysis of HA-IKKε wt- and HA-IKKε KD-m-expressing cells (and HA-GFP as a control) demonstrated lack of kinase activity in KD-m IKKε, due to lack of phosphorylation of p65 and IRF3. Indicated cell lines were treated with 50 ng/ml doxycycline for 16 hours then lysed and processed for western blotting. Vinculin is shown as a loading control.

Table 3.3 – Relative abundance of secondary kinases detected by mass spectrometry analysis of in vitro kinase assay samples. Filtering out kinases detected in samples where phosphorylation of PSAT1 was not detected and kinases also detected in the lysis buffer blank, in which there was no organic material, left just the single kinase: TBK1. A close family member of IKKε, TBK1 is known to phosphorylate some of the same substrates as IKKε and can interact with IKKε in a heterodimer formation. TBK1 seems a likely candidate for explaining PSAT1 phosphorylation in the presence of HA-IKKε KD-m.

		Flp-In 293 HA-IKKε wt						Flp-In 293 HA-IKKε KD-m						LB		
		-	-	+	+	+	+	-	-	+	+	+	+	-	-	Doxycycline (50 ng/ml)
		+	+	+	+	+	+	+	+	+	+	+	+	+	+	PSAT1 (5 pmol)
Kinase	Uniprot_ID	+	+	+	+	-	-	+	+	+	+	-	-	+	+	ATP (1 mM)
BAZ1B	BAZ1B_HUMAN						2984.297	1244.2386		1932.4476	1664.1875			1010.9791	523.2176	
CDK18	CDK18_HUMAN				8059.8924					18069.624						
CDK20	CDK20_HUMAN	4881.7174		252.9605	8059.8924				6960.912	18069.624					5088.713	
DGKζ	DGKZ_HUMAN									2510.598			74612.3			
PKM	KPYM_HUMAN	1223.5914	573.5077	465.7423	1252.4022	97916.303	10113.117	325.5534		703.5075	427.4682	5867.518	3579.418	328.6298	763.5995	
PKLR	KPYR_HUMAN	15599.382	2871.2116	3290.1434	822.2336			4212.142	7084.466	1254.5984				6255.358	8062.362	
MAP4K4	M4K4_HUMAN									3064.0263						
MAPK1	MK01_HUMAN		196.211											206.956		
MRCKγ	MRCKG_HUMAN		2665.1312		6143.4025		45871.793	731.4015		1053.4261		712.704	3018.451	5424.6431	1517.7981	
NDKB	NDKB_HUMAN													591.1352		
NEK8	NEK8_HUMAN							208.9046								
PRKDC	PRKDC_HUMAN	70420.367	3839.5279	39533.753	61751.09	40776.476	695714.4	26604.793		6971.3174	58455.848	666900.83	713109.68	26189.511	20657.385	
PRPF4B	PRP4B_HUMAN			754.9553	623.1387			996.1896								
PRPS2	PRPS2_HUMAN					1239.5348										
ROCK1	ROCK1_HUMAN								933.3302		1037.8053					
SIK3	SIK3_HUMAN														680.6587	
TBK1	**TBK1_HUMAN**	**2859.8696**	**2677.8666**	**61437.209**	**73636.002**	**219105.02**	**529151.51**	**12995.058**	**13025.734**	**87509.731**	**170499.4**	**46110.77**	**823044.6**			
ULK1	ULK1_HUMAN													337.8299		
VRK2	VRK2_HUMAN														1432.261	

3.5 Development of Flp-In 293 HA-PSAT1 phospho-mutant and -mimic cell lines

Whilst PSAT1 Ser331 phosphorylation has been previously reported, it has only been identified as part of high throughput studies. Therefore, little focus had been given to either the phosphosite or kinases that can phosphorylate it and any potential role for the site in protein function remained unexplored.

To address this, a model in which the phosphorylation status of the enzyme could be modulated was developed. Based on a similar model previously used to modulate the phosphorylation of PHGDH[326], point mutagenesis was used to introduce serine > alanine or serine > glutamic acid mutations at the Ser331 residue of PSAT1, to inhibit or mimic phosphorylation respectively. By mimicking the general size, shape and chemical properties of phosphorylated and un-phosphorylated serine residues at a neutral pH, alanine can easily represent an un-phosphorylated serine residue and glutamic acid can potentially act as a phosphorylated serine residue (Figure 3.10 A). These two modifications not being serine residues means that instead of being subject to dynamic regulation of phosphorylation by kinases and phosphatases, they are permanent fixtures. Generating a PSAT1 S>A or S>E mutant therefore allows control over the phosphorylation status of the enzyme and evaluation of functional differences between its un-phosphorylated and phosphorylated states. To generate PSAT1 S>A and S>E mutants, a cDNA clone of the open reading frame of *PSAT1* in a *pGEM-T* plasmid backbone was purchased from Sino Biological (Beijing, China) and point mutagenesis PCR was used to specifically modify the Ser331 residue. The resultant *PSAT1 wt*, *PSAT1 S > A* and *PSAT1 S > E* DNA sequences were cloned into the Flp-In 293 compatible *pcDNA5.5* vector, adding an HA-tag to each protein in the process. Similar to HA-IKKε models, this allowed the generation of doxycycline inducible Flp-In 293 HA-PSAT1 cell lines. As indicated previously, the Flp-In 293 system was an optimal model for the comparison of the differentially phosphorylated proteins. Inserted genes are typically integrated into the host genome at a single site and at the same site every time. This ensures equal expression of gene inserts under the control of the same promoter in different cell lines. Equal gene expression of mutant variants makes it easy to compare functional differences between alternate versions of the same protein.

To generate new Flp-In 293 cell lines, parental Flp-In 293 cells were co-transfected with the desired *pcDNA5.5 HA-PSAT1* plasmid and another plasmid called *pOG44*, which contains a gene encoding the enzyme Flp recombinase under the control of a constitutive promoter. Transfection of *pOG44* into the host cell results in production of Flp recombinase. This induces

homologous recombination of the FRT-flanked *HA-PSAT1* gene, contained within the *pcDNA5.5* plasmid, with FRT sites in the Flp-In 293 host genome. Successful recombination also introduces a hygromycin resistance gene to the host genome, so following transfection, successful integration of *HA-PSAT1* genes was selected for by hygromycin treatment. This process was performed for each HA-PSAT1 variant and 3 independent pools of new Flp-In 293 cell lines were generated for each variant; Flp-In 293 HA-PSAT1 wt, Flp-In 293 HA-PSAT1 S>A and Flp-In 293 HA-PSAT1 S>E. In each cell line, HA-PSAT1 expression was under the control of a doxycycline inducible promoter (Figure 3.10 B). Each pool was validated for expression of HA-PSAT1 variants and expression of the HA-tagged enzyme across the different pools was found to be roughly equal. The data presented in Figure 3.10 was obtained using cells from the first pool generated. These were the same cells used for experiments assessing the function of phosphorylation of the PSAT1 Ser331 residue.

Induction of HA-PSAT1 wt, HA-PSAT1 S>A and HA-PSAT1 S>E in each Flp-In 293 cell line was validated by using quantitative real-time polymerase chain reaction (qRT-PCR) analysis to measure doxycycline-mediated induction of *PSAT1* messenger RNA (mRNA) levels. Treatment of Flp-In 293 HA-PSAT1 wt, Flp-In 293 HA-PSAT1 S>A and Flp-In 293 HA-PSAT1 S>E cells with doxycycline for 16 hours strongly induced *PSAT1* mRNA levels (Figure 3.10 C). As expected from using the Flp-In 293 system, no significant difference in the induction of *PSAT1* mRNA was observed between the different cell lines, indicating equal gene transcription. To check that the upregulation of mRNA levels also translated into protein expression, western blotting was used to validate the doxycycline-mediated induction of HA-PSAT1 protein. Treatment of Flp-In 293 HA-PSAT1 cells with doxycycline for 16 hours led to stable induction of the protein in all 3 cell lines (Figure 3.10 D). Intriguingly, despite qRT-PCR analysis demonstrating equal gene transcription, densitometry analysis quantification of protein levels in the different Flp-In 293 HA-PSAT1 cell lines showed differential expression of the HA-PSAT1 protein variants. Compared to the expression of the wt protein, HA-PSAT1 S>A protein was expressed to a significantly lower level and HA-PSAT1 S>E was expressed to a significantly higher level (Figure 3.10 E). Since the comparison of mRNA expression showed no clear differences, this suggested that the mutation of the PSAT1 Ser331 residue might be specifically regulating the enzyme post-translationally.

The differential protein expression will be further discussed later (see 3.9), but regardless, the Flp-In 293 system was successfully used to generate 3 new cell lines that expressed wt and mutant versions of the PSAT1 protein when treated with doxycycline. This model was subsequently used to explore the functional impact of mutating the Ser331 residue for PSAT1.

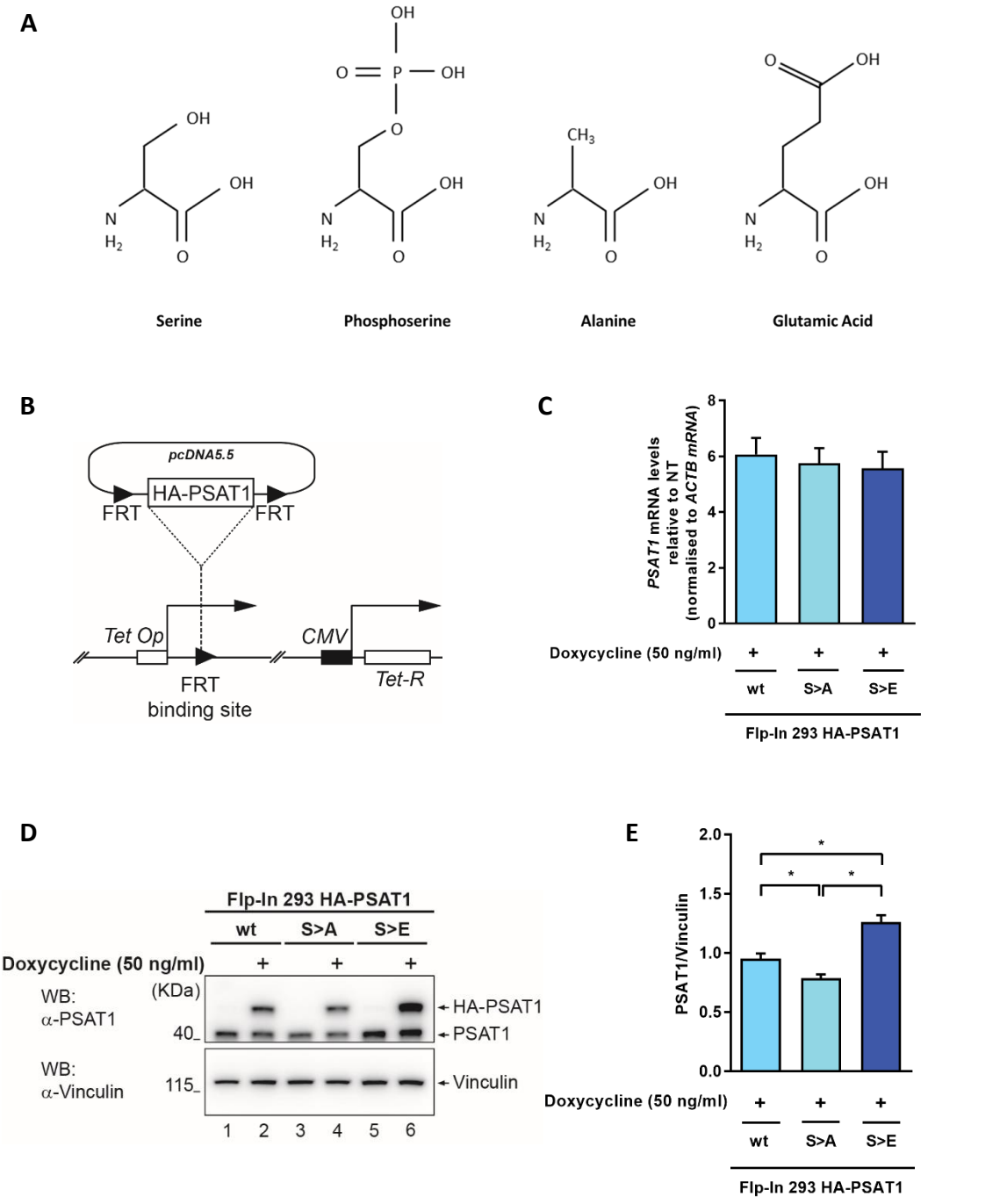

Figure 3.10 – Induction of HA-tagged PSAT1 wt and phosphomutant/mimic variants in Flp-In 293 cells. (A) Visual representation of how mutation of serine to alanine or glutamic acid can physically mimic either serine or phosphoserine respectively. In addition to physical similarities, chemical similarities exist at physiological pH 7.4, both serine and alanine exhibit neutral charges whereas phosphoserine and glutamic acid are negatively charged. **(B)** Schematic representation of incorporation of HA-PSAT1 at FRT sites in the Flp-In 293 genome. **(C)** qRT-PCR analysis, measuring induction of *HA-PSAT1 wt*, *HA-PSAT1 S>A* and *HA-PSAT1 S>E* mRNA upon treatment of indicated Flp-In 293 HA-PSAT1 cell lines with 50 ng/ml doxycycline for 16 hours. mRNA levels were expressed as fold changes relative to non-treated basal levels of *PSAT1* mRNA in the corresponding cell lines and normalised to *ACTB* (β-Actin) mRNA. n=4 independent experiments, mean ± SEM. No significant differences were observed using one-way ANOVA with Bonferroni *post-hoc* tests. **(D)** Western blot demonstrating induction of HA-PSAT1 wt, HA-PSAT1 S>A and HA-PSAT1 S>E protein upon treatment of corresponding Flp-In 293 HA-PSAT1 cell lines with 50 ng/ml doxycycline for 16 hours. Vinculin is shown as loading control. **(E)** Densitometry analysis quantification of HA-PSAT1 protein levels expressed in different Flp-In 293 HA-PSAT1 mutant cell lines, normalised to vinculin protein levels. n=11 independent experiments, mean ± SEM, *p < 0.05 as measured by one-way ANOVA with Bonferroni *post-hoc* tests.

3.6 Development of MDA-MB-453 PSAT1 wt, S>A and S>E cell lines

In addition to the development of Flp-In 293 HA-PSAT1 cell lines, a breast cancer cell line expressing PSAT1 wt and mutant variants was also generated. To select the cell line which PSAT1 would be introduced to, a model where the functional implications of PSAT1 mutation could be directly addressed was desired. To find such a model, cell growth in serine-free medium was assessed via IncuCyte analysis. A fully functioning SBP allows cells to survive conditions where external supplies of serine are lacking, as the cells can synthesise sufficient serine intracellularly to compensate for the external deprivation and maintain proliferation. Lack of expression of one or more enzymes of the SBP causes cells to lose the ability to biosynthesise serine themselves, triggering dependency on exogenous serine. By identifying a breast cancer cell line that failed to grow in serine-free medium, due to a lack of PSAT1 expression, reintroduction of PSAT1 wt or mutant variants could be used to assess relative mutant function by evaluating ability to rescue serine-free medium growth.

To determine the ability of the breast cancer cell line panel to proliferate in serine-free medium, each cell line was plated in a 96-well plate and, 24 hours later, the culture medium was changed for either serine - medium, or serine - medium which had been reconstituted with serine to act as whole medium. The IncuCyte Zoom was then used to track cell growth over the following days. Measuring confluency at given time points and calculating changes in confluency over 72 hours allowed detection of statistically significant changes in proliferative rates. ZR-75-1, T47D, MDA-MB-453, MDA-MB-231 and MCF7 cell lines all exhibited significant growth retardation when deprived of exogenous serine (Figure 3.11 A). Example growth curves for these cell lines are shown in Figure 3.11 B-F and show that although proliferative rates in ZR-75-1 and T47D were significantly reduced, cultures eventually grew to confluency over the course of the experiment. This indicated that these cell lines still featured active, albeit perhaps less efficient, serine biosynthesis. Contrastingly, a much stronger effect on proliferation was seen in the MDA-MB-453, MDA-MB-231 and MCF7 cell lines, with proliferation being more or less completely inhibited in the absence of exogenous serine (Figure 3.11 A and D-F). The serine biosynthesis enzyme protein expression profile for each breast cancer cell line was then assessed to identify why MDA-MB-453, MDA-MB-231 and MCF7 exhibited such a reduced capacity to grow in serine-free conditions (Figure 3.12). For MDA-MB-231, this is because the cell line lacks expression of the first enzyme of the pathway, PHGDH. Both MCF7 and MDA-MB-453 however, are unable to grow due to lack of PSAT1 expression, making them good candidate cell lines for the reintroduction of PSAT1. A cell line lacking endogenous PSAT1 expression represents a good

model for exploring the functionality of mutant PSAT1 proteins. A lack of interference of functional endogenous protein means exogenous PSAT1 function can be judged on its own merit. MDA-MB-453 was selected as the cell line to which PSAT1 would be introduced as it only lacked PSAT1 expression, whereas MCF7 also exhibited low levels of the PSPH protein.

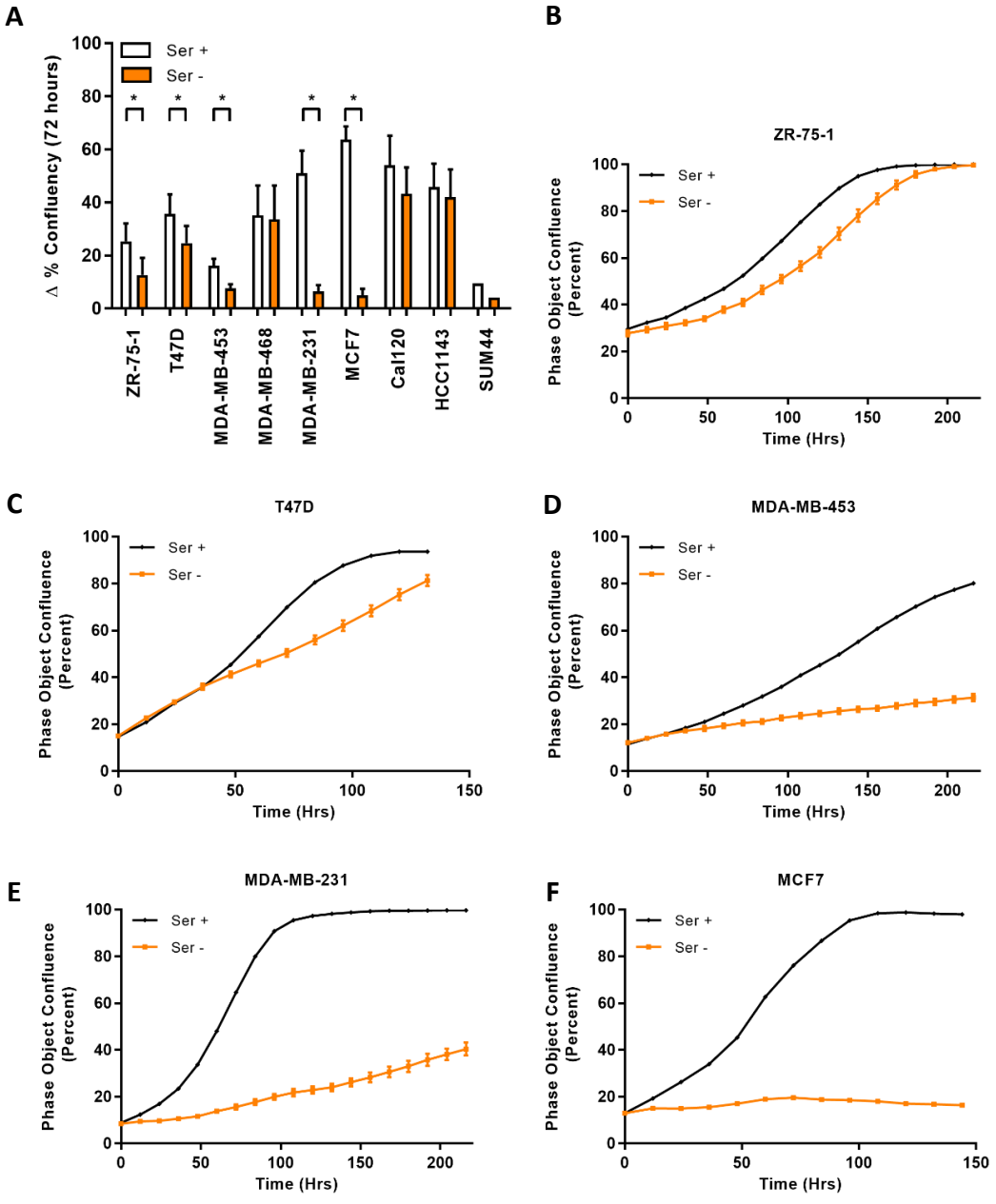

Figure 3.11 – Serine deprivation impairs the growth of a subset of breast cancer cell lines. Growth of breast cancer cell lines was measured by tracking cell confluency over time using the IncuCyte Zoom. **(A)** Serine deprivation significantly slows proliferation of ZR-75-1, T47D, MDA-MB-231, MDA-MB-453 and MCF7 breast cancer cell lines. Cell lines were plated in full medium which was replaced with either serine - medium, or serine - medium reconstituted with serine, 24 hours later. Delta confluency was calculated between 0 and 72 hours to identify statistically significant differences in cell proliferation. n≥4 independent experiments in all cell lines with the exception of SUM44, where only n=1 independent experiment was performed, mean ± SEM, * $p<0.05$ as measured by two-tailed Student's t-test. **(B-F)** Representative IncuCyte growth curves from single experiments with ZR-75-1 (B), T47D (C), MDA-MB-453 (D), MDA-MB-231 (E) and MCF7 (F). Mean ± SD.

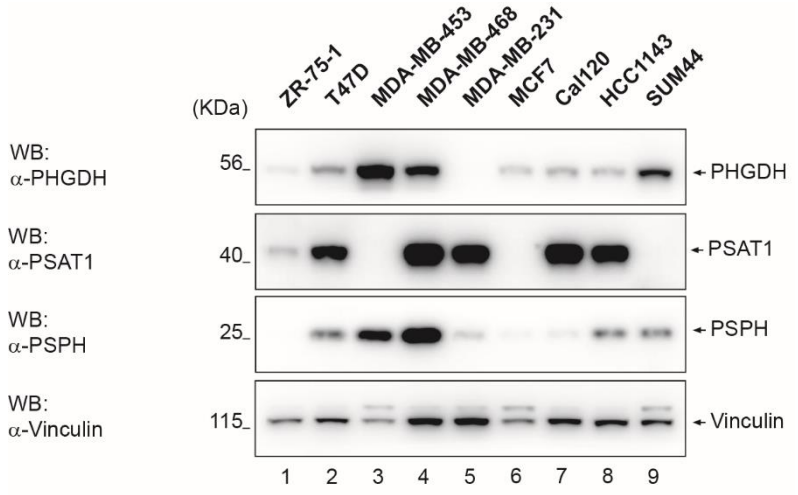

Figure 3.12 – Serine biosynthesis enzyme protein expression profile of a panel of breast cancer cell lines. Western blot analysis of basal PHGDH, PSAT1 and PSPH protein expression in indicated breast cancer cell lines. MDA-MB-453 and MCF7 exhibit reduced growth in serine-deprived conditions due to a lack of PSAT1 protein. MDA-MB-231 exhibits reduced growth in serine-deprived conditions due to a lack of PHGDH. Vinculin is shown as a loading control.

To generate MDA-MB-453 cell lines with inducible PSAT1 expression, the *PSAT1 wt*, *PSAT1 S>A* and *PSAT1 S>E* genes were cloned from the *pcDNA5.5* vector into the *pTRIPZ* lentiviral vector, following which the vectors were transduced into MDA-MB-453 cells via lentiviral infection. As the *pTRIPZ* vector contains a puromycin resistance gene, successful transduction of the *pTRIPZ PSAT1* vector was selected for using puromycin. 3 new inducible PSAT1 cell lines were therefore generated; MDA-MB-453 PSAT1 wt, MDA-MB-453 PSAT1 S>A and MDA-MB-453 PSAT1 S>E.

To confirm successful transduction of inducible PSAT1 genes, the 3 MDA-MB-453 PSAT1 cell lines were treated with 500 ng/ml doxycycline for 16 hours and qRT-PCR was used to detect induction of *PSAT1* mRNA levels. Treatment of all 3 MDA-MB-453 PSAT1 cell lines induced substantial fold-increases in *PSAT1* mRNA levels; roughly 75-fold, 90-fold and 55-fold increases in MDA-MB-453 PSAT1 wt, S>A and S>E cells respectively (Figure 3.13 A). Unlike mRNA induction in Flp-In 293 HA-PSAT1 cells, doxycycline induction of *PSAT1* mRNA in the breast cancer cells resulted in significantly different amounts of gene transcription, with *PSAT1 S>A* mRNA levels induced significantly more than *PSAT1 S>E* mRNA levels. This indicated that in the MDA-MB-453 models, the PSAT1 genes were differentially expressed. Western blotting was subsequently used to evaluate PSAT1 protein induction. Doxycycline treatment induced PSAT1 protein expression in all three cell lines (Figure 3.13 B). However, as with the mRNA levels, densitometry analysis quantification of the relative PSAT1 protein levels revealed significantly different expression between protein variants. The PSAT1 wt protein was induced to a significantly higher level than either mutant variant (Figure 3.13 C). Since qRT-PCR analysis had revealed significant differences in PSAT1 expression at the mRNA level, densitometry analysis protein expression values were

normalised to mRNA levels to determine whether some of the differential expression could be explained by differences in gene transcription. Following normalisation, PSAT1 S>E protein levels showed no significant difference from PSAT1 wt protein levels, indicating the reduced protein induction was a result of reduced gene expression. However, PSAT1 S>A protein levels were still significantly lower than the wt protein levels (Figure 3.13 D). This suggested that, as in the Flp-In 293 HA-PSAT1 model, an uncharacterised post-translational modification might be regulating the enzyme protein levels. Irrespective of this, stable PSAT1 protein expression in MDA-MB-453 cells demonstrated successful generation of a breast cancer cell line where PSAT1 expression could be tightly controlled and generation of another model where the functional implications of PSAT1 Ser331 mutation could be assessed.

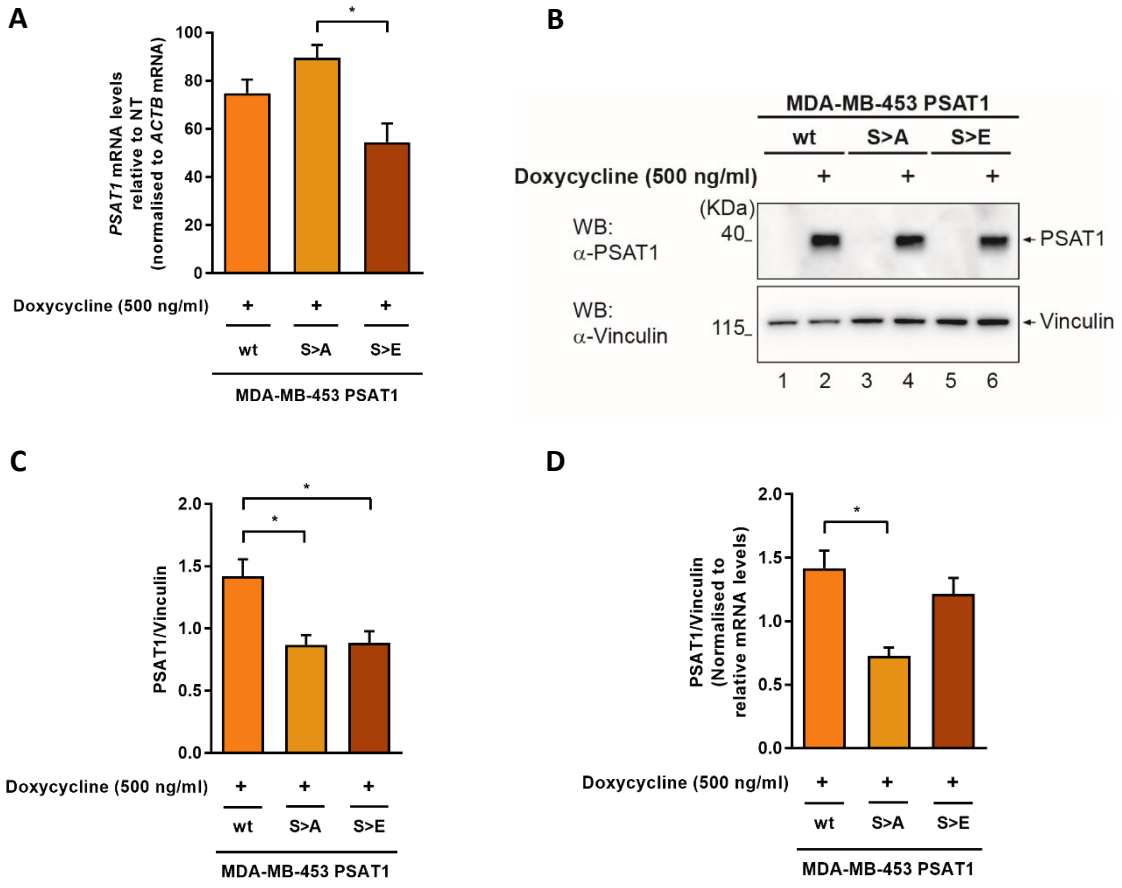

Figure 3.13 – Induction of PSAT1 wt and mutant variants in MDA-MB-453 cells. (A) qRT-PCR analysis measuring *PSAT1* mRNA levels in MDA-MB-453 PSAT1 cell lines following treatment with 500 ng/ml doxycycline for 16 hours. mRNA levels were expressed as fold changes relative to non-treated basal levels of *PSAT1* mRNA in the corresponding cell lines and normalised to *ACTB (*β-Actin) mRNA levels. n=3 independent experiments, mean ± SEM, *p<0.05 as measured by one-way ANOVA with Bonferroni *post-hoc* tests. **(B)** Western blot analysis demonstrating induction of PSAT1 wt, PSAT1 S>A and PSAT1 S>E proteins in corresponding modified MDA-MB-453 cell lines upon treatment with 500 ng/ml doxycycline for 16 hours. Vinculin is shown as a loading control. **(C)** Densitometry analysis quantification of induced PSAT1 protein levels in MDA-MB-453 cells, normalised to vinculin. n=3 independent experiments, mean ± SEM, *p<0.05 as measured by one-way ANOVA with Bonferroni *post-hoc* tests. **(D)** Additional normalisation of densitometry analysis from (C), normalising relative protein levels to mRNA levels from (A).

3.7 Assessing the impact of Ser331 mutation on enzymatic activity

Phosphorylation of enzymes is a frequent post-translational modification that often regulates enzyme activity. In order to evaluate what impact, if any, modification of the PSAT Ser331 residue would have on enzyme activity, the wt and mutant PSAT1 proteins were assessed for their ability to rescue growth inhibition in serine-free medium. As previously established, MDA-MB-453 cells fail to grow in serine-free medium, but Flp-In 293 cells express all 3 SBP enzymes to sufficient degrees to sustain proliferation in the absence of serine. Therefore, it was unsurprising to find that, when measuring growth in serine deprivation using the IncuCyte Zoom, parental Flp-In 293 cells continued to grow to confluency in the absence of exogenous serine, albeit with a significant decrease in proliferative rates (Figure 3.14). If Flp-In 293 HA-PSAT1 cells can sustain proliferation in serine-free medium, attempts to characterise HA-PSAT1-dependent growth rescue would be complicated. Therefore, a method by which Flp-In 293 proliferation in serine-free medium could be inhibited was sought.

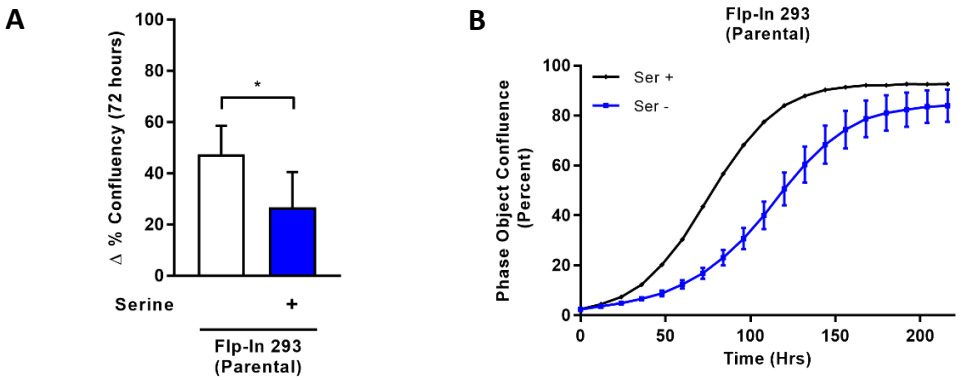

Figure 3.14 – Flp-In 293 cells exhibit impaired but maintained growth in serine deprived conditions. Parental Flp-In 293 cells were plated in complete medium which, 24 hours later, was replaced with either serine - medium (Ser -) or serine - medium reconstituted with serine (Ser +) and growth was tracked by measurement of cell confluency over time using the IncuCyte Zoom. **(A)** Delta confluency was calculated between 0 and 72 hours to identify statistically significant differences in proliferative rates. n=3 independent experiments, mean ± SEM, *p<0.05 as measured by paired two-tailed Student's t-test. **(B)** Representative IncuCyte growth curve from a single experiment with Flp-In 293 parental cells. Mean ± SD.

To inhibit the growth of Flp-In 293 cells in serine-free medium and subsequently compare the ability of HA-PSAT1 wt, HA-PSAT1 S>A and HA-PSAT1 S>E to rescue that growth inhibition, endogenous PSAT1 expression was suppressed. To achieve endogenous knockdown whilst maintaining inducible expression of HA-PSAT1 upon doxycycline treatment, 3 *PSAT1*-targeting siRNA oligos, which specifically targeted the non-coding sequences of the *PSAT1* mRNA (which are absent from the HA-PSAT1 sequences), were transfected into Flp-In 293 HA-PSAT1 cells for 72 hours. Cells were simultaneously treated with doxycycline for the final 16 hours to induce HA-PSAT1 in the absence of endogenous enzyme expression. To validate stable HA-PSAT1

induction and endogenous PSAT1 knockdown, western blotting was used. As expected, the transfection of non-coding targeting siRNA successfully suppressed endogenous PSAT1 expression in all 3 Flp-In 293 HA-PSAT1 cell lines and, whilst inducible protein levels were slightly reduced, HA-PSAT1 wt, HA-PSAT1 S>A and HA-PSAT1 S>E proteins were all successfully induced with doxycycline treatment (Figure 3.15).

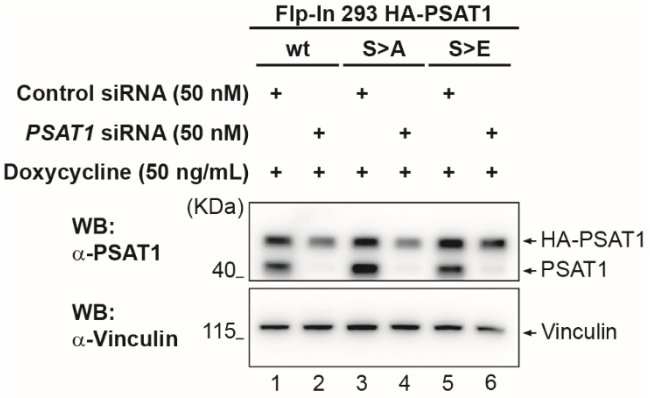

Figure 3.15 – Stable induction of HA-PSAT1 wt and mutant variants in the absence of endogenous expression. Western blot demonstrating the knockdown of endogenous PSAT1 in indicated Flp-In 293 HA-PSAT1 cells by siRNA and induction of HA-tagged variant. Indicated cell lines were transfected with 3 siRNA oligos targeting the non-coding sequence of *PSAT1* mRNA or a single non-targeting control oligo to a final concentration of 50 nM for 72 hours. Cells were simultaneously treated with 50 ng/ml doxycycline for the final 16 hours, achieving HA-tagged PSAT1 expression in the absence of endogenous protein. Vinculin is shown as a loading control.

Suppression of endogenous PSAT1 had the desired effect on the proliferation of Flp-In 293 cells. Evaluating cell growth using the IncuCyte Zoom, it was found that *PSAT1* siRNA had no impact on proliferation when serine was present in the medium, but substantially inhibited growth in serine deprived conditions (Figure 3.16 A), demonstrating the importance of the pathway when nutrient availability is compromised. With a model in place in which suppression of PSAT1 could inhibit the growth of Flp-In 293 cells, the ability of HA-PSAT1 to rescue growth could be assessed and compared between wt and mutant variants. Suppression of endogenous PSAT1 was confirmed to significantly reduce growth in serine-free medium in all three Flp-In 293 HA-PSAT1 cell lines, and although doxycycline treatment had no significant proliferative effect on the cells when endogenous PSAT1 and exogenous serine were both present (Figure 3.16 B), the induction of HA-PSAT1 rescued the serine deprived growth of each cell line when endogenous PSAT1 was suppressed (Figure 3.16 C-E). Importantly, whilst induction of the HA-tagged enzyme resulted in complete growth rescue of the cells expressing either HA-PSAT1 wt or the HA-PSAT1 S>E mutant, cells expressing HA-PSAT1 S>A still demonstrated a significantly reduced growth over 72 hours compared to the siRNA control, demonstrating that the HA-PSAT1 S>A mutant could not wholly compensate for the absence of the endogenous enzyme. This indicated that phosphorylation of PSAT1 Ser331 was important for continued proliferation of cells in serine-deprived conditions.

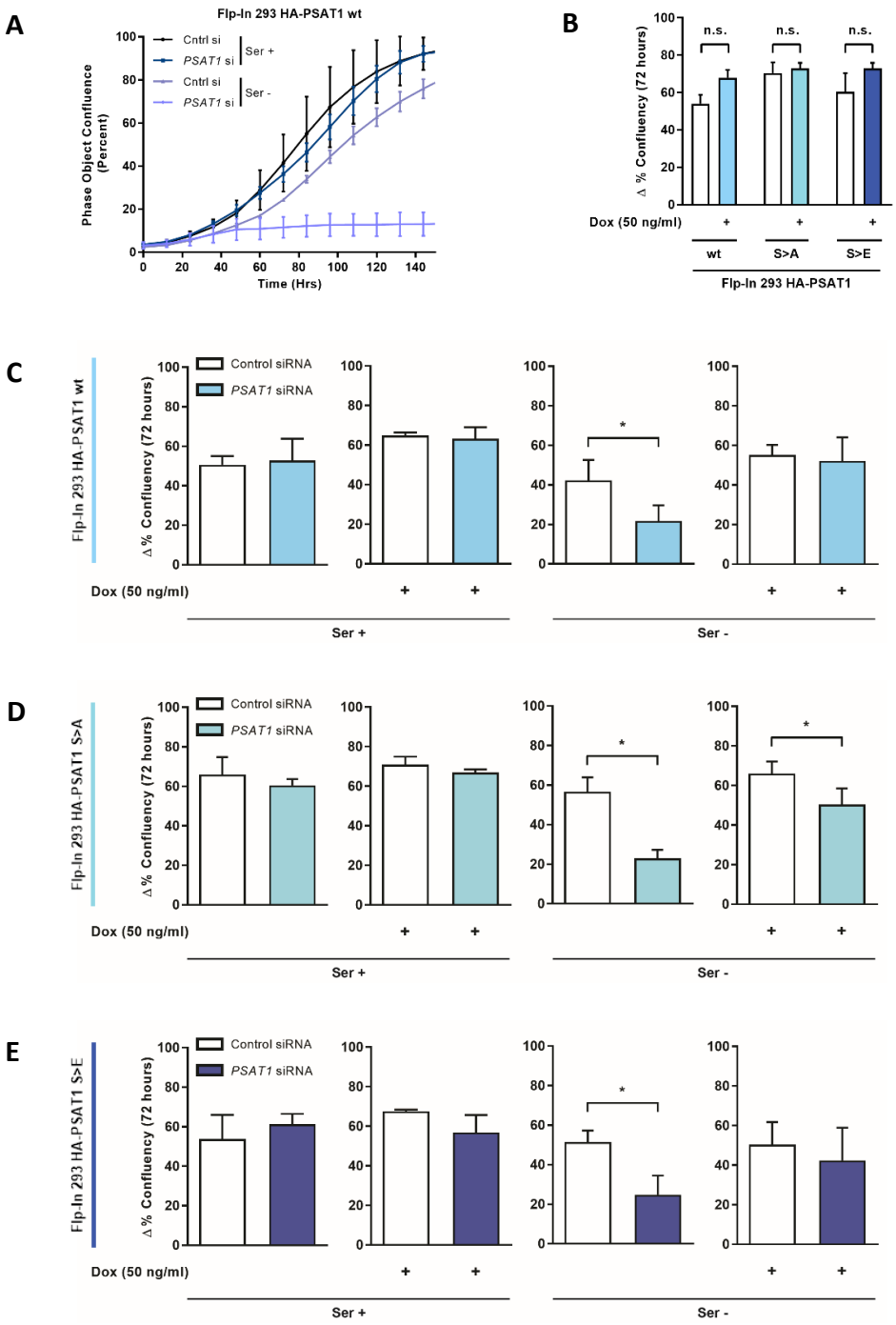

Figure 3.16 – Rescue of growth of Flp-In 293 cells in serine-free medium in the absence of endogenous PSAT1 by HA-PSAT1 wt and mutant proteins. Flp-In 293 HA-PSAT1 cells were transfected with *PSAT1* siRNA as in 3.15 and growth over subsequent days in either serine - medium (Ser -) or serine - medium reconstituted with serine (Ser +), was tracked via measurement of confluency using the IncuCyte Zoom. Delta confluency was calculated between 0 and 72 hours to identify statistically significant differences in cell proliferation. **(A)** Representative IncuCyte growth curve from a single experiment with Flp-In 293 HA-PSAT1 wt cells. Flp-In 293 HA-PSAT1 wt cells grow at a marginally reduced rate in serine-free medium and knockdown of endogenous PSAT1 only inhibits growth in serine deprived conditions. Mean ± SD. **(B)** Delta confluency of control siRNA-transfected Flp-In 293 HA-PSAT1 cells with or without 50 ng/ml doxycycline treatment. n=3 independent experiments, mean ± SEM, no significant differences were detected using a two-way ANOVA with Bonferroni *post-hoc* tests **(C-E)** Delta confluency of siRNA-transfected Flp-In 293 HA-PSAT1 wt (C), HA-PSAT1 S>A (D) and HA-PSAT1 S>E (E) cells in Ser + or Ser - medium over 72 hours with or without 50 ng/ml doxycycline treatment. HA-PSAT1 wt and HA-PSAT1 S>E completely rescue Ser – growth diminished by knockdown of endogenous serine, whereas HA-PSAT1 S>A fails to fully restore growth. Control siRNA, Ser + data is the same data as presented as in (B) and is used here for further comparison with *PSAT1* siRNA-transfected cells. n=3 independent experiments, mean ± SEM, *p<0.05 as measured by paired t-tests.

It is worth noting that, although the proliferative effect of the doxycycline-mediated induction of HA-PSAT1 variants in Flp-In 293 cells was assessed (Figure 3.16 B), it was only assessed in "basal" conditions (i.e. control siRNA-transfected cells with exogenous serine present in the medium). Whilst it would be interesting and informative to perform a comprehensive analysis of the growth of cells in the presence or absence of HA-tagged wild-type or mutant PSAT1 in all the conditions detailed in Figure 3.16 C-E, such an analysis could not be sufficiently performed here, as variability in the data prevented the identification of statistically significant differences when comparing more than two groups of data. Indeed, it would be important to perform further data collection for this experiment in the future to facilitate a more in-depth analysis. For the purposes of this thesis, the statistical analysis for each condition was exclusively performed between two groups; where endogenous PSAT1 was present (control siRNA-transfected cells), and where it was suppressed (*PSAT1* siRNA-transfected cells), facilitating the main aim of the experiment to compare the activity of the HA-tagged PSAT1 variants to that of the endogenous.

In the MDA-MB-453 PSAT1 cell models, culturing cells in serine-free medium substantially impaired growth rates in all 3 cell lines. Unlike what was observed in the Flp-In 293 cells however, treatment of all 3 MDA-MB-453 PSAT1 cell lines with doxycycline seemed to rescue the growth inhibition induced by serine deprivation (Figure 3.17). This indicated that the enzymatic activities of PSAT1 wt, PSAT1 S>A and PSAT1 S>E in MDA-MB-453 cells were equally sufficient to support serine production to a level high enough to sustain growth in serine-free medium.

Since the expression of HA-PSAT1 S>A in the Flp-In 293 cell model was found to be insufficient to rescue growth in serine-deprived conditions in the absence of endogenous serine and since it had previously been established that the protein expression of the HA-PSAT1 S>A mutant was lower than that of the wt or S>E variants upon treatment of cells with doxycycline, it was hypothesised that the reduced growth rescue ability of HA-PSAT1 S>A was attributable to reduced PSAT1 protein expression resulting in reduced overall serine production. This hypothesis was directly addressed by measuring the serine production from the different HA-PSAT1 proteins using labelled metabolite analysis, allowing evaluation of the comparative amount of serine produced when each HA-PSAT1 mutant was expressed. As with the previous labelled metabolite analysis, cells were prepared by Dr Ruoyan Xu and mass spectrometry detection of labelled metabolites was performed by Dr Christian Frezza and Dr Sofia De Costa.

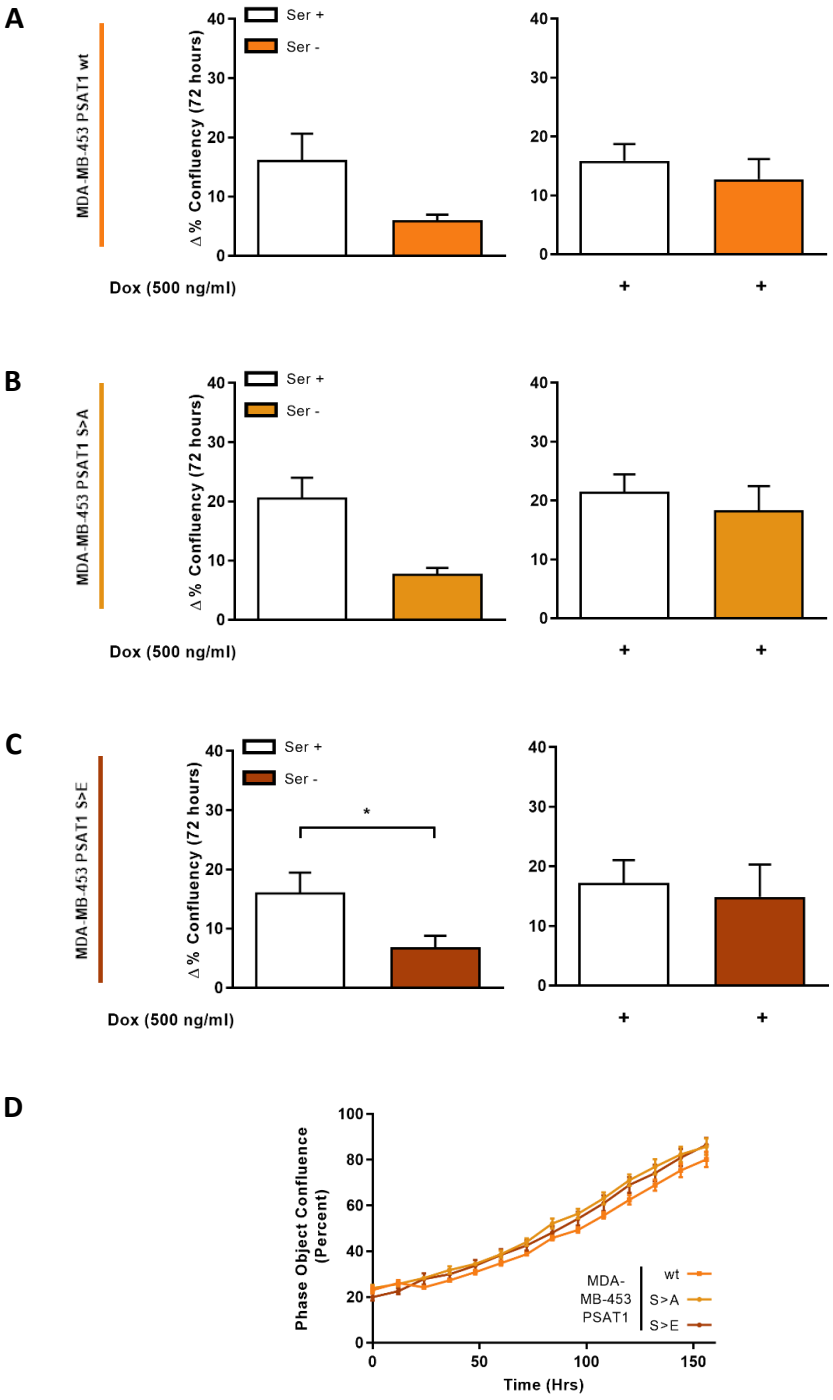

Figure 3.17 PSAT1 wt and mutant proteins rescue growth inhibition of MDA-MB-453 cells in serine-free medium. MDA-MB-453 PSAT1 cells were grown in either serine - medium (Ser -), or serine - medium reconstituted with serine (Ser +) and treated with 500 ng/ml doxycycline to induce PSAT1 expression. Growth with and without doxycycline treatment was tracked by measurement of cell confluency over time using the IncuCyte Zoom. Delta confluency was measured between 0 and 72 hours to identify statistically significant changes in proliferation. **(A-C)** Delta confluency of MDA-MB-453 PSAT1 wt (A), MDA-MB-453 PSAT1 S>A (B) and MDA-MB-453 PSAT1 S>E (C) cells in Ser + and Ser - medium over 72 hours with and without 500 ng/ml doxycycline treatment. Non-treated cell lines show diminished proliferation in Ser - medium, which is wholly rescued by induction of PSAT1 wt, PSAT1 S>A and PSAT1 S>E. n=3 independent experiments, mean ± SEM, *p<0.05 as measured by paired t-tests. **(D)** Representative IncuCyte growth curves for a single experiment with MDA-MB-453 PSAT1 wt, S>A and S>E cell lines treated with doxycycline in serine-free medium, demonstrating equivalent growth rescue. Mean ± SD.

As in the IncuCyte experiments, endogenous PSAT1 was suppressed in Flp-In 293 cells using non-coding sequence-targeting siRNA oligos prior to induction of the HA-tagged PSAT1 variants and incubation of cells with labelled metabolites. Doxycycline-treated Flp-In 293 HA-PSAT1 cells were then incubated with ^{15}N-labelled glutamine to track the incorporation of the amino group into phosphoserine and ultimately serine itself. This allowed evaluation of the efficiency of the aminotransferase reaction and therefore assessment of comparative HA-PSAT1 enzyme activity. To identify differences in metabolite labelling, the amount of labelled serine and glycine detected was calculated as a percentage of total serine and glycine. Surprisingly, whilst the HA-PSAT1 S>A mutant variant displayed a reduced ability to rescue growth of Flp-In 293 cells in serine-free conditions, labelled metabolite flux analysis showed no significant differences in the incorporation of glutamine-derived nitrogen into serine or glycine between the different HA-PSAT1 variants. Indeed, the proportion of synthesised serine and glycine within the cells was steady at about 8-10% of the total intracellular pool across each cell line. This indicated equal amounts of serine biosynthesis with different HA-PSAT1 variants (Figure 3.18), suggesting the reduced proliferation of Flp-In 293 cells expressing HA-PSAT1 S>A in serine-free conditions was not due to a reduction in the amount of serine produced.

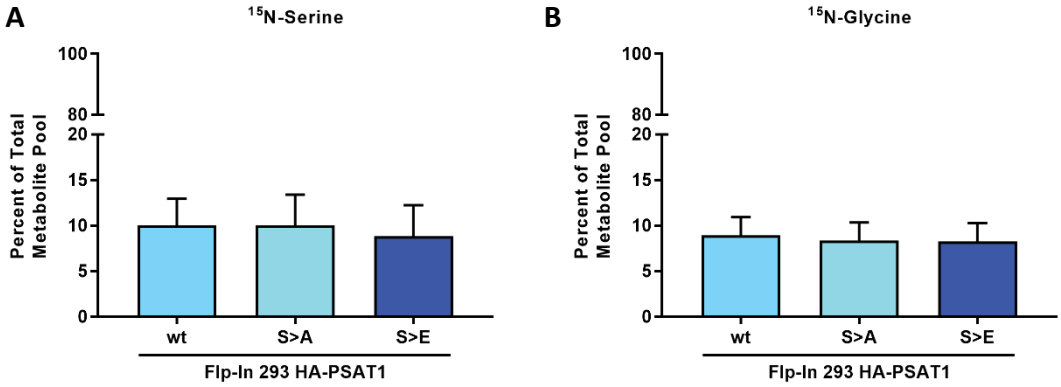

Figure 3.18 – Modulation of PSAT1 Ser331 residue has no effect on serine biosynthesis. Labelled metabolite analysis using Flp-In 293 HA-PSAT1 cells tracked the incorporation of ^{15}N derived from labelled glutamine into **(A)** serine and **(B)** glycine, thereby measuring the efficiency of the PSAT1 reaction catalysed by the different HA-PSAT1 variants. Flp-In 293 HA-PSAT1 cells were transfected with 3 siRNA oligos targeting the non-coding sequences of *PSAT1* mRNA or a single non-targeting control oligo to a final concentration of 50 nM for 72 hours. Cells were treated with 50 nM doxycycline simultaneously for the final 48 hours, to induce expression of the respective HA-PSAT1 variant and, for the final 24 hours, were cultured in medium containing ^{15}N-labelled glutamine by Dr Ruoyan Xu. Following this, ^{15}N-labelled metabolites were detected by mass spectrometry analysis performed by Dr Christian Frezza and Dr Sofia De Costa. Data is expressed as the percentage of the total metabolite concentration that is labelled, indicating the percent of serine and glycine within the cell containing nitrogen derived from glutamine. n=3 independent experiments, raw data from each independent experiment is available in supplementary Tables 7.4, 7.5 and 7.6 on the provided CD, mean ± SEM. No significant differences were detected using one-way ANOVA with Bonferroni *post-hoc* tests.

This data therefore indicated that the reduced proliferation of HA-PSAT1 S>A-expressing Flp-In 293 HA-PSAT1 cells in serine-free medium was instead attributable to an alternative, as yet uncharacterised role of PSAT1. Until such a role is determined, it is difficult to speculate why the PSAT1 S>A mutant did not demonstrate reduced growth rescue of MDA-MB-453 cells in serine-free medium but, importantly, the lack of difference in serine production between the different HA-PSAT1 mutants at least demonstrates that the Ser331 residue is not a site of any distinct importance for the primary enzymatic activity of PSAT1.

3.8 Assessing the impact of Ser331 mutation on PSAT1 containing protein complexes

As evidence suggested that the phosphorylation of PSAT1's Ser331 site was not an important event for regulation of its primary enzymatic activity, attention was turned to other functional roles the phosphorylation of this residue might play. Characterisation of the PSAT1 crystal structure in *Escherichia coli* and *Mycobacterium tuberculosis* has indicated that the enzyme exists as a homodimer[339-341] and the structure of human PSAT1, publicly available in the Protein Data Bank (PDB) (www.rscb.org)[342] as part of the worldwide PDB (www.wwpdb.org)[343], shows the same dimer formation (PDB ID 3E77 – Lehtio *et al.* Structural Genomics Consortium (SGC). Human phosphoserine aminotransferase in complex with PLP). Furthermore, evidence in yeast models demonstrating formation of a protein complex containing yeast homologs of PHGDH and SHMT suggests that the PSAT1 enzyme might complex with other SBP enzymes in human cells[288]. As protein phosphorylation is also known to regulate potential protein-protein interactions, it was hypothesised that the mutation of Ser331 on PSAT1 might impact the interaction of PSAT1 either with itself, or with other serine biosynthesis enzymes.

To test this hypothesis, the Flp-In 293 HA-PSAT1 model was used. Taking advantage of the HA-tag on the inducible PSAT1 protein, cell lysates from doxycycline-treated Flp-In 293 HA-PSAT1 (or HA-GFP as a control) cell lines were incubated with anti-HA antibody-conjugated agarose beads to perform a HA-pulldown. This purified HA-PSAT1 from cell lysates. To check for protein-protein interaction, presence of endogenous PSAT1 and other enzymes of the SBP in the pull-down samples was evaluated using western blotting. This allowed assessment of potential differences in protein-protein interaction between HA-PSAT1 mutant variants (Figure 3.19). Pull-down of HA-PSAT1 from Flp-In 293 cells resulted in strong enrichment of HA-PSAT1 in resultant purified lysate samples. Furthermore, interaction of HA-PSAT1 with endogenous PSAT1 was confirmed due to detection of endogenous PSAT1 in the pull-down samples. This indicated that HA-PSAT1 was dimerising with the endogenous protein. Importantly, this dimerisation did not appear to involve phosphorylation of the Ser331 residue. Endogenous PSAT1 appeared equally in the pull-down samples containing HA-PSAT1 wt, HA-PSAT1 S>A and HA-PSAT1 S>E. This indicated that both mutant proteins maintained endogenous dimerisation.

Interestingly, PHGDH was also present in the pull-down assay samples, indicating that it too was purified from lysates via HA-PSAT1 (Figure 3.19 A). This suggested formation of a protein complex containing both PHGDH and PSAT1 proteins in Flp-In 293 cells and is the first indication of an interaction between serine biosynthesis enzymes in human cells. Similar to the interaction

with endogenous PSAT1, the interaction of HA-PSAT1 with PHGDH was unaffected by the mutation of the Ser331 residue, with PHGDH detected in the pull-down samples containing HA-PSAT1 S>A and HA-PSAT1 S>E the same way as it was in the sample containing HA-PSAT1 wt.

To determine whether PHGDH was directly interacting with HA-tagged PSAT1 or if it was only interacting with endogenous PSAT1, siRNA targeting the non-coding sequence of *PSAT1* mRNA was used to suppress the endogenous enzyme and the pull-down was repeated with only the HA-variants expressed. In the absence of endogenous PSAT1, PHGDH was still purified from lysates during the pull-down, indicating direct interaction with the HA-tagged enzyme (Figure 3.19 B). Collectively, this data demonstrates that, as well as enzymatic activity, phosphorylation of PSAT1 residue Ser331 is a post-translational modification that is entirely dispensable for protein-protein interactions.

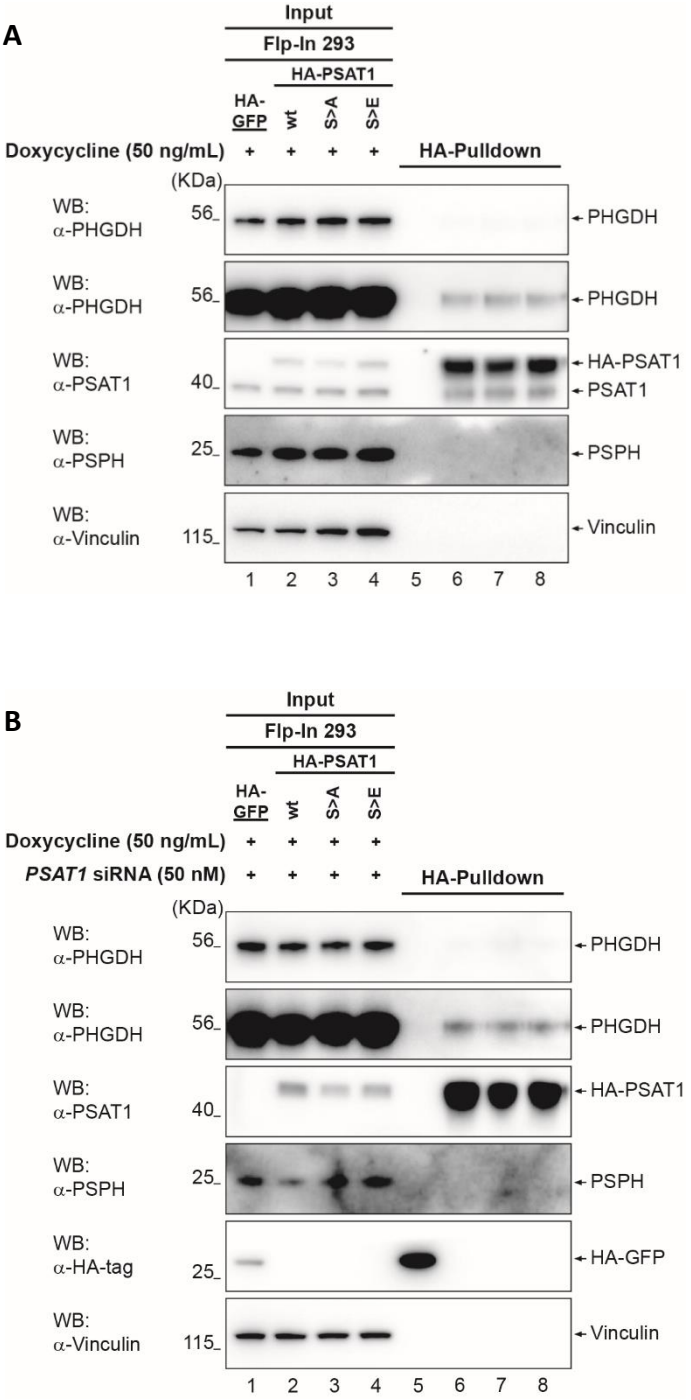

Figure 3.19 – HA-PSAT1 wt and mutant variants interact with endogenous PSAT1 and PHGDH. Western blots from HA-tag pull-down purification of Flp-In 293 HA-PSAT1 cell lysates, demonstrating the protein-protein interactions of all variants of HA-PSAT1 with endogenous PSAT1 and PHGDH. Flp-In 293 HA-GFP control cells and Flp-In 293 HA-PSAT1 wt, Flp-In 293 HA-PSAT1 S>A and Flp-In 293 HA-PSAT1 S>E cells were **(A)** treated with 50 ng/ml doxycycline for 16 hours or **(B)** transfected with 3 siRNA oligos targeting the non-coding sequence of *PSAT1* mRNA or a single non-targeting control oligo to a final concentration of 50 nM for 72 hours. siRNA-transfected cells were simultaneously treated with 50 ng/ml doxycycline for the final 16 hours. Cells from (A) and (B) were lysed and lysates were used in an HA-pulldown for purification of HA-tagged proteins. Lanes 1 to 4 demonstrate the input samples and lanes 5-8 demonstrate the purified HA-pulldown lysates. Presence of endogenous PSAT1 and PHGDH in lanes 6-8 indicate protein interaction with HA-PSAT1. Vinculin is shown as a loading control in the input.

3.9 PSAT1 Ser331 is an important residue for protein stability

As phosphorylation of PSAT1 Ser331 appeared to be dispensable for both enzymatic activity and protein-protein interaction, attention was turned to another possible role for protein phosphorylation and the importance of Ser331 phosphorylation in the regulation of protein stability was investigated.

Initial induction tests of the Flp-In 293 HA-PSAT1 mutant cell lines did in fact indicate a role for the phosphosite in protein stability when, in spite of equal expression of the wt and mutant variants at the mRNA level, the mutant proteins exhibited significantly different levels of protein expression compared to PSAT1 wt. Indeed, the PSAT1 S>E mutant protein was expressed at a significantly higher level than the wt and the PSAT1 S>A mutant protein was expressed to a significantly lower level (Figure 3.10). Similarly, initial induction of the MDA-MB-453 PSAT1 mutant cell lines exhibited significantly lower expression of PSAT1 S>A than PSAT1 wt, in spite of marginally higher mRNA levels (Figure 3.13). These data seemed to indicate that the S>A mutant was always expressed to a lesser degree than the wt protein, which is potentially indicative of lower protein stability. Therefore, to evaluate comparative protein stability, a two-fold approach was taken. Firstly, the rate of protein degradation was assessed using a pulse chase experiment and secondly, the comparative rate of PSAT1 induction was determined by performing a doxycycline-induction time course. Once again, the Flp-In 293 system is a particularly good system for comparison of mutant versions of the same protein as inducible expression is typically equal, due to the single insertion of inducible genes at the same point in the genome, under the same promoters. This is exhibited in the lack of significant difference in mRNA expression of the HA-PSAT1 variants in the Flp-In 293 cells versus the comparatively variable mRNA expression in MDA-MB-453 PSAT1 cells. For this reason, the Flp-In 293 HA-PSAT1 cells were used as a more reliable model for assessing protein stability.

A pulse chase experiment is useful for evaluating the relative stability of inducible proteins over time. The stimulus for induction of the protein is applied for a limited window of time in a “pulse” and is subsequently washed away. Representative samples are then taken at set intervals following the removal of the stimulus to “chase” the degradation of the protein over time as no more protein is induced to replace what is degraded. For this experiment in Flp-In 293 HA-PSAT1 cells were treated with doxycycline for 16 hours and washed, then representative cell samples were harvested at 24-hour intervals up to 96 hours. Subsequently, a western blot was performed to visualise relative protein degradation and densitometry analysis was used to quantify relative amounts of HA-PSAT1 remaining after the initial pulse. Across the 3 HA-PSAT1 cell lines, the

amount of HA-PSAT1 protein remaining was always expressed as a portion of the initial induction of the PSAT1 variant from that cell line (i.e. starting quantities of HA-PSAT1 wt, HA-PSAT1 S>A and HA-PSAT1 S>E were equally defined as a value of 1.0). Quantification of the western blot demonstrated that whilst no significant differences were observed between the degradation curves of the HA-PSAT1 variants, a subtle but distinct and repeatable trend was apparent, in that HA-PSAT1 S>A degraded marginally faster than HA-PSAT1 wt with a half-life of roughly 32 hours vs the wt half-life of 38. Conversely, HA-PSAT1 S>E remained expressed for slightly longer, exhibiting a half-life of around 48 hours (Figure 3.20).

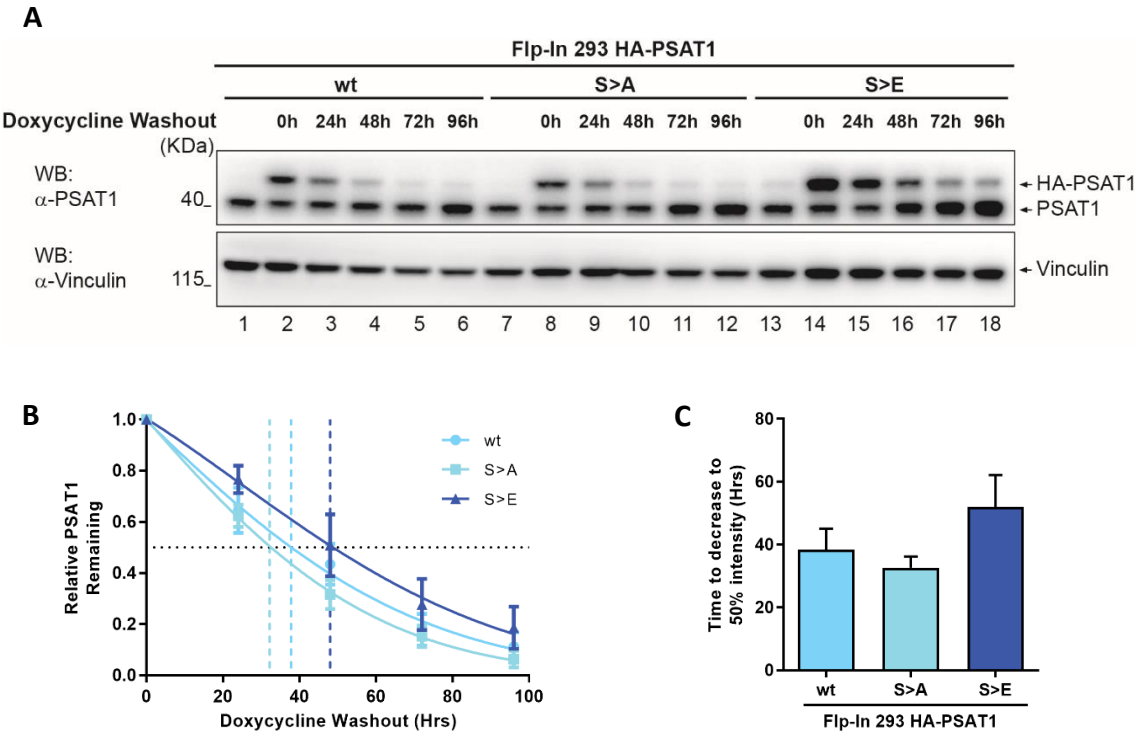

Figure 3.20 – Mutation of PSAT1 Ser331 residue alters the protein degradation rate. Pulse chase experiment characterising the relative degradation rates of HA-PSAT1 wt, HA-PSAT1 S>A and HA-PSAT1 S>E proteins. Corresponding Flp-In 293 HA-PSAT1 cell lines were treated with 50 ng/ml doxycycline for 16 hours, which was subsequently washed away. Representative cell samples were harvested at 24-hour intervals up to 96 hours to track degradation. **(A)** Western blot demonstrating the degradation of HA-tagged PSAT1 after initial induction. Vinculin is shown as a loading control. **(B and C)** Densitometry analysis quantification of HA-PSAT1 protein levels at 24, 48, 72 and 96 hours relative to initial induced level of HA-PSAT1 wt, HA-PSAT S>A and HA-PSAT1 S>E respectively. Comparative degradation curves (B) demonstrated marginally slower degradation of S>E mutant and faster degradation of S>A mutant. The average half-life (C) of S>E PSAT1 mutant was higher than that of the S>A mutant. n=4 independent experiments, mean ± SEM.

After characterisation of HA-PSAT1 degradation, attention was turned to assessing relative rates of HA-PSAT1 protein induction. To evaluate induction rates, the 3 Flp-In 293 HA-PSAT1 cell lines were treated with doxycycline at 2 hourly intervals, up to 10 hours, to induce HA-PSAT1 protein at different time points and generate a curve of steadily increasing protein levels over time. As

with the pulse chase experiment, a western blot was performed to visualise the increase in HA-PSAT1 protein levels and densitometry analysis was used to quantify the induction over the time scale. To quantify relative protein levels, all protein quantities were normalised to the final induced level of wt PSAT1 at 10 hours, which was defined as a value of 1.0. This allowed determination of the relative time it would take for protein levels of HA-PSAT1 S>A or HA-PSAT1 S>E mutants to accumulate to equal levels of HA-PSAT1 wt.

After 10 hours of doxycycline induction, HA-PSAT1 S>E levels were significantly higher than levels of HA-PSAT1 wt and HA-PSAT1 S>A. After just 8 hours of doxycycline induction, the HA-PSAT1 S>E protein had accumulated to levels equivalent to that of the HA-PSAT1 wt protein after 10 hours. This indicated that the HA-PSAT1 S>E protein accumulated faster than the wt protein. On the other hand, the HA-PSAT1 S>A protein failed to accumulate to levels equivalent to that of the HA-PSAT1 wt protein by the end of the 10-hour experiment. This data indicated that the HA-PSAT1 S>A protein accumulated slower than the HA-PSAT1 wt protein (Figure 3.21).

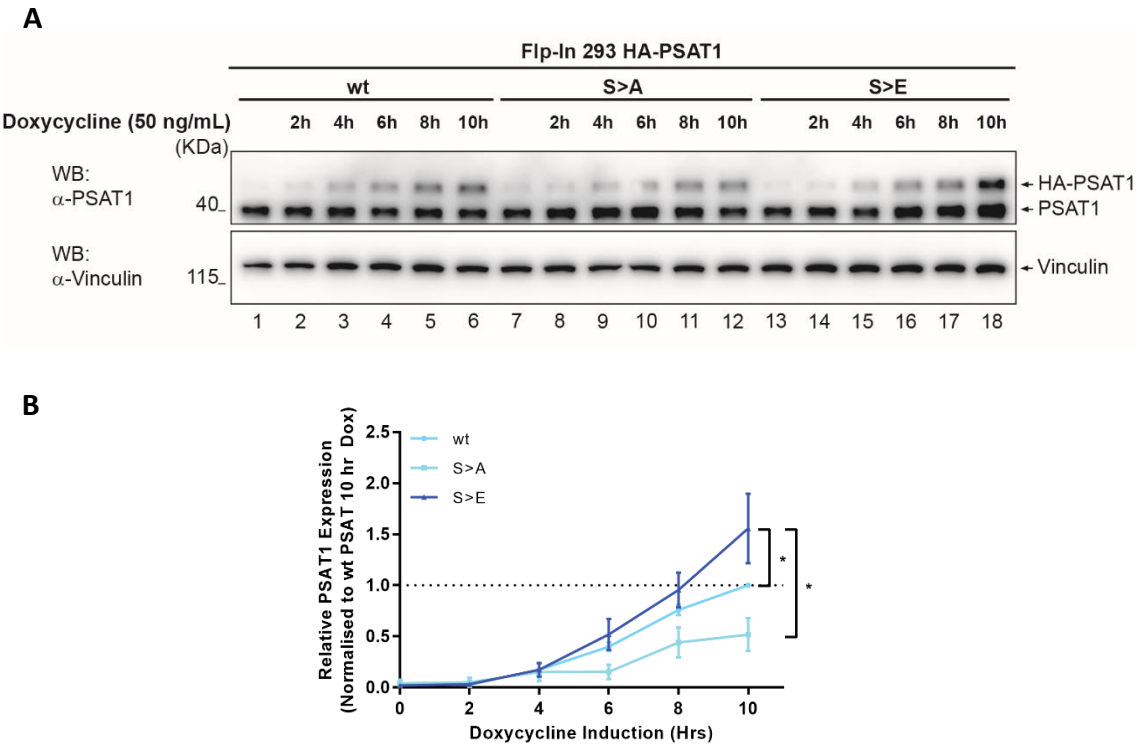

Figure 3.21 – Mutation of PSAT1 Ser331 significantly alters HA-PSAT1 accumulation rate. Doxycycline induction time course characterising the relative rate of accumulation of HA-PSAT1 wt, HA-PSAT1 S>A and HA-PSAT1 S>E proteins. Indicated Flp-In 293 HA-PSAT1 cell lines were treated with 50 ng/ml doxycycline for 2, 4, 6, 8 or 10 hours to track HA-tagged protein induction. **(A)** Western blot demonstrating the relative induction rates of the different HA-PSAT1 variants. Vinculin is shown as a loading control. **(B)** Densitometry analysis quantification of HA-PSAT1 protein levels from all variants at all time points, relative to the quantified level of HA-PSAT1 wt at 10 hours of doxycycline induction, was used to visualise relative induction rates for the different HA-PSAT1 variants. HA-PSAT1 S>E mutant protein levels at 10 hours are significantly higher than HA-PSAT1 wt or HA-PSAT1 S>A protein levels. n=3 independent experiments, mean ± SEM, *p<0.05 as measured by two-way repeated measures ANOVA with Bonferroni *post-hoc* tests.

Together, these data demonstrate a slower accumulation and faster degradation of the HA-PSAT1 S>A mutant and, conversely, a faster accumulation and slower degradation of the HA-PSAT1 S>E mutant. This supports the hypothesis that the Ser331 residue is an important residue for protein stability. One which, if phosphorylated, might promote stabilisation and accumulation of the protein.

3.10 Discussion

This chapter described the characterisation of PSAT1 as a novel IKKε substrate, phosphorylated in an IKKε-dependent manner at serine residue Ser331, and detailed the experiments leading to the identification of Ser331 as an important serine residue for PSAT1 protein stability, thereby demonstrating a novel mechanism of post-translational regulation of the enzyme mediated by IKKε. Various transcription factors have been reported to regulate either all 3 serine biosynthesis enzymes at a transcriptional level, including c-Myc and NRF2[315,324], or specific enzymes of the pathway, such as tumour suppressive kinase protein kinase C zeta (PKCζ) which has been shown to suppress genetic expression of PHGDH and PSAT1[326]. However, very little is known about how the enzymes of the pathway are regulated at a post-transcriptional level. The same study identifying PKCζ as a regulator of PHGDH and PSAT1 gene expression also reported the PKCζ-mediated phosphorylation of PHGDH at 2 highly conserved threonine residues (Thr57 and Thr78) to be an important post-translational modification that negatively regulates PHGDH's enzymatic activity[326], but beyond this, no other post-translational modifications known to regulate PHGDH function have been reported. Furthermore, nothing is currently known about the post-translational regulation of the other enzymes of the SBP.

PSAT1 Ser331 phosphorylation

Phosphoproteomic analysis, highlighting differentially phosphorylated peptides in IKKε-expressing Flp-In 293 cells, identified PSAT1 as significantly more phosphorylated at serine residue Ser331 in the presence of IKKε. Using an *in vitro* kinase assay, PSAT1 was confirmed to be a target of an IKKε-dependent phosphorylation. Importantly however, whilst the *in vitro* kinase assay confirmed that phosphorylation of PSAT1 Ser331 was IKKε-dependent, it proved difficult to definitively confirm that IKKε was directly phosphorylating the enzyme. The identification of phosphorylation of PSAT1 in the samples containing HA-IKKε KD-m initially indicated the kinase-dead IKKε mutant had retained some residual kinase activity. However, this hypothesis was quickly discounted as extensive data had previously confirmed the lack of activity in the mutant kinase. Instead, it became evident that the presence of a secondary kinase in the reaction mixture had led to the phosphorylation of PSAT1 in these samples. Fortunately, mass spectrometry analysis of assay samples allowed identification of other kinases present and a list of 18 was defined (Table 3.3). The only kinase from that list that was present in all the samples where phosphorylation was detected and was also not detected in the control sample was TBK1. Notably, TBK1 is the only other kinase of the 18 which has previously been shown to be associated with IKKε function. It was therefore hypothesised that TBK1 was phosphorylating

PSAT1 in the presence of HA-IKKε KD-m. This raised the question of whether IKKε was phosphorylating PSAT1 at all, or if it was just required for TBK1 to phosphorylate the enzyme.

Attempts were made to unravel this and identify which the phosphorylating kinase was by performing an *in vitro* kinase assay using recombinant IKKε and/or TBK1, but unfortunately, this experiment failed to re-produce PSAT1 phosphorylation due to inactivity of the recombinant kinases. There are various possible reasons why the recombinant kinases failed to be active, including lack of kinase auto-phosphorylation. A possible contributing factor is the absence of IKKε and TBK1 adaptor molecules and scaffolding proteins during the recombinant kinase assay, which could have been present when performing the HA-purified kinase assay. For example, IKKε is known to require K63-linked polyubiquitination for full activity, which might not have been present on the recombinant protein[344]. Another example is the scaffolding proteins that assist the formation of functional IKKε and TBK1 heterodimers. In order to properly dimerise, IKKε and TBK1 require scaffolding proteins like nucleosome assembly protein 1 (NAP1), TANK or similar to NAP1 TBK1 adaptor (SINTBAD) (reviewed by Chau, 2008[85]). Such adaptors were not present in the recombinant kinase experiment, but notably, TANK was detected in the HA-purified *in vitro* kinase assay samples. This suggests it was purified in complex with IKKε and indicates that combination of recombinant IKKε and TBK1 with TANK protein might facilitate the formation of functional dimers and be sufficient to elicit PSAT1 phosphorylation, but this would undoubtedly require experimental validation. If this hypothesis were true however, it would imply an IKKε/TBK1 heterodimer was responsible for PSAT1 phosphorylation, not either kinase individually. This hypothesis is in fact supported by the existing *in vitro* kinase assay data presented in this chapter. TBK1 was detected in all assay samples, which should suggest PSAT1 would be phosphorylated if the kinase could phosphorylate it alone. Instead, PSAT1 phosphorylation was only detected in samples were HA-IKKε and TBK1 were present simultaneously, suggesting an IKKε/TBK1 heterodimer is required for the phosphorylation. This would also be in agreement with the substantial overlap in substrates that is observed between the two kinases, as both IKKε and TBK1 have repeatedly been shown to phosphorylate the same residues on proteins, including IRF3[86], cRel[82] and p65[194].

Phosphorylation of PSAT1 at serine residue Ser331 has previously been reported in a number of studies using high throughput techniques, including studies aiming to determine the phosphoproteome of breast cancer tissues[345], lung cancer cells[346] and melanoma cells[347] to name a selection. Importantly, no pre-existing studies have attempted to characterise the functional relevance of phosphorylation of this residue, making the experiments described in this chapter the first real effort to do so.

PSAT1 Ser331 phosphorylation in enzyme activity

The experiments described here support the hypothesis that PSAT1's Ser331 residue is an important site for regulation of protein stability, demonstrating that, compared to the wild-type protein, the phospho-mimic PSAT1 S>E mutant protein showed characteristics of greater stability and the phospho-mutant PSAT1 S>A protein exhibited the opposite phenotype. Interestingly, whilst the data indicates phosphorylation of PSAT1 Ser331 promotes accumulation of protein levels, it appeared insufficient to alter serine biosynthesis itself. Modulation of the PSAT1 Ser331 residue failed to demonstrate any significant effect on the production of serine when serine biosynthesis was measured using labelled metabolite analysis. Despite this, it is difficult to completely rule out the prospect that phosphorylation of PSAT1 Ser331 might have some impact on enzyme activity. Firstly, and most strikingly, previous work has detailed the existence of an alternate, shorter PSAT1 isoform. This isoform is lacking 46 amino acids between Val290 to Ser337 compared to the canonical full-length protein. Importantly, this shorter version of the enzyme has been shown to be substantially lacking in enzymatic activity compared to the dominantly expressed full-length protein[348]. This suggests something within this 46-amino acid sequence is important for enzymatic function. According to the PSAT1 entry in the PhosphoSitePlus® database[338], multiple residues within this sequence of the protein are targets of post-translational modifications, including several ubiquitination and acetylation targets, but phosphorylation of Ser331 stands out as the second most reported modification within the sequence and as the only phosphorylation target in the full-length PSAT1 protein that is not present in the shorter sequence. It is impossible to speculate on the relative importance of other PSAT1 post-translational modifications without further investigation into their functions, but considering that the activity of PHGDH, another serine biosynthesis enzyme, has been shown to depend on protein phosphorylation events[326], it is not unreasonable to imagine that phosphorylation of Ser331 might contribute to the increased activity of the full-length protein.

It is also worth considering that Ser331 is just a solitary post-translational modification site on the protein. Phosphorylation of Ser331 might represent just one of several PSAT1 post-translational modifications that serve to regulate enzyme activity. It is possible that Ser331 phosphorylation does contribute to the regulation of PSAT1 function but cannot regulate the function enough on its own to significantly impact serine production. Instead Ser331 phosphorylation might act in tandem with other phosphorylation events to modulate activity of the enzyme. Once again utilising information from the PhosphoSitePlus® database[338], numerous other phosphorylation sites on PSAT1 have been described. As with Ser331 however, each of these sites have been characterised in studies using mass throughput techniques and no other

functional residues have yet been reported. It does seem unlikely however, that IKKε itself phosphorylates PSAT1 at any other residues. Not only was no other significant change in PSAT1 phosphorylation detected during the phosphoproteomic analysis, but no further overlap of at least 3 out of 4 residues from IKKε's optimal phosphorylation motif[197] was detected in the PSAT1 sequence. Therefore, if PSAT1 is phosphorylated at other sites, it is likely these events are IKKε-independent.

Another point to consider is that, although the experiments detailed here show that the residue is dispensable for protein-protein interactions, the phosphorylation of the residue might serve to alter substrate interaction dynamics and alter the affinity of PSAT1 for either phosphohydroxypyruvate or glutamate, thereby indirectly regulating the activity of the enzyme. The effect of PSAT1 Ser331 phosphorylation on substrate affinity is therefore also something that should be investigated.

It is also worth recognising that the experimental conditions used to assess enzyme activity via labelled metabolite analysis might have served to mask detectable differences in serine production between HA-PSAT1 wt and HA-PSAT1 mutant variants. Although the flux analysis experiment showed no change in serine production upon mutation of the PSAT1 Ser331 residue, this experiment was performed in the presence of extracellular serine. This means that even though the SBP was active, the Flp-In 293 cells in which the labelled metabolite analysis was performed were not wholly dependent on *de novo* serine production for survival. It is possible that, in such circumstances, the amount of serine produced via PSAT1 is low enough that even an activity deficient variant of the enzyme could be active enough to produce the same amount of serine as the wild-type enzyme, thereby masking differences in mutant enzyme capacity. To address this limitation, it would be worth repeating the experiment in conditions where cells are deprived of extracellular serine, are forced to rely solely on the SBP for survival and are therefore utilising each of the serine biosynthesis enzymes to their maximal capacity. Considering a diminished ability for the HA-PSAT1 S>A mutant enzyme to rescue the growth of Flp-In 293 cells in serine-free medium, it is possible that differences in serine production could be observed in these conditions.

PSAT1 Ser331 phosphorylation in proliferation

Should the phosphorylation of Ser331 be entirely uninvolved in PSAT1's role in serine production, the fact that the phospho-mutant HA-PSAT1 S>A protein exhibited a lesser ability to rescue growth of Flp-In 293 cells in serine-free medium would suggest that PSAT1 Ser331 phosphorylation is important for an undetermined secondary function of the enzyme that

supports cell survival in nutrient-deprived conditions. One possibility to explore is that PSAT1 has been shown to regulate cyclin D1 stability by indirectly inhibiting GSK3β, preventing cyclin D1 phosphorylation to stabilise the protein, sustaining cell cycle progression and proliferation[310]. It is possible that the marked decrease in HA-PSAT1 S>A protein levels, associated with reduced protein stability, is insufficient to reduce serine production, but is enough to impact inhibition of GSK3β, thereby reducing proliferation. Examination of the cell cycle profile, cyclin D1 stability and cell cycle progression markers in cells expressing the various PSAT1 mutant proteins would be valuable to determine the effect of PSAT1 Ser331 phosphorylation on its ability to regulate cyclin D1 protein stability. If phosphorylation of PSAT1 Ser331 is involved in the regulation of cyclin D1 and cell cycle progression, this might help explain why, in a study examining the phosphoproteome of different human breast cancer cases, the phosphorylation appeared to associate with the more aggressive triple-negative subtype of breast cancer[345].

It is worth noting that, although the HA-PSAT1 S>A mutant exhibited a reduced ability to rescue Flp-In 293 cell growth in serine-deprived conditions, the same diminished rescue ability was not observed in MDA-MB-453 cells expressing PSAT1 S>A. At this time, it is difficult to speculate why this might be, but it should be recognised that there are fundamental differences between the cell line models that might help explain the discrepancy. Primarily, the Flp-In 293 cell model is a cell line model which basally expresses all three serine biosynthesis enzymes and, as a result, can survive in serine-free conditions until endogenous PSAT1 is suppressed. MDA-MB-453 does not express any detectable PSAT1 protein at a basal level and therefore cannot survive without extracellular serine. It is therefore likely that MDA-MB-453, whilst still dependent on serine that it can get from the extracellular environment, has adapted to survive independently of the serine biosynthesis enzymes. If PSAT1 has a secondary effect on proliferation in Flp-In 293 cells, potentially via regulation of cyclin D1 protein stability, it stands to reason that the MDA-MB-453 cell line, which does not express PSAT1 basally, regulates proliferation independently of PSAT1. As a cancer cell line, alternative mechanisms for overriding the cell cycle will likely have been developed. This would suggest that when PSAT1 is suddenly reintroduced upon doxycycline treatment of MDA-MB-453 PSAT1 cells, the enzyme serves only to facilitate the production of serine, allowing cells to survive in the absence of extracellular serine, but not conferring any secondary proliferative advantage. It could therefore be hypothesised that if phosphorylation of PSAT1 Ser331 is an important post-translational modification for the regulation of proliferation, then the modulation of this residue would have little effect in MDA-MB-453 cells. Since labelled metabolite analysis has indicated that the different HA-PSAT1 protein variants can synthesise equal amounts of serine, it would therefore be expected that the different PSAT1 variants in

MDA-MB-453 cells also produce equal amounts and rescue growth in serine-deprived conditions equally. If testing the effect of expression of HA-PSAT1 wt, HA-PSAT1 S>A or HA-PSAT1 S>E mutant proteins on cyclin D1 protein stability in Flp-In 293 cells, it would be interesting to test the effect of the mutant proteins on cyclin D1 in MDA-MB-453 cells as well, to ascertain whether the enzyme would have any proliferative role in the breast cancer cell line or not.

Clinical implications of PSAT1 Ser331 phosphorylation

With the context of breast cancer in mind, obvious questions over the pathophysiological relevance of IKKε-dependent PSAT1 phosphorylation in breast cancer are raised by the identification the Ser331 phosphosite, especially considering the lack of significant effect on enzymatic activity upon modulation of the phosphosite.

As mentioned above, the reduced ability for the HA-PSAT1 S>A mutant to rescue growth in serine-free conditions suggest that the phosphosite is important for cell growth or survival in some manner. Furthermore, whilst the data presented here cannot go far enough to fully elucidate clear evidence of a physiological benefit to PSAT1 Ser331 phosphorylation, evidence in the literature base does at least suggest that the site is actively phosphorylated in a subset of breast cancers associated with particularly poor prognosis. As mentioned above, in a high throughput analysis of the phosphoproteome of multiple patient-derived breast cancer tissues, PSAT1 Ser331 phosphorylation was reported at a substantially higher degree in tissues coming from patients with a more aggressive, triple negative subtype disease[345]. This indicates that phosphorylation of the enzyme might contribute to disease progression in some, as yet uncharacterised, way and suggests the phosphosite might be prognostic for poor patient outcome.

Interestingly, this apparent association of PSAT1 Ser331 phosphorylation with a specific breast cancer subtype is in contrast to the activity of IKKε in breast cancer, which has been shown to be oncogenic without any distinct correlation to disease subtype[195]. However, in spite of the overall lack of correlation of IKKε expression with tumour subtype, a subset of IKKε-driven triple-negative breast cancer has been described. Termed “immunomodulatory”, this subtype of triple negative breast cancer is distinct, due to an activated JAK/STAT cytokine signalling network which has been shown to be driven by IKKε expression[213]. Therefore, whilst expression of the kinase itself shows no clear correlation with breast cancer subtype, it is clear that IKKε activity is associated with certain subsets of triple negative classified tumours. This activity might be responsible for the increased PSAT1 Ser331 phosphorylation observed in patients with tumours exhibiting the triple-negative phenotype.

IKKε-dependent phosphorylation of other serine biosynthesis enzymes

The question remains as to whether IKKε's post-translational regulation of the serine biosynthesis enzymes is limited to PSAT1, or if the other enzymes are potential substrates. Current evidence suggests the answer to this question is that IKKε specifically acts on PSAT1, since neither PHGDH nor PSPH phosphorylation was detected in the phosphoproteomic analysis performed in the early stages of this project. Searching for potential IKKε phosphosites in the PHGDH and PSPH sequences using IKKε's optimal phosphorylation motif[197] and looking for at least 3 out of 4 overlapping residues, did identify residues in both PHGDH and PSPH that matched the sequence targeted by the kinase, namely PHGDH serine residue Ser166 and PSPH serine residue Ser114. Whilst this does suggesting phosphorylation might be possible, according to information contained within the PHGDH and PSPH entries in the PhosphoSitePlus database[338], neither of these sites have ever been previously reported as phosphorylated. This raises a question over whether these residues would even be phosphorylatable *in vivo* at all and suggests that neither of these proteins could be legitimate IKKε substrates in the way PSAT1 is. This would imply that the regulation of the SBP by IKKε is centred specifically around the second enzyme of the pathway. This would be in accordance with the fact that, despite PHGDH being the subject of genetic amplification in breast cancer[304,305], the ability for PSAT1 to generate glutamine-derived α-KG to fuel the TCA cycle means it provides more direct growth benefits to tumours than PHGDH[305].

Given the importance of the donation of serine-derived carbon to one-carbon metabolism in cancer for the maintenance of redox balance, it would also be important to address whether SHMT, the enzyme catalysing the catabolism of serine to glycine and the donation of serine-derived carbon to the one-carbon cycle, might also be a target of IKKε phosphorylation. Again, no SHMT phosphopeptide was detected in the phosphoproteomic analysis, but overlap of the optimal IKKε motif with the sequence of either SHMT isoform (SHMT1 catalyses the reaction in the cytosol and SHMT2 catalyses the reaction in the mitochondria) revealed three potential IKKε target sites on SHMT1; Ser164, Ser169 and Ser473 and five potential sites on SHMT2; Ser5, Ser187, Ser192, Ser322 and Ser470. Of these identified residues, SHMT1 Ser169 and SHMT2 Ser5 and Ser192 all demonstrated overlap of 4 out of 4 possible residues from the optimal recognition motif, demonstrating a strong potential for phosphorylation of these residues by IKKε. However, as with PHGDH and PSPH, most of these identified potential phosphosites have not been previously reported. Only SHMT2 Ser470 having been reported in a single study using mass-throughput analysis techniques[349]. Especially considering the lack of identified phosphopeptide for any other serine related enzyme, it therefore seems likely that PSAT1 is the only serine

biosynthesis enzyme subject to IKKε-dependent phosphorylation. To confirm this hypothesis however, it would be important to perform further *in vitro* kinase assays to definitively rule out IKKε-dependent phosphorylation of the other enzymes.

Phosphorylation of other metabolic proteins by IKKε

In addition to the finding of PSAT1 Ser331 phosphorylation in IKKε-expressing cells, several other metabolic proteins were identified to be significantly more phosphorylated in the presence of kinase expression. These enzymes included glycolytic enzymes fructose bisphosphate aldolase at serine residue Ser46, gamma enolase at residue Ser40 and triosephosphate isomerase at residues Ser58 and Ser273. Phosphorylation of fructose bisphosphate aldolase Ser46, gamma enolase Ser40 and triosephosphate isomerase Ser58 residues have all been previously reported in the PhosphoSitePlus® database[338], but as before, only in mass-throughput studies. Interestingly, no previous reports have been made regarding triosephosphate isomerase Ser273. Therefore, the finding of IKKε-dependent increased phosphorylation is possibly the first identification of this phosphosite. Again, whether phosphorylation of this site would have any functional role is a question that is yet to be answered. It is worth noting that Ser46 of fructose bisphosphate aldolase, Ser40 of gamma enolase and Ser273 of triosephosphate isomerase are all conserved residues in mouse and rat protein sequences. Whether this implies any further importance to a residue for protein function is arguable, but conservation of a residue across species at least suggests it is possible that these residues are important for the function of these enzymes and that IKKε might promote glycolytic activity by phosphorylating them.

The identification of 3 glycolysis enzymes exhibiting increased phosphorylation in the presence of IKKε expression clearly indicates the potential for the kinase to play a role in glycolysis. This is in agreement with previous findings demonstrating a link between IKKε and the upregulation of glycolytic rates. In dendritic cells, IKKε promotes a metabolic shift to aerobic glycolysis upon early activation of the cells[106] and in pancreatic cancer cells, an IKKε dependent-shift to aerobic glycolysis has been shown to sustain cellular proliferation[189]. In dendritic cells, this shift has been reported to be initiated by AKT-dependent phosphorylation of glycolytic enzyme hexokinase II, which is associated with localisation of the enzyme to the mitochondria where it can directly use mitochondrial ATP to maximise its enzymatic efficiency, boosting the glycolytic rate. In pancreatic cancer cells, IKKε-mediated metabolic regulation has been shown to be attributable to the activation of an AKT-dependent phosphorylation cascade which results in stabilisation and nuclear retention of c-Myc, thereby promoting proliferation and glycolysis-related gene expression. This action is dependent on the phosphorylation of GSK3β at serine residue Ser9,

which inhibits the GSK3β-mediated phosphorylation of c-Myc that promotes its nuclear export. Intriguingly, the induction of the aerobic glycolysis phenotype observed in the Flp-In 293 HA-IKKε cells appears independent of both of these described mechanisms, as investigation of the phosphoproteomic analysis detected no significant changes in hexokinase II, GSK3β or c-Myc phosphorylation in the IKKε-expressing cells. Whilst the lack of changes in phosphorylation status of these proteins would need to be experimentally validated, using western blotting or similar techniques, the phosphoproteomic analysis at least indicates a lack of involvement of these mechanisms in IKKε-driven metabolic reprogramming in Flp-In 293 HA-IKKε cells. Consequently, this suggests that the kinase-dependent rewiring of cellular metabolism occurs via a previously uncharacterised mechanism in this particular system.

The phosphoproteomic analysis also demonstrated significantly increased phosphorylation of GFPT1, the enzyme controlling the flow of glucose-derived carbon into the hexosamine biosynthesis pathway, at serine residue Ser261. Phosphorylation of GFPT1 Ser261 has been linked to the induction of GFPT1 enzymatic activity, as the site corresponds to key catalytic residue Ser243 in a splice variant of the enzyme[336,337]. Increased phosphorylation of this residue in IKKε-expressing cells therefore suggests IKKε might promote hexosamine biosynthesis. Other enzymes of the hexosamine biosynthesis pathway, such as UDP-N-acetylhexosamine pyrophosphorylase (UAP1) and GFPT isoenzyme 2 (GFPT2), have been shown to be overexpressed in prostate cancer and support disease development by promoting epithelial-mesenchymal transition and protecting against endoplasmic reticulum stress[350,351]. At the same time, the hexosamine biosynthesis pathway has also been shown to act in a tumour suppressive fashion in a subset of prostate cancers[352]. It is therefore unclear what role, if any, the hexosamine biosynthesis pathway might play in a breast cancer setting, but whether or not IKKε is capable of inducing activity of pathway is certainly an avenue worth exploring. Unfortunately, the performed labelled metabolite analysis failed to detect any metabolite products from the hexosamine biosynthesis pathway so, from the current metabolomics data available, it is difficult to assess the effect that the kinase might have on the pathway without further research.

Phosphorylation of other non-metabolic proteins by IKKε

From a non-metabolic standpoint, the phosphoproteomic analysis also revealed significantly decreased phosphorylation of YAP1 at serine residue Ser61 and significantly increased phosphorylation of histone deacetylase 2 (HDAC2) at residue Ser394 in IKKε-expressing cells. Both of these events are notable. Phosphorylation of YAP1 Ser61 has been shown to contribute to the inhibition of pro-proliferative, oncogenic Hippo pathway signalling. Whilst it should be

noted that phosphorylation of YAP1 Ser61 alone is insufficient to inhibit Hippo pathway oncogenesis[353], decreased phosphorylation of this residue in IKKε-expressing cells suggests that the kinase might at least contribute to the maintenance of a YAP1-dependent oncogenic signal to promote cancer development. In agreement with this, IKKε has been previously linked to cancer development through YAP1 in gliomas, where the kinase has been shown to stabilise YAP1 by decreasing phosphorylation of YAP1 Ser127. This increases YAP1 transcriptional activity which initiates a feedback loop, reinforcing kinase expression through suppression of IKKε-targeting microRNA miR-let-7b/i[173]. Identification of IKKε-dependent decreased YAP1 Ser61 phosphorylation in the phosphoproteomic analysis therefore supports the findings in gliomas, demonstrating a close regulation of Hippo pathway oncogenic activity by the kinase through the regulation of YAP1 protein stability.

Phosphorylation of HDAC2 Ser394 is also an event which can be linked to cancer development. Phosphorylation of this residue has been shown to be important for HDAC2 enzyme activity[354] and HDAC2 overexpression correlates with tumour aggressiveness in breast cancer[355]. Accordingly, HDAC2 has been shown to contribute to breast cancer development by indirectly upregulating DNA-damage response genes like RAD51 through the suppression of microRNA's that inhibit such genes[356]. The increased phosphorylation of HDAC2 by IKKε therefore implies that the kinase might also contribute to cancer development through the promotion of HDAC2 activity, which has not previously been considered as part of the kinases oncogenic potential.

PHGDH/PSAT1 dimer formation in human cell lines

Finally, although it has been mentioned earlier that the PSAT1 Ser331 residue was shown to be inessential for the dimerisation of HA-PSAT1 with endogenous PSAT1 or the interaction of PSAT1 with PHGDH, the data presented in this chapter demonstrating the interaction of PSAT1 interaction with PHGDH represent the first characterisation of a PHGDH/PSAT1 protein-protein interaction in human cell lines. Indeed, in yeast, the yeast homologs of the serine biosynthesis enzymes Ser33 and Ser3 (isoforms of PHGDH) and Shm2 (SHMT) have been shown to interact in a protein complex called SESAME with yeast homologs of PKM2 and SAM synthetases, but no such interactions have as yet been detailed in human cells. It is unlikely that the protein complex observed in the pull-down assay is representative of a human variant of the SESAME complex, since attempts to probe for PKM2 and SHMT demonstrated no pull-down of those enzymes and Ser1 (the yeast homolog of PSAT1) was absent from the SESAME complex. This suggests the interaction observed might represent an as yet uncharacterised complex that contains PHGDH and PSAT1. Other proteins present in such a complex could be identified using mass

spectrometry analysis of HA-pulldown samples and could help elucidate what kind of protein complex is formed, or indicate what its potential function might be.

Concluding remarks

In summary, this chapter has detailed efforts to characterise the IKKε-dependent metabolic phenotype in both a Flp-In 293 system and a more physiological breast cancer cell line model. The kinase was found to significantly increase intracellular serine biosynthesis, a particularly important pathway for rapidly proliferating cells. Consequently, IKKε was shown to be required for the phosphorylation of serine enzyme PSAT1 at a residue that regulates protein stability. As the kinase therefore potentially promotes PSAT1 protein accumulation, the effects of IKKε expression of the serine biosynthesis enzyme protein levels were next explored. The results of such experiments are described in the next chapter.

Chapter 4

Results II

IKKε transcriptionally regulates serine biosynthesis enzymes

4.1 IKKε regulates serine biosynthesis enzyme protein levels in Flp-In 293 cells and breast cancer cell lines

The findings of the previous chapter detailed a mechanism through which PSAT1, upon phosphorylation at serine residue Ser331 in an IKKε-dependent manner, was stabilised at the protein level, leading to faster accumulation and slower degradation of the protein. It was therefore hypothesised that modulation of IKKε expression in Flp-In 293 HA-IKKε cells or human breast cancer cell lines might directly impact the serine biosynthesis enzyme and lead to upregulation of the PSAT1 protein. To test this hypothesis, Flp-In 293 HA-IKKε and Flp-In 293 HA-GFP cells were treated with doxycycline for 16 hours, inducing HA-tagged kinase expression or HA-tagged GFP as a control. The potential impact of HA-IKKε induction on the protein levels of PSAT1 and other serine biosynthesis enzymes was subsequently assessed via western blotting (Figure 4.1).

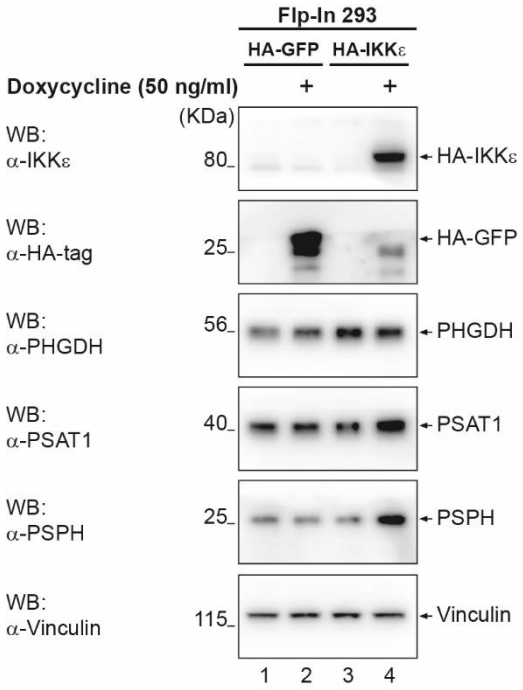

Figure 4.1 – Induction of HA-IKKε in Flp-In 293 cells upregulates PSAT1 and PSPH protein levels. Western blot demonstrating effect of IKKε expression on serine biosynthesis enzyme protein levels in Flp-In 293 cells. Indicated Flp-In 293 cell lines were treated with 50 ng/ml doxycycline for 16 hours inducing HA-GFP or HA-IKKε. PSAT1 and PSPH protein levels were upregulated upon induction of HA-IKKε expression. Vinculin is shown as a loading control.

Treatment of Flp-In 293 HA-IKKε cells with doxycycline led to upregulation of PSAT1, whereas doxycycline treatment of Flp-In 293 HA-GFP cells had no impact of the enzyme's protein levels, confirming that induction of IKKε leads to upregulation of PSAT1 in Flp-In 293 cells. This suggested that the kinase might be phosphorylating and stabilising the enzyme in Flp-In 293

cells, as was hypothesised. Surprisingly, whilst PHGDH protein levels were unaffected by induction of IKKε, PSPH protein levels were upregulated, similar to PSAT1, by expression of the kinase. This indicated that upregulation of the serine biosynthesis enzymes might not be limited to the PSAT1 enzyme and, since the phosphoproteomic analysis did not indicate that IKKε induced PSPH phosphorylation, might not be solely attributable to substrate phosphorylation.

Since PSPH protein levels were unexpectedly found to be upregulated by expression of IKKε, it was also questioned whether SHMT, the enzyme that catalyses the breakdown of serine to glycine and regulates the entry of serine-derived carbon into the one-carbon cycle, might be regulated by the kinase as well. Specifically, it was wondered whether SHMT2, the mitochondrial isoform of the enzyme and the isoform that has been more frequently linked to cancer progression due to its role in maintaining redox balance[320,357-359], might be regulated. To investigate this, protein levels of SHMT2 upon doxycycline treatment of Flp-In 293 HA-GFP or HA-IKKε cells were investigated via western blotting, using the same samples from Figure 4.1.

Treatment of Flp-In 293 HA-GFP or HA-IKKε cells with doxycycline had no effect on the protein levels of SHMT2 (Figure 4.2), demonstrating that the kinase does not regulate the enzyme. This demonstrated that IKKε-mediated protein regulation of enzymes related to serine biosynthesis in Flp-In 293 cells is limited to PSAT1 and PSPH.

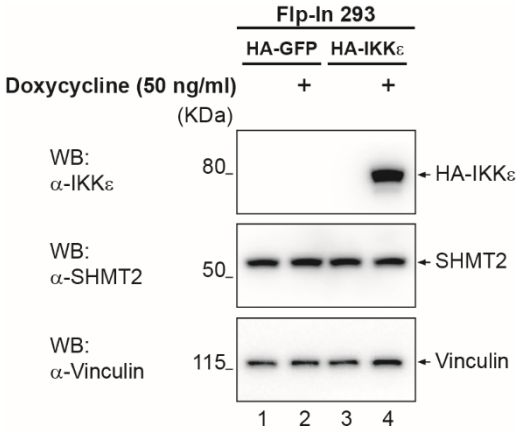

Figure 4.2 – Induction of HA-IKKε expression in Flp-In 293 cells has no effect on SHMT2 protein levels. Western blot indicating SHMT2 protein levels in indicated Flp-In 293 cells upon treatment with 50 ng/ml doxycycline for 16 hours. No change in SHMT2 protein levels was observed upon HA-IKKε induction. Vinculin is shown as a loading control.

To determine whether IKKε was regulating PSAT1 and PSPH protein levels in a more physiological model, the panel of 9 breast cancer cell lines was transfected with a pool of *IKBKE*-targeting siRNA oligos, to suppress IKKε, or a non-targeting control siRNA oligo for 72 hours.

Following transfection, serine biosynthesis enzyme protein levels were evaluated via western blotting (Figure 4.3). Subsequently, protein levels were quantified using densitometry analysis in order to determine changes IKKε-mediated in serine biosynthesis enzyme protein expression (Figure 4.4).

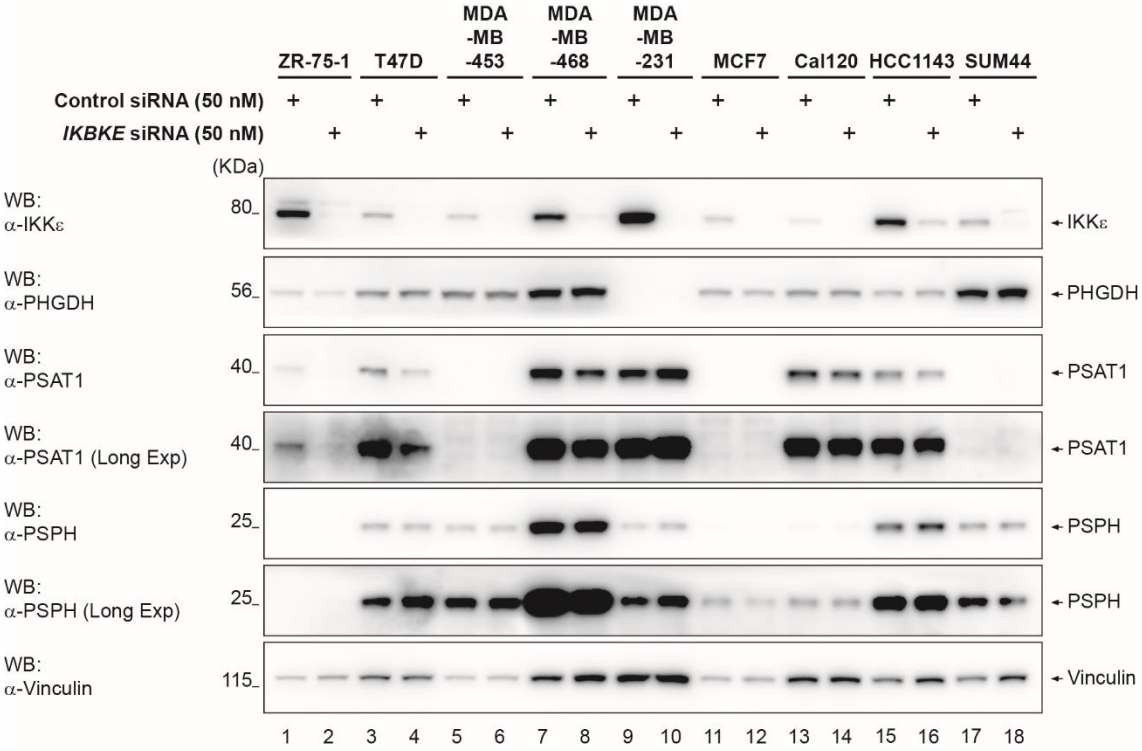

Figure 4.3 – siRNA-mediated suppression of IKKε in breast cancer cell lines reduces serine biosynthesis enzyme protein levels. Western blot of IKKε and serine biosynthesis enzyme protein levels following transfection of indicated breast cancer cell lines with *IKBKE*-targeting siRNA. Indicated breast cancer cell lines were transfected with a pool of 4 *IKBKE*-targeting siRNA oligos, to suppress IKKε, or a single non-targeting control oligo to a final concentration of 50 nM for 72 hours. Quantification of protein levels is shown in Figure 4.4. Vinculin is shown as a loading control.

In agreement with the findings in Flp-In 293 cells, siRNA-mediated suppression of IKKε expression significantly reduced PSAT1 protein levels in 5 out of 9 breast cancer cell lines tested. Of the remaining cell lines, only MDA-MB-231 failed to show any significant change in PSAT1 protein levels, as MDA-MB-453, MCF7 and SUM44 do not basally express the protein to any detectable level. Additionally, significant decreases in PHGDH and PSPH protein levels were detected in the ZR-75-1 and MDA-MB-468 cell lines. Together, this data validates evidence in Flp-In 293 cells of IKKε-mediated regulation of the protein levels of the serine biosynthesis enzymes. Furthermore, demonstration of a significant IKKε-mediated regulation of serine biosynthesis enzymes in human breast cancer cells supports the hypothesis that the kinase regulates serine biosynthesis enzymes in human breast tumours. Importantly, PSAT1 represents

a key focal point of regulation of the pathway by IKKε, being repeatedly regulated by the kinase across multiple cell lines, potentially reflecting the fact that it is phosphorylated in an IKKε-dependent manner.

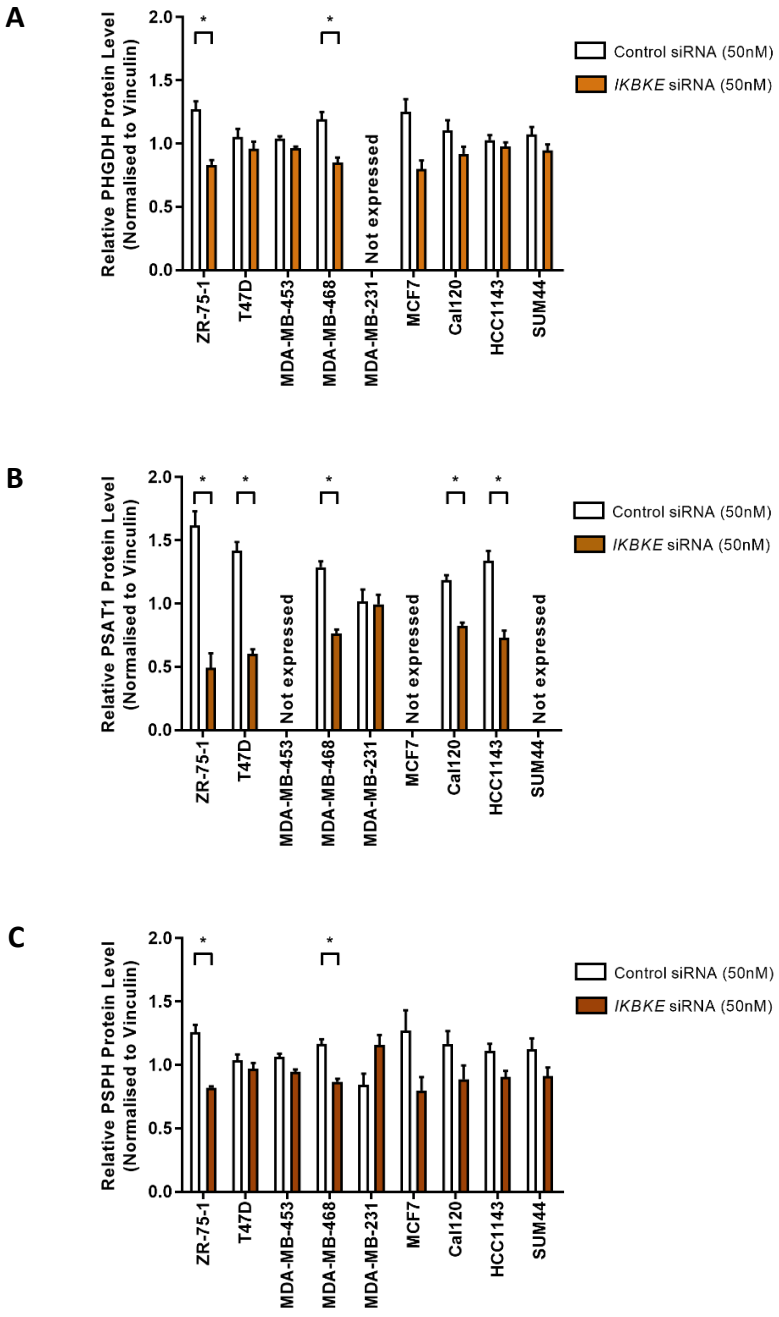

Figure 4.4 – Quantification of reduction in serine biosynthesis enzyme protein levels in breast cancer cell lines upon transfection of *IKBKE* siRNA. Densitometry quantification analysis of **(A)** PHGDH, **(B)** PSAT1 and **(C)** PSPH protein levels upon transfection of indicated breast cancer cell lines with *IKBKE*-targeting siRNA and subsequent suppression of IKKε protein. PSAT1 protein levels were significantly reduced by IKKε siRNA transfection in all breast cancer cell lines where it is expressed, with the exception of MDA-MB-231. PHGDH and PSPH protein levels were significantly reduced by suppression of the kinase in ZR-75-1 and MDA-MB-468 cell lines. Serine enzyme densitometry per sample was quantified as a percentage of total protein densitometry and normalised to vinculin. n≥3 independent experiments, mean ± SEM, *p<0.05 as measured by paired t-test.

4.2 IKKε regulates serine biosynthesis enzyme transcription

Whilst the regulation of the PSAT1 protein by IKKε was expected, due to results from the previous chapter demonstrating that phosphorylation of the enzyme in an IKKε-dependent manner resulted in protein stabilisation, the findings that expression of the kinase regulated protein levels of PSPH in Flp-In 293 HA-IKKε cells and PHGDH and PSPH in ZR-75-1 and MDA-MB-468 breast cancer cell lines were unexpected. As previously discussed, existing evidence suggested that IKKε-mediated phosphorylation of PHGDH and PSPH is unlikely, suggesting a mechanism of regulation for the enzymes other than substrate phosphorylation. Therefore, the effect of IKKε expression on the transcription of the serine biosynthesis enzymes was evaluated.

Flp-In 293 HA-IKKε and Flp-In 293 HA-GFP cells were treated with doxycycline for 16 hours to induce HA-IKKε or HA-GFP respectively. mRNA levels of *PHGDH*, *PSAT1* and *PSPH* were subsequently measured using qRT-PCR. Changes in serine biosynthesis enzyme transcript levels were evaluated as fold changes versus basal levels in untreated Flp-In 293 HA-GFP samples. As expected, treatment of Flp-In 293 HA-GFP cells with doxycycline had no effect on the mRNA levels of the serine biosynthesis enzymes. However, treatment of Flp-In 293 HA-IKKε cells with doxycycline significantly upregulated mRNA levels of all three serine biosynthesis enzymes, indicating that IKKε regulates *PHGDH*, *PSAT1* and *PSPH* at a transcriptional level, in addition to the post-translational regulation of the PSAT1 protein via phosphorylation (Figure 4.5).

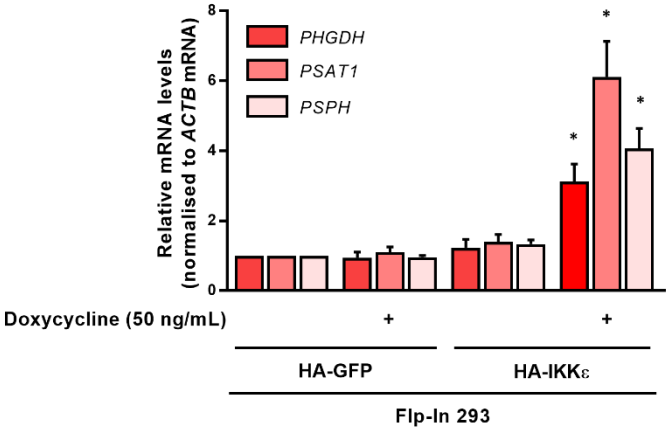

Figure 4.5 – Induction of HA-IKKε in Flp-In 293 cells upregulates serine biosynthesis enzyme mRNA levels. qRT-PCR analysis measuring *PHGDH*, *PSAT1* and *PSPH* mRNA levels upon treatment of Flp-In 293 cells with 50 ng/ml doxycycline for 16 hours. Doxycycline treatment of Flp-In 293 HA-IKKε, but not Flp-In 293 HA-GFP cells significantly upregulated *PHGDH*, *PSAT1* and *PSPH* mRNA levels. mRNA levels are presented as relative fold change values from HA-GFP non-treated samples and normalised to *ACTB* (β-Actin) mRNA levels. n=4 independent experiments, mean ± SEM, *p<0.05 as measured by two-way ANOVA with Bonferroni *post-hoc* tests.

To determine whether the upregulation of serine biosynthesis enzyme transcript levels was a result of increased IKKε kinase activity in doxycycline-treated cells, the effect of induction of HA-IKKε wt and HA-IKKε KD-m, a mutant variant of the kinase featuring a K38A point mutation in the protein kinase domain that ablates kinase activity (Figure 3.1), on *PSAT1* mRNA was assessed and compared. Whilst induction of HA-IKKε wt led to a significant increase in *PSAT1* mRNA levels as before, induction of HA-IKKε KD-m, failed to elicit the same upregulation (Figure 4.6). This demonstrated that upregulation of the serine biosynthesis enzymes upon doxycycline treatment of Flp-In 293 HA-IKKε cells was a consequence of elevated IKKε kinase activity in the cells, suggested that the transcriptional upregulation of the enzymes was a result of kinase activity-dependent IKKε downstream signalling.

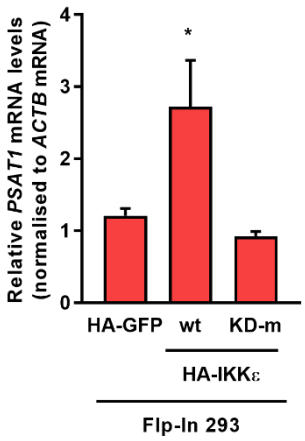

Figure 4.6 – Transcriptional upregulation of *PSAT1* mRNA requires IKKε kinase activity. qRT-PCR analysis of *PSAT1* mRNA levels in Flp-In 293 HA-GFP, HA-IKKε wt or HA-IKKε KD-m cell lines upon treatment with 50 ng/ml doxycycline for 16 hours. *PSAT1* mRNA levels are expressed as a fold change versus basal mRNA levels in non-treated cells. Induction of HA-IKKε wt but not HA-IKKε KD-m significantly upregulated *PSAT1* mRNA levels, demonstrating dependency on IKKε kinase activity for transcriptional regulation of serine biosynthesis enzymes. *PSAT1* mRNA levels are normalised to *ACTB* (β-Actin) mRNA levels. n=3 independent experiments, mean ± SEM, *p<0.05 as measured by two-way ANOVA with Bonferroni *post-hoc* tests.

Given the hypothesised involvement of fellow IKK family member and close IKKε relation TBK1 in the phosphorylation of PSAT1, it was questioned whether the kinase might also be involved in IKKε-mediated transcriptional regulation of the serine biosynthesis enzymes. To address this question, *TBK1*-targeting siRNA was used to facilitate induction of HA-IKKε in Flp-In 293 cells in the absence of TBK1. Flp-In 293 HA-IKKε cells were transfected with a pool of siRNA oligos targeting *TBK1* mRNA, to suppress TBK1, or a non-targeting control oligo for 72 hours. Cells were

simultaneously treated with doxycycline for the final 16 hours to induce HA-IKKε without the interference of TBK1.

Induction of HA-IKKε in TBK1 silenced Flp-In 293 cells resulted in upregulation of PSAT1 and PSPH proteins to a level roughly equivalent to what was observed in cells where TBK1 had not been suppressed (Figure 4.7 A). Similarly, at the transcript level, there was no significant difference in IKKε-driven *PSAT1* mRNA upregulation in cells transfected with *TBK1* siRNA compared to cells transfected with control siRNA (Figure 4.7 B). Suppression of TBK1 also had no clear effect on basal *PSAT1* mRNA levels or PHGDH, PSAT1 and PSPH protein levels, indicating that the IKK-related kinase has no role in maintaining the expression of the enzymes of the SBP. Together, these data demonstrate that, whilst seemingly involved in the phosphorylation of PSAT1, TBK1 is inessential for IKKε-mediated upregulation of serine biosynthesis enzyme transcription and protein levels in Flp-In 293 cells. This also indicates that upregulation of serine biosynthesis enzymes is not a function shared by both non-canonical IKK's, but is instead a unique activity of IKKε.

To determine whether IKKε was also regulating serine biosynthesis enzyme transcription in breast cancer cells, kinase expression was silenced in the panel of 9 breast cancer cell lines by using siRNA as before (see 4.1). Following siRNA transfection, *PHGDH*, *PSAT1* and *PSPH* mRNA levels in *IKBKE* siRNA-transfected cells were compared to mRNA levels in control siRNA-transfected cells to identify any IKKε-mediated effect on serine biosynthesis enzyme transcription (Figure 4.8).

In line with what was observed at the protein level, siRNA-mediated IKKε silencing in breast cancer cell lines significantly reduced *PSAT1* mRNA levels in the majority of cell lines tested. Of the cell lines where *IKBKE* siRNA reduced PSAT1 protein levels, only *PSAT1* mRNA levels in Cal120 failed to show a corresponding reduction in response to IKKε suppression. Whilst not significant, the *PHGDH* mRNA levels in ZR-75-1 and MDA-MB-468 cells also showed a trend of reduction upon IKKε silencing, which is in agreement with the significant reduction observed in PHGDH protein levels observed in these cell lines when the kinase was suppressed. Similarly, *PSPH* mRNA levels showed a trend of IKKε siRNA-mediated reduction in MDA-MB-468 cells. No clear trend was observed for *PSPH* mRNA in ZR-75-1 cells however, despite the significant reduction in protein levels observed upon kinase suppression in that cell line. This suggests that, in this cell line, PSPH might be regulated by an IKKε-dependent post-translational mechanism rather than regulation at a transcriptional level. Interestingly, whilst not significant (although this is more than likely due to the limited analytical power of the one-sample t-test required to measure

statistical differences in fold changes between two samples), a strong increase in *PHGDH*, *PSAT1* and *PSPH* mRNA levels was observed in MDA-MB-231 cell. Although this did not appear to translate to any clear increasing trend in serine enzyme protein levels, this does suggest that in MDA-MB-231 cells, IKKε suppresses the transcription of the enzymes of the serine biosynthesis pathway rather than promoting it.

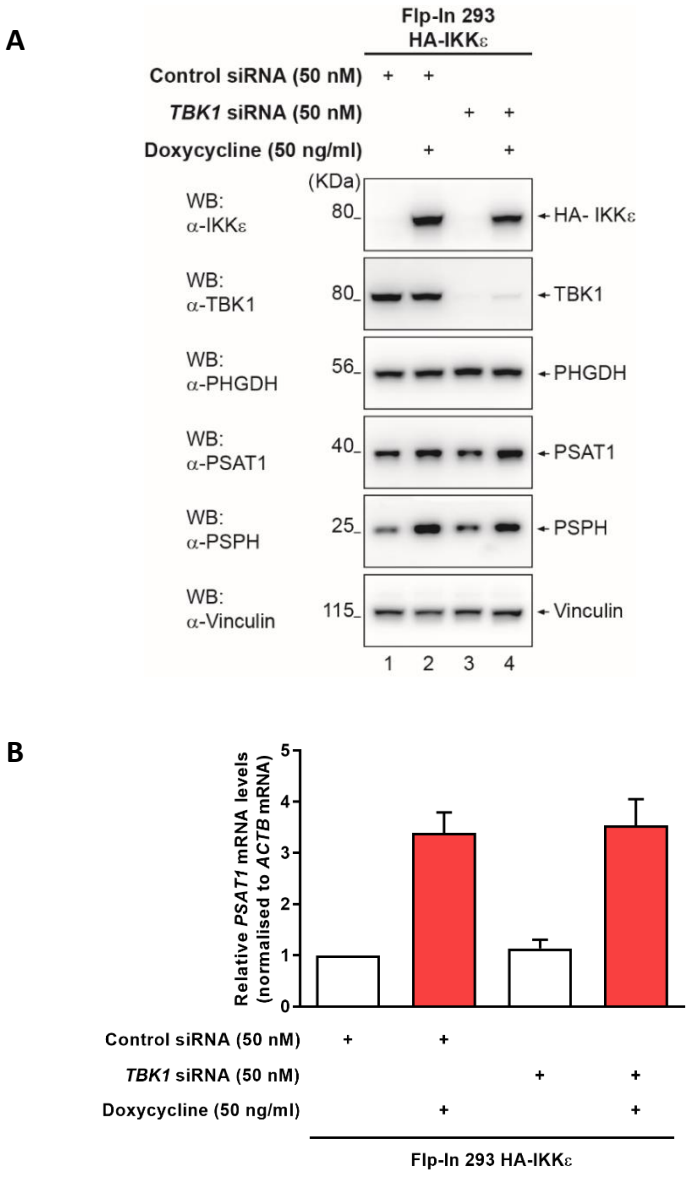

Figure 4.7 – IKKε-mediated regulation of serine biosynthesis enzymes is independent of TBK1. Flp-In 293 HA-IKKε cells were transfected with a pool of 4 siRNA oligos targeting *TBK1* or a single non-targeting control oligo at a final concentration of 50 nM for 72 hours. In the final 16 hours, 50 ng/ml doxycycline was added to the cells to induce HA-IKKε expression in the absence of TBK1. **(A)** Western blot demonstrating the effective knockdown of TBK1 protein levels and the effect HA-IKKε induction on PSAT1 and PSPH protein levels in the presence and absence of TBK1. HA-IKKε still upregulated PSAT1 and PSPH in cells where TBK1 expression was suppressed. Vinculin is shown as a loading control. **(B)** qRT-PCR analysis of *PSAT1* mRNA levels upon the induction of HA-IKKε in Flp-In 293 HA-IKKε cells transfected with either control or *TBK1* siRNA. mRNA levels were expressed as fold changes versus non-treated, control siRNA-transfected cells and normalised to *ACTB* (β-Actin) mRNA levels. n=3 independent experiments, mean ± SEM, *p<0.05 as measured by two-way ANOVA with Bonferroni *post-hoc* tests.

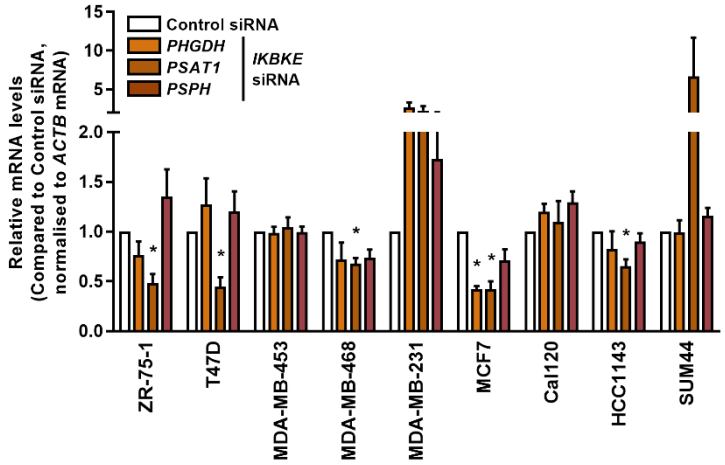

Figure 4.8 – Suppression of IKKε expression in select breast cancer cell lines significantly reduces serine biosynthesis enzyme mRNA levels. qRT-PCR analysis of *PHGDH*, *PSAT1* and *PSPH* mRNA levels in indicated breast cancer cell lines following suppression of IKKε. Cells were transfected with a pool of 4 siRNA oligos targeting *IKBKE,* to suppress IKKε, or a single non-targeting control oligo to a final concentration of 50 nM for 72 hours, following which *PHGDH*, *PSAT1* and *PSPH* mRNA levels were measured by qRT-PCR. mRNA levels in *IKBKE* siRNA-transfected cells were presented as a fold change versus basal levels in control siRNA-transfected cells and normalised to *ACTB* (β-Actin) mRNA levels. *PSAT1* mRNA levels were significantly reduced in ZR-75-1, T47D, MDA-MB-468, MCF7 and HCC1143 cell lines. *PHGDH* mRNA levels were significantly reduced in MCF7 cells. n≥3 independent experiments, mean ± SEM, *p<0.05 as measured by one-sample t-test comparing fold change values to a hypothetical mean of 1.0.

In order to confirm that the observed reduction in serine biosynthesis enzyme protein and mRNA levels was a consequence of IKKε suppression and not a result of an off-target effect of a particular siRNA oligo, the pool of four oligos used to knock down the kinase was deconvoluted in ZR-75-1, T47D and MDA-MB-468 cells. siRNA oligos were transfected individually to identify any unusual effects that might occur with one oligo but not the other three. When used as an oligo pool, each individual oligo was used at a concentration of 12.5 nM, making the total concentration of the siRNA oligo pool 50 nM. When used individually, the concentration at which each siRNA oligo was transfected was increased to 50 nM to match the total concentration present in the siRNA oligo pool and keep transfection concentrations consistent. Cells were transfected with siRNA oligo pools or single oligos for 72 hours and subsequently, knockdown of IKKε was confirmed via western blotting. The consequences of IKKε silencing on PSAT1 protein and mRNA level were also assessed using western blotting and qRT-PCR respectively.

Transfecting each oligo individually suppressed IKKε protein levels generally equally across the three cell lines used for the pool deconvolution. Suppression of IKKε through individual transfection of three out of the four oligos used in the pool had similar effects on PSAT1 protein levels, reducing expression of the enzyme. Only one oligo (oligo #6) consistently failed to induce

a downregulation of PSAT1 protein levels as a result of transfection (Figure 4.9 A). When evaluating the effect of individual oligos on *PSAT1* mRNA levels, similar results were observed. In ZR-75-1 cells, two of the four oligos used reduced *PSAT1* mRNA levels. In T47D cells, three of the oligos reduced mRNA levels and, in MDA-MB-468 cells, all four oligos reduced *PSAT1* mRNA levels (Figure 4.9 B-D). This indicated that the observed transcriptional downregulation of the serine biosynthesis enzymes in breast cancer cells transfected with *IKBKE*-targeting siRNA was dependent specifically on IKKε silencing and was not an off-target effect of one particular siRNA oligo used.

Together, these data demonstrate that induction of HA-IKKε induces expression of serine biosynthesis enzymes at a transcriptional level in Flp-In 293 cells and that this mRNA induction corresponds to a protein level induction for PSAT1 and PSPH. This also suggests that PHGDH is regulated post-translationally in Flp-In 293 cells in a manner different to PSAT1 and PSPH. These data also provide evidence that expression of IKKε maintains the expression of serine biosynthesis enzymes in a panel of breast cancer cell lines. Taken together, these data reveal that IKKε is a central regulator of the enzymes of the serine biosynthesis pathway in Flp-In 293 and human breast cancer cells.

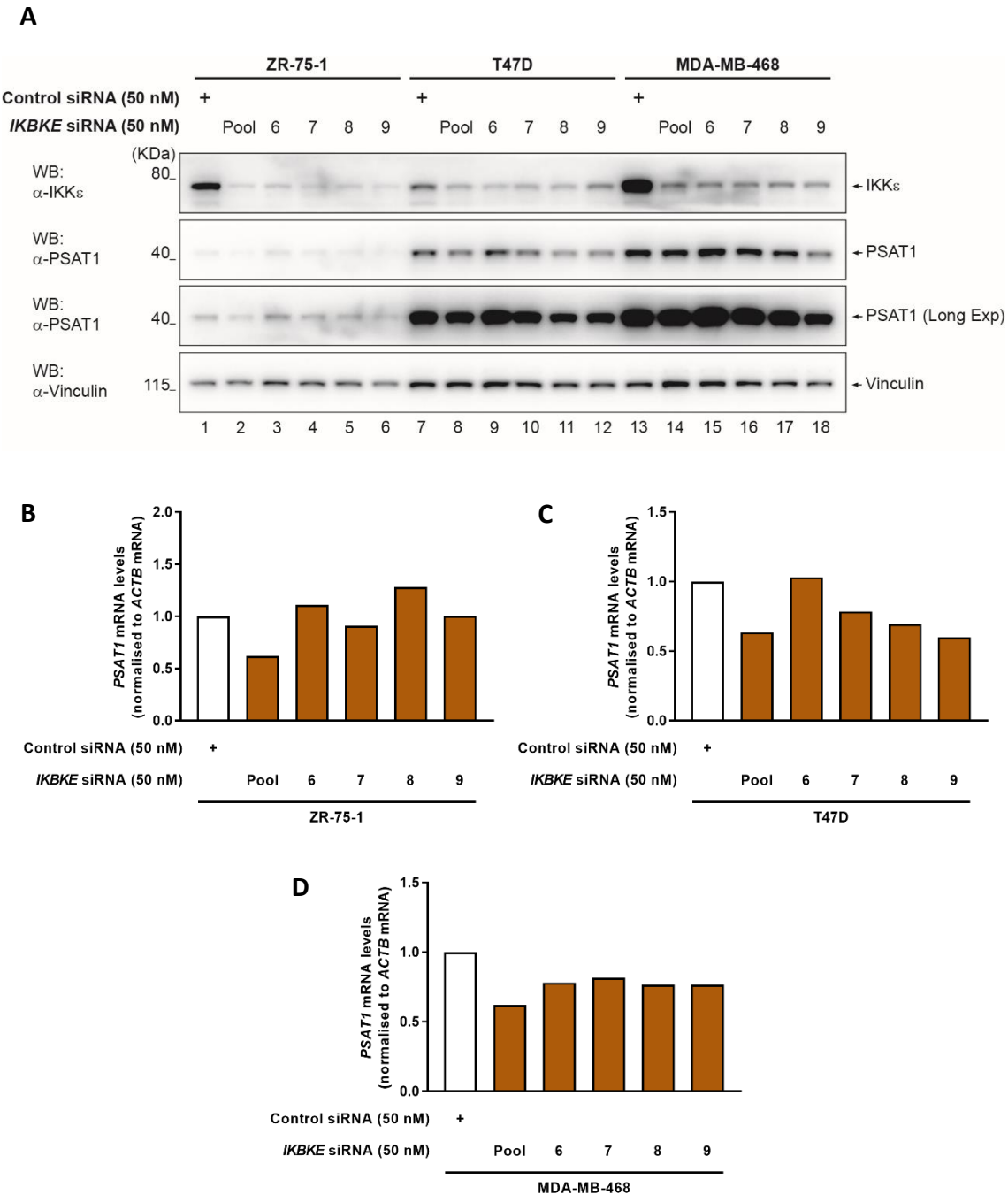

Figure 4.9 – *IKBKE* siRNA oligo pool deconvolution. ZR-75-1, T47D and MDA-MB-468 breast cancer cell lines were transfected for 72 hours with either a pool of 4 *IKBKE*-targeting siRNA oligos or a single *IKBKE*-targeting siRNA oligo, to suppress IKKε expression, or a single non-targeting control oligo to a final concentration of 50 nM for 72 hours. **(A)** Western blot demonstrating the knockdown of IKKε and PSAT1 protein suppression by the siRNA oligo pool or single oligos. Vinculin is shown as a loading control. **(B-D)** qRT-PCR analysis of *PHGDH*, *PSAT1* and *PSPH* mRNA levels in **(B)** ZR-75-1, **(C)** T47D and **(D)** MDA-MB-468 breast cancer cell lines following suppression of IKKε with either single *IKBKE*-targeting siRNA oligos or a combined pool of 4 oligos. mRNA levels in *IKBKE* siRNA-transfected cells were presented as a fold change versus basal levels in control siRNA-transfected cells and normalised to *ACTB* (β-Actin) mRNA levels. *PSAT1* mRNA levels were consistently reduced by *IKBKE* siRNA oligos 7 and 9, and by oligo 8 in 2 out of 3 cell lines tested. n=2 independent experiments.

4.3 Expression of IKKε adaptor proteins in Flp-In 293 and breast cancer cells

Whilst *PHGDH*, *PSAT1* and *PSPH* mRNA and PSAT1 and PSPH proteins were upregulated by induction of HA-IKKε in doxycycline-treated Flp-In 293 cells, this pattern of regulation was not consistent across the panel of breast cancer cell lines. Some cell lines, like T47D, exhibited just significant downregulation of *PSAT1* mRNA and PSAT1 protein upon transfection of IKKε siRNA, whereas some cell lines, such as MDA-MB-468, showed significant reductions in all three enzyme protein levels and *PSAT1* mRNA, with a trend of reduction in *PHGDH* and *PSPH* mRNA, suggesting regulation of all three enzymes together. The reason for this discrepancy between cell lines was unclear, however it is known that IKKε requires specific adaptor proteins to carry out its signalling activities and different conformations of these adaptor proteins can affect the kind of signalling that the kinase induces[85]. It was therefore questioned whether different adaptor protein expression between cell lines might explain the differential regulation of the serine biosynthesis enzymes that was observed.

To address this question, the expression of 4 main non-canonical IKK adaptor proteins; optineurin, SINTBAD, NAP1 and TANK, was assessed via western blotting in non-treated and doxycycline-treated Flp-In 293 HA-GFP and Flp-In 293 HA-IKKε cells and the control siRNA-transfected breast cancer cell line samples from Figure 4.3, as control siRNA transfection was represented the "basal" state in both that experiment and in the labelled metabolite analysis experiment described in chapter 3 (see 3.2). This allowed evaluation of the expression profile of IKKε adaptors in conditions where serine biosynthesis was known to be elevated and serine biosynthesis enzyme levels were known to be increased.

All four adaptor proteins were expressed in Flp-In 293 cells but, more intriguingly, treatment of Flp-In 293 HA-IKKε cells with doxycycline and subsequent induction of HA-IKKε resulted in a marginal upward shift in the detected protein bands for SINTBAD, NAP1 and TANK (Figure 4.10). Whilst it would require further experimental validation, such a shift is typically indicative of protein phosphorylation, suggesting that these three adaptors are phosphorylated when IKKε is induced. Whether this implies that the specific adaptor complex that forms in Flp-In 293 cells upon induction of HA-IKKε is one that involves SINTBAD, NAP1 and TANK but not optineurin, remains to be seen, but it is certainly possible that interaction with these three adaptor proteins is required for the induction of serine biosynthesis enzyme mRNA and PSAT1 and PSPH protein in Flp-In 293 cells.

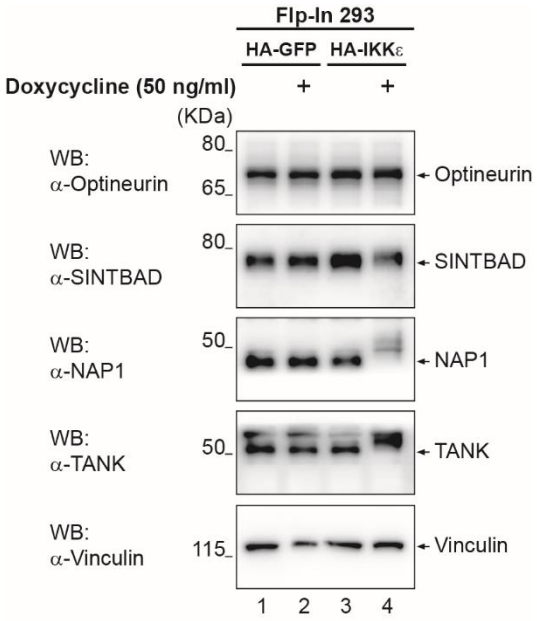

Figure 4.10 – Expression of IKKε adaptor proteins in Flp-In 293 cells. Western blot demonstrating the expression of known IKKε adaptor proteins optineurin, SINTBAD, NAP1 and TANK in Flp-In 293 HA-GFP and Flp-In 293 HA-IKKε cells. Cells were treated with 50 ng/ml doxycycline for 16 hours as indicated. Minor shift in molecular weight of SINTBAD, NAP1 and TANK protein bands in doxycycline-treated Flp-In 293 HA-IKKε cells is potentially indicative of increased phosphorylation. Vinculin is shown as a loading control.

Unfortunately, examining the expression profiles of adaptor proteins in breast cancer cell lines by western blotting failed to provide any explanation for the variable nature of serine biosynthesis enzyme regulation in the cell lines. Between cell lines where IKKε either regulates no serine enzyme proteins (MDA-MB-231), just PSAT1 (such as T47D), or multiple serine biosynthesis enzymes (such as MDA-MB-468) no clearly observable pattern of adaptor expression was detected (Figure 4.11). This therefore made it difficult to draw conclusions about the involvement of specific adaptor proteins in the regulation of serine biosynthesis enzymes by IKKε in the context of breast cancer cell lines. Furthermore, no minor size shifts were observed in any of the proteins in this experiment, making it difficult to even hypothesise which adaptors are more likely to be involved than others.

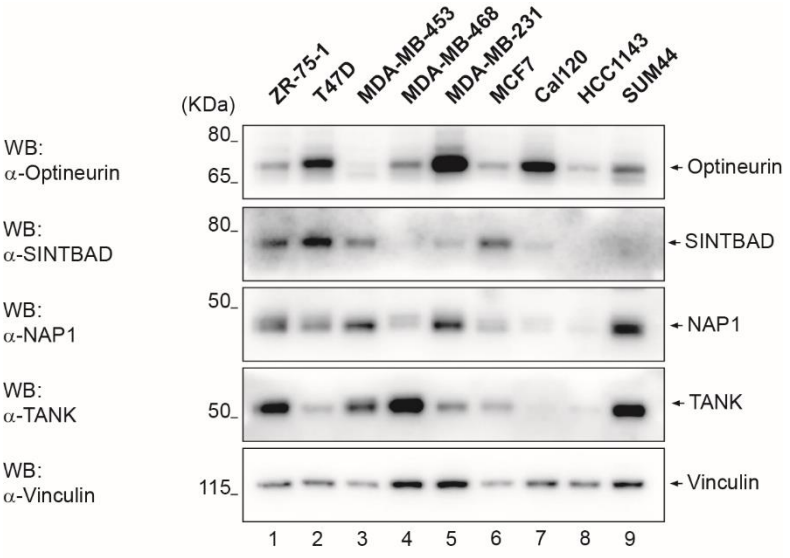

Figure 4.11 – Expression of IKKε adaptor proteins in the panel of human breast cancer cell lines. Western blot demonstrating the expression pattern of the four IKKε adaptor proteins across the panel of human breast cancer cell lines. Samples for each indicated cell line were the same samples which were transfected with a single non-targeting control oligo at a final concentration of 50 nM for 72 hours from Figure 4.3, to represent the expression of adaptor proteins in "basal" conditions from this experiment. Each cell line appears to express the four adaptors in a unique pattern. Notably, Cal120 and HCC1143 express little to no detectable levels of SINTBAD, NAP1 or TANK. Vinculin is shown as a loading control.

4.4 Activation of canonical IKKε signalling pathways in IKKε-expressing cells

Since induction of IKKε in Flp-In 293 HA-IKKε cells was seen to transcriptionally upregulate the enzymes of the serine biosynthesis pathway and, correspondingly, kinase silencing in breast cancer cell lines suppressed mRNA levels of serine biosynthesis enzymes, the mechanism by which the kinase induced the transcriptional regulation necessary to upregulate the enzymes was investigated. The established downstream signalling pathways of IKKε (discussed in 1.2.3.2) involve the activation of 2 major intracellular transcriptional programmes, induced by the IKKε-mediated activation of NF-κB and IFNβ signalling. Therefore, it was hypothesised that activation of one of these transcriptional programmes might be responsible for the upregulation of *PHGDH*, *PSAT1* and *PSPH* mRNA levels upon IKKε induction. Before testing this hypothesis, the activation of canonical IKKε downstream signalling pathways in doxycycline-treated Flp-In 293 HA-IKKε cells was confirmed by western blotting for key markers of NF-κB and IFNβ pathway activation.

Whilst IKKε is not capable of inducing IκBα-degradation and canonical activation of NF-κB alone, due its inability to phosphorylate both serine residues necessary for proteasomal degradation[79], the kinase is capable of directly phosphorylating select NF-κB subunits to regulate transcriptional activity independently of IκBα degradation. For instance, IKKε can directly phosphorylate p65 at serine residues Ser468 and Ser536 to promote p65 transactivation activity[83,194] independently of canonical NF-κB activation. Therefore, IKKε induction of NF-κB signalling was evaluated by immunoblotting for p65 and phosphorylation of p65 at residue Ser468. To assess IKKε-mediated induction of IFNβ signalling, phosphorylation of IRF3 at serine residue Ser396, a site directly phosphorylated by IKKε to induce dimerisation, nuclear translocation and transcriptional activity[90], was evaluated by western blotting. The subsequent activation of downstream JAK/STAT signalling, necessary for induction of the IFNβ-dependent transcriptional response, was also assessed by immunoblotting for the phosphorylation of STAT1 at tyrosine residue Tyr701, a site whose phosphorylation is indicative of STAT1 activation[360].

Flp-In 293 HA-GFP or Flp-In 293 HA-IKKε cells were treated with doxycycline for 16 hours to induce HA-GFP and HA-IKKε expression respectively. Following treatment, the selected markers of NF-κB and IFNβ pathway activation were subsequently detected via western blotting (Figure 4.12). Treatment of the Flp-In 293 HA-IKKε cells, but not Flp-In 293 HA-GFP cells, with doxycycline resulted in increased phosphorylation of p65 at serine residue Ser468, indicative of increased p65 transcriptional activity in cells expressing HA-IKKε. Similarly, phosphorylation of IRF3 Ser396 and STAT1 Tyr701 phosphorylation was increased in doxycycline-treated Flp-In 293

HA-IKKε cells but not Flp-In 293 HA-GFP cells, indicating an HA-IKKε-dependent increase in IRF3 activation and JAK/STAT signalling pathway activity respectively. Together, this data demonstrates the activation of canonical IKKε signalling pathways upon its induction in Flp-In 293 cells.

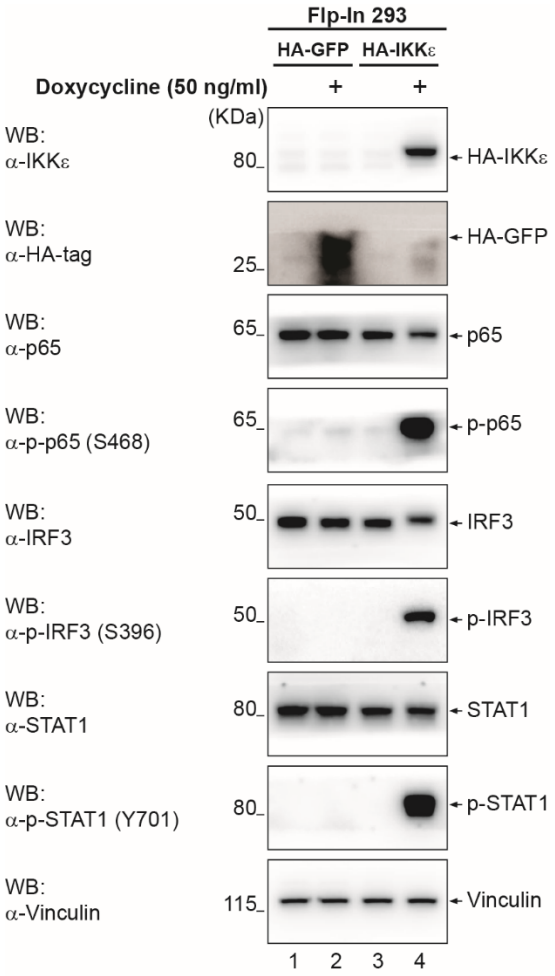

Figure 4.12 – Induction of NF-κB and IFNβ signalling in Flp-In 293 HA-IKKε cells. Western blot analysis of NF-κB and IFNβ pathway activation in Flp-In 293 HA-GFP and Flp-in 293 HA-IKKε cells treated with 50 ng/ml doxycycline for 16 hours. Phosphorylation of p65 at serine residue Ser468 (S468) was used as a readout for NF-κB pathway activation, and phosphorylation of IRF3 at Ser396 (S396) and STAT1 at tyrosine residue Tyr701 (Y701) as a readout for IFNβ signalling activation. Induction of HA-IKKε but not HA-GFP induced phosphorylation of p65, IRF3 and STAT1 indicating activation of NF-κB and IFNβ signalling. Vinculin is shown as a loading control.

Activation of canonical IKKε signalling pathways was also assessed in the panel of 9 human breast cancer cell lines, by using western blotting to evaluate the basal phosphorylation status of p65 Ser468, IRF3 Ser396 and STAT1 Tyr701. Control siRNA-transfected samples from Figure 4.3 were used again here, as the activation of IKKε-mediated signalling pathways in conditions where the expression of serine biosynthesis enzymes were elevated compared to IKKε siRNA-transfected cells was to be investigated. Phosphorylation status of p65, IRF3 and STAT1 in the

breast cancer cell lines was compared to the induced level of phosphorylation of the proteins that was observed in Flp-In 293 HA-IKKε cells upon doxycycline treatment, as a positive control for immunoblot detection of protein phosphorylation (Figure 4.13). Phosphorylation of p65 at serine residue Ser468 was detected to varying degrees in all breast cancer cell lines with the exception of SUM44 indicating variable activation of NF-κB signalling. In contrast, no clear phosphorylation of IRF3 was detected in any of the breast cancer cell lines. Some cell lines tested demonstrated phosphorylation of STAT1 at Tyr 701, but considering the lack of detectable IRF3 phosphorylation upstream, it seems likely that this phosphorylation is attributable to factors other than the activation of JAK/STAT signalling by IKKε rather than it being representative of active IFNβ signalling. This data suggests that although initial induction of the kinase in Flp-In 293 cells results in strong activation of both branches of IKKε signalling, in breast cancer, where IKKε expression is established and constitutive, the kinase primarily signals via NF-κB only in terms of recognised downstream signalling. This is in agreement with data presented by Boehm *et al.* upon initial identification of IKKε as a transforming kinase, where activation of IRF3 and IFNβ signalling was shown to be dispensable for IKKε's oncogenic activity[195].

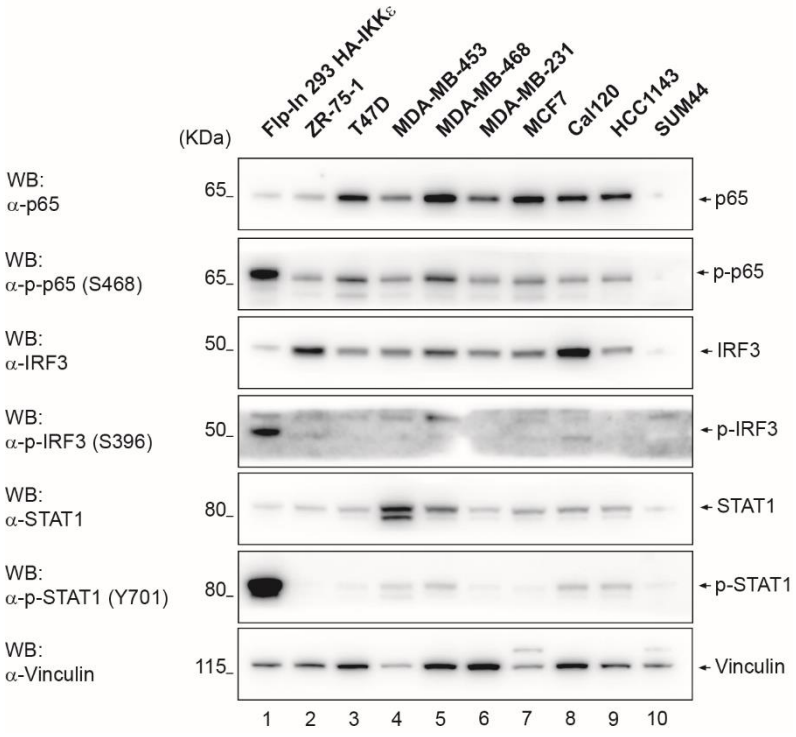

Figure 4.13 – Basal activation of NF-κB and IFNβ signalling in human breast cancer cell lines. Western blot demonstrating the basal phosphorylation of p65 Ser468 (S468), IRF3 Ser396 (S396) and STAT1 Tyr701 (Y701) as a readout for activation of NF-κB and IFNβ signalling. Samples for each indicated cell line were the same samples which were transfected with a single non-targeting control oligo at a final concentration of 50 nM for 72 hours from Figure 4.3, to represent the "basal" activation of signalling pathways in this experiment. Vinculin is shown as a loading control.

4.5 Evaluating the effect of IKKε on serine enzyme expression in a model of IKKε-driven transformation

As initial induction of the kinase in Flp-In 293 cells was found to significantly upregulate the serine biosynthesis enzymes and IKKε-mediated regulation of the enzymes was observed in breast cancer cell lines, it was questioned whether the regulation of serine biosynthesis might occur in the early stages of IKKε-mediated cellular transformation and whether regulation of the serine enzymes might contribute to the early stages of IKKε-driven tumour formation. To test this, a model where IKKε expression induced transformation was required. IKKε was originally identified as a transforming kinase in 2007 but, importantly, was only shown to induce cellular transformation in the presence of a constitutively active form of MEK (MEK^{DD})[195]. The Flp-In 293 HA-IKKε cell model used to explore the effect of the kinase on metabolism does not feature constitutively active MEK and, accordingly, proliferation of doxycycline-treated Flp-In 293 HA-IKKε cells slows over the first 12 hours of induction compared to the doxycycline-treated Flp-In 293 HA-GFP cells (Figure 4.14), as expression of the kinase alone is insufficient for transformation. This effect was likely attributable to the activation of IFNβ signalling, which culminates in the activation of cytotoxic signals as part of the innate immune response, but regardless prevented the evaluation of the effect of IKKε expression on PHGDH, PSAT1 and PSPH in transformation using the Flp-In 293 HA-IKKε model.

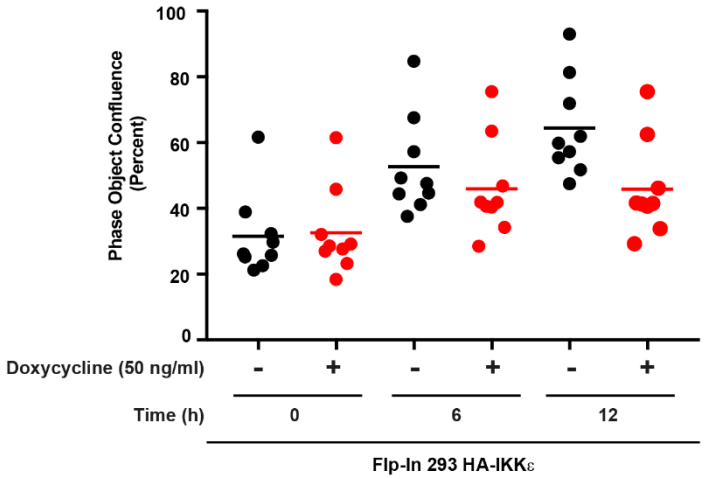

Figure 4.14 – Induction of HA-IKKε in Flp-In 293 cells induces proliferation arrest. Comparison of growth of non-treated Flp-In 293 HA-IKKε cells and cells treated with 50 ng/ml doxycycline over 12 hours was assessed by measuring cell confluency at 0, 6 and 12 hours following the addition of doxycycline using the IncuCyte Zoom. Despite equal confluency at 0 hours, confluency of doxycycline-treated Flp-In HA-IKKε cells after 12 hours of treatment is reduced compared to the confluency of non-treated Flp-In 293 HA-IKKε cells, indicating a decreasing proliferative rate. n=9 independent experiments.

In the same study which identified IKKε as a transforming kinase, a cell line model termed "HA1E-M" was developed, in which HEK293 cells expressed hTERT, SV40 LT and ST, and featured constitutively active MEK^{DD}. The addition of IKKε expression to these cells was therefore enough to render the cells oncogenic and a cell line expressing IKKε was developed as a transformed line (HA1E-M F-IKKε) for comparison to the IKKε-lacking HA1E-M cell line. These HA1E-M and HA1E-M F-IKKε cell lines represent a model in which expression of the kinase is sufficient to tip the scales in favour of oncogenic cellular transformation. Since induction of IKKε in Flp-In 293 cells, which are themselves a modified version of the HEK293 cell line, resulted in induction of serine biosynthesis enzymes transcriptionally without transformation, and suppression of the kinase in select transformed breast cancer cells reduced transcription of PSAT1, it was questioned whether expression of IKKε would also induce serine biosynthesis enzyme regulation in HA1E-M F-IKKε cells when it was transforming. To answer this question, basal expression of PHGDH, PSAT1 and PSPH protein was assessed and compared between HA1E-M and HA1E-M F-IKKε cells using western blotting. Additionally, basal *PSAT1* mRNA levels were compared between the two cell lines using qRT-PCR. IKKε expression in HA1E-M F-IKKε cells was also suppressed by transfecting cells with a pool of *IKBKE*-targeting siRNA oligos for 72 hours, after which serine biosynthesis enzyme protein expression was evaluated using western blotting to determine the effect of modulating established kinase expression in this alternate HEK293 cell model.

Surprisingly, no difference in PHGDH, PSAT1 or PSPH protein expression was observed between the HA1E-M and HA1E-M F-IKKε cell lines. In agreement with this, no significant difference in *PSAT1* mRNA levels was detected between the two cell lines either, despite clear expression of the kinase in the HA1E-M F-IKKε cells. Similarly, siRNA-mediated silencing of IKKε in HA1E-M F-IKKε cells showed no significant reduction in the protein of any of the serine biosynthesis enzymes (Figure 4.15). This data therefore demonstrated that IKKε was not regulating serine biosynthesis enzyme expression in the HA1E-M F-IKKε cell model.

To understand why regulation of serine biosynthesis enzymes might not have been observed in these cells, the activation of IKKε-mediated downstream signalling was evaluated. As before, activation of canonical IKKε downstream signalling pathways was confirmed by investigating key markers of pathway activation, including phosphorylation of p65 at serine residue Ser468 as an indicator of NF-κB activity, and phosphorylation of IRF3 and STAT1 at serine residue Ser396 and tyrosine residue Tyr701 respectively as markers for IFNβ signalling (see 4.4). These markers for the activation of IKKε's downstream signalling were assessed in the HA1E-M and HA1E-M F-IKKε cell lines in basal conditions using western blotting and compared to levels of pathway activation resulting from induction of HA-IKKε in Flp-In 293 cells following doxycycline treatment.

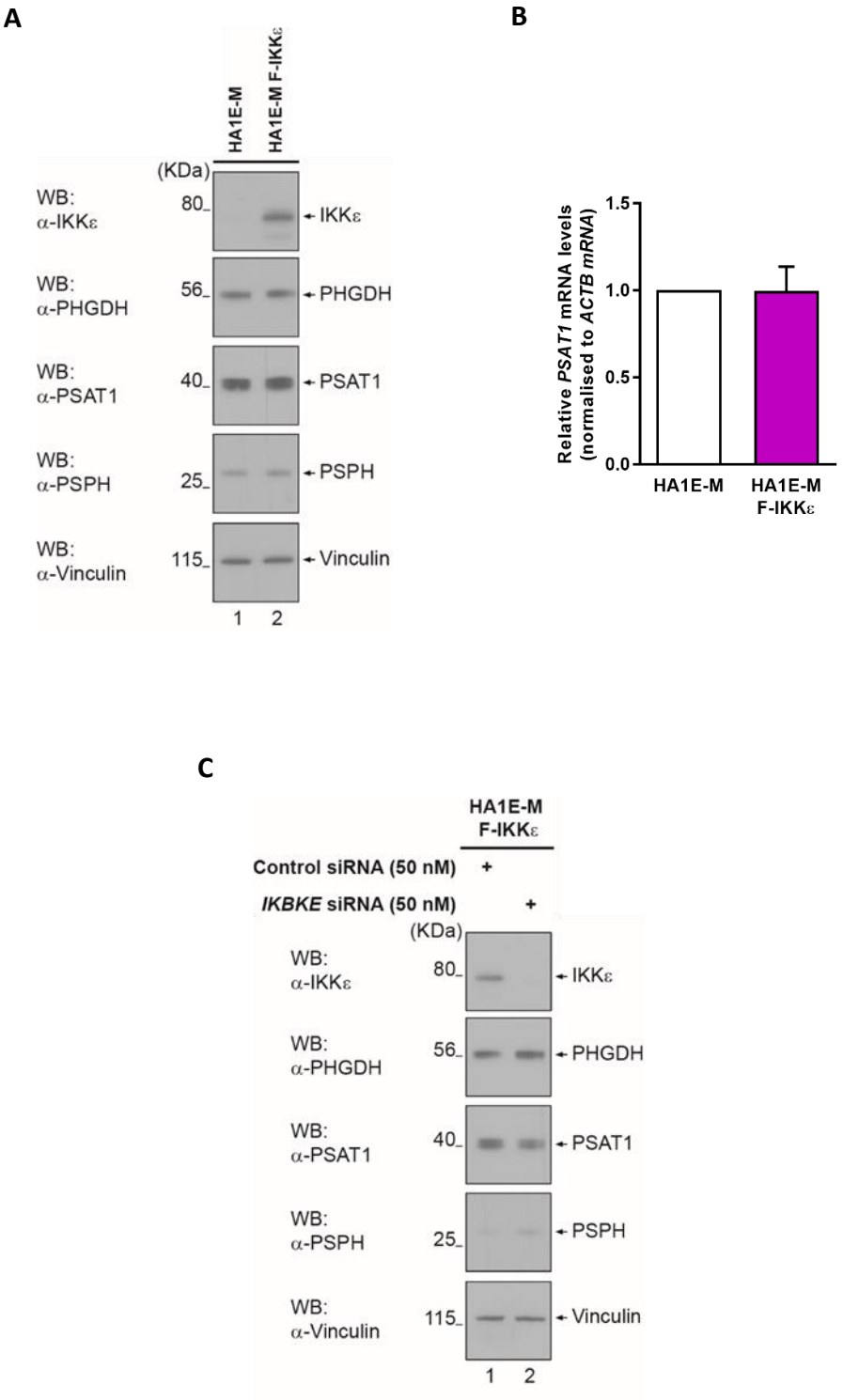

Figure 4.15 – Serine biosynthesis enzymes are not regulated by IKKε in HA1E-M and HA1E-M F-IKKε cells. (A) HA1E-M and HA1E-M F-IKKε cells were cultured and lysed for western blot analysis of basal protein levels of IKKε, PHGDH, PSAT1 and PSPH. No difference between PHGDH, PSAT1 and PSPH protein levels were observed between the 2 cell lines. **(B)** qRT-PCR analysis of *PSAT1* mRNA levels in HA1E-M F-IKKε cells relative to levels in HA1E-M cells. *PSAT1* mRNA levels were normalised to *ACTB* (β-Actin) mRNA levels. n=3 independent experiments, mean ± SEM. No significant differences were detected using a one sample t-test, comparing values to a hypothetical mean of 1.0. **(C)** Western blot analysis of HA1E-M F-IKKε cells transfected with a pool of 4 *IKBKE*-targeting siRNA oligos, to suppress IKKε, or a single non-targeting control oligo to a final concentration of 50 nM for 72 hours allowed assessment of the effect of kinase suppression on serine biosynthesis enzymes. No difference between PHGDH, PSAT1 and PSPH protein levels was detected between cells in which IKKε was silenced and cells transfected with control, non-targeting siRNA.

Unexpectedly, no signs of signalling activity downstream of the kinase were detected in these HA1E-M F-IKKε cells (Figure 4.16). No phosphorylation of either p65 residue Ser468 or IRF3 residue Ser396 was detected. Furthermore, whilst some phosphorylation of STAT1 Tyr701 was observed, no clear difference between phosphorylation was seen in the IKKε-expressing HA1E-M F-IKKε cells versus the HA1E-M cells, suggesting that the STAT1 phosphorylation detected in these cell line models was IKKε-independent. IKKε itself was found to exhibit no detectable phosphorylation of serine residue Ser172 when expressed in HA1E-M F-IKKε cells either. As previously mentioned, phosphorylation of IKKε residue Ser172 is highly indicative of kinase activity and is auto-phosphorylated by the kinase itself when active. Together, this data therefore indicates that the kinase expressed in these HA1E-M F-IKKε cells is not inducing activation of any established signalling pathway downstream of IKKε, due to inactivity of the kinase itself. This explains the lack of regulation of the serine biosynthesis enzymes in this cellular model, as this requires active kinase activity as has previously been demonstrated in this chapter (Figure 4.6).

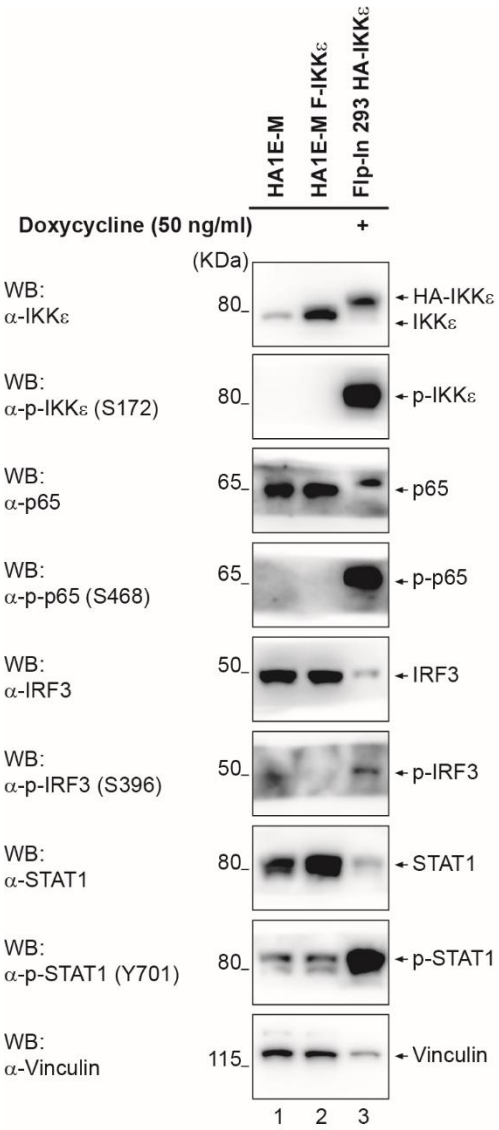

Figure 4.16 – IKKε signalling appears to be inactive in these HA1E-M F-IKKε cells. Western blot analysis of NF-κB and IFNβ signalling pathway activation in HA1E-M and HA1E-M F-IKKε cells compared to Flp-In 293 HA-IKKε cells treated with 50 ng/ml doxycycline for 16 hours. Phosphorylation of p65 Ser468 was used as a readout for NF-κB activation and phosphorylation of IRF3 Ser396 and STAT1 Tyr701 was used as a readout for IFNβ signalling. Despite expression of IKKε in HA1E-M F-IKKε cells, no indication of canonical IKKε signalling was detected, indicating inactive kinase signalling. Vinculin is shown as a loading control.

4.6 IKKε-mediated serine biosynthesis enzyme regulation is independent of autocrine/paracrine IFNβ signalling

Since the primary function of the kinase involves the induction of IFNβ signalling and the activation of an IFNβ-mediated transcriptional programme, attempts to understand the IKKε-mediated transcriptional regulation of *PHGDH*, *PSAT1* and *PSPH* first focussed on investigating the role of IFNβ signalling. Despite the fact that the no clear evidence of IFNβ-mediated signalling was observed in the panel of breast cancer cell lines, the pathway was strongly activated in the Flp-In 293 HA-IKKε cells upon induction of the kinase. Considering the effect on the serine biosynthesis enzymes was so broad in the Flp-In 293 cells, it was questioned whether the observed transcriptional upregulation of the enzymes could be attributable to the activation of an IFNβ-mediated transcriptional programme. Interferon signalling involves the secretion of IFNβ from activated cells, where upon it activates the interferon receptor (IFNAR) on the cell surface in an autocrine or paracrine manner. Therefore, to address the involvement of IFNβ signalling in IKKε's regulation of the serine biosynthesis enzymes, this IFNβ signalling loop was targeted using multiple techniques.

Firstly, the activation of the IFNAR in response to IFNβ was inhibited using a competitive binding antibody specific to the receptor. This blocked the binding of IFNβ to the receptor, thereby inhibiting the activation of the JAK/STAT signalling cascade and preventing the activation of the IFNβ-mediated transcriptional programme. Flp-In 293 HA-IKKε or Flp-In 293 HA-GFP cells were pre-treated with the IFNAR blocking antibody for 2 hours prior to 16 hours of doxycycline treatment to induce HA-IKKε or HA-GFP respectively. Following doxycycline treatment, the induction of PSAT1 and PSPH protein levels was assessed using western blotting and *PHGDH*, *PSAT1* and *PSPH* mRNA by qRT-PCR. mRNA levels in IFNAR pre-treated cells were compared to the level of induction in Flp-In 293 HA-IKKε cells upon doxycycline treatment without IFNAR treatment as was shown in Figure 4.5, as the IFNAR pre-treated samples were run in parallel with those samples as part of the same experiment.

Inhibition of IFNAR activation by pre-treatment with the IFNAR blocking antibody reduced the phosphorylation of STAT1 Tyr701 in the presence of IKKε expression, indicating a reduction of JAK/STAT signalling activation, which is in accordance with functional inhibition of the IFNAR. Induction of HA-IKKε in the presence of the IFNAR blocking antibody exhibited the same level of PSAT1 and PSPH protein induction as induction of the kinase without the blocking antibody. Similarly, no significant difference in the induction of *PHGDH*, *PSAT1* and *PSPH* mRNA levels was detected between the doxycycline-treated and IFNAR-pre-treated Flp-In 293 HA-IKKε cells and

those cells not treated with the blocking antibody (Figure 4.17). This data demonstrated that although the IFNAR blocking antibody successfully inhibited the activation of the JAK/STAT signalling cascade in response to IKKε expression, the blocking of IFNAR activation had no inhibitory effect on the induction of serine biosynthesis enzymes. This therefore indicated that the transcriptional regulation of PHGDH, PSAT1 and PSPH by IKKε is independent of the IFNβ stimulated transcriptional programme.

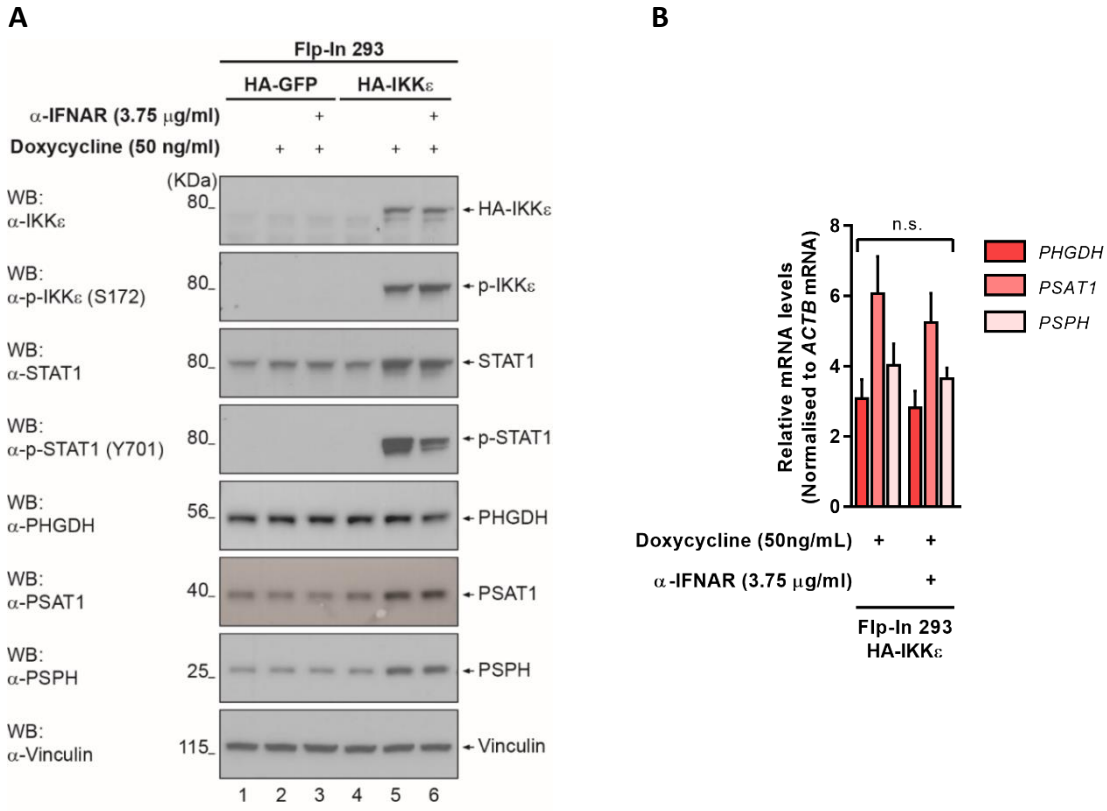

Figure 4.17 – IKKε-mediated upregulation of serine biosynthesis enzymes is independent of IFNAR activation. Flp-In 293 HA-GFP and HA-IKKε cells were treated with 3.75 μg/ml IFNAR blocking antibody for 2 hours, after which 50 ng/ml doxycycline was added for 16 hours to induce HA-GFP or HA-IKKε whilst blocking IFNAR activation. **(A)** Western blotting analysis of PSAT1 and PSPH protein upregulation upon blocking of IFNAR activation. Decreased phosphorylation of STAT1 Tyr 701 (Y701) in response to IKKε induction in IFNAR treated cells indicates successfully reduced IFNAR activation. PSAT1 and PSPH proteins were upregulated by IKKε even when IFNAR activation was blocked. **(B)** qRT-PCR analysis of *PHGDH*, *PSAT1* and *PSPH* mRNA levels upon treatment of Flp-In 293 HA-IKKε cells with 50 ng/ml doxycycline for 16 hours with or without IFNAR blocking antibody pre-treatment. mRNA levels are normalised relative to non-treated basal levels in Flp-In 293 HA-GFP cells and compared to mRNA levels in doxycycline-treated Flp-In 293 HA-IKKε cells from Figure 4.5, of which the α-IFNAR pre-treated samples were run as part of the same experiment. mRNA levels were normalised to *ACTB* (β-Actin) mRNA levels. No significant difference was detected between *PHGDH*, *PSAT1* or *PSPH* mRNA levels in doxycycline-treated Flp-In 293 HA-IKKε cells and doxycycline-treated Flp-In 293 HA-IKKε cells pre-treated with the IFNAR blocking antibody, as measured by two-way ANOVA with Bonferroni *post-hoc* tests. n=4 independent experiments, mean ± SEM.

Whilst JAK/STAT mediated IFNβ transcriptional regulation was therefore concluded to be uninvolved in the regulation of serine biosynthesis enzymes by IKKε, it was questioned whether the kinase might induce another endocrine signalling loop to regulate serine enzyme

transcription. The involvement of cytokine secretion in this process was therefore addressed using a conditioned medium experiment. Flp-In 293 HA-GFP and Flp-In 293 HA-IKKε cells were treated with doxycycline for 16 hours to induce HA-GFP and HA-IKKε expression respectively and allow secretion of cytokines released from the Flp-In 293 cells into the culture medium. The medium from these cells was subsequently collected, filtered to remove any cell contaminants and applied to receiving Flp-In 293 HA-GFP cells for 24 hours. As the medium from HA-IKKε cells contained IKKε-dependent cytokines, applying the medium to Flp-In 293 cells would therefore replicate the downstream cytokine-mediated signalling induced by the kinase in the Flp-In 293 HA-GFP cells without requiring the expression of IKKε. This then allowed evaluation of the role of an endocrine signalling loop in the regulation of serine biosynthesis enzymes by IKKε.

Since other signalling pathways are less well defined, activation of IKKε-driven cytokine signalling was confirmed by evaluating the phosphorylation of STAT1 at tyrosine residue Tyr701 using western blotting as a readout for IFNβ signalling activation (Figure 4.18). In accordance with the secretion of IFNβ by IKKε-expressing cells, application of medium conditioned by doxycycline-treated Flp-In 293 HA-IKKε cells induced phosphorylation of STAT1 at tyrosine residue Tyr701. This indicated IFNβ-dependent activation of the IFNAR and the JAK/STAT signalling cascade and confirmed the presence of IKKε-dependent cytokines capable of endocrine signalling in the conditioned medium. However, even though IKKε-dependent cytokine signalling was induced in Flp-In HA-GFP cells upon application of the conditioned medium, the conditioned medium had no effect on the protein levels of either PSAT1 or PSPH. This therefore suggested that regulation of serine biosynthesis enzymes in Flp-In 293 HA-IKKε cells was independent of a cytokine endocrine signalling loop.

IKKε has also been shown to function downstream of cytokine signalling pathways as well as upstream. For instance, in the activation of the JAK/STAT signalling cascade, IKKε regulates the initial activation of the pathway through phosphorylation of IRF3, but also regulates the pathway downstream of IFNAR activation through the direct phosphorylation of STAT1 at serine residue Ser708, which promotes ISGF3 formation and can enhance the induction of interferon stimulated genes (ISGs), as well as control the induction of an IKKε-dependent subtype of ISGs[99,102]. It was therefore noted that Flp-In 293 HA-GFP cells do not basally express IKKε, meaning that cytokine signalling pathways in which IKKε plays upstream and downstream rolls might not be properly activated. It was questioned whether regulation of serine biosynthesis enzymes might be regulated by such a cytokine signalling pathway. To address this question, medium conditioned by doxycycline-treated Flp-In 293 HA-IKKε cells was applied to breast cancer cell lines ZR-75-1 and T47D which express IKKε basally.

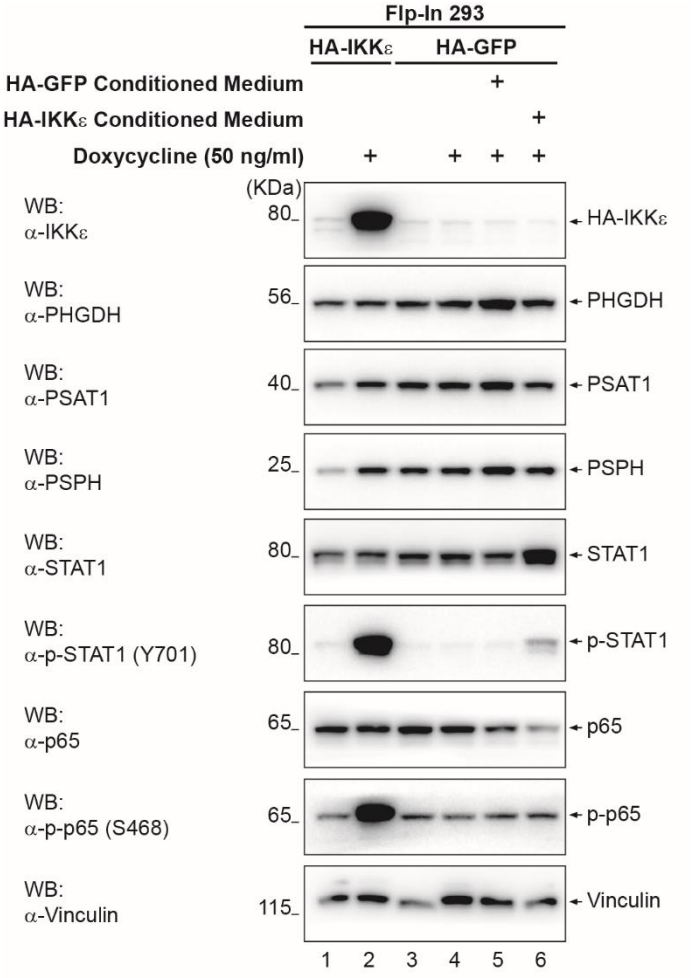

Figure 4.18 – IKKε-mediated upregulation of serine biosynthesis enzymes in Flp-In 293 cells is independent of endocrine signalling. Flp-In 293 HA-GFP or HA-IKKε cells were treated with 50 ng/ml doxycycline for 16 hours. The culture medium from those cells was subsequently collected, filtered and applied to receiving Flp-In 293 HA-GFP cells for 24 hours, to activate cytokine signalling in HA-GFP cells mediated by cytokines secreted from HA-GFP- or HA-IKKε-expressing cells. Phosphorylation of STAT1 Tyr701 and p65 Ser468 indicates IFNβ and NF-κB activation respectively. Activation of IFNβ signalling in particular is indicative of active cytokine signalling in receiving cells. Receiving cells were also treated with 50 ng/ml doxycycline for 24 hours to control for the presence of doxycycline in the conditioned medium. No upregulation of serine biosynthesis enzymes was detected in cells cultured with Flp-In 293 HA-IKKε conditioned medium. Vinculin is shown as a loading control.

As with Flp-In 293 HA-GFP cells, application conditioned medium to both ZR-75-1 and T47D cells induced phosphorylation of STAT1, indicating activation of cytokine induced signalling in the form of JAK/STAT signalling. However, even with the presence of basal IKKε expression in the breast cancer cells lines, and therefore the potential for the contribution of the kinase to downstream signalling, application of conditioned medium failed to upregulate PSAT1 or PSPH proteins in either ZR-75-1 or T47D cell lines (Figure 4.19 and Figure 4.20). Together, this data demonstrated that the regulation of serine biosynthesis enzymes by IKKε was wholly independent of an endocrine signalling loop and the secretion of cytokines.

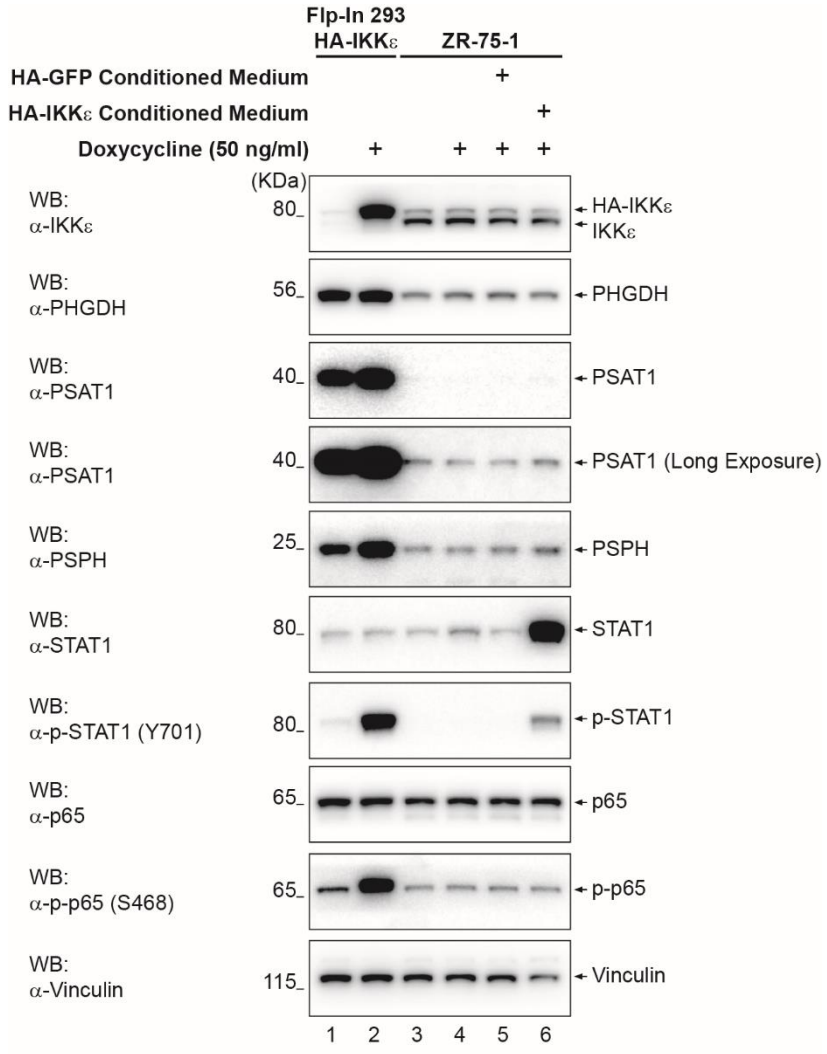

Figure 4.19 – IKKε-mediated upregulation of serine biosynthesis enzymes in ZR-75-1 cells is independent of endocrine signalling. Flp-In 293 HA-GFP and Flp-In 293 HA-IKKε conditioned medium was prepared as in Figure 4.18 and applied to receiving ZR-75-1 breast cancer cells for 24 hours. As before, induction of STAT1 Tyr701 phosphorylation indicated active cytokine signalling in receiving cells. Despite activation of cytokine signalling, no upregulation of serine biosynthesis enzymes was detected in ZR-75-1 breast cancer cells cultured with Flp-In 293 HA-IKKε conditioned medium. ZR-75-1 cells were also treated with 50 ng/ml doxycycline for 24 hours, controlling for the presence of doxycycline in the conditioned medium. Vinculin is shown as a loading control.

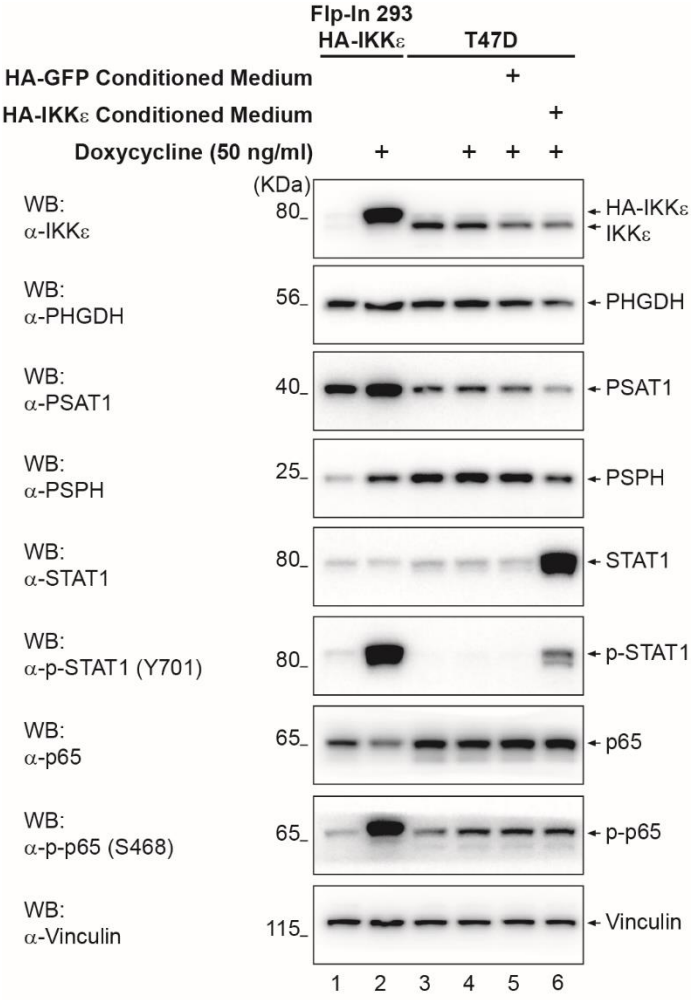

Figure 4.20 – IKKε-mediated upregulation of serine biosynthesis enzymes in T47D cells is independent of endocrine signalling. Medium conditioned by doxycycline-treated Flp-In 293 HA-GFP and Flp-In 293 HA-IKKε was prepared as in Figure 4.18 and applied to T47D breast cancer cells for 24 hours to induce cytokine signalling. STAT1 Tyr701 phosphorylation confirmed active cytokine signalling in T47D cells. No upregulation of serine biosynthesis enzymes was detected in T47D breast cancer cells cultured with Flp-In 293 HA-IKKε conditioned medium. In addition to treatment with Flp-In 293 cell conditioned medium, T47D cells were also treated with 50 ng/ml doxycycline for 24 hours to control for doxycycline in the conditioned medium. Vinculin is shown as a loading control.

4.7 Induction of serine biosynthesis enzymes by IKKε is independent of p65 and IRF3 signalling

Although the regulation of serine biosynthesis enzymes was found to be independent of a cytokine controlled endocrine signalling network, it was still uncertain whether IKKε-mediated phosphorylation of its canonical targets; IRF3 and NF-κB subunits like p65, was important for the regulation of serine biosynthesis enzymes transcriptionally. Therefore, this was directly addressed through the siRNA-mediated suppression of IRF3 and p65.

Flp-In 293 HA-GFP and Flp-In 293 HA-IKKε cells were transfected with single siRNA oligos targeting either *RELA* or *IRF3* mRNA, to suppress p65 an IRF3 protein expression respectively, or a non-targeting control oligo for 72 hours. For the final 16 hours, doxycycline was added to the siRNA-transfected cells to induce HA-GFP or HA-IKKε in the absence of p65 or IRF3 protein expression. Subsequently, knockdown of p65 and IRF3 protein levels was validated via western blotting and induction of *PHGDH*, *PSAT1* and *PSPH* mRNA levels was evaluated using qRT-PCR (Figure 4.21).

Western blotting showed that transfection of *RELA* and *IRF3*-targeting siRNA resulted in effective knockdown of p65 and IRF3 proteins respectively and demonstrated induction of HA-IKKε protein upon doxycycline treatment in the absence of p65 and IRF3 (Figure 4.21 A). This allowed evaluation of the role of canonical IKKε signalling pathways in the upregulation of *PHGDH*, *PSAT1* and *PSPH* mRNA levels (Figure 4.21 B, C and D). Consistent with previous findings, qRT-PCR analysis of serine biosynthesis enzyme mRNA levels demonstrated that doxycycline treatment of control siRNA-transfected Flp-In 293 HA-IKKε cells resulted in an upregulation of *PHGDH*, *PSAT1* and *PSPH* mRNA levels. Notably, suppression of p65 and IRF3 protein levels appeared to slightly downregulate basal mRNA levels of the enzymes, suggesting that NF-κB and IFNβ signalling may play a minor role in maintaining the basal expression of *PHGDH*, *PSAT1* and *PSPH* mRNA.

Importantly however, doxycycline treatment of Flp-In 293 HA-IKKε cells in which p65 and IRF3 protein levels had been suppressed via siRNA-mediated knockdown still resulted in an upregulation of the SBP enzyme mRNA levels. Comparing the fold-change in mRNA levels in doxycycline-treated *RELA* or *IRF3*-targeting siRNA-transfected cells with the fold-change in control siRNA-transfected cells revealed relatively consistent levels of doxycycline-dependent induction for all three SBP enzyme mRNA's. This data therefore demonstrates that, although both p65 and IRF3 may be involved in maintaining basal expression of the serine biosynthesis

enzymes, neither transcription factor is required for the IKKε-mediated upregulation of *PHGDH*, *PSAT1* or *PSPH* mRNA levels that is observed upon doxycycline treatment of Flp-In 293 HA-IKKε cells. By extension, this indicates that the IKKε-dependent transcriptional regulation of the serine biosynthesis enzymes is independent of both NF-κB and IFNβ signalling.

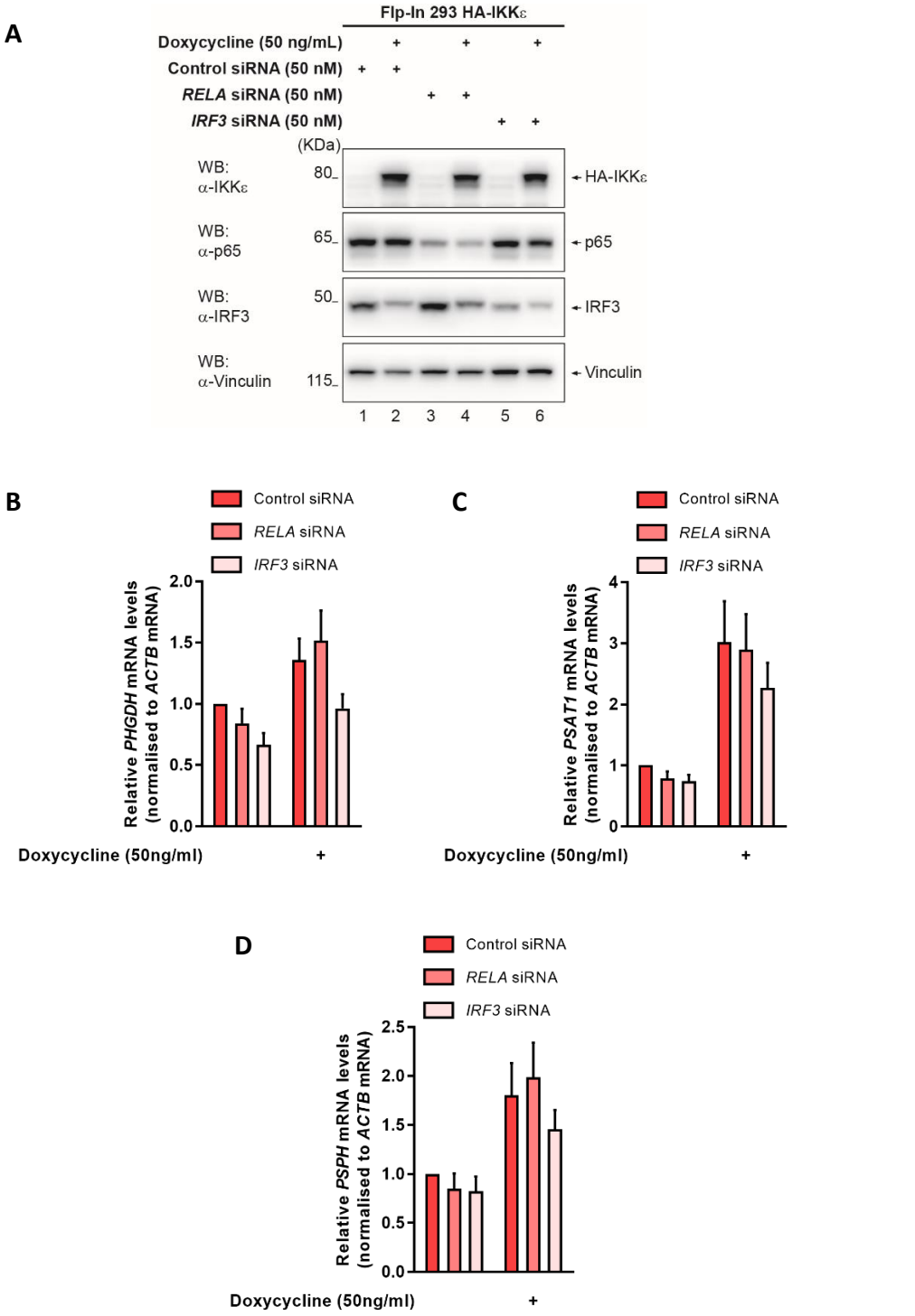

Figure 4.21 – Transcriptional upregulation of serine biosynthesis enzymes by IKKε is independent of p65 or IRF3. Flp-In 293 HA-IKKε cells were transfected with single siRNA oligos targeting *RELA* or *IRF3* mRNA, to suppress p65 and IRF3 protein levels respectively, or a non-targeting control oligo at a final concentration of 50 nM for 72 hours. 50 ng/ml doxycycline was added for the final 16 hours to induce HA-IKKε expression in the absence of p65 or IRF3 protein expression. **(A)** Western blot analysis demonstrating the knockdown of p65 and IRF3 proteins following transfection of Flp-In 293 HA-IKKε cells with *RELA*- and *IRF3*-targeting siRNA. Vinculin is shown as a loading control. **(B-D)** qRT-PCR analysis of **(A)** *PHGDH*, **(B)** *PSAT1* and **(C)** *PSPH* mRNA levels in *RELA*- or *IRF3*-targeting siRNA-transfected Flp-In 293 HA-IKKε cells upon treatment with 50 ng/ml doxycycline for 16 hours. Serine biosynthesis enzyme mRNA levels in *RELA* or *IRF3* siRNA-transfected cells were calculated as fold differences versus enzyme levels in non-treated, control siRNA-transfected cells and normalised to *ACTB* (β-Actin) mRNA. No statistically significant difference was detected between said conditions when measured using a two-way ANOVA with Bonferroni *post-hoc* tests. n=3 independent experiments, mean ± SEM.

4.8 Discussion

Following the findings detailed in chapter 3, demonstrating that serine biosynthesis enzyme PSAT1 is phosphorylated at serine residue Ser331 in an IKKε-dependent manner and that this phosphorylation promoted PSAT1 protein stability, this chapter set out to investigate whether modulation of IKKε expression in Flp-In 293 HA-IKKε or human breast cancer cells could lead to the corresponding modulation of PSAT1 protein levels. Consistently with IKKε-mediated phosphorylation increasing PSAT1 protein stability, it was found that induction of HA-IKKε in Flp-In 293 cells led to the upregulation of the PSAT1 protein and suppression of IKKε in the panel of breast cancer cell lines resulted in a decrease in PSAT1 protein levels in all PSAT1-expressing cell lines tested with only one exception (MDA-MB-231). Interestingly however, upregulation of PSPH in doxycycline-treated Flp-In 293 HA-IKKε cells and downregulation of PHGDH and PSPH proteins in IKKε siRNA-transfected ZR-75-1 and MDA-MB-468 breast cancer cell lines was also observed alongside PSAT1 regulation. Since the hypothesis for PSAT1 protein regulation involved the IKKε-dependent phosphorylation of the enzyme increasing protein stability, observing regulation of other serine biosynthesis enzymes by the kinase was somewhat surprising, since evidence pointed to the fact that neither PHGDH nor PSPH would be phosphorylated by the kinase (see 3.10).

Transcriptional regulation of PHGDH, PSAT1 and PSPH by IKKε

The regulation of other serine biosynthesis enzymes by IKKε led to the question of whether regulation of the enzymes was occurring at a transcriptional level. It was subsequently identified that induction of HA-IKKε expression in Flp-In 293 cells led to a transcriptional upregulation of *PHGDH*, *PSAT1* and *PSPH* expression and, similarly, transcriptional regulation of the enzymes by the kinase was observed in breast cancer cell lines as well. This demonstrated that, in addition to the regulation of the pathway through post-translational regulation of the PSAT1 protein, IKKε regulated the serine biosynthesis pathway at a transcriptional level by upregulating mRNA levels of the pathway enzymes.

The finding that, in Flp-In 293 cells at least, the enzymes of the pathway were all regulated transcriptionally, even when only PSAT1 and PSPH were regulated at the protein level, was partially unexpected, though consistent with what is already known about transcriptional regulators of the serine biosynthesis enzymes, as many regulate the enzymes all together as a full set, including TGFβ[361], c-Myc[315] and ATF4[324,362]. The fact that all three enzymes were regulated transcriptionally, whereas only two proteins were regulated however, suggests that

IKKε regulates the serine biosynthesis enzymes at two distinct levels. Transcriptionally, to promote mRNA production, and at a translational level, either preventing mRNA translation of PHGDH/promoting mRNA translation of PSAT1 and PSPH or degrading PHGDH protein/stabilising PSAT1 and PSPH proteins post-translationally. Although this work has already shown how IKKε can post-translationally modify PSAT1 to promote protein stability, it is difficult to speculate about post-transcriptional regulation of the other enzymes at this stage, since very little is currently known about the regulation of PHGDH or PSPH proteins.

Phosphorylation vs. transcriptional regulation

A key question is, if IKKε regulates PSAT1 protein stability through phosphorylation and PSAT1 transcription through upregulation of mRNA levels, which of these two regulatory processes contributes more to the overall upregulation of the PSAT1 protein, and which is more important for the enhanced serine biosynthesis observed in HA-IKKε-expressing Flp-In 293 cells? Whilst it is admittedly difficult to definitively answer this question without further investigation, evidence does suggest that the transcriptional regulation contributes to a greater extent than the phosphorylation of the protein. Whereas increased gene expression of serine enzymes is well known to boost serine biosynthesis[304,305,324], changing PSAT1 phosphorylation status appeared to have no discernible impact on production of serine intracellularly, as evidenced by the labelled metabolite analysis performed with Flp-In 293 HA-PSAT1 wt, S>A and S>E mutants (see 3.7). The possibility that phosphorylation of PSAT1 Ser331 could still contribute to enzymatic activity despite the findings from the labelled metabolite analysis has been discussed extensively in chapter 3 (see 3.10), but in the context of IKKε-mediated upregulation of serine biosynthesis activity, the data presented throughout this thesis certainly appear to indicate that the increased serine production observed in HA-IKKε-expressing cells is a consequence of IKKε's effect on the serine biosynthesis pathway as a whole and the upregulation of *PHGDH*, *PSAT1* and *PSPH* transcription, rather than the phosphorylation of PSAT1.

It is possible that, whilst increasing protein stability, the phosphorylation of PSAT1 in Flp-In 293 cells is not sufficient to induce accumulation of PSAT1 protein levels to a degree necessary for an observable increase in serine biosynthesis in the same way that transcriptional upregulation is. Evidence from the *in vitro* kinase assay described in chapter 3 (see 3.4) suggests that TBK1 can phosphorylate PSAT1 Ser331 in the presence of a kinase-dead mutant variant of IKKε (IKKε KD-m). It would therefore be expected that if PSAT1 is phosphorylated in Flp-In 293 cells expressing HA-IKKε wt, then it would also be phosphorylated in Flp-In 293 cells expressing HA-IKKε KD-m. If the phosphorylation alone was sufficient to induce protein accumulation, this

would mean that the induction of HA-IKKε in KD-m would result in upregulation of PSAT1. Instead, induction of HA-IKKε KD-m in Flp-In 293 cells, which has no effect on serine biosynthesis enzyme mRNA levels, failed to upregulate PSAT1 protein levels. This therefore provides further evidence of the fact that upregulation of PSAT1 protein by IKKε in Flp-In 293 cells requires a corresponding upregulation of *PSAT1* mRNA. As with the lack of the effect of mutation of the PSAT1 Ser 331 residue on serine biosynthesis, this suggests that transcriptional regulation of PSAT1 by the kinase is a far more crucial aspect of IKKε's ability to increase intracellular serine production than the phosphorylation of PSAT1.

Unequal regulation of serine biosynthesis enzymes across cell lines

Another major question is, why are the serine biosynthesis enzymes not regulated equally across all the cell lines tested? Whilst all three enzymes were regulated at the transcriptional level in Flp-In 293 cells, things were less consistent in the breast cancer cell lines. Transcriptional regulation of *PSAT1* alone was commonly observed and only MCF7 showed a significant reduction in any other serine biosynthesis enzyme mRNA levels (*PHGDH* in this instance), whilst other cell lines like MDA-MB-468 simply showed a trend of reduction of other enzymes.

It was hypothesised that the regulation of the enzymes might require availability of a specific conformation of IKKε adaptor proteins. In Flp-In 293 cells, evidence suggested that induction of HA-IKKε led to possible phosphorylation of SINTBAD, NAP1 and TANK adaptor proteins, as protein bands exhibited characteristic phosphoshifts when examined by western blotting. In addition to this, TANK was detected within the *in vitro* kinase assay samples (see 3.4), having likely been purified as part of the HA-IKKε pulldown through interaction with the kinase, demonstrating that at least one of these three adaptors formed a stable interaction with IKKε. This indicated that interaction of IKKε with TANK and potentially with SINTBAD and NAP1 occurred in Flp-In 293 HA-IKKε cells upon induction of the kinase and suggested that this particular conformation of adaptor proteins might facilitate the signalling activity that induced the serine biosynthesis enzymes. When searching for evidence of this in breast cancer cell lines, as an explanation for the differential regulation of serine biosynthesis enzymes between cell lines, no clear pattern of expression of these adaptor proteins was observable, even amongst the breast cancer cell lines where more than just PSAT1 appeared to be regulated by the kinase (although this experiment did offer hints as to why IKKε might regulate mitochondrial function in some breast cancer cell lines but not others (see 5.2 and 5.7)). Indeed, cell lines like T47D expressed all the adaptor proteins, yet only PSAT1 was regulated. MDA-MB-468 expressed high levels of TANK protein and seemed to regulate all three enzymes similar to what was observed

in Flp-In 293 cells. However, ZR-75-1, MDA-MB-453 and SUM44 also expressed high levels of TANK and failed to show consistent regulation of PHGDH, PSAT1 and PSPH transcriptionally. The explanation for why some enzymes are regulated by the kinase in some breast cancer cell lines but not others remains unfortunately elusive.

Negative transcriptional regulation of serine biosynthesis enzymes by IKKε in MDA-MB-231

One point of interest with regards to the IKKε-mediated regulation of serine biosynthesis enzymes in breast cancer is the apparent negative regulation of *PHGDH*, *PSAT1* and *PSPH* mRNA levels by the kinase in the MDA-MB-231 breast cancer cell line. The serine biosynthesis pathway is not of any particular functional relevance in the MDA-MB-231 cell line, as it is not fully active due to a lack of PHGDH protein expression. These cells therefore cannot synthesise their own serine and, accordingly, cannot survive in serine-free medium (see 3.6). Nevertheless, even if the whole pathway is not hugely important for the cell line, growth benefits could still be offered via the contribution of the PSAT1 reaction to the incorporation of glutamine-derived carbon in the TCA cycle. It is therefore interesting that the upregulation of serine biosynthesis enzyme mRNA levels upon siRNA-mediated suppression of IKKε suggests that the kinase might actively be suppressing *PHGDH*, *PSAT1* and *PSPH* mRNA levels in MDA-MB-231 cells.

Considering the importance of the serine biosynthesis pathway in breast cancer, this might suggest that IKKε is instead acting in a tumour suppressive role in this cell line. Although this would be surprising for a kinase that, till now, had previously only been linked to tumour formation, other IKK's have been demonstrated to have tumour suppressive roles in the past, including IKKα's role in inhibiting the formation and progression of squamous cell carcinoma[135-137] and the controversial role of IKKβ in mesenchymal cells in the development of colitis-associated cancer (CAC) where expression of IKKβ has been shown to play both tumour promoting and tumour suppressive roles[139,140] (see 1.3.1). It is therefore not entirely impossible to hypothesise a scenario where IKKε might also act unexpectedly in a tumour suppressive fashion. Evidence at least supports the hypothesis that IKKε is not driving the proliferation of MDA-MB-231 cells by the fact that suppression of the IKKε in MDA-MB-231 cells failed to inhibit proliferative rate (Figure 3.3), indicating that that the cell line does not require expression of the kinase for proliferation. On the other hand, suppression of the kinase also did not result in an increase in proliferative rates, indicating that IKKε is not necessarily restricting the growth of the cell line either. From a functional standpoint, this negative regulation of *PHGDH*, *PSAT1* and *PSPH* mRNA levels by IKKε in MDA-MB-231 does not translate through to the protein levels (Figure 4.4), indicating that some uncharacterised mechanism maintains protein expression in

the face of mRNA downregulation by IKKε. Considering that modulation of IKKε in MDA-MB-231 has no bearing on proliferation, it appears likely that the effect of kinase modulation on the serine biosynthesis enzymes in this setting is inconsequential. Nevertheless, the fact that the effect of kinase suppression in this singular cell line is so different is notable and would be worth investigating further.

Lack of IKKε-mediated serine biosynthesis enzyme regulation in HA1E-M cells

In addition to identifying transcriptional regulation of the serine biosynthesis enzymes by IKKε in Flp-In 293 and breast cancer cell lines, a model in which the kinase was directly inducing cellular transformation was used to investigate whether the serine enzymes were regulated by IKKε in the early stages of oncogenic transformation.

The model was one defined by Boehm *et al.* in 2007, in the same study wherein IKKε was identified as a transforming kinase[195], and is a HEK293 cell line system expressing hTERT, SV40 LT and ST and a constitutively active version of MEK^{DD}. Termed "HA1E-M", the addition of IKKε expression to this model is sufficient to tip the balance of cellular transformation in favour of oncogenesis. When the effect of IKKε expression on serine biosynthesis enzymes in this model was investigated, it was done so by comparing the expression of PHGDH, PSAT1 and PSPH proteins in HA1E-M cells to expression in a stable IKKε-expressing equivalent cell line; HA1E-M F-IKKε. The expression of serine biosynthesis enzymes in the HA1E-M F-IKKε cells was also compared to their expression in HA1E-M F-IKKε cells wherein IKKε had been suppressed using siRNA. In both comparisons, no clear reproducible change in enzyme protein levels was detected, suggesting no IKKε-dependent regulation of the enzymes was occurring in this cell model. Surprisingly, this was found to be explainable by an unexpected lack of established IKKε signalling in these cell lines. No phosphorylation of known IKKε targets p65, IRF3 or STAT1 was found to occur in an IKKε-dependent manner and auto-phosphorylation of the kinase, indicative of kinase activity, could not be detected in the HA1E-M F-IKKε cells. The kinase expressed in these particular HA1E-M cells therefore appeared inactive, despite IKKε providing the cells with the ability to grow in an anchorage-independent manner. An explanation for the apparent lack of kinase activation remains elusive. It is possible that, over time in culture, the cells have adapted to the constant presence of the kinase and no longer exhibit the same key markers of downstream pathway activation as those that are observed upon the short-term induction of the kinase in the doxycycline-treated Flp-In 293 cells. Alternatively, the wrong markers may have been examined. Phosphorylation of p65 at Ser468 by IKKε has indeed been shown to facilitate regulation of NF-κB signalling[83], but when confirming activation of the pathway by the kinase in

HA1E-M cells, Boehm *et al.* demonstrated that expression of IKKε reduced cytoplasmic levels of both IκBα and NF-κB subunit p50 and increased nuclear localisation of NF-κB p50[195]. In addition to phosphorylation of p65 Ser468, these readouts should be evaluated in the HA1E-M and HA1E-M F-IKKε cells used in this project to properly confirm whether the kinase is indeed activating NF-κB signalling in these cells.

To attempt to recapitulate the short-term activation of the kinase observed in doxycycline-treated Flp-In 293 cells, it would be worth mimicking the physiological activation of the kinase by treating HA1E-M F-IKKε cells with toll-like receptor (TLR) agonists LPS or Poly(I:C). This would stimulate TLR activation and its downstream signalling to provide an activating signal for IKKε and therefore allow potential evaluation of the role of short-term activated IKKε in regulating the serine biosynthesis enzymes in the HA1E-M cell model. Importantly however, the activation of TLR's does not exclusively activate IKKε. A variety of signalling pathways are activated in response to receptor activation, meaning such an experiment might not be sufficient to conclude on the specific role of IKKε. Instead, a different HA1E-M cell line model could prove more useful in this regard. In the same 2007 study, several IKKε-expressing HA1E-M cell lines were created, including a version containing a myristoylated, constitutively active kinase. By comparing the expression of the serine biosynthesis enzymes in the myristoylated-IKKε-expressing cells, where Boehm *et al.* have already shown that the kinase induces NF-κB activation and is therefore active and signalling[195], to the HA1E-M cells without IKKε and even to HA1E-M F-IKKε cells with the inactive kinase, it would be possible to definitively conclude whether PHGDH, PSAT1 or PSPH are regulated by IKKε in the HA1E-M cell model or not.

In spite of the lack of PHGDH, PSAT1 and PSPH regulation by IKKε in the HA1E-M F-IKKε cells, it is worth noting that experiments performed by another member of the Bianchi lab, Dr Ewa Wilcz-Villega, have successfully offered some insight into the role of serine biosynthesis in IKKε-driven cellular transformation. Dr Wilcz-Villega has found that mimicking the inflammatory conditions found in a tumour microenvironment by treating MCF-10A cells with medium conditioned by patient-derived M1 and M2 macrophages induces IKKε expression and promotes the transformation of cells as measured by an increased ability for cells to grow in an anchorage-independent manner in a soft agar colony formation assay. In the context of serine biosynthesis, this effect was effectively blocked by the addition of recently described PHGDH inhibitor, NCT-502[363], to the cells, thus indicating that the serine biosynthesis pathway is an important contributor to the IKKε-driven acquisition of transformed properties. The role of serine biosynthesis in this model of IKKε-mediated transformation is therefore something that should be investigated further.

Canonical IKKε-signalling pathways are dispensable for regulation of serine biosynthesis

As well as identifying the transcriptional regulation of the serine biosynthesis enzymes by IKKε, the other major finding of this chapter is that said regulation is independent of established IKKε signalling and the NF-κB and IFNβ pathways. This was surprising, given that the major transcriptional programmes that IKKε is known to induce as part of its main functions involve both NF-κB and IFNβ signalling, but is significant in the context of the project and the therapeutic options it might present for breast cancer patients. Herein is evidence for a breast cancer oncogene regulating the activity of a pathway that has been extensively linked to breast cancer development independently of the NF-κB pathway. As discussed in chapter 1 (see 1.3.3.1), therapeutic targeting of NF-κB activation remains a poor strategy for therapeutic intervention in IKKε-driven breast cancers. Whilst the kinase has been primarily linked to breast cancer through both the induction of IκBα degradation and canonical NF-κB activation[192,195] and the activation of NF-κB independently of IκBα degradation via direct phosphorylation of NF-κB subunits[82,194], other NF-κB-independent mechanisms of IKKε-mediated oncogenesis have been described. Such mechanisms include the direct promotion of the stabilisation of YAP1 in gliomas[173], the phosphorylation and inhibition of FOXO3a in lung cancers[177] and in breast cancer, the induction of expression of a truncated ERα, ERα-36, in ER negative breast cancers that induces cyclin D1 and c-Myc[211,212]. The NF-κB independent regulation of serine biosynthesis enzymes to promote serine biosynthesis might therefore represent a novel NF-κB independent mechanism by which IKKε expression can promote cell growth and cancer development and provide a host of new therapeutic targets for drug development.

IKKε, serine biosynthesis and oxidative stress in breast cancer

Whether or not the upregulation of the serine biosynthesis pathway actively contributes to IKKε's ability to support breast cancer development remains to be seen. However, some indirect evidence from the labelled metabolite analysis described in chapter 3 (see 3.2) does suggest that the upregulation of PHGDH, PSAT1 and PSPH by IKKε could indeed benefit rapidly proliferating cancer cells.

One of the primary ways that increased serine biosynthesis can support rapid proliferation and cancer development is by contributing to the maintenance of intracellular redox balance. Serine is catabolised to glycine by SHMT, which removes a carbon unit from serine and donates it to the one-carbon cycle, an important by-product of which is NADPH to support the production of key cellular anti-oxidant glutathione[320]. Although SHMT2, the mitochondrial isoform of SHMT that primarily facilitates this process and the isoform that has been most linked with cancer

progression[320,357-359], showed no significant upregulation at the protein level upon induction of HA-IKKε in Flp-In 293 cells, evidence from the labelled metabolite analysis suggests that expression of IKKε does promote anti-oxidant production in breast cancer cells. It was found that suppression of IKKε in T47D cells reduced intracellular glutathione levels (Figure 3.6). This therefore suggests that upregulation of IKKε in breast cancer contributes to the maintenance of glutathione levels within the cells and that the kinase might help to maintain intracellular redox balance. Considering IKKε upregulated serine biosynthesis in T47D cells, this IKKε-dependent increase in cellular glutathione levels could be explained via an increase in the flux of serine-derived carbon into one-carbon metabolism. Indeed, even if SHMT2 itself is not regulated by the kinase, increased serine biosynthesis can increase the flow of glucose-derived carbons towards glycine, thereby increasing the contribution of glucose-derived carbon into the one-carbon metabolic cycles and facilitating the maintenance of redox balance through glutathione reduction. With this in mind, it would be prudent to evaluate the effect of IKKε suppression in T47D breast cancer cells on intracellular ROS levels, as this would allow evaluation of whether the kinase does indeed provide such a mechanism for ROS detoxification in this context.

Concluding remarks

The data presented in this chapter follows up on the work from the previous chapter, in which the phosphorylation of PSAT1 in an IKKε-dependent manner was shown to promote protein stability, by providing evidence that expression of IKKε in Flp-In 293 HA-IKKε cells and a panel of human breast cancer cell lines upregulates PSAT1 protein levels. Unexpectedly, in addition to PSAT1, other serine biosynthesis enzymes were found to be regulated by the kinase, indicating that regulation of the enzymes was not solely attributable to substrate phosphorylation. This subsequently led to the finding that IKKε regulates serine biosynthesis enzymes at a transcriptional level to enhance serine production. Importantly, the transcriptional regulation of *PHGDH*, *PSAT1* and *PSPH* mRNA levels by IKKε was found to be independent of the kinases known functions in NF-κB and IFNβ signalling, suggesting that expression of the kinase in Flp-In 293 cells and breast cancer cell lines activates other, previously uncharacterised transcriptional programmes. What this transcriptional programme might be, what the transcription factor responsible for its activation is and how the kinase induces that transcription factor were the next major questions to be asked. Efforts to answer these questions are therefore described in the next chapter.

Chapter 5

Results

IKKε regulates serine biosynthesis enzymes via mitochondrial inhibition

Disclaimer: Whilst such instances are clearly indicated previously in the materials and methods and again in the following text and figure legends, the data demonstrating the effect of IKKε on oxygen consumption rate (presented in Figures 5.1 and 5.2) were acquired by Dr Ruoyan Xu. Similarly, the samples sent for assessment of IKKε's effect on mitochondrial membrane potential via TMRM staining with collaborator Professor Gyorgy Szabadkai at University College London, London, UK were prepared with the assistance of Dr Ruoyan Xu, who prepared the samples for the experiment presented in Figure 5.3 (samples for the experiment presented in Figure 5.6 were prepared by the author). These data were included with the intention to provide context for the work examining the role of ATF4 in IKKε-mediated regulation of the serine biosynthesis enzymes, as the changes in OCR provided the key reason for investigating ATF4.

5.1 Identification of potential serine biosynthesis enzyme-regulating transcription factors

The results described in the previous chapter provided evidence for the transcriptional upregulation of serine biosynthesis enzymes by IKKε. Experiments performed in Flp-In 293 HA-IKKε cells, wherein p65 or IRF3 proteins were suppressed using siRNA targeting *RELA* and *IRF3* mRNA respectively to inhibit canonical NF-κB or IFNβ activation, found that the transcriptional upregulation of *PHGDH*, *PSAT1* and *PSPH* mRNA in response to induction of HA-IKKε was wholly independent of the kinases established NF-κB- or IFNβ-mediated signalling. Therefore, the regulation of serine enzymes by IKKε was deemed to be via alternative signalling activities.

In order to identify other potential transcription factors capable of upregulating *PHGDH*, *PSAT1* and *PSPH* mRNA in response to induction of HA-IKKε in doxycycline-treated Flp-In 293 cells, a two-pronged approach was taken. Firstly, a promoter analysis was performed to identify transcription factor binding sites in the promoter regions of the serine biosynthesis enzyme genes. Simultaneously, existing literature was searched to identify transcription factors which had been previously been reported to induce *PHGDH*, *PSAT1* and *PSPH* expression.

The promoter analysis was performed in collaboration with Professor Claude Chelala and Dr Ai Nagano (Barts Cancer Institute, London, UK) and studied the peak Histone H3 methylation regions upstream of the *PHGDH*, *PSAT1* and *PSPH* genes, searching for potential transcription factor binding sites. Since a transcription factor that regulates all three enzymes in HA-IKKε-expressing Flp-In 293 cells was sought, the lists of identified transcription factors with potential binding sites in each gene promoter were subsequently compared to highlight common factors between the three genes. The resulting list was then cross-referenced with the literature base to identify factors that might be regulated upon induction of the kinase (Table 5.1).

Several transcription factors with predicted binding sites in the promoter regions of all three serine biosynthesis enzyme genes were identified as having potential links to IKKε. These factors therefore represented possible candidates for regulating the serine biosynthesis enzymes in response to induction of the kinase. Such factors included members of the ccaat-enhancer-binding protein (C/EBP) family C/EBPβ and C/EBPδ and transcription factor specificity protein 1 (SP1), all of which have been shown to be activated by IKKε[364-366]. Importantly, the links between these factors and IKKε all involve or require p65 and active NF-κB signalling to some degree[364,366]. Similarly, E1A-associated protein p300 (EP300), a histone acetyltransferase which can bind to

IRF3 to drive transcription can be linked to IKKε through IKKε's ability to induce nuclear translocation of IRF3[367,368].

Unfortunately, the fact that the links between IKKε and these transcription factors all depended on the activity of p65 or IRF3 demonstrated that none of them were likely to be responsible for the observed transcriptional regulation of the serine biosynthesis enzymes. Indeed, the previous chapter confirmed that neither p65 nor IRF3 were essential for the upregulation of *PHGDH*, *PSAT1* or *PSPH* mRNA upon induction of HA-IKKε in Flp-In 293 cells. This means that transcription factors which depend on p65 or IRF3 could not be involved, as such factors would have been unable to function upon the knockdown of p65 or IRF3 and enzyme induction would have been inhibited as a result. That this was not the outcome therefore indicates that the responsible transcription factor must function independently of p65 or IRF3. Consequently, none of the transcription factors identified in the promoter analysis were deemed to be suitable candidates to explain the observed phenotype and instead, attention was turned back to the existing literature, to identify transcription factors that had previously been shown to be regulators of *PHGDH*, *PSAT1* and *PSPH* expression.

From a literature search, it was apparent that two major transcription factors, which were absent from the promoter analysis, have been reported to induce transcription of the three serine biosynthesis enzymes. Firstly, c-Myc has been shown upregulate *PHGDH*, *PSAT1* and *PSPH* mRNA levels (and *SHMT1* and *SHMT2* mRNA as well) in tumours driven by the oncogene and accordingly, ChIP-qPCR analysis has demonstrated the binding of c-Myc to enhancer regions in the *PHGDH*, *PSAT1* and *PSPH* genes[315,369]. Secondly, ATF4, a key stress-responding transcription factor, has been reported to be a master regulator of serine biosynthesis having repeatedly been shown to transcriptionally upregulate serine biosynthesis enzyme mRNA levels in mouse cell lines, drosophila and in human cancer cells and, in agreement with this, has been shown to upregulate the enzymes downstream of NRF2 to support glutathione and nucleotide production in NSCLC[324,370-372].

The absence of c-Myc and ATF4 from the promoter analysis suggested that the analysis that was performed was incomplete, that it was likely not searching the full promoter sequences for the three genes and was therefore unlikely to be detecting all the possible transcription factor binding sites. Nevertheless, c-Myc and ATF4 represented promising candidates for the regulation of the pathway by IKKε. Indeed, IKKε has been shown to promote c-Myc nuclear translocation via activation of AKT to promote an aerobic glycolysis phenotype and support

pancreatic cancer growth[189], demonstrating a strong link between the kinase and c-Myc in the context of cellular metabolism.

Before investigating the role of c-Myc however, the results of the labelled metabolite analysis were recalled (Figures 3.5 and 3.6). When mapping the metabolic response to modulation of IKKε in Flp-In 293 cells and T47D breast cancer cells, it was concluded that the kinase was inducing an aerobic glycolysis-like state, with an increase in anabolic biosynthesis (in the form of increased serine biosynthesis), an increase in lactate production and a decrease in the incorporation of glucose-derived carbon in the intermediates of the TCA cycle. Reduced entry of glucose-derived carbon into the mitochondria and the TCA cycle is one of the key features of classical aerobic glycolysis and is one of the main reasons why cancer cells do not display typical mitochondrial respiration via OXPHOS.

That IKKε was regulating mitochondrial metabolism was interesting. The kinase has been previously demonstrated to associate with the mitochondria through interaction with mitochondrial antiviral-signaling (MAVS) protein[373] and a previous study examining the effect of IKKε on cellular metabolism in dendritic cells demonstrated that the kinase can induce aerobic glycolysis by promoting the interaction of glycolytic enzyme hexokinase II with the mitochondria[106]. More importantly, as this project has demonstrated, IKKε regulates serine biosynthesis activity, inducing expression of serine biosynthesis enzymes in both Flp-In 293 cells and breast cancer cells. This is particularly notable, as regulation of mitochondrial function has recently been linked with the regulation of serine biosynthesis activity via ATF4. A 2016 study by Bao *et al.* identified that mitochondrial dysfunction, triggered by a reduction in mitochondrial DNA and OXPHOS membrane complex expression, induced a retrograde mitochondria-to-nucleus signalling axis mediated by ATF4, which resulted in the transcriptional upregulation of *PHGDH*, *PSAT1* and *PSPH* and the enhancement of serine biosynthesis activity to support one-carbon metabolism[362].

Since the labelled metabolite analysis demonstrated that IKKε inhibited the mitochondrial uptake of glucose-derived carbon, it was therefore speculated that if the effect of the kinase on the mitochondria was sufficient to inhibit mitochondrial function, then the upregulation of *PHGDH*, *PSAT1* and *PSPH* mRNA levels could be a result of the same ATF4-mediated retrograde mitochondria-to-nucleus signalling. To address this, the question of whether expression of IKKε led to an inhibition of mitochondrial function was first investigated.

Table 5.1 – List of transcription factors with predicted binding sites in *PHGDH*, *PSAT1* and *PSPH* promoter regions. Promoter analysis performed in collaboration with Professor Claude Chelala and Dr Ai Nagano to identify potential transcription factor binding sites in the promoter regions of serine biosynthesis enzyme genes. Using data from the ENCODE project[374], the analysis was performed by searching for transcription factor binding sites located in regions of peak Histone H3 lysine 4 methylation (H3K4me3) near PHGDH, PSAT1 and PSPH gene start positions. Previous links of transcription factors to IKKε, as identified via a literature search, are indicated.

Transcription Factor	Link to IKKε
C/EBPβ	Activation and nuclear translocation induced by IKKε binding[365]
C/EBPδ	DNA binding activity induced by IKKε in response to LPS stimulation[364]
CHD2	
E2F1	
E2F4	
EP300	Binds to IRF3 via an IRF3 binding domain (IBiD) to drive transcription[367,368]
MAZ	
NFYB	
PHF8	
RCOR1	
REST	
RFX5	
SIN3AK20	
SP1	Induced by p52 in response to poly(I:C)-mediated IKKε activation[366]
TAF1	
TBP	
ZBTB33	
ZNF143	

5.2 IKKε inhibits mitochondrial function

In cells undergoing classical aerobic respiration, the TCA cycle fuels the electron transport chain (ETC), which is used to produce ATP in large quantities for energy storage. The final stages of the ETC involve the consumption of oxygen as an acceptor of the electrons passed along the intermembrane complexes (Figure 1.5). Therefore, in order to determine the effect of IKKε on classical mitochondrial function, cellular oxygen consumption rate (OCR) was measured by Dr Ruoyan Xu. In Flp-In 293 cells, the effect of induction of the kinase upon OCR was measured using Oroboros high resolution respirometry analysis. In breast cancer cell lines, the effect of siRNA-mediated suppression of IKKε on cellular OCR was measured using Seahorse extracellular flux analysis.

Flp-In 293 HA-IKKε wt or Flp-In 293 HA-IKKε KD-m cells were used to assess the effect of IKKε kinase activity on mitochondrial function. Cells were treated with doxycycline for 16 hours to induce kinase expression, following which OCR was measured in both non-treated and doxycycline-treated cells to compare cellular oxygen consumption before and after IKKε induction (Figure 5.1).

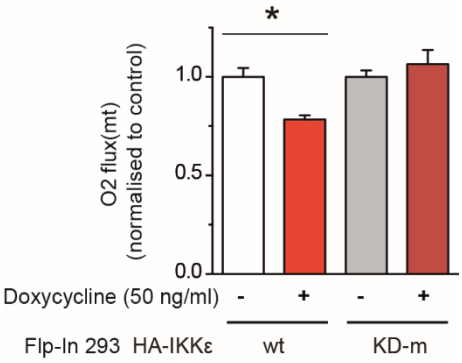

Figure 5.1 – Induction of HA-IKKε wt in Flp-In 293 cells reduces cellular oxygen consumption. Oroboros high resolution respirometry analysis of basal oxygen consumption in non-treated Flp-In 293 HA-IKKε wt or Flp-In 293 HA-IKKε KD-m cells compared to cells treated with 50 ng/ml doxycycline for 16 hours. Oxygen consumption values of doxycycline-treated cells were normalised to non-treated cells. IKKε reduces cellular oxygen consumption in a kinase activity-dependent manner. Experiment performed by Dr Ruoyan Xu. n≥3 independent experiments, mean ± SEM, *p<0.05 as measured by two-way ANOVA with Bonferroni *post-hoc* tests.

Treatment of Flp-In 293 HA-IKKε wt cells with doxycycline significantly reduced OCR. Conversely, doxycycline treatment of Flp-In 293 HA-IKKε KD-m cells failed to induce any significant change in cellular OCR. This indicated that expression of HA-IKKε induces a particular signalling axis which reduces cellular OCR in a kinase-dependent manner.

To determine whether IKKε was affecting OCR in human breast cancer cell lines, siRNA was used to suppress kinase expression as in previous experiments. Cells were plated and transfected with a pool of siRNA oligos targeting *IKBKE* mRNA, to suppress IKKε, or a single non-targeting control oligo for 72 hours. Following kinase knockdown, OCR was measured using Seahorse extracellular flux analysis to determine IKKε-dependent changes in oxygen consumption (Figure 5.2). Whilst basal OCR was of primary interest to this project, other parameters, such as maximal and spare respiratory capacity were also measured for each cell line upon IKKε suppression. Representative data for these parameters is presented for each cell line in the supplementary material (see supplementary materials: Figure 7.1).

Suppression of the kinase in breast cancer cells led to significant increases in OCR in 6 out of the 9 cell lines tested, indicating that IKKε suppresses cellular oxygen consumption in a subset of breast cancer cell lines. This supports the findings in Flp-In 293 cells upon induction of the kinase and together, these data demonstrate that IKKε significantly impairs mitochondrial oxygen consumption.

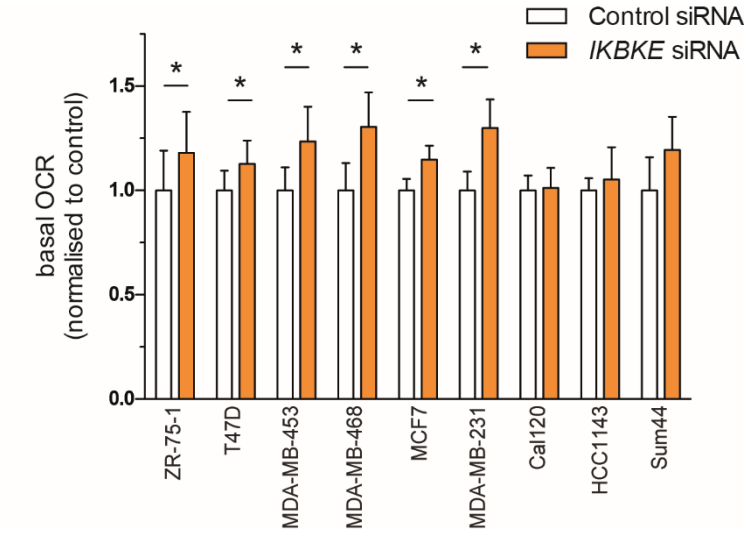

Figure 5.2 – Suppression of IKKε increases cellular oxygen consumption in a subset of breast cancer cell lines. Seahorse extracellular flux analysis of basal oxygen consumption rate in *IKBKE* siRNA-transfected breast cancer cell lines. Indicated cell lines were transfected with a pool of 4 siRNA oligos targeting *IKBKE* mRNA, to suppress IKKε, or a single non-targeting control oligo at a final concentration of 50 nM. 24 hours post-transfection, cells were trypsinised and re-plated into a Seahorse plate and 48 hours later, OCR was measured using the Seahorse XF96 analyser. All OCR values were normalised to the protein concentration of each sample well (measured by a BCA assay), then additionally normalised to the OCR in cells transfected with non-targeting control siRNA. IKKε suppression significantly increased OCR in 6 out of the 9 cell lines tested. Experiment performed by Dr Ruoyan Xu. n≥3 independent experiments, mean ± SEM, *p,0.05 as measured by paired, two-tailed Student's t-test.

In addition to evaluating the kinases effect on OCR, the effect of IKKε on mitochondrial activity was also investigated by measuring mitochondrial membrane potential. Active mitochondria feature a strong negatively charged polarity across the inner mitochondrial membrane due to

the function of the electron transport chain. As the activity decreases, the membrane depolarises. This change in polarity can therefore be exploited to measure mitochondrial activity, by staining cells with tetramethylrhodamine, methyl ester (TMRM), a positively charged dye that accumulates in mitochondria proportionally to the membrane potential. TMRM dye does not accumulate in inactive mitochondria with a depolarised membrane, therefore meaning that dye intensity correlates with mitochondrial activity. This experiment was also performed by Dr Ruoyan Xu, in collaboration with Professor Gyorgy Szabadkai (University College London, London, UK), who measured TMRM staining intensity in cells using the ImageXpress Micro XL High-Content Imaging system.

Flp-In 293 HA-IKKε wt or Flp-In 293 HA-IKKε KD-m cells were plated, treated with doxycycline for 16 hours to induce kinase expression and subsequently stained with TMRM dye to evaluate mitochondrial activity (Figure 5.3).

Similar to the analysis of OCR upon induction of HA-IKKε, treatment of Flp-In 293 HA-IKKε wt cells with doxycycline for 16 hours significantly reduced TMRM staining intensity, whereas doxycycline treatment of Flp-In 293 HA-IKKε KD-m cells failed to induce any significant change in staining intensity. This, in agreement with findings on IKKε's effect on cellular oxygen consumption, demonstrated that IKKε inhibits mitochondrial activity in a manner dependent on kinase activity. Additionally, this confirms that the IKKε-dependent reduction in OCR is attributable to the inhibition of mitochondrial activity and the suppression of the electron transport chain.

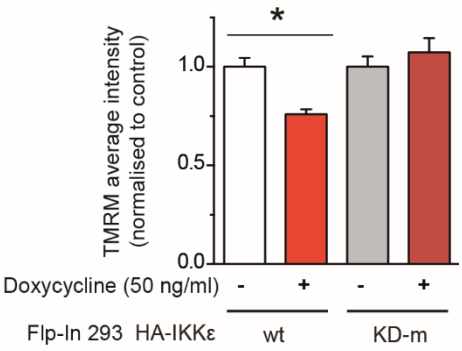

Figure 5.3 – Induction of HA-IKKε wt in Flp-In 293 cells reduces mitochondrial membrane potential. Tetramethylrhodamine, methyl ester (TMRM) staining analysis of mitochondrial membrane potential as a readout for mitochondrial activity in non-treated Flp-In 293 HA-IKKε wt or Flp-In 293 HA-IKKε KD-m cells compared to cells treated with 50 ng/ml doxycycline for 16 hours. Staining intensity was measured using the ImageXpress Micro XL High-Content Imaging system and intensity in doxycycline-treated cells was normalised to that of non-treated cells. IKKε significantly reduces mitochondrial sequestration of TMRM dye in a kinase-dependent manner, indicating a significant reduction in mitochondrial membrane potential and therefore, mitochondrial activity. Experiment performed by Dr Ruoyan Xu in collaboration with Professor Gyorgy Szabadkai. n≥3 independent experiments, mean ±SEM, *p<0.05 as measured by two-way ANOVA with Bonferroni *post-hoc* tests.

5.3 IKKε controls glucose-carbon entry into the TCA cycle via PDHA1

As previously mentioned, data from the labelled metabolite analysis demonstrated that IKKε-expressing cells exhibited reduced incorporation of glucose-derived carbon into the TCA cycle. In order to confirm whether the reduction in mitochondrial respiration induced by the kinase was attributable to this diversion of substrate away from the TCA cycle it was questioned how exactly the kinase was preventing the mitochondrial uptake of glucose-derived carbon.

To identify potential effectors of IKKε's effect on the mitochondria, the results of the phosphoproteomic analysis, identifying proteins exhibiting significant changes in phosphorylation in HA-IKKε-expressing Flp-In 293 cells, were recalled (Table 3.2). Several metabolic proteins were identified as significantly more phosphorylated when IKKε was expressed, including PSAT1 as described in chapter 3. In the context of mitochondrial inhibition however, it was particularly intriguing to find that pyruvate dehydrogenase E1 component subunit alpha (PDHA1) was significantly more phosphorylated at serine residue Ser232 in HA-IKKε-expressing cells. Phosphorylation of PDHA1 at Ser232 inhibits the activity of the enzyme[375,376]. That this residue was significantly more phosphorylated in IKKε-expressing cells indicates that the kinase inhibits PDHA1 activity.

PDHA1 is a central component of the pyruvate dehydrogenase complex, which catalyses the conversion of pyruvate to acetyl-CoA for entry into the mitochondrial TCA cycle. In essence, the enzyme complex is the gatekeeper for the entry of glucose-derived carbon into the TCA cycle. IKKε inducing an inhibitory phosphorylation of an essential subunit of the complex could explain the decrease of glucose-derived carbon in the TCA cycle and the reduced mitochondrial function in kinase-expressing cells. However, overlap of IKKε's optimal phosphorylation motif[197] with the PDHA1 sequence surrounding Ser232 exhibited no overlap in residues other than the requisite phosphorylated serine (Figure 5.4). This, combined with the fact that PDHA1 is a mitochondrial protein inaccessible to the kinase, indicated that PDHA1 Ser232 is not a direct substrate of IKKε.

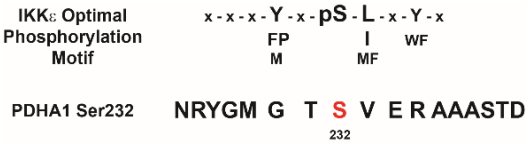

Figure 5.4 – PDHA1 is likely not a direct substrate of IKKε. IKKε's optimal phosphorylation motif as described by Hutti *et al.* 2006[197] compared with the amino acid sequence surrounding the PDHA1 Ser232 residue, identified as significantly more phosphorylated in IKKε-expressing cells. With the exception of the serine residue, no overlap of residues was detected between IKKε's optimally recognised sequence and the PDHA1 sequence, indicating that PDHA1 is unlikely to be an IKKε substrate.

This suggested that, rather than direct phosphorylation similar to phosphorylation of PSAT1 Ser331 by IKKε, the kinase induced PDHA1 Ser232 phosphorylation indirectly through the activation of a signalling cascade. To attempt to validate the detected IKKε-dependent phosphorylation of the enzyme, western blotting was used to evaluate PDHA1 Ser232 phosphorylation levels in Flp-In 293 HA-IKKε cells upon treatment with doxycycline (Figure 5.5).

No clear difference in PDHA1 Ser232 phosphorylation was observed between non-treated and doxycycline-treated cells via western blot. This was confirmed by densitometry quantification analysis of the blot, performed by normalising total PDHA1 and p-PDHA1 (Ser232) protein levels to vinculin, to account for differences in loading, followed by normalisation of phosphorylated protein levels to total protein levels, to account for any changes in PDHA1 expression that might be induced by IKKε. The fact that no differences in Ser232 phosphorylation were observed upon treatment of Flp-In 293 HA-IKKε cells with doxycycline indicated that the kinase was unable to induce stable phosphorylation of PDHA1. It is worth noting however, that kinase phosphorylations are often highly transient events, meaning it is possible that IKKε does induce PDHA1 Ser232 phosphorylation, but that it does so in a dynamic manner that is difficult to detect via western blotting. Therefore, alternative methods of evaluating the role of PDHA1 in IKKε-mediated mitochondrial inhibition were used.

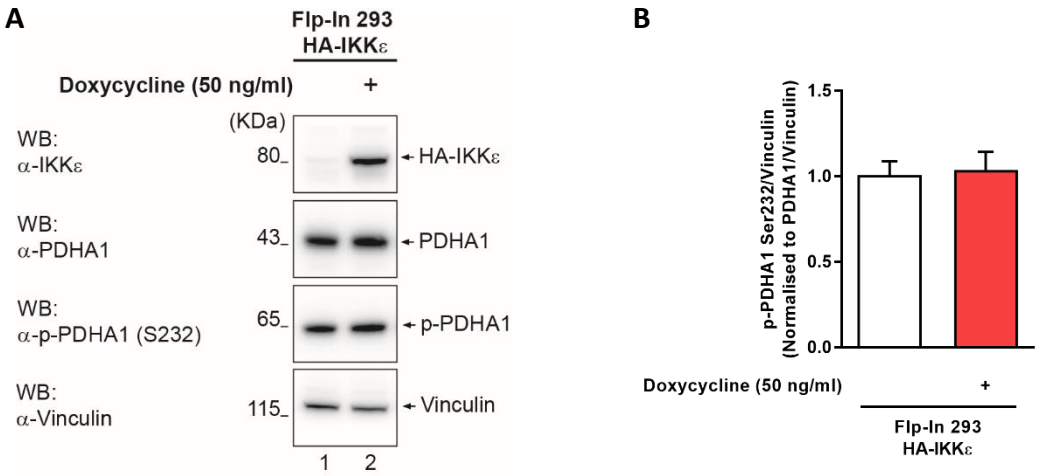

Figure 5.5 – Induction of HA-IKKε in Flp-In 293 cells has no impact on levels of stable PDHA1 phosphorylation. (A) Western blot analysis of total PDHA1 protein levels and PDHA1 Ser232 (S232) phosphorylation in either non-treated Flp-In 293 HA-IKKε cells or cells treated with 100 ng/ml doxycycline for 16 hours to induce kinase expression. Vinculin is shown as a loading control. **(B)** Densitometry quantification analysis of PDHA1 Ser232 phosphorylation levels in doxycycline-treated cells versus non-treated cells. Total PDHA1 and p-PDHA1 Ser232 densitometry per sample was quantified as a percentage of total protein densitometry and normalised to vinculin, then p-PDHA1 Ser232 densitometry was further normalised to total PDHA1. PDHA1 Ser232 phosphorylation was unchanged by induction of HA-IKKε with doxycycline. n=3 independent experiments, mean ± SEM. No significant differences were detected when measured using a paired, two-tailed Student's t-test.

To better clarify the role of PDHA1 in IKKε-mediated mitochondrial regulation in Flp-In 293 cells, pyruvate dehydrogenase complex activity was forcibly induced in the presence of IKKε induction through treatment of Flp-In 293 HA-IKKε cells with dichloroacetate (DCA). Phosphorylation of PDHA1 at serine residue Ser232 is typically controlled by a kinase called pyruvate dehydrogenase kinase (PDK) which phosphorylates the enzyme to inhibit the pyruvate dehydrogenase complex[377]. DCA can activate PDHA1 by inhibiting PDK[378]. Therefore, treatment of HA-IKKε-expressing Flp-In 293 cells with DCA should prevent IKKε's effect on the mitochondria, if it is mediated by inhibition of PDHA1, by maintaining activation of the enzyme in the presence of the kinase. The effect of combined treatment of Flp-In 293 HA-GFP or Flp-In 293 HA-IKKε cells with DCA and doxycycline on mitochondrial activity was evaluated using TMRM staining with the help of Professor Gyorgy Szabadkai (Figure 5.6).

In agreement with previous data, treatment of Flp-In 293 HA-IKKε cells, but not Flp-In 293 HA-GFP cells, with doxycycline significantly reduced TMRM staining intensity within the cells, confirming an IKKε-dependent inhibition of mitochondrial activity. Importantly, whilst treatment of either Flp-In 293 HA-GFP or Flp-In 293 HA-IKKε cells with DCA alone had no significant impact on TMRM intensity, combined treatment of Flp-In 293 HA-IKKε cells with DCA and doxycycline completely abolished the kinase-dependent decrease in TMRM staining. This indicated that the reduction in mitochondrial activity by the HA-IKKε was mediated through inhibition of the activity of the pyruvate dehydrogenase complex and that this phenotype was rescuable with therapeutic intervention.

Together, these data confirm that, as indicated by the labelled metabolite analysis, IKKε supports an aerobic glycolysis-like phenotype by having an inhibitory effect on the mitochondria, reducing mitochondrial respiration as measured by oxygen consumption and membrane potential. This inhibition is controlled by the IKKε-dependent inhibition of pyruvate dehydrogenase activity, resulting in an inhibition of the conversion of pyruvate to acetyl-CoA and the uptake of glucose-derived carbon to the mitochondria. This therefore explains the reduction in glucose-derived carbon incorporation in TCA cycle metabolites observed in the labelled metabolite analysis performed in IKKε-expressing cells (see 3.2).

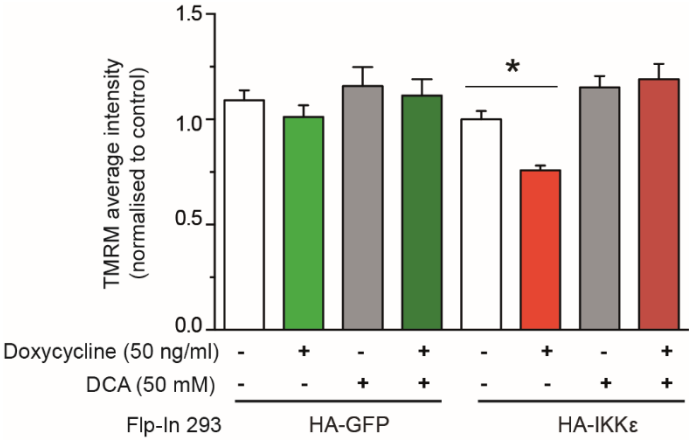

Figure 5.6 – DCA pre-treatment rescues HA-IKKε-mediated inhibition of the mitochondria in Flp-In 293 cells. TMRM staining analysis of mitochondrial membrane potential in Flp-In 293 HA-GFP or Flp-In 293 HA-IKKε cells treated with 50 ng/ml doxycycline, 50 mM DCA or a combination of doxycycline and DCA for 16 hours. Staining intensity was measured using the ImageXpress Micro XL High-Content Imaging system and intensity in doxycycline, DCA or doxycycline and DCA-treated cells was normalised to the intensity in non-treated Flp-In 293 HA-IKKε cells. Neither doxycycline nor DCA had any significant impact on TMRM staining intensity in Flp-In 293 HA-GFP cells. Treatment of Flp-In 293 HA-IKKε cells with doxycycline for 16 hours significantly reduced TMRM staining intensity as before, consistent with decreased mitochondrial activity, but combination of doxycycline treatment with DCA prevented this HA-IKKε-dependent decrease, indicating that the kinase blocks mitochondrial function through reversible inhibition of the pyruvate dehydrogenase complex. Experiment performed in collaboration with Professor Gyorgy Szabadkai. n=3 independent experiments, mean ± SEM, *p<0.05 as measured by two-way ANOVA with Bonferroni *post-hoc* tests.

5.4 IKKε-mediated transcriptional upregulation of *PHGDH*, *PSAT1* and *PSPH* in Flp-In 293 cells requires ATF4

As previously mentioned, mitochondrial dysfunction has previously been demonstrated to upregulate the enzymes of the serine biosynthesis pathway via ATF4-mediated retrograde mitochondria-to-nucleus signalling[362]. Confirmation that the IKKε-induced reduction in mitochondrial utilisation of glucose-derived carbon is accompanied by a reduction in mitochondrial function suggested that the expression of the kinase would be sufficient to activate the same ATF4-mediated retrograde signalling axis. It was therefore hypothesised that IKKε's effect on the enzymes of the serine biosynthesis pathway was mediated by ATF4. Accordingly, the involvement of the transcription factor on IKKε-mediated upregulation of *PHGDH*, *PSAT1* and *PSPH* mRNA levels was investigated.

Flp-In 293 HA-IKKε cells were transfected with a single *ATF4*-targeting siRNA oligo or a non-targeting control oligo for 72 hours, with doxycycline being added for the final 16 hours. This allowed the induction of the kinase in the absence of ATF4 expression and therefore evaluation of the role that ATF4 plays in the IKKε-mediated transcriptional regulation of the serine biosynthesis enzymes (Figure 5.7). The data shown is using single oligo suppression of ATF4, but the experiment was also repeated with a pool of 4 *ATF4*-targeting siRNA oligos to control for off-target effects.

The first observation that was noted was that treatment of Flp-In 293 HA-IKKε cells with doxycycline resulted in an increase in overall ATF4 protein levels. Whilst total protein levels of a transcription factor do not necessarily correlate with transcriptional activity, meaning an increase in ATF4 protein levels may not be indicative of increased activity, this at least indicated some regulation of the transcription factor by the kinase. Furthermore, transfection of the siRNA oligo effectively suppressed ATF4 protein levels which could not then be rescued by induction of the kinase. More interestingly, whereas induction of HA-IKKε successfully increased PSAT1 and PSPH protein levels and significantly upregulated *PHGDH*, *PSAT1* and *PSPH* mRNA levels as expected in the control siRNA-transfected cells, the transfection of cells with ATF4 targeting siRNA not only reduced basal levels of PHGDH, PSAT1 and PSPH protein and mRNA, but also completely abrogated IKKε's ability to induce the enzymes at a protein or mRNA level. This indicated that the observed upregulation of serine biosynthesis enzymes in IKKε-expressing cells was mediated by ATF4-dependent transcriptional upregulation of the enzyme mRNA levels.

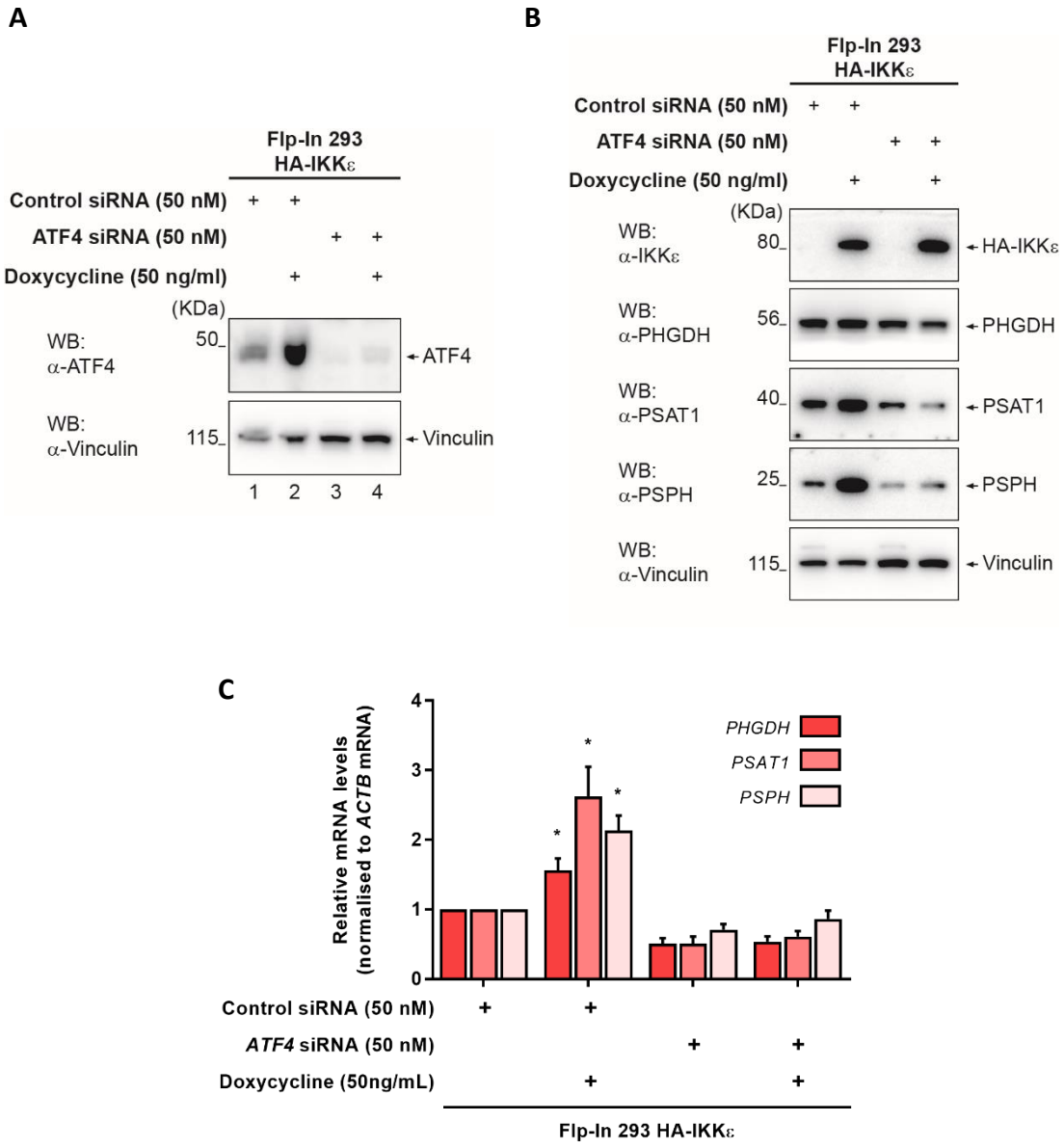

Figure 5.7 – HA-IKKε-mediated upregulation of serine biosynthesis enzymes in Flp-In 293 cells requires ATF4. Flp-In 293 HA-IKKε cells were transfected with a single *ATF4*-targeting siRNA oligo, to suppress the transcription factor, or a non-targeting control oligo at a final concentration of 50 nM for 72 hours. 50 ng/ml doxycycline was added for the final 16 hours to induce HA-IKKε in the absence of ATF4. **(A)** Western blot analysis demonstrating upregulation of ATF4 protein levels upon treatment of Flp-In 293 HA-IKKε cells with doxycycline and effective suppression of ATF4 protein following transfection of *ATF4* siRNA. **(B)** Western blot analysis examining the effect of doxycycline treatment on PHGDH, PSAT1 and PSPH protein levels in Flp-In 293 HA-IKKε cells where ATF4 is suppressed using siRNA. Doxycycline induces PSAT1 and PSPH protein upregulation as expected upon induction of IKKε, but suppression of ATF4 decreases basal PHGDH, PSAT1 and PSPH protein level and prevents HA-IKKε-mediated upregulation of PSAT1 and PSPH upon doxycycline treatment. Vinculin is shown as a loading control. **(C)** qRT-PCR analysis of the effect of doxycycline on serine biosynthesis enzyme mRNA levels in Flp-In 293 HA-IKKε cells transfected with *ATF4* siRNA. As before, doxycycline significantly upregulates *PHGDH*, *PSAT1* and *PSPH* mRNA levels in control siRNA transfected cells, but suppression of ATF4 inhibits HA-IKKε-mediated upregulation of enzyme mRNA levels. These data indicate ATF4 controls HA-IKKε-driven upregulation of serine biosynthesis enzymes. mRNA levels are presented as relative fold change values versus non-treated, control siRNA-transfected samples and normalised to *ACTB* (β-Actin) mRNA levels. n=4 independent experiments, mean ± SEM, *p<0.05 as measured by two-way ANOVA with Bonferroni *post-hoc* tests.

Together, these data confirm that the IKKε-mediated transcriptional regulation of serine biosynthesis enzymes in doxycycline-treated Flp-In 293 HA-IKKε cells is in fact a consequence of the effect of IKKε on the mitochondria. As determined earlier, expression of IKKε blocks the uptake of glucose-derived carbon into the TCA cycle and, as a consequence, mitochondrial OXPHOS is impaired. The inhibition of mitochondrial function is evidently sufficient to activate ATF4-mediated retrograde mitochondria-to-nucleus signalling, inducing transcriptional upregulation of the enzymes of the serine biosynthesis pathway.

5.5 ATF4 maintains serine biosynthesis enzyme expression in human breast cancer cell lines

As upregulation of the serine biosynthesis enzymes by HA-IKKε in Flp-In 293 cells was found to be mediated by ATF4, the role of this transcription factor in IKKε-mediated regulation of the enzymes in human breast cancer cell lines was also assessed.

Since mitochondrial dysfunction was found to be the driving force behind IKKε-mediated upregulation of *PHGDH*, *PSAT1* and *PSPH* in Flp-In 293 cells, it was hypothesised that the upregulation of the enzymes was occurring via a similar mechanism in breast cancer cell lines where the kinase also inhibited cellular oxygen consumption. Therefore, the effect of siRNA-mediated suppression of ATF4 on *PHGDH*, *PSAT1* and *PSPH* mRNA levels was investigated in ZR-75-1, T47D and MDA-MB-468 cell lines. These are cell lines where IKKε regulated the expression of one or more serine biosynthesis enzymes whilst also regulating OCR (see 4.1, 4.2 and 5.2), suggesting activation of ATF4 was responsible for the transcriptional upregulation of the enzymes in these cells. It was thus hypothesised that suppression of ATF4 in ZR-75-1, T47D and MDA-MB-468 cells would have the same effect on the expression of *PHGDH*, *PSAT1* and *PSPH* mRNA as suppression of IKKε did.

Breast cancer cell lines were transfected with a single *ATF4*-targeting siRNA oligo or a non-targeting control oligo for 72 hours, following which the effect of transcription factor knockdown on *PHGDH*, *PSAT1* and *PSPH* mRNA was assessed using qRT-PCR. These experiments were performed with the assistance of Miss Sheila Olendo Barasa, a master's degree student under supervision in the lab.

The effect of ATF4 suppression on the serine biosynthesis enzymes was much broader than the effect of IKKε suppression. Knockdown of ATF4 had a very general suppressive effect on all of the serine biosynthesis enzymes, significantly downregulating both *PHGDH* and *PSAT1* mRNA levels in ZR-75-1, T47D and MDA-MB-468 cells and *PSPH* in T47D cells (Figure 5.8 A). This is in contrast to the effect of IKKε knockdown in these cells, which primarily resulted in the significant downregulation of *PSAT1* mRNA with no consistent impact on *PHGDH* or *PSPH* mRNA (Figure 4.8). To ascertain whether this broad effect was limited to just the selected cell lines, the effect of siRNA-mediated suppression of ATF4 was validated in all of the other cell lines of the panel. Confirming what was seen in ZR-75-1, T47D and MDA-MB-468, ATF4 knockdown in the other breast cancer cell lines resulted in substantial downregulation of mRNA levels of all three serine

biosynthesis enzymes in all cell lines except Cal120 and HCC1143, where *PSPH* mRNA levels stayed mostly unaffected (see supplementary materials: Figure 7.2).

To determine whether this broad pattern of regulation would translate to the enzyme protein levels, western blotting was used to assess the effect of ATF4 knockdown on PHGDH, PSAT1 and PSPH protein levels in breast cancer cell lines. As before, this was primarily assessed in ZR-75-1, T47D and MDA-MB-468 cells, but this for this experiment, the effect of knockdown on the enzyme protein levels was also evaluated in MDA-MB-231, as the only PSAT1-expressing cell line where IKKε inhibited OCR but did not upregulate PSAT1, and HCC1143, as a cell line where IKKε regulated PSAT1 but had no effect on OCR. As with the qRT-PCR experiments, these experiments were performed with the assistance of Miss Sheila Olendo Barasa.

Akin to the findings at the mRNA level, ATF4 suppression broadly and consistently downregulated the protein levels of all three enzymes in all the cell lines tested, even in MDA-MB-231 and HCC1143 (Figure 5.8 B). Comparatively, suppression of IKKε led to a consistent reduction in PSAT1 protein levels in all PSAT1-expressing cell lines (except MDA-MB-231), but had no consistent effect on the other enzymes of the pathway (Figures 4.3 and 4.4). This reduction in PHGDH, PSAT1 and PSPH protein levels upon ATF4 knockdown was also validated in all other cell lines within the panel, further demonstrating the ubiquitous role of the transcription factor (see supplementary materials: Figure 7.3). Transcription factor knockdown was also assessed across the full panel of cell lines at the same time.

Together, these data confirm that ATF4 plays a much broader role in the regulation of PHGDH, PSAT1 and PSPH in breast cancer cell lines than IKKε does, and demonstrates ATF4's status as a master regulator of serine biosynthesis. In line with the fact that IKKε is just one of many factors capable of regulating ATF4 activity, it was unlikely that identical effects would be observed upon suppression of IKKε or ATF4. Indeed, these data highlight that IKKε's ability to regulate the serine biosynthesis enzymes in breast cancer cell lines is far more specific to PSAT1 than the ability of ATF4, and indicate that, as expected based on previous findings of the role of ATF4 in cancer[324,372,379], the transcription factor is likely frequently regulated independently of IKKε. Nevertheless, these data do confirm that ATF4 is an active regulator of the serine biosynthesis enzymes in the panel of breast cancer cell lines. This therefore maintains the possibility that, in cell lines where IKKε regulates mitochondrial function, the serine biosynthesis enzymes could theoretically be induced via the same ATF4-mediated retrograde signalling through which the kinase seems to regulate the enzymes in Flp-In 293 cells.

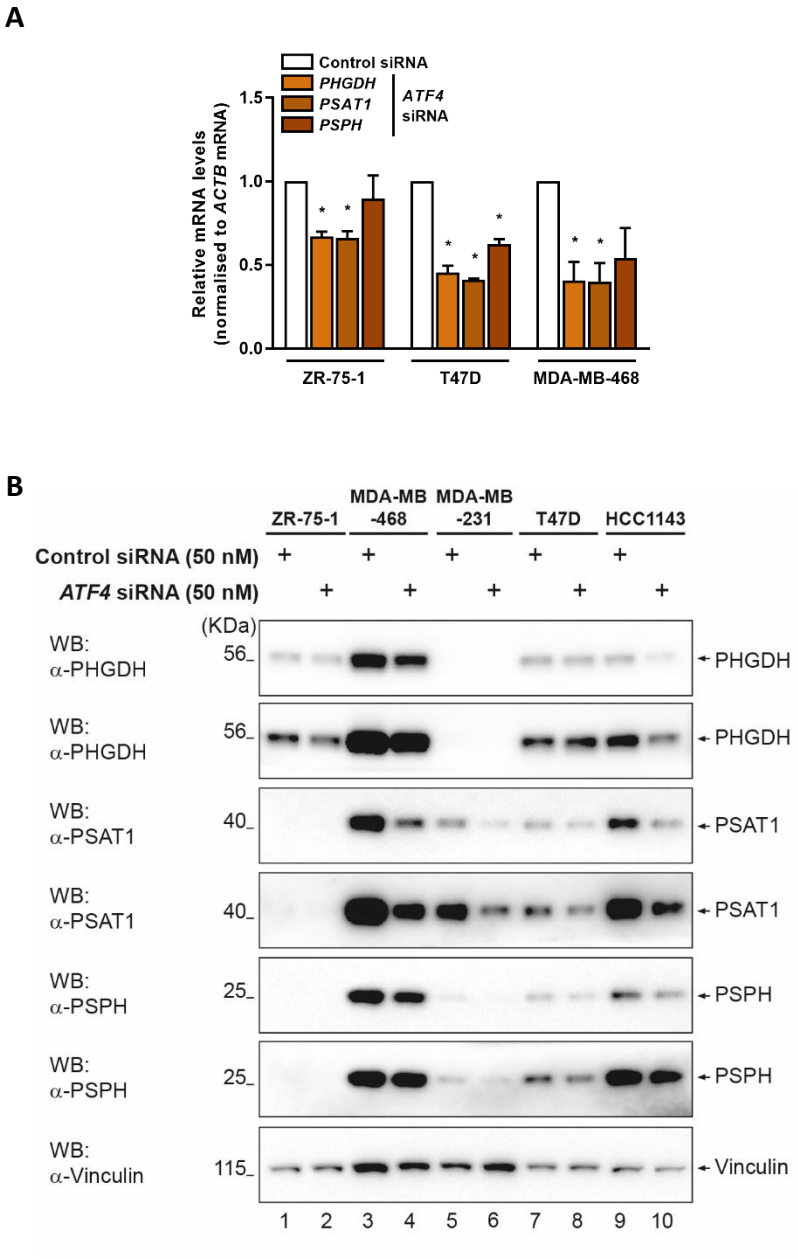

Figure 5.8 – ATF4 is an active master regulator of serine biosynthesis enzyme expression in human breast cancer cell lines. Indicated breast cancer cell lines were transfected with a single *ATF4*-targeting siRNA oligo or a non-targeting control oligo, at a final concentration of 50 nM for 72 hours. ATF4 suppression downregulated serine biosynthesis enzyme proteins and mRNA levels in all cell lines tested. **(A)** qRT-PCR analysis of *PHGDH*, *PSAT1* and *PSPH* mRNA levels in ZR-75-1, T47D and MDA-MB-468 breast cancer cell lines following ATF4 suppression. mRNA levels are presented as relative fold changes compared to control siRNA transfected cells and normalised to *ACTB* (β-Actin) mRNA levels. n=3 independent experiments, mean ± SEM, *p<0.05 as measured by one-sample t-test comparing fold change values to a hypothetical mean of 1.0. **(B)** Western blot analysis of PHGDH, PSAT1 and PSPH protein levels in ATF4 siRNA transfected ZR-75-1, MDA-MB-468, MDA-MB-231, T47D or HCC1143 breast cancer cells compared to cells transfected with control siRNA. Vinculin is shown as a loading control.

5.6 DCA inhibits IKKε-mediated upregulation of serine biosynthesis enzymes

As the IKKε-mediated regulation of serine biosynthesis enzymes in Flp-In 293 cells was found to be attributable to the mitochondrial dysfunction that results from the inhibition of pyruvate dehydrogenase and the corresponding reduction in the uptake of glucose-derived carbon to the mitochondria, it was questioned whether forced re-activation of pyruvate dehydrogenase would block the IKKε-mediated upregulation of serine biosynthesis enzymes. Treatment of Flp-In 293 HA-IKKε cells with DCA was previously found to be capable of preventing the mitochondrial inhibition induced by IKKε (see 5.2), so it was therefore hypothesised that if treatment with DCA reversed the mitochondrial inhibition, it would also prevent the IKKε-driven upregulation of the serine biosynthesis enzymes.

To test this hypothesis, Flp-In 293 HA-IKKε cells were plated and treated with doxycycline, DCA, or a combination of both doxycycline and DCA for 16 hours. This allowed induction of the kinase whilst activating mitochondrial uptake of glucose-derived carbon. Induction of *PSAT1* mRNA was subsequently assessed using qRT-PCR (Figure 5.9).

Surprisingly, it was found that treatment of Flp-In 293 HA-IKKε cells with DCA alone upregulated *PSAT1* mRNA similar to treatment of cells with doxycycline. This suggested that, instead of mitochondrial inhibition being required to activate ATF4, any modulation of mitochondrial function, positive or negative, might be sufficient to activate the retrograde signalling necessary to upregulate the serine biosynthesis enzymes. Importantly, the combination of DCA and doxycycline treatment had no synergistic effect on *PSAT1* mRNA levels. Instead, the level of induction that was observed with the combined treatment of Flp-In 293 HA-IKKε cells with doxycycline and DCA was similar to the level of induction observed when cells were treated with just doxycycline or DCA alone. This indicated that, when Flp-In 293 HA-IKKε cells were treated with DCA, the activation of pyruvate dehydrogenase was at least blocking IKKε-dependent increases in enzyme mRNA levels.

Since DCA alone upregulated *PSAT1* transcription, it was questioned whether the activation of pyruvate dehydrogenase was inducing the same retrograde mitochondria-to-nucleus signalling that IKKε does. Therefore, to address this, a western blot was performed to evaluate the protein levels of the ATF4 transcription factor, PHGDH, PSAT1 and PSPH in Flp-In 293 HA-GFP or Flp-In 293 HA-IKKε cells upon treatment with doxycycline, DCA, or a combination of both compounds for 16 hours (Figure 5.10 A). Subsequently, the protein levels of ATF4, PSAT1 and PSPH in these conditions were measured using densitometry quantification analysis (Figure 5.10 B-D).

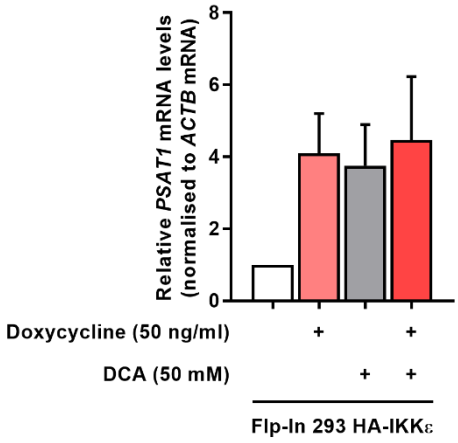

Figure 5.9 – DCA upregulates *PSAT1* mRNA levels independently but prevents further upregulation by IKKε. qRT-PCR analysis of *PSAT1* mRNA levels in Flp-In 293 HA-IKKε cells treated with 50 ng/ml doxycycline and 50 mM DCA as indicated for 16 hours. mRNA levels are presented as fold change values versus non-treated control samples and normalised to *ACTB* (β-Actin) mRNA levels. Doxycycline upregulated PSAT1 mRNA as expected but, surprisingly, so did DCA treatment alone. No additive effect was observed in the combined treatment, indicating that the mechanism by which the two treatments induced *PSAT1* mRNA were the same. Since DCA acts by modulation of mitochondrial activity, this supports the hypothesis that IKKε upregulates *PSAT1* mRNA via regulation of the mitochondria as well. n=5 independent experiments, mean ± SEM.

Western blotting quantification revealed that DCA treatment induced upregulation of ATF4 protein levels, similar to induction of IKKε (Figure 5.10 B). This therefore indicated that DCA was activating ATF4-mediated mitochondria-to-nucleus retrograde signalling, as predicted based on the observed upregulation of *PSAT1* mRNA levels following treatment of Flp-In 293 HA-IKKε cells with DCA. This seemingly confirmed the hypothesis that, rather than only being activated upon inhibition of the mitochondria, such signalling could potentially be activated by any modulation of mitochondrial function.

Importantly, in support of the findings at the *PSAT1* mRNA level, although induction of IKKε upregulated PSAT1 and PSPH proteins as expected, induction of the kinase alongside DCA treatment had no additive effect of upregulation of the enzymes (Figure 5.10 C and D). If DCA was regulating expression of the serine biosynthesis enzymes through modulation of mitochondrial activity and IKKε was inducing the enzymes via an alternate mechanism, then it would be expected that a combination of DCA treatment and doxycycline-mediated HA-IKKε induction would have a synergistic effect on the expression of the serine biosynthesis enzymes. In this instance, mRNA and protein levels would be expected to rise to a greater level following combined DCA and doxycycline treatment than with either treatment individually. That there is no additive effect at either the mRNA or protein level indicates that both treatments trigger the upregulation of the enzymes via the same mechanism. These data therefore further support the

hypothesis that regulation of *PHGDH*, *PSAT1* and *PSPH* by HA-IKKε in Flp-In 293 cells occurs via regulation of mitochondrial activity and induction of ATF4.

Interestingly, despite a lack of additive effect of the combination treatment on the serine biosynthesis enzymes, an additive effect was observed in terms of ATF4 protein induction. This suggests that the induction of ATF4 by IKKε and by DCA occur via different mechanisms. Importantly, the increased levels of ATF4 in the combined doxycycline and DCA-treated cells do not appear to reflect an increase in transcriptional activity compared to the single treatment conditions. Indeed, despite higher levels of ATF4 protein, the expression of the serine biosynthesis enzymes is not further increased, suggesting that the ATF4 protein induced by the combined treatment is less active overall than the protein induced by induction of IKKε or treatment with DCA alone. Potential explanations for this are discussed later (see 5.7).

Together, these data support the hypothesis that the transcriptional upregulation of serine biosynthesis enzymes is a direct consequence of mitochondrial inhibition by the kinase, mediated by the inhibition of the conversion of pyruvate to acetyl-CoA, the resulting mitochondrial dysfunction and the consequential activation of ATF4-mediated gene transcription.

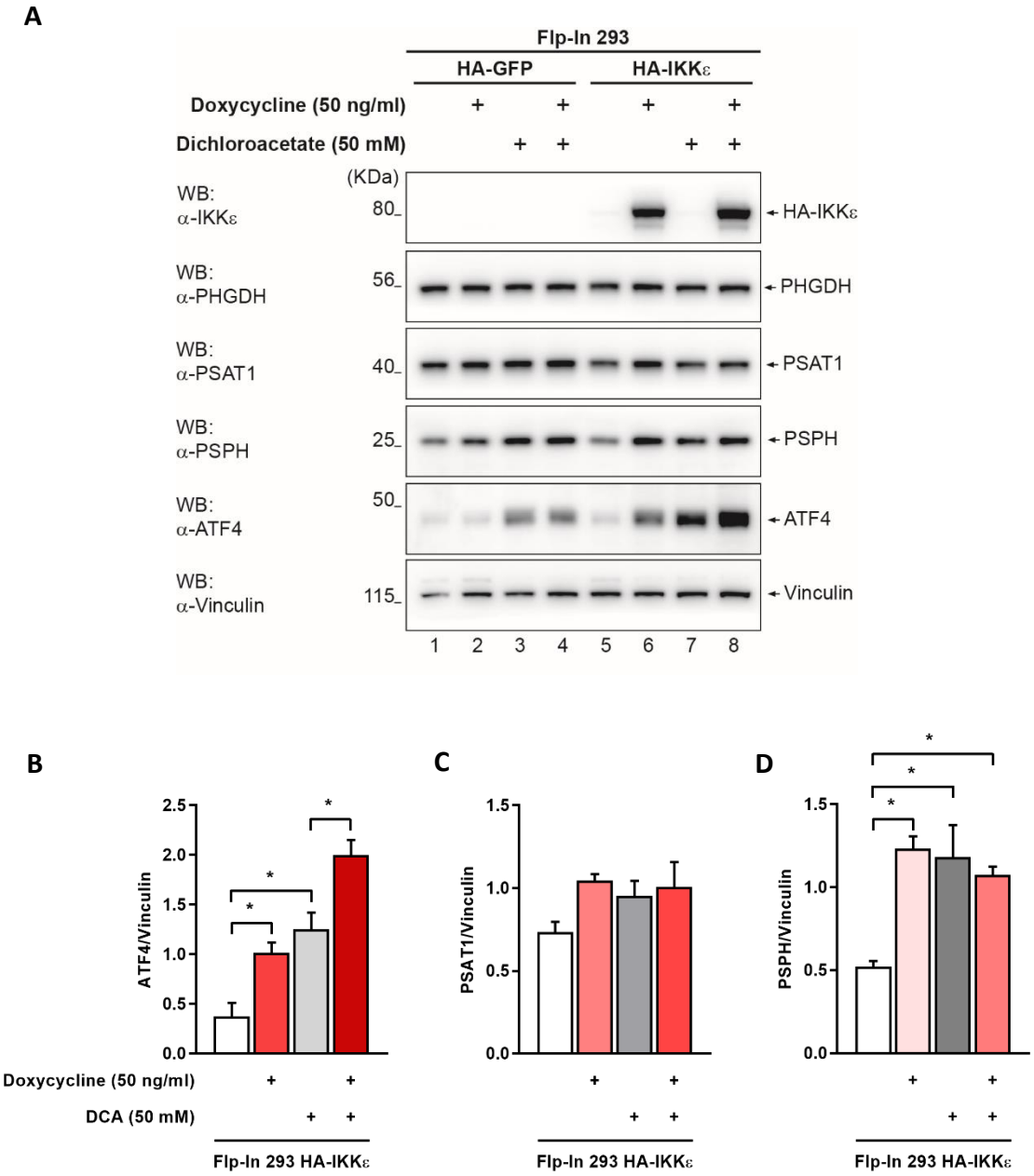

Figure 5.10 – DCA upregulates serine biosynthesis enzyme protein levels independently, but prevents further upregulation of PSAT1 and PSPH by IKKε. (A) Western blot analysis of the effect of doxycycline and DCA on PHGDH, PSAT1, PSPH and ATF4 protein levels in Flp-In 293 HA-GFP or Flp-In 293 HA-IKKε cells. Cells were treated with 50 ng/ml doxycycline and 50 mM DCA as indicated for 16 hours. Vinculin is shown as a loading control. **(B-D)** Densitometry quantification analysis of ATF4 **(B)**, PSAT1 **(C)** and PSPH **(D)** protein levels in Flp-In 293 HA-IKKε cells. Protein densitometry per sample was quantified as a percentage of total protein densitometry and normalised to vinculin. Treatment of cells with doxycycline upregulated ATF4, PSAT1 and PSPH protein levels in agreement with previous findings. DCA also upregulated PSAT1 and PSPH protein levels alone, supporting findings at the *PSAT1* mRNA level. This is potentially attributable to a significant increase in ATF4 protein levels upon DCA treatment. No additive effect of doxycycline and DCA was observed with PSAT1 and PSPH proteins, but ATF4 protein levels were significantly higher in the cells treated with both compounds combined than in cells treated with either compound individually. n=4 independent experiments, mean ± SEM, *p<0.05 as measured by two-way ANOVA with Bonferroni *post-hoc* tests.

5.7 Discussion

After chapter 4 described the finding that induction of HA-IKKε in Flp-In 293 cells not only upregulated PSAT1 protein levels, as was expected based on the hypothesis that IKKε-dependent phosphorylation would increase protein stability, but also upregulated PSPH protein levels and transcriptionally upregulated *PHGDH*, *PSAT1* and *PSPH*, it became clear that the kinase was broadly affecting the activity of the serine biosynthesis pathway via a mechanism independent of substrate phosphorylation. Importantly, this mechanism was also shown to be independent of "classical" IKKε signalling activities, with NF-κB subunit p65 and IFNβ signalling factor IRF3 both being found to be inessential for the transcriptional upregulation of serine biosynthesis enzymes. It was therefore evident that the kinase was regulating the serine biosynthesis pathway transcriptionally via a previously uncharacterised mechanism. This chapter described the efforts undergone to identify this mechanism and a transcription factor responsible for the upregulation of *PHGDH*, *PSAT1* and *PSPH* expression.

IKKε-mediated mitochondrial inhibition

Recent studies have described the interaction of IKKε with the mitochondria to varying degrees, either promoting the association of secondary enzymes with the organelle[106], or interacting with it itself[373]. As labelled metabolite analysis had identified an IKKε-dependent decrease in the incorporation of glucose-derived carbon in TCA cycle metabolites, it was hypothesised that the kinase was actively inhibiting mitochondrial function in addition to the upregulation of serine biosynthesis activity.

It was found that IKKε inhibited the uptake of glucose-derived carbon in the mitochondria by blocking the conversion of pyruvate to acetyl-CoA, which in turn decreased mitochondrial OXPHOS. What currently remains unclear, is how exactly the kinase exerts its effect on the mitochondria. Considering that the inhibitory effect can be blocked by treatment with DCA, which induces activation of pyruvate dehydrogenase, the regulation of mitochondrial function by IKKε appears to involve the inhibition of pyruvate dehydrogenase activity. In favour of this hypothesis, PDHA1, a central subunit of the pyruvate dehydrogenase complex, was identified as part of the phosphoproteomic described in chapter 3 (see 3.3) to be significantly more phosphorylated in IKKε-expressing cells at serine residue Ser232. Phosphorylation of PDHA1 at Ser232 is known to be a site linked with inactivity of the enzyme[375,376], therefore suggesting that IKKε inhibits pyruvate dehydrogenase complex activity through inducting the phosphorylation of PDHA1. Overlap of IKKε's optimal phosphorylation recognition motif[197] with the amino acid

sequence surrounding the PDHA1 Ser232 phosphosite showed little sequence matching, indicating that PDHA1 is unlikely to be a direct substrate of the kinase.

Pyruvate dehydrogenase complex subunits are typically phosphorylated by members of the pyruvate dehydrogenase kinase family, and PDHA1 Ser232 is usually phosphorylated by pyruvate dehydrogenase kinase 1 (PDK1), though it is possible other kinases could also phosphorylate the residue[376]. Considering that IKKε's inhibition of the mitochondria was completely rescued by treatment of cells with DCA, a PDK1 inhibitor[380], it is possible that the kinase inhibits PDHA1 by activating PDK1. PDK1 is known to be activated by high levels of acetyl-CoA and ATP and, conversely, be inhibited by high levels of pyruvate and ADP, but has also been shown to be activated by phosphorylation at threonine residue Thr338 by mitochondria-translocated phosphoglycerate kinase 1 (PGK1)[381] and at residue Thr346 by AKT[382]. PGK1 can be translocated to the mitochondria by EGFR activation, which has been shown to activate IKKε in non-small cell lung cancer[383] and it is well characterised that IKKε can activate AKT directly[384]. Therefore, whilst PDK1 phosphorylation was unable to be detected in IKKε-expressing cells via the phosphoproteomic analysis, it is possible that IKKε could activate PDK1 by indirectly inducing Thr338 or Thr346 phosphorylation, thereby promoting the inactivation of PDHA1 and pyruvate dehydrogenase activity. It would therefore be worth evaluating the effect of IKKε on the activity of PDK1 in future work to either confirm or deny this hypothesis.

IKKε significantly regulated mitochondrial activity and OCR in Flp-In 293 cells and in 6 out of 9 breast cancer cell lines tested and, although not significant, a trend of upregulated OCR upon IKKε suppression in the SUM44 cell line was also observed. Only the Cal120 and HCC1143 cell lines showed no change in OCR upon siRNA-mediated suppression of IKKε. When trying to consider why these cell lines might be different, the activation of IKKε canonical signalling was first considered. As reported in chapter 4 (see 4.4 and Figure 4.13) none of the breast cancer cell lines tested demonstrated phosphorylation of IRF3 suggesting that, in accordance with findings that signalling via IRF3 is dispensable for IKKε-driven transformation[195], IFNβ signalling was inactivated in breast cancer. Cal120 and HCC1143 did show evidence of STAT1 phosphorylation, but so did MDA-MB-453 and MDA-MB-468 which feature OCR regulation upon IKKε suppression, suggesting that the absence of OCR regulation in Cal120 and HCC1143 is independent of STAT1 phosphorylation. Similarly, p65 was phosphorylated in all breast cancer cell lines tested with the exception of SUM44 indicating that presence or absence of NF-κB activation would not explain the differential regulation of OCR between cell lines either. Together this demonstrated that the regulation of OCR in breast cancer cell lines was independent of activation of canonical IKKε signalling. Interestingly, assessing the expression of established IKKε adaptor proteins in the

panel of breast cancer cell lines offered some insight as to why Cal120 and HCC1143 might be different to the other cell lines tested. In HA-IKKε-expressing Flp-In 293 cells, evaluation of adaptor protein expression indicated that IKKε adaptor proteins SINTBAD, NAP1 and TANK were potentially phosphorylated, suggesting that these proteins might be acting as IKKε adaptors for signalling in those cells (see 4.3 and Figure 4.10). When looking at the expression profile of kinase adaptors in the breast cancer cell line panel, Cal120 and HCC1143 cells were found to express little to no SINTBAD, NAP1 or TANK, whereas the rest of the cell lines expressed all of the known adaptors (Figure 4.11). If the IKKε-mediated signalling that results in regulation of OCR requires the formation of a protein complex of IKKε with SINTBAD, NAP1 and/or TANK adaptor proteins, then the absence of these proteins in Cal120 and HCC1143 could explain the lack of effect of the kinase on OCR in these cell lines. It would therefore be interesting to test whether reintroduction of these adaptor proteins to Cal120 and HCC1143 cells could recapitulate IKKε's effect on OCR.

IKKε-mediated regulation of serine biosynthesis via ATF4

Irrespective of the mechanism, induction of IKKε in Flp-In 293 cells inhibits mitochondrial oxygen consumption and by extension mitochondrial activity by inhibiting the conversion of pyruvate to acetyl-CoA, thereby blocking the entry of glucose-derived carbon to the TCA cycle. Mitochondrial dysfunction has been shown to induce the activation of ATF4, which is believed to be a response to altered cellular redox balance and the oxidative stress that occurs upon the inhibition of the electron transport chain[362]. Indeed, the transcription factor has been shown to be crucial for the cellular response to redox imbalance. It is also activated as part of the integrated stress response to endoplasmic reticulum stress, specifically enhancing glutathione synthesis to maintain intracellular redox balance[385]. Disruption in mitochondrial activity induces an ATF4-mediated mitochondria-to-nucleus retrograde signalling axis that upregulates the serine biosynthesis enzymes[362]. The upregulated serine biosynthesis enzymes help maintain redox balance by providing cells with a mechanism by which glucose-derived carbon can be easily diverted into one-carbon metabolism in order to support production of reduced glutathione[320]. Accordingly, data described in this chapter demonstrated that IKKε upregulated enzymes of the serine biosynthesis pathway in an ATF4-dependent manner, indicating the mitochondrial dysfunction induced by the kinase is responsible for the transcriptional upregulation of the serine biosynthesis enzymes.

This demonstrates a much broader mechanism of regulation of serine biosynthesis by IKKε than the specific upregulation of PSAT1 through IKKε-dependent phosphorylation. With this in mind, and to further discuss a point debated in chapter 4 (see 4.8), it is necessary to consider the

relative importance of PSAT1 phosphorylation versus transcriptional regulation in the overall IKKε-driven upregulation of enzyme expression and serine biosynthesis. The data presented here in Figure 5.7 supports the conclusion reached in the previous chapter that transcriptional regulation supersedes protein phosphorylation for overall upregulation of the PSAT1 protein. Whilst suppression of ATF4 in Flp-In 293 HA-IKKε cells completely abolished IKKε's ability to upregulate PSAT1 and PSPH protein levels and *PHGDH*, *PSAT1* and *PSPH* mRNA levels, IKKε kinase activity was unaffected in these conditions, meaning PSAT1 should still be phosphorylated in an IKKε-dependent manner. The fact that no protein upregulation was observed therefore indicates that transcriptional regulation of the enzymes plays a more significant role in the regulation of total protein levels and that the primary regulation of serine biosynthesis by IKKε comes from the ATF4-mediated upregulation of gene transcription as a consequence of mitochondrial inhibition.

Interestingly, the data presented in Figure 5.9 and Figure 5.10 in this chapter seemingly indicate that ATF4 signalling is not solely induced by mitochondrial dysfunction, but rather by any modulation of mitochondrial activity. Treatment of both Flp-In 293 HA-GFP and Flp-In 293 HA-IKKε cells with mitochondrial activator DCA for 16 hours not only induced upregulation of ATF4 protein levels themselves, but also *PSAT1* mRNA levels, indicating that ATF4 transcriptional activity is induced as well. Notably, it is not clear what effect DCA treatment has on redox homeostasis within the cells over the course of 16 hours of treatment. One possible explanation is that, rather than ATF4 being activated by an increase in mitochondrial activity, DCA is unexpectedly inducing a mitochondrial stress response despite enhancing mitochondrial activity. DCA treatment and the resulting hyperactivation of the pyruvate dehydrogenase complex might lead to rapid depletion of available fuel and therefore lead to the activation of a stress response and ATF4 due to a lack of mitochondrial substrate availability. This could explain why the transcription factor was activated when, theoretically, mitochondrial function was maximised. Measuring intracellular ROS levels upon treatment of cells with DCA could help determine the effect of the compound on redox balance and ascertain how DCA is activating ATF4 signalling.

The data in Figure 5.10 and Figure 5.7 indicate that induction of HA-IKKε in Flp-In 293 HA-IKKε also upregulates ATF4 protein levels. Whilst total protein levels of a transcription factor do not necessarily correlate with its transcriptional activity, this at least indicated that the transcription factor was regulated by the kinase and the characteristic increase in *PHGDH*, *PSAT1* and *PSPH* mRNA levels upon induction of the kinase obviously supports the hypothesis that IKKε increases ATF4 transcriptional activity. Interestingly, whilst this data represents the first explicit

connection of IKKε with the induction of ATF4 transcriptional activity, the transcription factor has been indirectly linked with IKKε before, when it was found that the activation of TLR4 signalling in human monocytes, following treatment with LPS, activated ATF4 and induced its nuclear translocation, wherein it promoted the induction and secretion of key inflammatory cytokines like IL-6[386]. Whilst this activity was determined to be mediated by the TLR4-recruitment of MyD88 and the resulting activation of c-Jun N-terminal kinases (JNK), activation of toll-like receptors by LPS stimulation also induces IKKε and IKKε signalling activities[88]. The data presented here therefore represent a secondary mechanism by which activation of innate immune response signalling can promote the activation of ATF4 and, considering the role the transcription factor plays in serine biosynthesis, further emphasises the link between immunity and metabolism.

Intriguingly, our data suggest that IKKε might induce ATF4 protein levels via two alternative mechanisms. The evidence presented in this chapter demonstrates the induction of ATF4 protein levels and transcriptional activity as a result of IKKε-mediated mitochondrial inhibition. However, as previously discussed, DCA also induced ATF4 protein upregulation and transcriptional activity. Given DCA's mechanism of action, DCA-mediated upregulation of ATF4 almost certainly occurs via mitochondrial regulation. It would be expected then, that if induction of IKKε and treatment of cells with DCA both induced ATF4 transcriptional activity via regulation of mitochondrial activity, a combination of DCA treatment and induction of IKKε would have no additive effect on ATF4 protein levels or transcriptional activity. As Figure 5.9 and Figure 5.10 demonstrate, even though ATF4 transcriptional activity in combined DCA treatment and IKKε induction conditions appears equal, ATF4 protein levels are surprisingly significantly higher in cells treated with DCA and doxycycline together compared to cells treated with either compound individually. This additive effect on ATF4 protein levels suggests that induction of IKKε and treatment of cells with DCA induce ATF4 protein levels via two distinct mechanisms. This suggests that, although IKKε may upregulate ATF4 protein levels via regulation of mitochondrial activity, the kinase might also upregulate the transcription factor via a second, undetermined mechanism. It does however appear that if this hypothesis is proven correct, this unknown second mechanism is insufficient to induce activation of ATF4. As mentioned above, despite the additive effect on total protein levels, no additive effect on *PSAT1* mRNA or PSAT1 and PSPH protein was observed, suggesting ATF4 transcriptional activity was equal between conditions. This suggests that the additional ATF4 protein induced in the combined treatment condition was transcriptionally inactive. Further investigation would be necessary to identify whether IKKε was capable of upregulating ATF4 this way or not, but this would help explain why

when IKKε is induced but the mitochondria remain active, the protein levels of ATF4 can increase without an observable increase in transcription of the serine biosynthesis enzymes.

IKKε and ATF4 in breast cancer

Whilst the role of ATF4 in IKKε-mediated upregulation of serine biosynthesis enzymes in Flp-In 293 cells appears conclusive, the role that the transcription factor plays in IKKε's regulation of the enzymes in breast cancer remains less clear. The data presented in Figure 5.8 and supplementary Figures 7.1 and 7.2 demonstrate that the transcription factor is indeed maintaining expression of the enzymes in breast cancer and previous studies have also demonstrated a role for it in both lung cancer and breast cancer[324,387]. However, the consistency with which ATF4 was found to be regulating the enzymes across multiple cell lines demonstrated that it is activated far more broadly in breast cancer cell lines than just in cell lines where IKKε regulates the mitochondria. Based on the findings in Flp-In 293 HA-IKKε cells it would be expected that, wherever IKKε regulated cellular OCR, the expression of all three serine biosynthesis enzymes would be downregulated upon suppression of the kinase. Instead, in certain cell lines, suppression of the kinase only regulated *PSAT1* mRNA and PSAT1 protein levels (Figure 4.4 and Figure 4.8). Additionally, *PSAT1* mRNA was also regulated in the HCC1143 cell line, where no effect on OCR was observed. Contrastingly, ATF4 suppression frequently downregulated mRNA and protein levels of all three enzymes in all of the breast cancer cell lines tested. Active ATF4 signalling in the panel of breast cancer cell lines suggests that IKKε does have the potential to act via ATF4 in cell lines where it regulates the mitochondria, but perhaps instead of IKKε expression leading to an induction of ATF4 activity as is seen in Flp-In 293 cells, which would lead to the regulation of all three serine biosynthesis enzymes, IKKε might just modify pre-existing ATF4 transcriptional activity in breast cancer cells to upregulate PSAT1, similar to how the kinase modifies STAT1 transcriptional activity to promote the activation of additional IKKε-dependent STAT1 target genes[99]. This is consistent with the fact that ATF4 is not solely regulated by IKK in cancer, with the kinase instead being just one of many factors known to induce ATF4 transcriptional activity[324,372,379].

It is also likely that IKKε-mediated regulation of serine biosynthesis enzymes across numerous breast cancer cell lines cannot be simply pinned down to the activity of a single transcription factor. Whilst the role of NF-κB and IFNβ signalling in the regulation of serine biosynthesis in Flp-In 293 cells has been shown to be minimal, the roles of these signalling pathways and resulting transcriptional programmes should be properly assessed in breast cancer cell lines. Whilst preliminary experiments have indicated a similarly inessential role for NF-κB signalling in breast

cancer cells, the role of IRF3 and IFNβ signalling is less clear, sometimes appearing to be partially involved, sometimes appearing to have no role. Given that experiments investigating the activation of IFNβ signalling in the breast cancer cell line panel indicated that the pathway is inactive in the cell lines used, it seems contradictory to suggest that siRNA-mediated suppression of IRF3 would have any impact on these cell lines, but further validation of the roles of both the NF-κB and IFNβ signalling pathways may allow some clarification of the role that ATF4 and other IKKε downstream targets play in the regulation of serine biosynthesis in breast cancer.

Activation of alternative transcription factors by IKKε in breast cancer

It would also be worth further exploring additional transcription factors that might be involved in breast cancer cell lines. Whilst the promoter analysis that was performed and described at the start of this chapter (see 5.1) highlighted other transcription factors that might regulate *PHGDH*, *PSAT1* and *PSPH* together, none of these potential factors were deemed to be suitable candidates for the regulation of the enzymes in Flp-In 293 cells. Links between IKKε and C/EBPβ, C/EBPδ, SP1 and EP300 all required the involvement of NF-κB subunit p65 or IFNβ-signalling factor IRF3[364-368]. Since neither NF-κB or IFNβ signalling were found to be necessary for the regulation of the serine biosynthesis enzymes by IKKε in Flp-In 293 cells, the role of these transcription factors in those cells was considered to likely be minor compared to ATF4. However, given the lack of clarity of the role of ATF4 in the regulation of serine biosynthesis enzymes by IKKε in breast cancer cells, it would be prudent to revisit some of these other potential transcription factors to re-assess their involvement. Additionally, in light of findings in pancreatic cancer demonstrating that IKKε-driven metabolic reprogramming in a Myc-dependent manner promotes proliferation[189] the involvement of c-Myc in IKKε-mediated upregulation of *PHGDH*, *PSAT1* and *PSPH* mRNA should also be examined.

Concluding remarks

To summarise, the data presented in this final results chapter expands on the findings from the labelled metabolite analysis experiment described in chapter 3, detailing how IKKε regulates mitochondrial function to promote a phenotype akin to aerobic glycolysis within Flp-In 293 cells and breast cancer cell lines. Following the findings regarding the inessential nature of IKKε's canonical NF-κB and IFNβ signalling activities in the kinases ability to enhance serine biosynthesis, it was found that IKKε's inhibitory effect on the mitochondria induced the activation of an ATF4-mediated retrograde mitochondria-to-nucleus signalling axis which in turn upregulates *PHGDH*, *PSAT1* and *PSPH*, demonstrating how the kinases effect on anabolic serine metabolism is a key consequence of its effect on the mitochondria.

Chapter 6

Discussion

6.1 Overview

Although identified as a major breast cancer oncogene in 2007, amplified and overexpressed in around 30% of human breast cancer cases[195], therapeutic options for targeting and treating IKKε-driven cancers remain limited by the fact that the primary mechanism of oncogenesis in breast cancer is attributed to aberrant activation of NF-κB. The impracticalities of targeting NF-κB signalling for therapeutic intervention in cancer have been discussed previously (see 1.3.3.1) and given the ubiquitous nature of NF-κB signalling in tissues, prolonged inhibition can have severely detrimental effects, including immunosuppression. Furthermore, attempts to develop NF-κB inhibitors for cancer therapy have thus far yielded few promising compounds. This means that in order to effectively treat IKKε-driven breast cancers, a greater understanding of the full scope of IKKε's oncogenic potential is required and alternative therapeutic targets must be identified so that the cancer can be treated without inhibiting NF-κB.

IKKε regulates cellular metabolism in breast cancer cells

Cellular metabolism is frequently and dramatically altered in most human cancers, with classical oxidative phosphorylation being suppressed in favour of aerobic glycolysis. In aerobic glycolysis, glycolytic rates and lactate production are substantially increased and glucose-derived carbon is diverted away from the mitochondria and the TCA cycle in favour of its utilisation in biosynthetic pathways. Various oncogenes and cancer promoting processes have previously been shown to be master regulators of cellular metabolism. For example; c-Myc is known to increase the expression of glucose transporters and glycolytic enzymes, increase lactate production and promote glutaminolysis[264-266,268,269]; HIF1α has been shown to upregulate glucose transporters, glycolytic enzymes and lactate dehydrogenase to enhance glycolysis and also upregulates PDK to inhibit mitochondrial metabolism[222-224,250-253] and finally; tumour suppressor p53 reportedly inhibits glycolysis by suppressing glucose transporters and upregulating TP53-induced glycolysis and apoptosis regulator (TIGAR), which subsequently suppresses fructose-2,6-bisphosphate protein levels and lowers glycolytic rate, and promotes OXPHOS by upregulating synthesis of cytochrome c oxidase 2 (SCO2) to increase cytochrome c oxidase protein[293,294,388]. The data presented in this thesis propose IKKε, a central player in the innate immune response[86-88,99,102] and transforming kinase, involved in the oncogenic activation of NF-κB signalling[192,194,195], as an oncogenic kinase capable of regulating cellular metabolism via target protein phosphorylation equally as substantially as major oncogenic transcription factors like c-Myc and HIF1α, which modulate metabolism via regulation of gene expression.

Previous work has identified roles for other members of the IKK family of kinases in the regulation of cellular metabolism. As per p53's role as a tumour suppressor and a suppressor of aerobic glycolysis, loss of p53 was found to increase kinase activities of IKKα and IKKβ and, as a result, increase NF-κB activation, which subsequently increased the rate of glycolysis and upregulated glucose transporter GLUT3[389]. Similarly, in B-cell lymphomas, IKKβ-driven activation of NF-κB was found to be required for the localisation of glucose transporter GLUT1 to the cell surface[390], further demonstrating the promotion of glycolytic metabolism by IKKβ and the activation of the canonical NF-κB pathway. Conversely, IKK and NF-κB activation can also promote oxidative phosphorylation over aerobic glycolysis. Recent studies have demonstrated that IKKβ facilitates cancer cell adaptation to glutamine depravation, phosphorylating and inhibiting PFKFB3 to down-regulate aerobic glycolysis when glutamine sources are limited[391] and, in muscle cells, IKKα has been reported to promote oxidative metabolism by inducing mitochondrial biogenesis via the activation of the non-canonical NF-κB pathway and upregulation of peroxisome proliferator-activated receptor-gamma (PPAR-γ) coactivator-1 beta (PGC1-β)[392]. Along a similar line, p65-mediated NF-κB signalling in MEFs has been reported to actively promote oxidative phosphorylation in response to glucose starvation by transcriptionally upregulating the expression of SCO2 via p53[393]. These studies demonstrate how the activation of canonical IKK's and NF-κB signalling can both promote or limit an aerobic glycolysis phenotype in a context-dependent manner.

Whilst the regulation of aerobic glycolysis by canonical IKK's has been shown to involve positive or negative regulation, recent years have also the non-canonical IKK's TBK1 and IKKε increasingly linked to the regulation of cellular metabolism specifically through the promotion of aerobic glycolysis. TBK1 has been shown to be involved in the metabolic response to obesity. Both IKKε and TBK1 kinase activity is significantly increased in the adipocytes of obese mice on high fat diets[104] and mice with an adipocyte-specific knockout of TBK1 failed to become obese when fed with a high-fat diet due to substantial increases in oxygen consumption and energy expenditure in white adipose tissue. This indicated that TBK1 suppressed mitochondrial respiration. Indeed, the kinase has subsequently been shown to suppress mitochondrial respiration by inactivating AMPK-induced mitochondrial biogenesis[394]. Although IKKε and TBK1 share some overlap in phosphorylation targets and signalling activities, it remains to be seen whether the regulation of AMPK activity is unique to TBK1's functional capacity or not. More relevant to this project therefore, is how previous work has demonstrated a strong link between IKKε and aerobic glycolysis.

In dendritic cells, proper cellular activation was shown to require an early metabolic switch to aerobic glycolysis that is dependent on TBK1 and IKKε. In this context, the kinases promote the association of glycolytic enzyme hexokinase II with the mitochondria, facilitating direct use of mitochondrial ATP and thereby enhancing the glycolytic rate[106]. Furthermore, whilst it remains to be seen whether TBK1 would regulate cellular metabolism in a cancer setting, IKKε has been clearly shown to promote aerobic glycolysis in pancreatic cancer, where the kinase induces an AKT/GSK3β/c-Myc phosphorylation cascade that culminates in nuclear translocation of c-Myc and c-Myc-dependent induction of an aerobic glycolysis phenotype[189]. The non-canonical IKK's have therefore been shown to regulate cellular metabolism via multiple distinct mechanisms. IKKε in particular promotes aerobic glycolysis both via direct interaction with a glycolytic enzyme and indirectly via the activation of oncogenic c-Myc, demonstrating that the kinase regulates cellular metabolism in a versatile manner. Intriguingly, the data presented within this thesis propose a novel alternate mechanism of IKKε-mediated metabolic regulation. This thesis presents a 2-pronged mechanism, through which the kinase inhibits mitochondrial respiratory activity and induces cellular biosynthetic activity to promote an aerobic glycolysis-like metabolic state.

Labelled metabolite analysis was used to identify key IKKε-dependent changes in the metabolic state of HEK cells and breast cancer cells. It was found that the kinase had 2 major effects. Specifically, a reduction in the incorporation of glucose-derived carbon in TCA-cycle metabolites and an increase in the incorporation of glucose-derived carbon in amino-acids serine and glycine. This indicated that expression of IKKε was inhibiting classical respiratory mitochondrial function and increasing the *de novo* biosynthesis of serine. Using a combination of oroboros, seahorse extracellular flux analysis and TMRM mitochondrial staining in cells, the kinase was confirmed to reduce mitochondrial respiration. A phosphoproteomic analysis, identifying significantly more or less phosphorylated proteins in IKKε-expressing HEK cells, was performed to identify a potential mechanism for IKKε's metabolic regulation. This data suggested the kinase was inhibiting mitochondrial activity by indirectly inducing an inhibitory phosphorylation of PDHA1, the central gatekeeper for the entry of glucose-derived carbon into the TCA cycle. Treatment of IKKε-expressing cells with DCA, a pyruvate dehydrogenase activator, successfully reversed IKKε-induced mitochondrial inhibition, thereby confirming that the kinase inhibits the mitochondrial uptake of glucose-derived carbon via the blocking of pyruvate dehydrogenase activity. Given that IKKε is capable of directly activating AKT[384], which has been shown in previous work to be able to phosphorylate and activate PDK1 to indirectly inhibit pyruvate dehydrogenase[382], it is likely that the kinase inhibits pyruvate dehydrogenase via the

phosphorylation and activation of AKT. This hypothesis requires further experimental validation, but regardless, even though IKKε has previously been linked to the regulation of oxygen consumption in high-fat diet fed mice[103], in cancer, previous links between IKKε and metabolism have primarily demonstrated the focussed effect of the kinase on a single glycolytic enzyme[106], or demonstrated that the kinase regulated glycolysis independently of any effect on mitochondrial oxygen consumption[189]. This makes the data presented here the first indication in cancer cells that, in addition to enhancing glycolytic reactions, the kinase also promotes aerobic glycolysis by suppressing mitochondrial respiration.

IKKε upregulates serine biosynthesis via mitochondrial inhibition and ATF4

The other major effect of IKKε on the intracellular metabolic state that was observed during the labelled metabolite analysis was a significant increase in the incorporation of glucose-derived carbon in amino acids serine and glycine, indicative of an increase in serine biosynthesis from glucose. The serine biosynthesis pathway branches from the mainline glycolytic reactions as PHGDH converts 3-phosphoglycerate to phosphohydroxypyruvate. PSAT1 and PSPH subsequently catalyse the addition of an amino group and the removal of a phospho group respectively to produce serine (Figure 1.9). Previous work has identified PHGDH as an oncogene, subject to a recurrent genetic amplification in ER- breast cancer and melanoma[304,305]. Accordingly, the serine biosynthesis pathway is of particular importance for rapidly proliferating cells and cancer cells for two key reasons.

Firstly, in aerobic glycolysis, glucose-derived carbon is diverted from the mitochondria, preventing replenishment of TCA cycle intermediates and OXPHOS. Since, in addition to its role in mitochondrial respiration, the TCA cycle is important for various biosynthetic reactions, it is beneficial for proliferating cells to maintain TCA intermediate levels in the absence of glucose-derived carbon incorporation. The primary alternate source of carbon in many cancers is glutamine. The second reaction of the serine biosynthesis pathway, catalysed by PSAT1, transfers an amino group from glutamine-derived glutamate to phosphohydroxypyruvate leaving TCA intermediate α-KG and producing phosphoserine respectively. The production of α-KG via the PSAT1 reaction means that serine biosynthesis can therefore contribute to the fuelling of the TCA cycle with glutamine-derived carbon. Indeed, the serine biosynthesis pathway has been shown to account for a substantial proportion of glutamine anaplerosis (TCA cycle refuelling) in breast cancer[305]. Secondly, the break-down of serine to glycine involves the donation of one-carbon units to one-carbon metabolism, which is well known to help maintain redox balance and supports nucleotide production and DNA methylation in cancer[320,322,323,395].

Outside of the genetic amplification of PHGDH, multiple transcription factors, proteins and enzymes have been shown to induce upregulation of the serine biosynthesis enzymes in cancer including c-Myc[315], ATF4[324,387], p73[325] and PKCζ[326]. Expression of IKKε in HEK and breast cancer cells was found to transcriptionally upregulate serine biosynthesis enzymes, accounting for the increased serine biosynthesis observed in cells expressing the kinase. Therefore, a transcription factor that induced the enzymes in response to IKKε expression was sought. Mitochondrial dysfunction has been previously reported to induce ATF4-mediated retrograde mitochondria-to-nucleus signalling to upregulate serine biosynthesis enzymes[362] and accordingly, the upregulation of serine biosynthesis enzymes was found to require ATF4 expression, indicating that the enzymes were regulated as a consequence of mitochondrial inhibition.

ATF4 has been repeatedly linked to activation of the serine biosynthesis enzymes in previous work. The transcription factor has been shown to be upregulated by NRF2[396], which itself can be activated downstream of K-Ras to induce ATF4[397]. Accordingly, in lung cancer, activation of NRF2 has been shown to induce transcriptional upregulation of the serine biosynthesis enzymes via activation of ATF4[324]. Similarly, in ER- breast cancer, ATF4 was recently reported to be essential for the transcriptional upregulation of PSAT1, which was necessary to drive cell proliferation through the regulation of cyclin D1 protein stability[387], although, in this setting, the mechanism behind the activation of ATF4 was not characterised. This thesis presents the hypothesis that IKKε is an indirect activator of ATF4 in breast cancer, demonstrating a previously uncharacterised mechanism of ATF4 activation and presenting the kinase as a novel regulator of serine biosynthesis enzyme expression in cancer.

PSAT1 is phosphorylated in an IKKε-dependent manner to promote protein stability

During the phosphoproteomic analysis of differentially phosphorylated proteins in IKKε-expressing cells, PSAT1 was also identified as significantly more phosphorylated at serine residue Ser331. The enzyme was subsequently confirmed to be phosphorylated at this residue in a manner dependent on IKKε using an *in vitro* kinase assay. Studies using high-throughput techniques to analyse the phosphoproteome of cells had previously reported phosphorylation of the residue[345-347,349,398-402], but no known previous work had characterised the relevance of the phosphosite for enzyme function. Generating a model of mutated PSAT1 proteins in which residue Ser331 was mutated to mimic (S>E, phosphomimic) or inhibit phosphorylation (S>A, phosphomutant)[326], possible effects of PSAT1 Ser331 phosphorylation on enzyme function were assessed, examining serine production, protein-protein interactions and protein stability. The Ser331 residue was found to be an important residue for protein stability, with subtle but

measurable differences in protein stability being observed between phosphomimic and phosphomutant PSAT1 using pulse chase and induction time course assays. This study marks, not only the first investigation into the functional relevance of phosphorylation of the PSAT1 Ser331 residue, but also represents the first known characterisation of any post-translational modification that regulates the function of the enzyme. As overexpression of PSAT1 has been shown to promote cancer growth[309,310,312], it seems likely that phosphorylation of PSAT1 by IKKε could represent a mechanism by which the kinase can increase PSAT1 protein levels and promote cell proliferation. Whilst a lack of validated tools for detection of PSAT1 phosphorylation have limited the chance to detect phosphorylation in breast cancer cell lines, the data presented here provides some evidence for this phosphorylation event occurring. Specifically, suppression of IKKε in the Cal120 breast cancer cell line led to a significant decrease in PSAT1 protein levels without a corresponding decrease in mRNA levels, indicating post-translational regulation. IKKε-dependent phosphorylation of PSAT1 Ser331 modifying protein stability therefore represents a strong candidate to explain increased protein levels in the presence of IKKε-expression in this cell line. Additionally, whilst phosphorylation of PSAT1 Ser331 in breast cancer cell lines was not directly examined as part of this work, previous work has detected phosphorylation of the enzyme in human breast cancer tissues, confirming that it occurs in a cancer context. Analysis of the phosphoproteome of 77 breast cancer samples spanning different disease subtypes found greater PSAT1 Ser331 phosphorylation in samples coming from a triple-negative breast tumour[345]. This indicates that the phosphorylation of PSAT1 Ser331 correlates with a more aggressive tumour subtype and worse prognosis, implying that phosphorylation of this residue in an IKKε-dependent manner might contribute to poor disease outcome.

Together, the data presented in this thesis present IKKε as a master regulator of cell metabolism in both HEK cells and breast cancer cell lines, capable of inducing profound changes to intracellular metabolic networks. Through the inhibition of mitochondrial respiration, attributable to indirect inhibition of pyruvate dehydrogenase activity; the upregulation of serine biosynthesis activity, as a consequence of mitochondrial inhibition and finally; the direct regulation of PSAT1 phosphorylation to promote protein stability, the kinase induces a metabolic state in which mitochondrial OXPHOS is reduced, whilst biosynthetic processes are increased. This combined with an increase in lactate secretion as observed by labelled metabolite analysis indicate that IKKε shifts the metabolic state of cells towards a phenotype that bears striking similarities to classical aerobic glycolysis, presenting metabolic regulation as a possible mechanism of IKKε-driven oncogenesis in breast cancer.

6.2 Future work

One of the main ambitions of this project was to identify an NF-κB-independent mechanism of IKKε-mediated oncogenesis. In this thesis, the effect of the kinase on intracellular metabolism has been investigated and a dual mechanism of upregulation of serine biosynthesis activity has been described. The serine biosynthesis pathway is a particularly important pathway in cancers for reasons extensively described throughout this thesis, but a major outstanding question from this project is whether the mechanism described here, where IKKε regulates mitochondrial metabolism and consequently serine biosynthesis, is in fact of importance to the progression of human breast cancer or not. Specifically, it remains to be seen whether the IKKε-mediated upregulation of serine biosynthesis forms a part of IKKε's oncogenic potential and important future experiments are required to begin to answer this question.

Identifying IKKε-mediated regulation of PSAT1 in human cancer cases

In breast cancer cell lines, the primary effect of IKKε expression on the serine biosynthesis pathway appears to focus on the upregulation of PSAT1, either transcriptionally or post-translationally. This is of particular interest as, unlike PHGDH, the enzyme has not previously been indicated to be the subject of genetic amplification, instead relying on the action of other oncogenic transcription factors like Myc to be upregulated in cancer. In fact, when performing preliminary immunohistochemical staining of PSAT1 in patient tissue, it seems that overall expression of PSAT1 in any breast tissue is rather low, which is also supported by data in the human protein atlas, which shows no detectable PSAT1 expression in normal breast tissue and relatively low expression in breast cancer tissue compared to other cancer types[403,404]. It is possible that in cancer tissues where expression is higher, IKKε is responsible.

Notably, the same preliminary immunohistochemical staining indicates that PSAT1 expression in breast tumour tissue might correlate with inflammation of the tumour microenvironment. Considering that data from Dr Ewa Wilcz-Villega, a fellow lab member, demonstrates induction of IKKε in MCF-10A cells by macrophage conditioned medium, this could indicate that induction of IKKε in breast tissue as a result of inflammation represents a mechanism by which the serine biosynthesis enzyme is upregulated in human breast tissue. Similarly, it is worth acknowledging that bioinformatic biclustering analysis of the METABRIC dataset[405], kindly performed by Professor Gyorgy Szabadkai (University College London, London, UK), revealed that PSAT1 expression correlated with IKKε expression when stratifying tumours based on mitochondrial gene expression. This indicated that in tumours where mitochondrial function is impaired, IKKε

might be regulating the expression of the enzyme. Indeed, further work must be done to evaluate the link between IKKε and PSAT1 in patients. The aforementioned immunohistochemical staining of PSAT1 is a good place to start in this regard, as staining the same tissue samples for IKKε will allow identification of the presence of any correlation between the kinase and PSAT1 within the tissues. Furthermore, applying similar sample stratifications and biclustering analysis to other large cancer gene expression datasets, such as the breast cancer dataset within The Cancer Genome Atlas (TCGA)[406,407], would be prudent, to help try and identify a link between IKKε and the enzyme in larger numbers of patients.

Identifying a function for IKKε-mediated regulation of serine biosynthesis in cancer

PSAT1 has previously been found to be important for breast cancer progression both as part of the serine biosynthesis pathway and as an independent enzyme. For example, as has been previously discussed, the aminotransferase reaction that PSAT1 catalyses during its primary function in serine biosynthesis is beneficial to cancer cells as it provides a mechanism for glutamine anaplerosis of the TCA cycle. This allows cells to replenish TCA intermediates in the absence of glucose-derived carbon entry and allows the continuation of the biosynthetic reactions that use TCA metabolites as precursors. Accordingly, many cancers rely on the utilisation of glutamine to refuel TCA cycle intermediates[227] and exhibit glutamine addiction and susceptibility to glutaminolysis inhibition[234,235]. Indeed, although the overall contribution of PSAT1 to TCA cycle anaplerosis remains open for debate, findings from Possemato *et al.* have demonstrated that, in breast cancer cell lines where PHGDH is genetically amplified, suppression of PHGDH has little impact on intracellular serine levels, but does significantly impair the production of α-KG from glutamine[305], which indicates that the contribution of PSAT1 to anaplerosis is not an insubstantial one. Whilst labelled metabolite analysis was performed in IKKε-expressing cells using ^{13}C-labelled glucose and ^{15}N-labelled nitrogen, these experiments have been unable to provide substantial information regarding the contribution of glutamine-derived carbon to the TCA cycle in the presence of IKKε. In order to properly address the effect that the kinase has on glutamine TCA anaplerosis, it would be important to perform labelled metabolite analysis using ^{13}C-labelled glutamine, as this would allow measurement of the incorporation of glutamine-derived carbon into TCA cycle intermediates.

Upregulation of serine biosynthesis also allows cells to overcome a major obstacle that arises as tumour size increases. As a tumour expands beyond the limits of oxygen perfusion from the existing vasculature, hypoxic regions begin to emerge. Whilst induction of hypoxia is well established to be beneficial for tumour cells, promoting aerobic glycolysis and inducing other

pro-proliferative factors like VEGF (see 1.4.3.1), hypoxic conditions can have adverse effects on tumour cells, specifically through the induction of oxidative stress and redox imbalance. In hypoxia, oxygen is unavailable as a terminal electron acceptor of the electron transport chain in the mitochondria. As a result, electrons in the chain will form reactive oxygen species (ROS)[408] that can induce cell death if left unaddressed. Induction of HIF1 transcriptional activity promotes the activation of genes that assist in the detoxification of ROS. One such example of these genes is SHMT2[320], the mitochondrial isoform of SHMT that catalyses the breakdown of serine to glycine. Serine catabolism actively supports cells at risk of ROS associated toxicity, as its conversion to glycine involves the removal of a one-carbon unit. This one-carbon unit is donated to one-carbon metabolism and directly contributes to the production of NADPH to support the reduction of glutathione to help detoxify ROS. Accordingly, suppression of SHMT2, thereby inhibiting serine catabolism has been reported to induce cell death in hypoxic neuroblastoma cell lines and reduce xenograft tumour formation *in vivo*[320]. As IKKε has been shown to upregulate serine biosynthesis and, specifically, the flux of glucose-derived carbon towards serine, it stands to reason that increases in synthesised serine by the kinase can benefit breast cancer progression by increasing the flux of glucose-derived carbon into the one-carbon pool.

From a non-serine biosynthesis stand-point, the enzyme has been shown to enhance cell proliferation through the activation of GSK-3β and subsequent stabilisation of cyclin D1 to drive cell cycle progression in both non-small cell lung cancer and ER- breast cancer[310,387]. Therefore, the upregulation of PSAT1 by IKKε could, at least theoretically, directly support cell growth in aerobic glycolysis like-conditions. The lack of basal PSAT1 expression initially suggests the MDA-MB-453 PSAT1 cell line model would be useful for investigating the role of the enzyme and its IKKε-dependent phosphorylation in the regulation of cyclin D1 protein stability in breast cancer. However, as has already been discussed, the lack of basal expression of PSAT1 might prevent any proliferative effect of the enzyme being detected in this context (see 3.10). Therefore, to evaluate the effect that IKKε could have on PSAT1's ability to regulate cyclin D1 stability, it would be more useful to begin by examining the effect of modulation of kinase expression on cyclin D1 protein levels in both Flp-In 293 cells and breast cancer cell lines, particularly in ZR-75-1 and T47D breast cancer cells, where siRNA-mediated suppression of IKKε is known to both significantly reduce proliferative rates (see 3.1.2) and PSAT1 expression (see 4.1 and 4.2).

Considering the ways that serine biosynthesis and specifically PSAT1 upregulation can therefore directly contribute to cancer progression, it certainly seems unlikely that IKKε would consistently upregulate PSAT1 in breast cancer cell lines without it providing any growth advantage to those cells. From a broader perspective than the possible investigative paths mentioned above, it

would first be useful to address the importance of PSAT1 in the growth of IKKε-expressing breast cancers, using siRNA to suppress enzyme expression and evaluating the effects on proliferation using the IncuCyte. This would help to identify which of these cell lines are dependent on PSAT1 for proliferation and therefore indicate whether upregulation of the enzyme by IKKε could be supporting their growth or not. Further to this, the importance of PSAT1 in transformation and tumour formation could also be assessed, using the doxycycline-inducible MDA-MB-453 PSAT1 mutant cell lines to examine the importance of PSAT1 in anchorage independent growth via a soft agar colony formation assay, or in tumour formation via a xenograft mouse model. It is worth keeping in mind however, that MDA-MB-453 cells are already transformed independently of PSAT1. Therefore, an alternative, perhaps more appropriate approach to investigate the role of PSAT1 in transformation might be to ectopically express the enzyme in untransformed breast epithelial cell line MCF-10A. Previous experiments have demonstrated that ectopic expression of PHGDH in MCF-10A is sufficient to induce transformed characteristics in the cells when grown in 3D cultures[304]. It would be interesting to evaluate the effect of PSAT1 expression in MCF-10A cells using a similar model. Additionally, introduction of both wt and S>A or S>E PSAT1 mutant variants into MCF-10A cells might also allow evaluation of the importance of the PSAT1 Ser331 phosphosite in transformation.

Alternatively, the HA1E-M model could be utilised to assess the role of the serine biosynthesis enzymes in IKKε-mediated transformation. When characterising IKKε as a transforming kinase, Boehm *et al.* used HA1E-M cells expressing a myristoylated form of IKKε (myr-IKKε) in a soft agar colony formation assay. They found that cells expressing myr-IKKε formed significantly more and larger colonies than cells expressing an empty vector[195]. Whilst the HA1E-M F-IKKε cells used within this project failed to show any significant regulation of the serine biosynthesis enzymes by the kinase, this was concluded to be a result of an inactive kinase within those cells. Therefore, it is possible that the constitutively active IKKε variant in the HA1E-M myr-IKKε cell line would exhibit kinase-mediated regulation of the serine biosynthesis enzymes. Should this be the case, the soft agar colony formation assay could be repeated whilst using siRNA, shRNA or even CRISPR/Cas9 technology to suppress PSAT1 expression. This would therefore allow evaluation of the importance of the enzyme and *de novo* serine synthesis in IKKε-mediated transformation.

Considering the main function of the serine biosynthesis pathway is to synthesise serine, it would also be interesting to investigate how modulation of IKKε expression would affect the ability of cell lines to grow in serine-free medium. Cell lines like MDA-MB-468 demonstrate both an IKKε-dependent regulation of the expression of serine biosynthesis enzymes and an ability to

maintain more or less equivalent growth rate in whole medium and serine-free medium. Evaluation of how suppression of IKKε would impact the ability of such cell lines to grow in serine deprived conditions would indicate whether the regulation of the pathway by the kinase would provide cells with a greater ability to tolerate nutrient-depleted conditions common to the regions of tumours with poor vasculature. In line with the SBPs ability to protect against redox imbalance, it would also be beneficial to evaluate levels of ROS in IKKε-expressing Flp-In 293 cells or breast cancer cells where a kinase-dependent reduction in OCR is observed. This would help determine whether inhibition of the mitochondria by IKKε is sufficient to induce redox imbalance. Following this, measuring ROS levels whilst suppressing PSAT1 could help demonstrate whether the regulation of serine biosynthesis levels protected breast cancer cells from oxidative stress induced by IKKε-mediated inhibition of the mitochondria.

Whilst it may prove difficult to untangle the involvement of IKKε-mediated regulation of serine biosynthesis from the other mechanisms by which the kinase has already been demonstrated to support cell growth (see 1.3.3) such experiments could at least begin to indicate whether the regulation of metabolism is simply a side effect of IKKε expression in cancer, or is a driving force of disease progression in its own right.

Does regulation of serine biosynthesis contribute to other functions of IKKε?

It would also be beneficial to investigate potential roles for the pathway in other known functions of the kinase without cancer in mind. For instance, it has been previously mentioned how regulation of metabolism by the kinase is crucial for the activation of dendritic cells[106]. Even though the mechanism of metabolic regulation in dendritic cells appears to be different to the one described here, it is worth questioning whether the kinase still regulates serine biosynthesis in this context and, if so, what role the pathway might play in the process of antigen presentation.

Furthermore, is the pathway important for the primary function of the kinase in the activation of the innate immune response? Findings detailed in chapter 4 demonstrated that activation of IRF3 and IFNβ signalling is dispensable for the regulation of serine biosynthesis enzymes by the kinase, but it would be interesting to investigate whether the enzymes themselves are important for the proper activation of IFNβ signalling. Excitingly, preliminary data as offered some indication that serine biosynthesis might be important for endocrine IFNβ signalling. An experiment was performed in which conditioned medium was collected from doxycycline-treated Flp-In 293 HA-IKKε cells in which siRNA was used to suppress PSAT1. The conditioned medium was then applied to T47D cells and the resulting activation of IFNβ signalling was

evaluated via western blotting (see supplementary materials: Figure 7.4). Medium from Flp-In 293 HA-IKKε cells where PSAT1 was present induced activation of the JAK/STAT signalling pathway, a key downstream pathway in IFNβ signalling to a greater extent than medium from cells where PSAT1 had been suppressed, as measured by western blot analysis of STAT1 Tyr701 phosphorylation. This indicates that the serine biosynthesis pathway is important for proper secretion of IFNβ from cells upon the activation of innate immune signalling and suggests a role for the pathway in IKKε-mediated cytokine secretion. It is possible that the role of serine in protein and nucleotide production makes the serine biosynthesis pathway important for initial cytokine production, but the exact reason for this phenotype remains to be determined. Irrespectively, this finding raises fascinating questions with potentially wide-reaching implications. Is the serine biosynthesis pathway important for all mechanisms of cytokine secretion? Would suppression of the pathway limit the effectiveness of an immune response? Further investigation would be prudent to better clarify the role of the pathway in cytokine production and secretion to help to begin to answer such questions.

6.3 Therapeutic implications

Should upregulation of serine biosynthesis be found to be important for IKKε-driven oncogenesis, it presents a handful of exciting potential therapeutic targets.

Glutaminase inhibitors

Focussing on the fact that elevated serine biosynthesis could facilitate glutamine anaplerosis in the face of IKKε's inhibitory effect on mitochondrial utilisation of glucose-derived carbon, it would be unsurprising if IKKε-expressing cells were using glutamine to a greater extent and were dependent on it for the replenishment of TCA cycle metabolites. Glutamine consumption could be easily measured in IKKε-expressing cells and future experiments can also examine the growth of these cells in glutamine-deprived medium to help to elucidate whether the kinase induces glutamine dependency in addition to inhibiting mitochondrial utilisation of glucose-derived carbon. Should a hypothesis of IKKε-mediated increased glutamine consumption and dependency be proven correct, this would suggest that cells expressing the kinase could be more susceptible to inhibition of glutaminolysis, using glutaminase inhibitors such as BPTES, which has previously shown efficacy in Myc-driven, glutamine-dependent tumours[409-412]; CB-839, which has demonstrated efficacy in triple negative breast cancer cell lines[413] and is currently in clinical trials; or recently described UPGL00004, which has been reported to exhibit greater stability than BPTES and CB-839 and has been demonstrated to inhibit the proliferation of triple negative breast cancer cell lines and suppress xenograft breast tumour formation in a mouse model[414,415].

If IKKε-driven cancers do indeed exhibit glutamine dependency, then inhibition of glutaminolysis through the targeted inhibition of glutaminase could be expected to be therapeutically effective. The sensitivity of IKKε-expressing cell lines to such an inhibitor could be easily assessed using a combination of the IncuCyte system and IC_{50} assays, which would help indicate the therapeutic potential of inhibiting glutaminolysis to target IKKε-driven cancer.

Importantly, the fact that glutaminase inhibitors like CB-839 and UPGL00004 have demonstrated efficacy in triple-negative breast cancer cell lines is particularly interesting[413,414]. This is the same subtype where it is indicated that PSAT1 Ser331 phosphorylation occurs to a greater extent[345]. Whilst data described in chapter 3 indicates that the phosphorylation of PSAT1 Ser331 has no discernible effect on its enzymatic activity, the possibility that, despite the findings of the flux analysis, phosphorylation of the enzyme can in fact still impact its activity has been extensively discussed, as has the possibility that the phosphorylation might alter substrate affinity (see 3.10). It is possible that phosphorylation of PSAT1 Ser331 improves its ability to metabolise

glutamate in some way. Should this be the case, this suggests that, in cancers where IKKε might be phosphorylating PSAT1, the kinase might be inducing glutamine dependency and such cancers would benefit from inhibition of glutaminolysis.

Whilst glutaminase inhibitors would successfully inhibit TCA cycle anaplerosis, the use of such compounds would not necessarily prevent the serine biosynthesis pathway from continuing to support tumour growth via its contribution to one-carbon metabolism. Therefore, rather than targeting glutaminolysis individually, targeting of the serine biosynthesis pathway as a whole would likely prove more successful, negatively impacting glutamine anaplerosis whilst simultaneously removing a major mechanism by which cells adapt to oxidative stress. The combined inhibition of these 2 major cancer-promoting processes could therefore potentially be highly effective.

PHGDH inhibitors

Several therapeutic strategies for the targeting of serine biosynthesis in cancer exist. Firstly, several groups have recently described the identification of novel PHGDH inhibitors. Mullarky *et al*. identified CBR-5884, from a screen of 800,000 compounds, as a non-competitive inhibitor of PHGDH and demonstrated both its ability to inhibit serine biosynthesis and its efficacy in inhibiting the proliferation of breast cancer cells with high serine biosynthesis activity[416]. Almost simultaneously, a separate study from Pacold *et al*. described the inhibitors NCT-502 and NCT-503. These inhibitors were shown to be effective at inhibiting serine biosynthesis both *in vitro* in breast cancer cell lines and *in vivo* in xenograft mouse models. Surprisingly, NCT-503 was found to not only impact the incorporation of glucose-derived carbon into the one-carbon pool, but also reduced the incorporation of carbon from exogenous serine as well, indicating that inhibition of the serine biosynthesis pathway also prevented the proper utilisation of exogenous serine[363]. Shortly following, a third study, from Wang *et al.* reported the discovery of PHGDH specific allosteric inhibitors PKUMDL-WQ-2101 and PKUMDL-WQ-2201, demonstrating strong efficacy of these compounds in PHGDH-dependent breast cancer cell lines like MDA-MB-468 and in xenograft mouse models using the same cell line[417].

These inhibitors stand as promising compounds both for the investigation of the role of the serine biosynthesis pathway in new contexts and for the treatment of cancers with upregulated serine biosynthesis activity. For example, CBR-5884 has been used to demonstrate the importance of serine biosynthesis in protecting Müller glial cells against oxidative stress[418] and NCT-503 has been used to reduce pulmonary fibrosis in an *in vivo* mouse model[419], demonstrating a previously uncharacterised role for the pathway in the retina and in lung tissue

scarring respectively. Furthermore, in clear cell renal cell carcinoma, where constitutive activation of HIF is an important part of the pathogenesis of the disease, PHGDH and serine biosynthesis has been shown to allow cells to overcome HIF2α inhibition and both NCT-503 and CBR-5884 have been demonstrated to reduce cellular proliferation and xenograft formation in clear cell renal cell carcinomas which are growing independently of HIF2α[420].

No inhibitors of either PSAT1 or PSPH have been described to date, possibly due to the fact that, compared to PHGDH, roles for PSAT1 and PSPH in cancer have only recently been identified, but also because, unlike production of NADH by PHGDH, PSAT1 and PSPH do not produce easily measurable by-products, which makes it difficult to measure the activity of these enzymes. Nevertheless, inhibition of PHGDH should sufficiently cut off the progression of serine biosynthesis at its earliest stage, thereby reducing substrate availability for PSAT1 and thus preventing it from contributing to glutaminolysis. Indeed, as previously mentioned, suppression of PHGDH expression has been shown to dramatically reduce the incorporation of glutamine-derived α-KG into the TCA cycle in cells with elevated serine biosynthesis activity[305], demonstrating how chemical inhibition of PHGDH could effectively inhibit glutamine anaplerosis.

However, whilst inhibition of serine production can block the contribution of glucose derived carbon to the one-carbon pool, this does not necessarily block the involvement of exogenous serine. Despite findings from Pacold *et al.* suggesting that inhibition of *de novo* serine synthesis can also reduce the donation of carbon derived from exogenous serine to the one-carbon pool[363], it is not clear whether this inhibition would be enough to completely diminish the redox balancing effect of serine for patient treatment. Therefore, strategies inhibiting serine catabolism must also be examined.

Dietary serine deprivation

To counter the involvement of exogenous serine, a serine and glycine-free diet has been proposed, designed to limit the SHMT-mediated conversion between the 2 amino acids. This strategy would obviously prove particularly effective in targeting cells lacking the ability to synthesise serine intracellularly, such as breast tumours like the one from which the MDA-MB-231 cell line was derived. These cells lack PHGDH expression and, as demonstrated in chapter 3, cannot survive in serine-free medium due to an inability to synthesise their own serine. A serine and glycine-free diet has been shown to be effective in p53-deficient xenograft tumour models, where removal of exogenous serine forces cells to rely on serine biosynthesis and lack of p53

prevents remodelling of metabolism to upregulate serine biosynthesis, thereby preventing cells from adapting to serine deprivation and triggering cell death as a result of oxidative stress[421].

Importantly however, deprivation of serine has also recently been shown to induce mitochondrial fragmentation attributable to disruption of mitochondrial fatty acid metabolism[422]. Whilst this experiment was performed in HCT-116 colon cancer cells, therefore demonstrating the potential efficacy of such a diet in cancer, it is currently unclear what effect serine deprivation would have on normal cells and whether the systemic nature of restricting serine in the diet would have potentially damaging off-target effects. Indeed, dietary serine deprivation has recently been shown to limit effector T-cell expansion in a mouse model infected by *Listeria monocytogenes*[423] indicating that a serine/glycine free diet might have a negative impact on a patient's immune capabilities. Furthermore, dietary intervention has also been shown to be less successful in circumstances where other factors can upregulate serine biosynthesis enzymes. For example, although efficacy has been observed in Myc-driven lymphomas, where serine biosynthesis enzymes could theoretically be upregulated, dietary restriction of serine and glycine was concurrently found to be less effective in K-Ras-driven pancreatic and intestinal mouse tumour models, where activation of K-Ras was explicitly shown to upregulate serine biosynthesis enzymes[322]. This calls into question the effectiveness of such a therapeutic regime in IKKε-driven breast cancers, where the kinase can upregulate serine biosynthesis enzymes and increase pathway activity.

In this circumstance, specifically blocking serine catabolism through the use of SHMT inhibitors may be a more suitable option. Along this line, several SHMT inhibitors have been characterised. Antifolate drug lometrexol has been found to inhibit the enzyme[424] and recent years have seen the emergence of small molecule inhibitors of both SHMT isoforms. In 2015, compounds capable of targeting the protozoan isoforms of the enzyme were described[425] and subsequently, human SHMT isoform inhibitors have been described using the protozoan inhibitors as a basis[426]. These compounds have been demonstrated to inhibit HCT-116 cell growth and were found to be particularly effective inhibitors of diffuse large B-cell lymphoma proliferation

Combining diet and inhibitor

Again, whilst these strategies targeting serine catabolism are promising, there is an issue. Whilst pharmaceutical inhibition of PHGDH with a small molecule inhibitor fails to account for the involvement of exogenous serine in tumour development, the removal of exogenous serine and inhibition of serine catabolism fail to account for the fact that unhindered serine biosynthesis can still contribute to glutamine anaplerosis. For this reason, it seems that the most effective

therapeutic strategy would involve a combination approach, in which a serine-free diet is maintained, depriving cells of exogenous serine and forcing them to rely on the serine biosynthesis pathway, whilst simultaneous treatment with a targeted inhibitor of PHGDH is administered to completely block *de novo* serine production within cells. This combined therapy should successfully prevent the donation of one-carbon units to redox balancing mechanisms, whilst also inhibiting glutamine anaplerosis. The resulting redox imbalance and reduction in TCA cycle biosynthetic activity should be sufficiently toxic in cancer cells.

Indeed, the efficacy of a combination of a serine/glycine free diet with metformin, an inhibitor of cellular anti-oxidant response, has already been evaluated and shown to have additive efficacy over either therapy alone[322], demonstrating how the effectiveness of a serine and glycine-free diet can be improved in combination with a secondary compound. It would be important to recognise that maintaining a serine-free diet would also put healthy cells into a state of dependency on *de novo* serine biosynthesis, therefore the delivery mechanism of the inhibitor drug should be carefully considered, as systemic delivery would likely result in substantial off target toxicity, but if that obstacle can be overcome, a combined therapy could prove to be a highly successful and useful tool for the targeting of both IKKε-driven tumours, as well as other tumours with elevated serine biosynthesis.

6.4 Concluding remarks

Ultimately, this thesis has taken the observation that IKKε regulates overall cellular metabolism and serine biosynthesis and identified a two-pronged regulatory mechanism by which the enzymes of the serine biosynthesis pathway can be regulated in breast cancer. Firstly, by direct substrate phosphorylation of PSAT1, the second pathway enzyme, to promote protein stability and possibly support proliferation and secondly, transcriptional upregulation of the enzymes by ATF4 following IKKε-mediated inhibition of the mitochondria. The importance of the serine biosynthesis pathway in cancer, particularly breast cancer, suggests that the upregulation of the pathway by IKKε might be a key part of IKKε's oncogenic activities. Whilst work remains to be done before conclusions can be properly drawn on this hypothesis, it is important to recognise that if IKKε-mediated regulation of serine biosynthesis is indeed important for IKKε-driven breast cancer progression, the fact that both regulatory mechanisms are independent of IKKε's canonical roles in NF-κB and IFNβ signalling promises to open up exciting new therapeutic options for the treatment of IKKε-driven breast cancer.

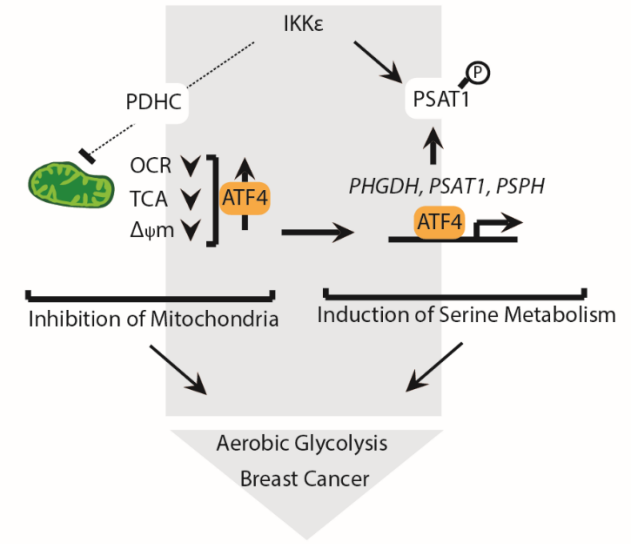

Figure 6.1 – Summary scheme. Schematic demonstrating the model proposed by this thesis, by which IKKε regulates intracellular metabolism. IKKε is proposed to directly inhibit mitochondrial function in cells in which it is expressed via inhibition of mitochondrial substrate uptake through the inhibitory phosphorylation of PDHA1. The subsequent inhibition of the pyruvate dehydrogenase complex (PDHC) reduces mitochondrial oxygen consumption, respiratory TCA cycle function and mitochondrial membrane potential. Consequently, a mitochondria-to-nucleus retrograde signalling pathway, mediated by the transcription factor ATF4, upregulates the expression of genes associated with the serine biosynthesis pathway to promote cell adaptation to mitochondrial inhibition. In parallel, IKKε directly regulates the serine biosynthesis pathway through the direct phosphorylation of PSAT1, leading to increased protein stability which potentially supports increased pathway activity. Together, these two parallel mechanisms serve to promote a cellular metabolic state akin to aerobic glycolysis (decreased mitochondrial respiration and increased biosynthesis in the form of serine production). This represents a previously uncharacterised function of the kinase and a potential mechanism by which the kinase could support breast cancer progression.

Chapter 7

Supplementary Materials

For IncuCyte-based growth tracking and measurement of cell confluency as a readout for cell proliferation, different processing definitions within the Zoom 2016B software (Essen Bioscience) were set up for each cell line. The parameters for each cell line's processing definition are detailed in Table 7.1

Table 7.1 – Processing definition parameters for the measurement of cell line confluency using the IncuCyte Zoom and Zoom 2016B software.

		Cleanup		Filters: Area (μm^2)		Filters: Eccentricity	
Cell Line	**Segmentation Adjustment**	**Hole Fill (μm^2)**	**Adjust Size (pixels)**	**Min**	**Max**	**Min**	**Max**
Flp-In 293	0.9	0	0	500	-	-	-
ZR-75-1	1.1	100	0	350	-	-	-
T47D	0.9	0	0	300	-	-	0.9915
MDA-MB-453	1.1	200	0	400	-	-	-
MDA-MB-468	1.4	50	-1	200	-	-	-
MDA-MB-231	0.8	0	0	300	-	-	0.9900
MCF7	1	0	0	300	-	-	0.9950
Cal120	1.2	0	0	300	-	-	0.9900
HCC1143	2	0	0	250	-	-	0.9900
SUM44	1.1	0	0	100	-	-	-

Heatmap and hierarchical clustering of significantly changing metabolite concentrations in doxycycline-treated Flp-In 293 HA-GFP and Flp-In 293 HA-IKKε cells or in *IKBKE*-targeting siRNA-transfected T47D cells as measured by labelled metabolite analysis using U-$^{13}C_6$-D-glucose are presented in Figures 3.5 and 3.6 respectively. The raw data from Dr Christian Frezza and Dr Sofia De Costa (MRC Cancer Unit, Cambridge, UK) and full details of total metabolite and ^{13}C- or ^{15}N-labelled metabolite concentrations detected in the experiments are provided in Table 7.2, included on the CD provided with this thesis.

Similarly, KEGGS pathway enrichment analysis of significantly differentially phosphorylated peptides in HA-IKKε-expressing Flp-In 293 cell clones compared to HA-GFP-expressing cells was presented in Figure 3.8 as a summary of the phosphoproteomic analysis and the selection of metabolic proteins with significantly altered phosphorylation status was presented in Table 3.2.

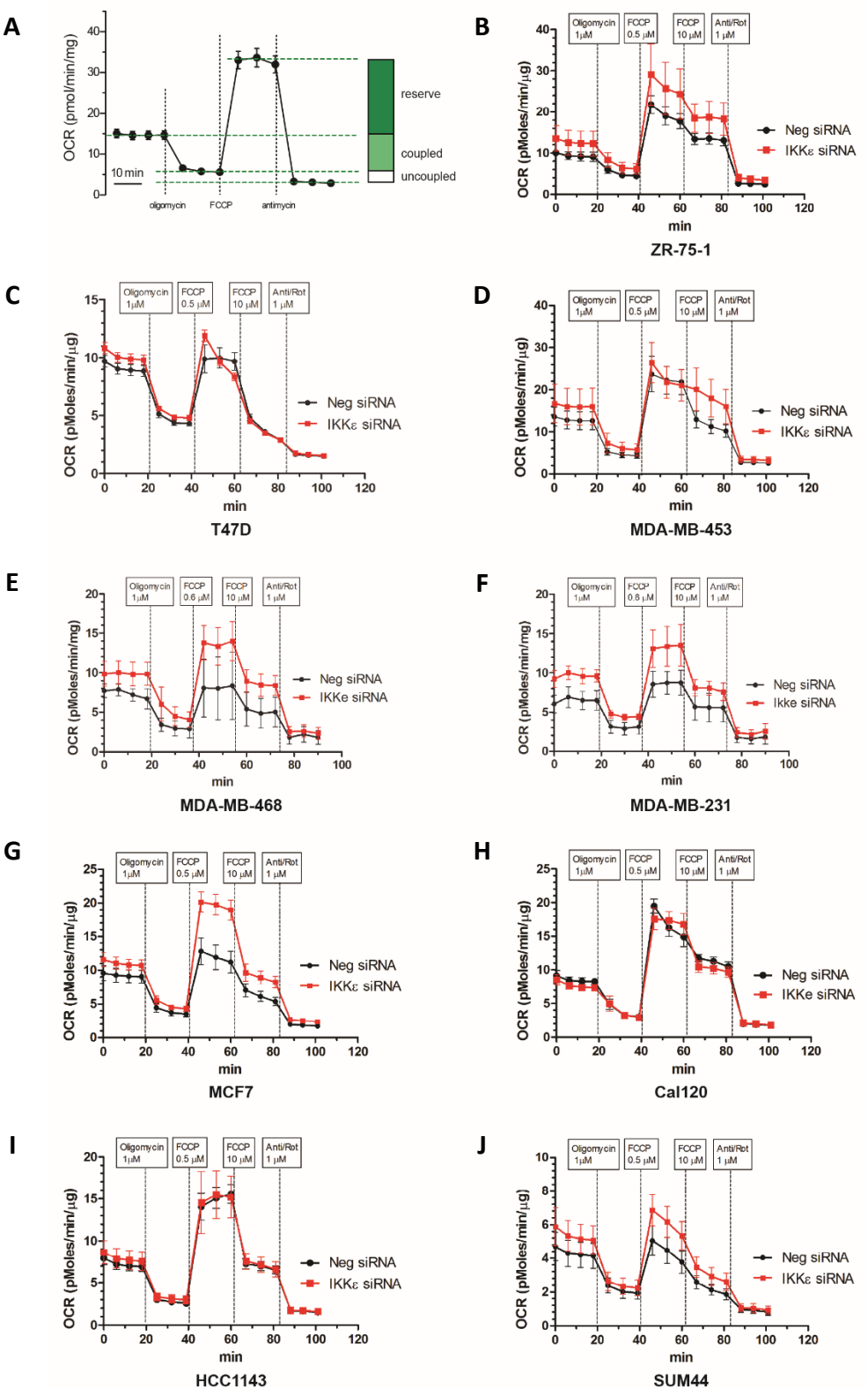

Figure 7.1 – Representative OCR curves demonstrating effect of siRNA-mediated suppression of IKKε on the mitochondrial respiratory profile of breast cancer cell lines. (A) Schematic demonstrating a breakdown of how the Seahorse XFe96 and addition of Oligomycin, FCCP, Rotenone and Antimycin A facilitates the characterisation of the mitochondrial respiratory profile of cellular samples, measuring basal, coupled, uncoupled and reserved respiratory capacities. **(B-J)** Representative OCR curves from single experiments examining the effect of siRNA-mediated suppression of IKKε on the mitochondrial respiratory profiles of ZR-75-1 (B), T47D (C), MDA-MB-453 (D), MDA-MB-468 (E), MDA-MB-231 (F), MCF7 (G), Cal120 (H), HCC1143 (I) and SUM44 (J) cells. Repeated OCR measurements were taken at 5-minute intervals, mean ± SD. Compiled data is presented in Figure 5.2, displaying data from at least 3 independent experiments per cell line.

The raw phosphoproteomic analysis data, detailing the log fold changes in phosphorylation of detected proteins and a heat map of significant changes, provided by Dr Pedro Cutillas and Dr Vinothini Rajeeve (Barts Cancer Institute, London, UK) following mass spectrometry analysis, is provided in Table 7.3 on the included CD.

The comparison of the relative enrichment of ^{15}N-serine and ^{15}N-glycine between Flp-In 293 cells expressing HA-PSAT1 wt, HA-PSAT1 S>A or HA-PSAT1 S>E was presented in Figure 3.18. The raw data from Dr Christian Frezza and Dr Sofia De Costa, detailing the peak area values from mass spectrometry analysis of total and labelled metabolites in three independent repeats are provided in Tables 7.4, 7.5 and 7.6 for each repeat. These tables are provided on the included CD. In each file, a sheet with the raw peak area data for each detected metabolite is accompanied by a sheet analysing the percentage of the total metabolite pool comprised by the detected ^{15}N-labelled ions for each metabolite.

In chapter 5, experiments were described in which the Seahorse XFe96 was used to measure IKKε-mediated changes in cellular oxygen consumption rate (OCR). The data presented in Figure 5.2 shows the effect of siRNA-mediated suppression of IKKε on basal OCR in a panel of 9 breast cancer cell lines. Analysis of cellular OCR using the Seahorse XFe96 uses various drugs to fully map the mitochondrial functional capacity; Oligomycin inhibits ATP synthase to characterise coupled oxygen consumption associated with mitochondrial ATP production, Carbonyl cyanide 4-(trifluoromethoxy)phenylhydrazone (FCCP) is an uncoupling agent that allows measurement of the maximum and reserve respiratory capacity of the mitochondria, and Rotenone and Antimycin A completely block the mitochondrial electron transport chain, thereby completely crashing mitochondrial respiratory capacity to determine the non-mitochondrial oxygen consumption of the cell (Figure 7.1 A). Although only the effect of IKKε on basal OCR was of interest for this project, the effect of the kinase on these other metabolic parameters was measured at the same time by Dr Ruoyan Xu. Representative Seahorse XFe96 OCR profile curves generated by Dr Xu are provided in Figure 7.1 B-J).

Also in chapter 5, *ATF4*-targeting siRNA was used to suppress expression of the transcription factor in Flp-In 293 cells and a panel of breast cancer cell lines (see 5.4 and 5.5). In breast cancer cell lines, suppression of ATF4 significantly downregulated *PHGDH* and *PSAT1* in ZR-75-1, T47D and MDA-MB-468 cell lines and *PSPH* in T47D cells (Figure 5.8 A). To validate that this broad effect was not limited to just the selected cell lines tested, the effect of ATF4 knockdown on serine biosynthesis enzyme transcription was validated in all other cell lines of the panel. As with ZR-75-1, T47D and MDA-MB-468, ATF4 knockdown substantially downregulated *PHGDH*, *PSAT1*

and *PSPH* mRNA levels in all other breast cancer cell lines within the panel with the exception of Cal120 and HCC1143, where *PSPH* mRNA levels were unaffected by knockdown of the transcription factor (Figure 7.2). The same broad effect was observed at the protein level in select cell lines (Figure 5.8 B) and this was also validated in all other cell lines of the panel. Similar to analysis of enzyme transcription, ATF4 knockdown consistently suppressed PHGDH, PSAT1 and PSPH proteins in every cell line (Figure 7.3). Together these data demonstrated ATF4's status as a master regulator of serine biosynthesis enzyme expression in breast cancer.

Notably, whilst effective knockdown of the transcription factor was validated via western blot in Flp-In 293 cells (Figure 5.7 A), attempts to validate the knockdown in the breast cancer cell line panel were less successful (Figure 7.3). Many cell lines appeared to give different unspecific bands when using the ATF4 antibody used in Flp-In 293 cells (Cell Signaling - #11815). A band corresponding to the size of band detected and validated in Flp-In 293 cells was detected in MDA-MB-453, MDA-MB-468 and MDA-MB-231 cells where *ATF4*-targeting siRNA effectively depleted the band intensity, confirming knockdown of the transcription factor, but other cell lines exhibited varying patterns of unspecific antibody binding, making it difficult to conclude on the effectiveness of knockdown in these contexts. qRT-PCR analysis of *ATF4* mRNA levels would help resolve this issue, but given that PHGDH, PSAT1 and PSPH are all confirmed downstream transcriptional targets of ATF4, corresponding suppression of the serine biosynthesis enzymes, which occurred in all cell lines transfected with *ATF4*-targeting siRNA was accepted as sufficient indication of effective suppression of the transcription factor in breast cancer cells.

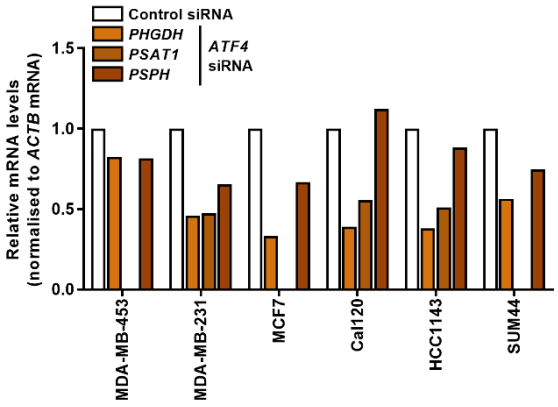

Figure 7.2 – siRNA-mediated ATF4 suppression broadly regulates serine biosynthesis enzyme transcription in all breast cancer cell lines. qRT-PCR analysis of *PHGDH*, *PSAT1* and *PSPH* mRNA levels in breast cancer cell lines transfected with a single *ATF4*-targeting siRNA oligo or a non-targeting control oligo at a final concentration of 50 nM for 72 hours. mRNA levels are presented as relative fold changes versus control siRNA transfected cells and normalised to *ACTB* (β-Actin) mRNA levels. Suppression of ATF4 recurrently suppressed *PHGDH* and *PSAT1* mRNA levels in all cell lines tested, and frequently suppressed *PSPH* mRNA levels. n=1 independent experiment per cell line.

Finally, chapter 6 discussed the potential role for IKKε-mediated regulation of serine biosynthesis in the kinases primary function activating IRF3 and IFNβ signalling in the innate immune system (see 6.2). A preliminary experiment investigating such a role was performed which indicated that the serine biosynthesis pathway is important for IKKε-mediated IFNβ secretion. Medium conditioned by Flp-In 293 cells expressing HA-IKKε in which PSAT1 was suppressed using siRNA (Figure 7.4 A) was applied to T47D cells and the activation of the IFNβ-mediated JAK/STAT signalling pathway was evaluated in receiving cells by western blot analysis of STAT1 Tyr701 phosphorylation (Figure 7.4 B). It was observed that medium conditioned by Flp-In 293 HA-IKKε cells where PSAT1 was suppressed induced less STAT1 Tyr 701 phosphorylation than medium conditioned by cells in which PSAT1 was still expressed, indicating that the serine biosynthesis pathway is important for IKKε-mediated IFNβ secretion and that upregulation of the serine biosynthesis pathway by IKKε might serve to support cytokine secretion in the innate immune system.

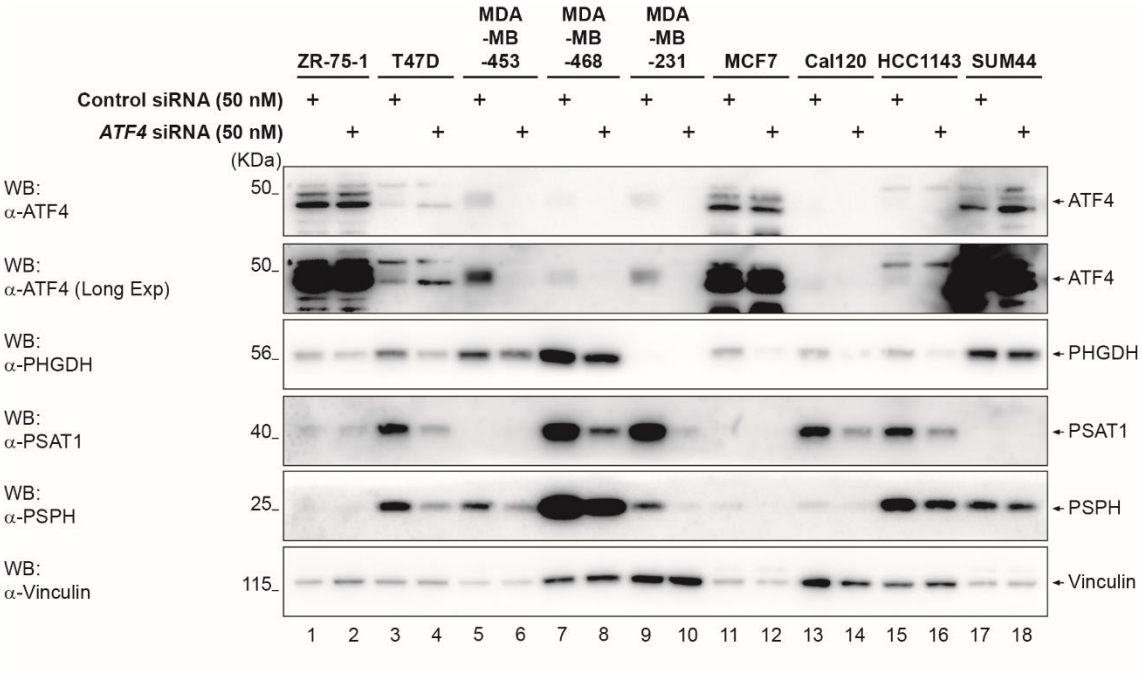

Figure 7.3 – siRNA-mediated suppression of ATF4 reduces serine biosynthesis enzyme protein levels in all breast cancer cell lines. Western blot of ATF4 and serine biosynthesis enzyme protein levels following transfection of indicated breast cancer cell lines with *ATF4*-targeting siRNA. Indicated breast cancer cell lines were transfected with a pool of 4 *ATF4*-targeting siRNA oligos, to suppress the transcription factor, or a single non-targeting control oligo to a final concentration of 50 nM for 72 hours. Effective knockdown was only validated in MDA-MB-453, MDA-MB-468 and MDA-MB-231 cell lines, being the only cell lines to clearly display bands corresponding to the band validated in Flp-In 293 cells (Figure 5.7 A), but transfection of siRNA resulted in reduction in PHGDH, PSAT1 and PSPH protein levels in most cell lines, indicative of ATF4 knockdown. Vinculin is shown as a loading control.

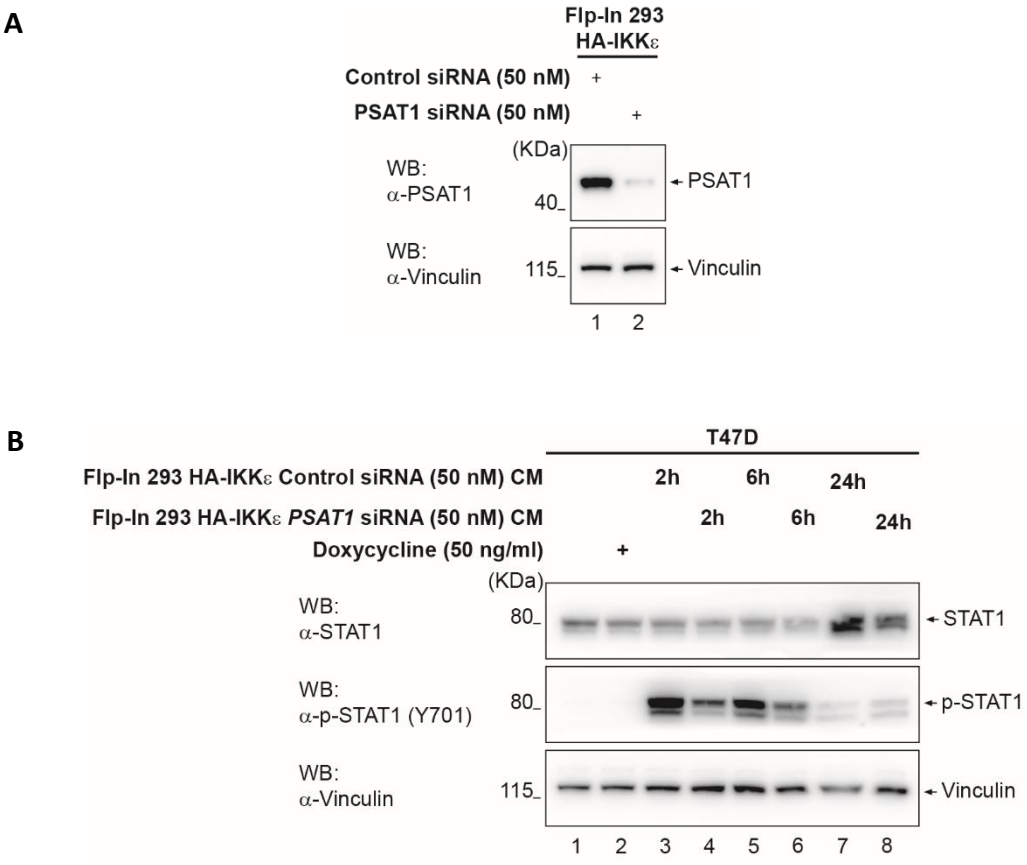

Figure 7.4 – Serine biosynthesis enzyme PSAT1 is important for IKKε-mediated IFNβ secretion. Analysis of STAT1 Tyr701 (Y701) phosphorylation in T47D cells following application of conditioned medium for 2 hours. **(A)** Medium was conditioned for 16 hours by Flp-In 293 HA-IKKε cells transfected with a pool of 4 *PSAT1*-targeting siRNA oligos or a single non-targeting control oligo to a final concentration of 50 nM for 72 hours and treated with 50 ng/ml doxycycline for the final 16 hours. PSAT1 suppression in medium-conditioning cells is demonstrated by western blotting. **(B)** Conditioned medium was filtered through a 0.22 µm pore-size filter and applied to receiving T47D cells for 2 hours. Activation of IFNβ-mediated JAK/STAT signalling was evaluated by western blot detection of relative STAT1 Tyr701 phosphorylation levels. Suppression of PSAT1 in medium-conditioning cells substantially reduced the phosphorylation of STAT1 Tyr701 in receiving cells, indicating that the enzyme is important for proper IFNβ secretion. Vinculin is shown as a loading control.

Bibliography

1 Takeuchi, O. & Akira, S. Pattern recognition receptors and inflammation. *Cell* **140**, 805-820, doi:10.1016/j.cell.2010.01.022 (2010).

2 Brubaker, S. W., Bonham, K. S., Zanoni, I. & Kagan, J. C. Innate immune pattern recognition: a cell biological perspective. *Annu Rev Immunol* **33**, 257-290, doi:10.1146/annurev-immunol-032414-112240 (2015).

3 Netea, M. G. *et al.* A guiding map for inflammation. *Nature immunology* **18**, 826-831, doi:10.1038/ni.3790 (2017).

4 Medzhitov, R. Origin and physiological roles of inflammation. *Nature* **454**, 428-435, doi:10.1038/nature07201 (2008).

5 Sarma, J. V. & Ward, P. A. The complement system. *Cell Tissue Res* **343**, 227-235, doi:10.1007/s00441-010-1034-0 (2011).

6 Serhan, C. N. & Savill, J. Resolution of inflammation: the beginning programs the end. *Nature immunology* **6**, 1191-1197, doi:10.1038/ni1276 (2005).

7 Serhan, C. N. Resolution phase of inflammation: novel endogenous anti-inflammatory and proresolving lipid mediators and pathways. *Annu Rev Immunol* **25**, 101-137, doi:10.1146/annurev.immunol.25.022106.141647 (2007).

8 Koh, T. J. & DiPietro, L. A. Inflammation and wound healing: the role of the macrophage. *Expert Rev Mol Med* **13**, e23, doi:10.1017/S1462399411001943 (2011).

9 Turabelidze, A. & Dipietro, L. A. Inflammation and wound healing. *Endodontic Topics* **24**, 26-38, doi:10.1111/etp.12012 (2011).

10 Coussens, L. M. & Werb, Z. Inflammation and cancer. *Nature* **420**, 860-867, doi:10.1038/nature01322 (2002).

11 Warrington, R., Watson, W., Kim, H. L. & Antonetti, F. R. An introduction to immunology and immunopathology. *Allergy Asthma Clin Immunol* **7 Suppl 1**, S1, doi:10.1186/1710-1492-7-S1-S1 (2011).

12 Bonilla, F. A. & Oettgen, H. C. Adaptive immunity. *J Allergy Clin Immunol* **125**, S33-40, doi:10.1016/j.jaci.2009.09.017 (2010).

13 Jaskiewicz, M., Conrath, U. & Peterhansel, C. Chromatin modification acts as a memory for systemic acquired resistance in the plant stress response. *EMBO reports* **12**, 50-55, doi:10.1038/embor.2010.186 (2011).

14 Quintin, J. *et al.* Candida albicans infection affords protection against reinfection via functional reprogramming of monocytes. *Cell host & microbe* **12**, 223-232, doi:10.1016/j.chom.2012.06.006 (2012).

15 Cheng, S. C. *et al.* mTOR- and HIF-1alpha-mediated aerobic glycolysis as metabolic basis for trained immunity. *Science* **345**, 1250684, doi:10.1126/science.1250684 (2014).

16 Netea, M. G., Quintin, J. & van der Meer, J. W. Trained immunity: a memory for innate host defense. *Cell host & microbe* **9**, 355-361, doi:10.1016/j.chom.2011.04.006 (2011).

17 Netea, M. G. & van der Meer, J. W. Trained Immunity: An Ancient Way of Remembering. *Cell host & microbe* **21**, 297-300, doi:10.1016/j.chom.2017.02.003 (2017).

18 Balkwill, F. & Mantovani, A. Inflammation and cancer: back to Virchow? *Lancet* **357**, 539-545, doi:10.1016/S0140-6736(00)04046-0 (2001).

19 Deng, T., Lyon, C. J., Bergin, S., Caligiuri, M. A. & Hsueh, W. A. Obesity, Inflammation, and Cancer. *Annu Rev Pathol* **11**, 421-449, doi:10.1146/annurev-pathol-012615-044359 (2016).

20 Hanahan, D. & Weinberg, R. A. Hallmarks of cancer: the next generation. *Cell* **144**, 646-674, doi:10.1016/j.cell.2011.02.013 (2011).

21 Ancrile, B., Lim, K. H. & Counter, C. M. Oncogenic Ras-induced secretion of IL6 is required for tumorigenesis. *Genes & development* **21**, 1714-1719, doi:10.1101/gad.1549407 (2007).

22 Ancrile, B. B., O'Hayer, K. M. & Counter, C. M. Oncogenic ras-induced expression of cytokines: a new target of anti-cancer therapeutics. *Mol Interv* **8**, 22-27, doi:10.1124/mi.8.1.6 (2008).

23 Shchors, K. *et al.* The Myc-dependent angiogenic switch in tumors is mediated by interleukin 1beta. *Genes & development* **20**, 2527-2538, doi:10.1101/gad.1455706 (2006).

24 Sunaga, N. *et al.* Oncogenic KRAS-induced interleukin-8 overexpression promotes cell growth and migration and contributes to aggressive phenotypes of non-small cell lung cancer. *International journal of cancer. Journal international du cancer* **130**, 1733-1744, doi:10.1002/ijc.26164 (2012).

25 Kortlever, R. M. *et al.* Myc Cooperates with Ras by Programming Inflammation and Immune Suppression. *Cell* **171**, 1301-1315 e1314, doi:10.1016/j.cell.2017.11.013 (2017).

26 Pages, F. *et al.* Immune infiltration in human tumors: a prognostic factor that should not be ignored. *Oncogene* **29**, 1093-1102, doi:10.1038/onc.2009.416 (2010).

27 Eiro, N. & Vizoso, F. J. Inflammation and cancer. *World J Gastrointest Surg* **4**, 62-72, doi:10.4240/wjgs.v4.i3.62 (2012).

28 Kiraly, O., Gong, G., Olipitz, W., Muthupalani, S. & Engelward, B. P. Inflammation-induced cell proliferation potentiates DNA damage-induced mutations in vivo. *PLoS genetics* **11**, e1004901, doi:10.1371/journal.pgen.1004901 (2015).

29 Lonkar, P. & Dedon, P. C. Reactive species and DNA damage in chronic inflammation: reconciling chemical mechanisms and biological fates. *International journal of cancer. Journal international du cancer* **128**, 1999-2009, doi:10.1002/ijc.25815 (2011).

30 Banning, D. P., O'Farrell, F. & Gooderham, N. J. Activation of the food derived carcinogen 2-amino-3,8-dimethylimidazo[4,5-f]quinoxaline by rat pleural cavity inflammatory cells. *Carcinogenesis* **14**, 2457-2462 (1993).

31 Henderson, J. P., Byun, J., Takeshita, J. & Heinecke, J. W. Phagocytes produce 5-chlorouracil and 5-bromouracil, two mutagenic products of myeloperoxidase, in human inflammatory tissue. *The Journal of biological chemistry* **278**, 23522-23528, doi:10.1074/jbc.M303928200 (2003).

32 Fedeles, B. I. *et al.* Intrinsic mutagenic properties of 5-chlorocytosine: A mechanistic connection between chronic inflammation and cancer. *Proc Natl Acad Sci U S A* **112**, E4571-4580, doi:10.1073/pnas.1507709112 (2015).

33 Gungor, N. *et al.* Genotoxic effects of neutrophils and hypochlorous acid. *Mutagenesis* **25**, 149-154, doi:10.1093/mutage/gep053 (2010).

34 Gilmore, T. D. Introduction to NF-kappaB: players, pathways, perspectives. *Oncogene* **25**, 6680-6684, doi:10.1038/sj.onc.1209954 (2006).

35 Karin, M. NF-kappaB as a critical link between inflammation and cancer. *Cold Spring Harbor perspectives in biology* **1**, a000141, doi:10.1101/cshperspect.a000141 (2009).

36 Hayden, M. S. & Ghosh, S. NF-kappaB, the first quarter-century: remarkable progress and outstanding questions. *Genes & development* **26**, 203-234, doi:10.1101/gad.183434.111 (2012).

37 Napetschnig, J. & Wu, H. Molecular basis of NF-kappaB signaling. *Annu Rev Biophys* **42**, 443-468, doi:10.1146/annurev-biophys-083012-130338 (2013).

38 Liu, T., Zhang, L., Joo, D. & Sun, S. C. NF-kappaB signaling in inflammation. *Signal Transduct Target Ther* **2**, doi:10.1038/sigtrans.2017.23 (2017).

39 Shih, V. F., Tsui, R., Caldwell, A. & Hoffmann, A. A single NFkappaB system for both canonical and non-canonical signaling. *Cell research* **21**, 86-102, doi:10.1038/cr.2010.161 (2011).

40 Oeckinghaus, A., Hayden, M. S. & Ghosh, S. Crosstalk in NF-kappaB signaling pathways. *Nature immunology* **12**, 695-708, doi:10.1038/ni.2065 (2011).

41 Sun, S. C. Non-canonical NF-kappaB signaling pathway. *Cell research* **21**, 71-85, doi:10.1038/cr.2010.177 (2011).

42 Xiao, G., Harhaj, E. W. & Sun, S. C. NF-kappaB-inducing kinase regulates the processing of NF-kappaB2 p100. *Molecular cell* **7**, 401-409 (2001).

43 Liao, G., Zhang, M., Harhaj, E. W. & Sun, S. C. Regulation of the NF-kappaB-inducing kinase by tumor necrosis factor receptor-associated factor 3-induced degradation. *The Journal of biological chemistry* **279**, 26243-26250, doi:10.1074/jbc.M403286200 (2004).

44 Vallabhapurapu, S. *et al.* Nonredundant and complementary functions of TRAF2 and TRAF3 in a ubiquitination cascade that activates NIK-dependent alternative NF-kappaB signaling. *Nature immunology* **9**, 1364-1370, doi:10.1038/ni.1678 (2008).

45 Senftleben, U. *et al.* Activation by IKKalpha of a second, evolutionary conserved, NF-kappa B signaling pathway. *Science* **293**, 1495-1499, doi:10.1126/science.1062677 (2001).

46 Sun, S. C. The noncanonical NF-kappaB pathway. *Immunol Rev* **246**, 125-140, doi:10.1111/j.1600-065X.2011.01088.x (2012).

47 Brown, K., Gerstberger, S., Carlson, L., Franzoso, G. & Siebenlist, U. Control of I kappa B-alpha proteolysis by site-specific, signal-induced phosphorylation. *Science* **267**, 1485-1488 (1995).

48 Traenckner, E. B. *et al.* Phosphorylation of human I kappa B-alpha on serines 32 and 36 controls I kappa B-alpha proteolysis and NF-kappa B activation in response to diverse stimuli. *The EMBO journal* **14**, 2876-2883 (1995).

49 Chen, Z. *et al.* Signal-induced site-specific phosphorylation targets I kappa B alpha to the ubiquitin-proteasome pathway. *Genes & development* **9**, 1586-1597 (1995).

50 Scherer, D. C., Brockman, J. A., Chen, Z., Maniatis, T. & Ballard, D. W. Signal-induced degradation of I kappa B alpha requires site-specific ubiquitination. *Proceedings of the National Academy of Sciences of the United States of America* **92**, 11259-11263 (1995).

51 Shen, R. R. & Hahn, W. C. Emerging roles for the non-canonical IKKs in cancer. *Oncogene* **30**, 631-641, doi:10.1038/onc.2010.493 (2011).

52 Ikeda, F. *et al.* Involvement of the ubiquitin-like domain of TBK1/IKK-i kinases in regulation of IFN-inducible genes. *The EMBO journal* **26**, 3451-3462, doi:10.1038/sj.emboj.7601773 (2007).

53 May, M. J., Larsen, S. E., Shim, J. H., Madge, L. A. & Ghosh, S. A novel ubiquitin-like domain in IkappaB kinase beta is required for functional activity of the kinase. *The Journal of biological chemistry* **279**, 45528-45539, doi:10.1074/jbc.M408579200 (2004).

54 Connelly, M. A. & Marcu, K. B. CHUK, a new member of the helix-loop-helix and leucine zipper families of interacting proteins, contains a serine-threonine kinase catalytic domain. *Cell Mol Biol Res* **41**, 537-549 (1995).

55 Mock, B. A., Connelly, M. A., McBride, O. W., Kozak, C. A. & Marcu, K. B. CHUK, a conserved helix-loop-helix ubiquitous kinase, maps to human chromosome 10 and mouse chromosome 19. *Genomics* **27**, 348-351, doi:10.1006/geno.1995.1054 (1995).

56 DiDonato, J. A., Hayakawa, M., Rothwarf, D. M., Zandi, E. & Karin, M. A cytokine-responsive IkappaB kinase that activates the transcription factor NF-kappaB. *Nature* **388**, 548-554, doi:10.1038/41493 (1997).

57 Mercurio, F. *et al.* IKK-1 and IKK-2: cytokine-activated IkappaB kinases essential for NF-kappaB activation. *Science* **278**, 860-866 (1997).
58 Regnier, C. H. *et al.* Identification and characterization of an IkappaB kinase. *Cell* **90**, 373-383 (1997).
59 Woronicz, J. D., Gao, X., Cao, Z., Rothe, M. & Goeddel, D. V. IkappaB kinase-beta: NF-kappaB activation and complex formation with IkappaB kinase-alpha and NIK. *Science* **278**, 866-869 (1997).
60 Zandi, E., Rothwarf, D. M., Delhase, M., Hayakawa, M. & Karin, M. The IkappaB kinase complex (IKK) contains two kinase subunits, IKKalpha and IKKbeta, necessary for IkappaB phosphorylation and NF-kappaB activation. *Cell* **91**, 243-252 (1997).
61 Lee, F. S., Peters, R. T., Dang, L. C. & Maniatis, T. MEKK1 activates both IkappaB kinase alpha and IkappaB kinase beta. *Proceedings of the National Academy of Sciences of the United States of America* **95**, 9319-9324 (1998).
62 Rothwarf, D. M., Zandi, E., Natoli, G. & Karin, M. IKK-gamma is an essential regulatory subunit of the IkappaB kinase complex. *Nature* **395**, 297-300, doi:10.1038/26261 (1998).
63 Yamaoka, S. *et al.* Complementation cloning of NEMO, a component of the IkappaB kinase complex essential for NF-kappaB activation. *Cell* **93**, 1231-1240 (1998).
64 Tang, E. D., Wang, C. Y., Xiong, Y. & Guan, K. L. A role for NF-kappaB essential modifier/IkappaB kinase-gamma (NEMO/IKKgamma) ubiquitination in the activation of the IkappaB kinase complex by tumor necrosis factor-alpha. *The Journal of biological chemistry* **278**, 37297-37305, doi:10.1074/jbc.M303389200 (2003).
65 Zhou, H. *et al.* Bcl10 activates the NF-kappaB pathway through ubiquitination of NEMO. *Nature* **427**, 167-171, doi:10.1038/nature02273 (2004).
66 Sun, L., Deng, L., Ea, C. K., Xia, Z. P. & Chen, Z. J. The TRAF6 ubiquitin ligase and TAK1 kinase mediate IKK activation by BCL10 and MALT1 in T lymphocytes. *Molecular cell* **14**, 289-301 (2004).
67 Srivastava, R., Burbach, B. J. & Shimizu, Y. NF-kappaB activation in T cells requires discrete control of IkappaB kinase alpha/beta (IKKalpha/beta) phosphorylation and IKKgamma ubiquitination by the ADAP adapter protein. *The Journal of biological chemistry* **285**, 11100-11105, doi:10.1074/jbc.M109.068999 (2010).
68 May, M. J. *et al.* Selective inhibition of NF-kappaB activation by a peptide that blocks the interaction of NEMO with the IkappaB kinase complex. *Science* **289**, 1550-1554 (2000).
69 Hu, Y. *et al.* Abnormal morphogenesis but intact IKK activation in mice lacking the IKKalpha subunit of IkappaB kinase. *Science* **284**, 316-320 (1999).
70 Takeda, K. *et al.* Limb and skin abnormalities in mice lacking IKKalpha. *Science* **284**, 313-316 (1999).
71 Li, Z. W. *et al.* The IKKbeta subunit of IkappaB kinase (IKK) is essential for nuclear factor kappaB activation and prevention of apoptosis. *The Journal of experimental medicine* **189**, 1839-1845 (1999).
72 Li, Q. *et al.* IKK1-deficient mice exhibit abnormal development of skin and skeleton. *Genes & development* **13**, 1322-1328 (1999).
73 Hu, Y. *et al.* IKKalpha controls formation of the epidermis independently of NF-kappaB. *Nature* **410**, 710-714, doi:10.1038/35070605 (2001).
74 Sil, A. K., Maeda, S., Sano, Y., Roop, D. R. & Karin, M. IkappaB kinase-alpha acts in the epidermis to control skeletal and craniofacial morphogenesis. *Nature* **428**, 660-664, doi:10.1038/nature02421 (2004).
75 Descargues, P. *et al.* IKKalpha is a critical coregulator of a Smad4-independent TGFbeta-Smad2/3 signaling pathway that controls keratinocyte differentiation.

Proceedings of the National Academy of Sciences of the United States of America **105**, 2487-2492, doi:10.1073/pnas.0712044105 (2008).

76 Suzuki, K. & Verma, I. M. Phosphorylation of SNAP-23 by IkappaB kinase 2 regulates mast cell degranulation. *Cell* **134**, 485-495, doi:10.1016/j.cell.2008.05.050 (2008).

77 Dondelinger, Y. *et al.* NF-kappaB-Independent Role of IKKalpha/IKKbeta in Preventing RIPK1 Kinase-Dependent Apoptotic and Necroptotic Cell Death during TNF Signaling. *Molecular cell* **60**, 63-76, doi:10.1016/j.molcel.2015.07.032 (2015).

78 Shimada, T. *et al.* IKK-i, a novel lipopolysaccharide-inducible kinase that is related to IkappaB kinases. *International immunology* **11**, 1357-1362 (1999).

79 Peters, R. T., Liao, S. M. & Maniatis, T. IKKepsilon is part of a novel PMA-inducible IkappaB kinase complex. *Molecular cell* **5**, 513-522 (2000).

80 Pomerantz, J. L. & Baltimore, D. NF-kappaB activation by a signaling complex containing TRAF2, TANK and TBK1, a novel IKK-related kinase. *The EMBO journal* **18**, 6694-6704, doi:10.1093/emboj/18.23.6694 (1999).

81 Tojima, Y. *et al.* NAK is an IkappaB kinase-activating kinase. *Nature* **404**, 778-782, doi:10.1038/35008109 (2000).

82 Harris, J. *et al.* Nuclear accumulation of cRel following C-terminal phosphorylation by TBK1/IKK epsilon. *Journal of immunology* **177**, 2527-2535 (2006).

83 Mattioli, I. *et al.* Inducible phosphorylation of NF-kappa B p65 at serine 468 by T cell costimulation is mediated by IKK epsilon. *The Journal of biological chemistry* **281**, 6175-6183, doi:10.1074/jbc.M508045200 (2006).

84 Kishore, N. *et al.* IKK-i and TBK-1 are enzymatically distinct from the homologous enzyme IKK-2: comparative analysis of recombinant human IKK-i, TBK-1, and IKK-2. *The Journal of biological chemistry* **277**, 13840-13847, doi:10.1074/jbc.M110474200 (2002).

85 Chau, T. L. *et al.* Are the IKKs and IKK-related kinases TBK1 and IKK-epsilon similarly activated? *Trends in biochemical sciences* **33**, 171-180, doi:10.1016/j.tibs.2008.01.002 (2008).

86 Fitzgerald, K. A. *et al.* IKKepsilon and TBK1 are essential components of the IRF3 signaling pathway. *Nature immunology* **4**, 491-496, doi:10.1038/ni921 (2003).

87 Sharma, S. *et al.* Triggering the interferon antiviral response through an IKK-related pathway. *Science* **300**, 1148-1151, doi:10.1126/science.1081315 (2003).

88 Hemmi, H. *et al.* The roles of two IkappaB kinase-related kinases in lipopolysaccharide and double stranded RNA signaling and viral infection. *The Journal of experimental medicine* **199**, 1641-1650, doi:10.1084/jem.20040520 (2004).

89 Paz, S. *et al.* Induction of IRF-3 and IRF-7 phosphorylation following activation of the RIG-I pathway. *Cell Mol Biol (Noisy-le-grand)* **52**, 17-28 (2006).

90 Lin, R., Heylbroeck, C., Pitha, P. M. & Hiscott, J. Virus-dependent phosphorylation of the IRF-3 transcription factor regulates nuclear translocation, transactivation potential, and proteasome-mediated degradation. *Molecular and cellular biology* **18**, 2986-2996 (1998).

91 Servant, M. J. *et al.* Identification of the minimal phosphoacceptor site required for in vivo activation of interferon regulatory factor 3 in response to virus and double-stranded RNA. *The Journal of biological chemistry* **278**, 9441-9447, doi:10.1074/jbc.M209851200 (2003).

92 Lin, R., Mamane, Y. & Hiscott, J. Multiple regulatory domains control IRF-7 activity in response to virus infection. *The Journal of biological chemistry* **275**, 34320-34327, doi:10.1074/jbc.M002814200 (2000).

93 Honda, K. & Taniguchi, T. IRFs: master regulators of signalling by Toll-like receptors and cytosolic pattern-recognition receptors. *Nature reviews. Immunology* **6**, 644-658, doi:10.1038/nri1900 (2006).

94 Sato, M. *et al.* Distinct and essential roles of transcription factors IRF-3 and IRF-7 in response to viruses for IFN-alpha/beta gene induction. *Immunity* **13**, 539-548 (2000).
95 Honda, K., Yanai, H., Takaoka, A. & Taniguchi, T. Regulation of the type I IFN induction: a current view. *International immunology* **17**, 1367-1378, doi:10.1093/intimm/dxh318 (2005).
96 Garcia-Sastre, A. & Biron, C. A. Type 1 interferons and the virus-host relationship: a lesson in detente. *Science* **312**, 879-882, doi:10.1126/science.1125676 (2006).
97 Seth, R. B., Sun, L. & Chen, Z. J. Antiviral innate immunity pathways. *Cell research* **16**, 141-147, doi:10.1038/sj.cr.7310019 (2006).
98 Fu, X. Y., Kessler, D. S., Veals, S. A., Levy, D. E. & Darnell, J. E., Jr. ISGF3, the transcriptional activator induced by interferon alpha, consists of multiple interacting polypeptide chains. *Proceedings of the National Academy of Sciences of the United States of America* **87**, 8555-8559 (1990).
99 Tenoever, B. R. *et al.* Multiple functions of the IKK-related kinase IKKepsilon in interferon-mediated antiviral immunity. *Science* **315**, 1274-1278, doi:10.1126/science.1136567 (2007).
100 Shuai, K., Schindler, C., Prezioso, V. R. & Darnell, J. E., Jr. Activation of transcription by IFN-gamma: tyrosine phosphorylation of a 91-kD DNA binding protein. *Science* **258**, 1808-1812 (1992).
101 Decker, T., Kovarik, P. & Meinke, A. GAS elements: a few nucleotides with a major impact on cytokine-induced gene expression. *Journal of interferon & cytokine research : the official journal of the International Society for Interferon and Cytokine Research* **17**, 121-134, doi:10.1089/jir.1997.17.121 (1997).
102 Ng, S. L. *et al.* IkappaB kinase epsilon (IKK(epsilon)) regulates the balance between type I and type II interferon responses. *Proceedings of the National Academy of Sciences of the United States of America* **108**, 21170-21175, doi:10.1073/pnas.1119137109 (2011).
103 Chiang, S. H. *et al.* The protein kinase IKKepsilon regulates energy balance in obese mice. *Cell* **138**, 961-975, doi:10.1016/j.cell.2009.06.046 (2009).
104 Reilly, S. M. *et al.* An inhibitor of the protein kinases TBK1 and IKK-varepsilon improves obesity-related metabolic dysfunctions in mice. *Nature medicine* **19**, 313-321, doi:10.1038/nm.3082 (2013).
105 Krawczyk, C. M. *et al.* Toll-like receptor-induced changes in glycolytic metabolism regulate dendritic cell activation. *Blood* **115**, 4742-4749, doi:10.1182/blood-2009-10-249540 (2010).
106 Everts, B. *et al.* TLR-driven early glycolytic reprogramming via the kinases TBK1-IKKvarepsilon supports the anabolic demands of dendritic cell activation. *Nature immunology* **15**, 323-332, doi:10.1038/ni.2833 (2014).
107 Dolcet, X., Llobet, D., Pallares, J. & Matias-Guiu, X. NF-kB in development and progression of human cancer. *Virchows Archiv : an international journal of pathology* **446**, 475-482, doi:10.1007/s00428-005-1264-9 (2005).
108 Xia, Y., Shen, S. & Verma, I. M. NF-kappaB, an active player in human cancers. *Cancer Immunol Res* **2**, 823-830, doi:10.1158/2326-6066.CIR-14-0112 (2014).
109 Chen, C., Edelstein, L. C. & Gelinas, C. The Rel/NF-kappaB family directly activates expression of the apoptosis inhibitor Bcl-x(L). *Molecular and cellular biology* **20**, 2687-2695 (2000).
110 Grossmann, M. *et al.* The anti-apoptotic activities of Rel and RelA required during B-cell maturation involve the regulation of Bcl-2 expression. *The EMBO journal* **19**, 6351-6360, doi:10.1093/emboj/19.23.6351 (2000).

111 Kreuz, S., Siegmund, D., Scheurich, P. & Wajant, H. NF-kappaB inducers upregulate cFLIP, a cycloheximide-sensitive inhibitor of death receptor signaling. *Molecular and cellular biology* **21**, 3964-3973, doi:10.1128/MCB.21.12.3964-3973.2001 (2001).
112 Micheau, O., Lens, S., Gaide, O., Alevizopoulos, K. & Tschopp, J. NF-kappaB signals induce the expression of c-FLIP. *Molecular and cellular biology* **21**, 5299-5305, doi:10.1128/MCB.21.16.5299-5305.2001 (2001).
113 Hinz, M. *et al.* NF-kappaB function in growth control: regulation of cyclin D1 expression and G0/G1-to-S-phase transition. *Molecular and cellular biology* **19**, 2690-2698 (1999).
114 Ko, H. M. *et al.* Platelet-activating factor-induced NF-kappaB activation enhances VEGF expression through a decrease in p53 activity. *FEBS letters* **580**, 3006-3012, doi:10.1016/j.febslet.2006.04.042 (2006).
115 Leychenko, A., Konorev, E., Jijiwa, M. & Matter, M. L. Stretch-induced hypertrophy activates NFkB-mediated VEGF secretion in adult cardiomyocytes. *PloS one* **6**, e29055, doi:10.1371/journal.pone.0029055 (2011).
116 Cabannes, E., Khan, G., Aillet, F., Jarrett, R. F. & Hay, R. T. Mutations in the IkBa gene in Hodgkin's disease suggest a tumour suppressor role for IkappaBalpha. *Oncogene* **18**, 3063-3070, doi:10.1038/sj.onc.1202893 (1999).
117 Lake, A. *et al.* Mutations of NFKBIA, encoding IkappaB alpha, are a recurrent finding in classical Hodgkin lymphoma but are not a unifying feature of non-EBV-associated cases. *International journal of cancer. Journal international du cancer* **125**, 1334-1342, doi:10.1002/ijc.24502 (2009).
118 Liu, X. *et al.* Mutations of NFKBIA in biopsy specimens from Hodgkin lymphoma. *Cancer Genet Cytogenet* **197**, 152-157, doi:10.1016/j.cancergencyto.2009.11.005 (2010).
119 Courtois, G. & Gilmore, T. D. Mutations in the NF-kappaB signaling pathway: implications for human disease. *Oncogene* **25**, 6831-6843, doi:10.1038/sj.onc.1209939 (2006).
120 Bredel, M. *et al.* NFKBIA deletion in glioblastomas. *N Engl J Med* **364**, 627-637, doi:10.1056/NEJMoa1006312 (2011).
121 Chaturvedi, M. M., Sung, B., Yadav, V. R., Kannappan, R. & Aggarwal, B. B. NF-kappaB addiction and its role in cancer: 'one size does not fit all'. *Oncogene* **30**, 1615-1630, doi:10.1038/onc.2010.566 (2011).
122 Anest, V. *et al.* A nucleosomal function for IkappaB kinase-alpha in NF-kappaB-dependent gene expression. *Nature* **423**, 659-663, doi:10.1038/nature01648 (2003).
123 Yamamoto, Y., Verma, U. N., Prajapati, S., Kwak, Y. T. & Gaynor, R. B. Histone H3 phosphorylation by IKK-alpha is critical for cytokine-induced gene expression. *Nature* **423**, 655-659, doi:10.1038/nature01576 (2003).
124 Hoberg, J. E., Popko, A. E., Ramsey, C. S. & Mayo, M. W. IkappaB kinase alpha-mediated derepression of SMRT potentiates acetylation of RelA/p65 by p300. *Molecular and cellular biology* **26**, 457-471, doi:10.1128/MCB.26.2.457-471.2006 (2006).
125 Song, L. L. *et al.* Notch-1 associates with IKKalpha and regulates IKK activity in cervical cancer cells. *Oncogene* **27**, 5833-5844, doi:10.1038/onc.2008.190 (2008).
126 Hao, L. *et al.* Notch-1 activates estrogen receptor-alpha-dependent transcription via IKKalpha in breast cancer cells. *Oncogene* **29**, 201-213, doi:10.1038/onc.2009.323 (2010).
127 Li, X. *et al.* Elevated microRNA-23a Expression Enhances the Chemoresistance of Colorectal Cancer Cells with Microsatellite Instability to 5-Fluorouracil by Directly Targeting ABCF1. *Curr Protein Pept Sci* **16**, 301-309 (2015).
128 Zhang, X. W. *et al.* Upregulation of microRNA-23a regulates proliferation and apoptosis by targeting APAF-1 in laryngeal carcinoma. *Oncology letters* **10**, 410-416, doi:10.3892/ol.2015.3238 (2015).

129 Yang, Z. *et al.* miR-23a promotes IKKalpha expression but suppresses ST7L expression to contribute to the malignancy of epithelial ovarian cancer cells. *British journal of cancer* **115**, 731-740, doi:10.1038/bjc.2016.244 (2016).
130 Lindholm, P. F., Bub, J., Kaul, S., Shidham, V. B. & Kajdacsy-Balla, A. The role of constitutive NF-kappaB activity in PC-3 human prostate cancer cell invasive behavior. *Clinical & experimental metastasis* **18**, 471-479 (2000).
131 Abraham, S., Zhang, W., Greenberg, N. & Zhang, M. Maspin functions as tumor suppressor by increasing cell adhesion to extracellular matrix in prostate tumor cells. *The Journal of urology* **169**, 1157-1161, doi:10.1097/01.ju.0000040245.70349.37 (2003).
132 Hall, D. C. *et al.* Maspin reduces prostate cancer metastasis to bone. *Urol Oncol* **26**, 652-658, doi:10.1016/j.urolonc.2007.07.017 (2008).
133 Luo, J. L. *et al.* Nuclear cytokine-activated IKKalpha controls prostate cancer metastasis by repressing Maspin. *Nature* **446**, 690-694, doi:10.1038/nature05656 (2007).
134 Mahato, R., Qin, B. & Cheng, K. Blocking IKKalpha expression inhibits prostate cancer invasiveness. *Pharmaceutical research* **28**, 1357-1369, doi:10.1007/s11095-010-0351-z (2011).
135 Liu, B. *et al.* A critical role for I kappaB kinase alpha in the development of human and mouse squamous cell carcinomas. *Proceedings of the National Academy of Sciences of the United States of America* **103**, 17202-17207, doi:10.1073/pnas.0604481103 (2006).
136 Maeda, G., Chiba, T., Kawashiri, S., Satoh, T. & Imai, K. Epigenetic inactivation of IkappaB Kinase-alpha in oral carcinomas and tumor progression. *Clinical cancer research : an official journal of the American Association for Cancer Research* **13**, 5041-5047, doi:10.1158/1078-0432.CCR-07-0463 (2007).
137 Park, E. *et al.* Reduction in IkappaB kinase alpha expression promotes the development of skin papillomas and carcinomas. *Cancer research* **67**, 9158-9168, doi:10.1158/0008-5472.CAN-07-0590 (2007).
138 Greten, F. R. *et al.* IKKbeta links inflammation and tumorigenesis in a mouse model of colitis-associated cancer. *Cell* **118**, 285-296, doi:10.1016/j.cell.2004.07.013 (2004).
139 Koliaraki, V., Pasparakis, M. & Kollias, G. IKKbeta in intestinal mesenchymal cells promotes initiation of colitis-associated cancer. *The Journal of experimental medicine* **212**, 2235-2251, doi:10.1084/jem.20150542 (2015).
140 Pallangyo, C. K., Ziegler, P. K. & Greten, F. R. IKKbeta acts as a tumor suppressor in cancer-associated fibroblasts during intestinal tumorigenesis. *The Journal of experimental medicine* **212**, 2253-2266, doi:10.1084/jem.20150576 (2015).
141 Chen, R. *et al.* Regulation of IKKbeta by miR-199a affects NF-kappaB activity in ovarian cancer cells. *Oncogene* **27**, 4712-4723, doi:10.1038/onc.2008.112 (2008).
142 Yang, Y. *et al.* MiR-503 targets PI3K p85 and IKK-beta and suppresses progression of non-small cell lung cancer. *International journal of cancer. Journal international du cancer* **135**, 1531-1542, doi:10.1002/ijc.28799 (2014).
143 Lee, D. F. *et al.* IKK beta suppression of TSC1 links inflammation and tumor angiogenesis via the mTOR pathway. *Cell* **130**, 440-455, doi:10.1016/j.cell.2007.05.058 (2007).
144 Nottingham, L. K. *et al.* Aberrant IKKalpha and IKKbeta cooperatively activate NF-kappaB and induce EGFR/AP1 signaling to promote survival and migration of head and neck cancer. *Oncogene* **33**, 1135-1147, doi:10.1038/onc.2013.49 (2014).
145 Jiang, R. *et al.* High expression levels of IKKalpha and IKKbeta are necessary for the malignant properties of liver cancer. *International journal of cancer. Journal international du cancer* **126**, 1263-1274, doi:10.1002/ijc.24854 (2010).

146 Schon, M. *et al.* KINK-1, a novel small-molecule inhibitor of IKKbeta, and the susceptibility of melanoma cells to antitumoral treatment. *Journal of the National Cancer Institute* **100**, 862-875, doi:10.1093/jnci/djn174 (2008).
147 Wu, L. *et al.* BMS-345541 sensitizes MCF-7 breast cancer cells to ionizing radiation by selective inhibition of homologous recombinational repair of DNA double-strand breaks. *Radiation research* **179**, 160-170, doi:10.1667/RR3034.1 (2013).
148 Yang, J., Amiri, K. I., Burke, J. R., Schmid, J. A. & Richmond, A. BMS-345541 targets inhibitor of kappaB kinase and induces apoptosis in melanoma: involvement of nuclear factor kappaB and mitochondria pathways. *Clinical cancer research : an official journal of the American Association for Cancer Research* **12**, 950-960, doi:10.1158/1078-0432.CCR-05-1220 (2006).
149 Yemelyanov, A. *et al.* Effects of IKK inhibitor PS1145 on NF-kappaB function, proliferation, apoptosis and invasion activity in prostate carcinoma cells. *Oncogene* **25**, 387-398, doi:10.1038/sj.onc.1209066 (2006).
150 Cilloni, D. *et al.* The NF-kappaB pathway blockade by the IKK inhibitor PS1145 can overcome imatinib resistance. *Leukemia* **20**, 61-67, doi:10.1038/sj.leu.2403998 (2006).
151 Olsen, L. S. *et al.* Anticancer agent CHS 828 suppresses nuclear factor-kappa B activity in cancer cells through downregulation of IKK activity. *International journal of cancer. Journal international du cancer* **111**, 198-205, doi:10.1002/ijc.20255 (2004).
152 Hjarnaa, P. J. *et al.* CHS 828, a novel pyridyl cyanoguanidine with potent antitumor activity in vitro and in vivo. *Cancer research* **59**, 5751-5757 (1999).
153 Hovstadius, P. *et al.* A Phase I study of CHS 828 in patients with solid tumor malignancy. *Clinical cancer research : an official journal of the American Association for Cancer Research* **8**, 2843-2850 (2002).
154 Zhuang, Z. *et al.* NEMO peptide inhibits the growth of pancreatic ductal adenocarcinoma by blocking NF-kappaB activation. *Cancer letters* **411**, 44-56, doi:10.1016/j.canlet.2017.09.018 (2017).
155 Habineza Ndikuyeze, G. *et al.* A phase I clinical trial of systemically delivered NEMO binding domain peptide in dogs with spontaneous activated B-cell like diffuse large B-cell lymphoma. *PloS one* **9**, e95404, doi:10.1371/journal.pone.0095404 (2014).
156 Chien, Y. *et al.* RalB GTPase-mediated activation of the IkappaB family kinase TBK1 couples innate immune signaling to tumor cell survival. *Cell* **127**, 157-170, doi:10.1016/j.cell.2006.08.034 (2006).
157 Barbie, D. A. *et al.* Systematic RNA interference reveals that oncogenic KRAS-driven cancers require TBK1. *Nature* **462**, 108-112, doi:10.1038/nature08460 (2009).
158 Ou, Y. H. *et al.* TBK1 directly engages Akt/PKB survival signaling to support oncogenic transformation. *Molecular cell* **41**, 458-470, doi:10.1016/j.molcel.2011.01.019 (2011).
159 Cooper, J. M. *et al.* TBK1 Provides Context-Selective Support of the Activated AKT/mTOR Pathway in Lung Cancer. *Cancer research* **77**, 5077-5094, doi:10.1158/0008-5472.CAN-17-0829 (2017).
160 Kim, J. Y. *et al.* Dissection of TBK1 signaling via phosphoproteomics in lung cancer cells. *Proceedings of the National Academy of Sciences of the United States of America* **110**, 12414-12419, doi:10.1073/pnas.1220674110 (2013).
161 Luo, J. *et al.* A genome-wide RNAi screen identifies multiple synthetic lethal interactions with the Ras oncogene. *Cell* **137**, 835-848, doi:10.1016/j.cell.2009.05.006 (2009).
162 Guo, J. Y. *et al.* Activated Ras requires autophagy to maintain oxidative metabolism and tumorigenesis. *Genes & development* **25**, 460-470, doi:10.1101/gad.2016311 (2011).
163 Yang, S. *et al.* Pancreatic cancers require autophagy for tumor growth. *Genes & development* **25**, 717-729, doi:10.1101/gad.2016111 (2011).

164 Pilli, M. *et al.* TBK-1 promotes autophagy-mediated antimicrobial defense by controlling autophagosome maturation. *Immunity* **37**, 223-234, doi:10.1016/j.immuni.2012.04.015 (2012).
165 Newman, A. C. *et al.* TBK1 kinase addiction in lung cancer cells is mediated via autophagy of Tax1bp1/Ndp52 and non-canonical NF-kappaB signalling. *PloS one* **7**, e50672, doi:10.1371/journal.pone.0050672 (2012).
166 Yang, S. *et al.* Autophagy Inhibition Dysregulates TBK1 Signaling and Promotes Pancreatic Inflammation. *Cancer Immunol Res* **4**, 520-530, doi:10.1158/2326-6066.CIR-15-0235 (2016).
167 Deng, T. *et al.* shRNA kinome screen identifies TBK1 as a therapeutic target for HER2+ breast cancer. *Cancer research* **74**, 2119-2130, doi:10.1158/0008-5472.CAN-13-2138 (2014).
168 Shiozawa, Y. *et al.* Human prostate cancer metastases target the hematopoietic stem cell niche to establish footholds in mouse bone marrow. *The Journal of clinical investigation* **121**, 1298-1312, doi:10.1172/JCI43414 (2011).
169 Kim, J. K. *et al.* TBK1 regulates prostate cancer dormancy through mTOR inhibition. *Neoplasia* **15**, 1064-1074 (2013).
170 Guan, H. *et al.* IKBKE is over-expressed in glioma and contributes to resistance of glioma cells to apoptosis via activating NF-kappaB. *The Journal of pathology* **223**, 436-445, doi:10.1002/path.2815 (2011).
171 Li, H. *et al.* Silencing of IKKepsilon using siRNA inhibits proliferation and invasion of glioma cells in vitro and in vivo. *International journal of oncology* **41**, 169-178, doi:10.3892/ijo.2012.1452 (2012).
172 Harvey, K. F., Zhang, X. & Thomas, D. M. The Hippo pathway and human cancer. *Nature reviews. Cancer* **13**, 246-257, doi:10.1038/nrc3458 (2013).
173 Zhang, Z. *et al.* IKBKE promotes glioblastoma progression by establishing the regulatory feedback loop of IKBKE/YAP1/miR-Let-7b/i. *Tumour biology : the journal of the International Society for Oncodevelopmental Biology and Medicine* **39**, 1010428317705575, doi:10.1177/1010428317705575 (2017).
174 Tian, Y. *et al.* MicroRNAs let-7b/i suppress human glioma cell invasion and migration by targeting IKBKE directly. *Biochemical and biophysical research communications* **458**, 307-312, doi:10.1016/j.bbrc.2015.01.105 (2015).
175 Chen, J. *et al.* Hyper activation of beta-catenin signalling induced by IKKepsilon inhibition thwarts colorectal cancer cell proliferation. *Cell proliferation* **50**, doi:10.1111/cpr.12350 (2017).
176 Chien, A. J. *et al.* Activated Wnt/beta-catenin signaling in melanoma is associated with decreased proliferation in patient tumors and a murine melanoma model. *Proceedings of the National Academy of Sciences of the United States of America* **106**, 1193-1198, doi:10.1073/pnas.0811902106 (2009).
177 Guo, J. P. *et al.* IKBKE phosphorylation and inhibition of FOXO3a: a mechanism of IKBKE oncogenic function. *PloS one* **8**, e63636, doi:10.1371/journal.pone.0063636 (2013).
178 Skurk, C. *et al.* The Akt-regulated forkhead transcription factor FOXO3a controls endothelial cell viability through modulation of the caspase-8 inhibitor FLIP. *The Journal of biological chemistry* **279**, 1513-1525, doi:10.1074/jbc.M304736200 (2004).
179 Gopinath, S. D., Webb, A. E., Brunet, A. & Rando, T. A. FOXO3 promotes quiescence in adult muscle stem cells during the process of self-renewal. *Stem Cell Reports* **2**, 414-426, doi:10.1016/j.stemcr.2014.02.002 (2014).
180 Chen, R. J., Ho, Y. S., Guo, H. R. & Wang, Y. J. Rapid activation of Stat3 and ERK1/2 by nicotine modulates cell proliferation in human bladder cancer cells. *Toxicological sciences : an official journal of the Society of Toxicology* **104**, 283-293, doi:10.1093/toxsci/kfn086 (2008).

181 Guo, J. *et al.* IKBKE is induced by STAT3 and tobacco carcinogen and determines chemosensitivity in non-small cell lung cancer. *Oncogene* **32**, 151-159, doi:10.1038/onc.2012.39 (2013).
182 Seccareccia, E. *et al.* The inhibitor of kappa B kinase-epsilon regulates MMP-3 expression levels and can promote lung metastasis. *Oncogenesis* **3**, e116, doi:10.1038/oncsis.2014.28 (2014).
183 Gialeli, C., Theocharis, A. D. & Karamanos, N. K. Roles of matrix metalloproteinases in cancer progression and their pharmacological targeting. *The FEBS journal* **278**, 16-27, doi:10.1111/j.1742-4658.2010.07919.x (2011).
184 Shay, G., Lynch, C. C. & Fingleton, B. Moving targets: Emerging roles for MMPs in cancer progression and metastasis. *Matrix biology : journal of the International Society for Matrix Biology* **44-46**, 200-206, doi:10.1016/j.matbio.2015.01.019 (2015).
185 Geng, B. *et al.* IkappaB-kinase-epsilon in the tumor microenvironment is essential for the progression of gastric cancer. *Oncotarget* **8**, 75298-75307, doi:10.18632/oncotarget.20778 (2017).
186 Guo, J. P. *et al.* Deregulation of IKBKE is associated with tumor progression, poor prognosis, and cisplatin resistance in ovarian cancer. *The American journal of pathology* **175**, 324-333, doi:10.2353/ajpath.2009.080767 (2009).
187 Hsu, S. *et al.* IKK-epsilon coordinates invasion and metastasis of ovarian cancer. *Cancer research* **72**, 5494-5504, doi:10.1158/0008-5472.CAN-11-3993 (2012).
188 Cheng, A. *et al.* IkappaB Kinase epsilon expression in pancreatic ductal adenocarcinoma. *American journal of clinical pathology* **136**, 60-66, doi:10.1309/AJCP2JJGYNIUAS2V (2011).
189 Zubair, H. *et al.* Glucose Metabolism Reprogrammed by Overexpression of IKKepsilon Promotes Pancreatic Tumor Growth. *Cancer research* **76**, 7254-7264, doi:10.1158/0008-5472.CAN-16-1666 (2016).
190 Hildebrandt, M. A. *et al.* Kinome expression profiling identifies IKBKE as a predictor of overall survival in clear cell renal cell carcinoma patients. *Carcinogenesis* **33**, 799-803, doi:10.1093/carcin/bgs018 (2012).
191 Moser, C. V. *et al.* The protein kinase IKKepsilon contributes to tumour growth and tumour pain in a melanoma model. *Biochemical pharmacology* **103**, 64-73, doi:10.1016/j.bcp.2015.12.016 (2016).
192 Eddy, S. F. *et al.* Inducible IkappaB kinase/IkappaB kinase epsilon expression is induced by CK2 and promotes aberrant nuclear factor-kappaB activation in breast cancer cells. *Cancer research* **65**, 11375-11383, doi:10.1158/0008-5472.CAN-05-1602 (2005).
193 Trembley, J. H. *et al.* Emergence of protein kinase CK2 as a key target in cancer therapy. *Biofactors* **36**, 187-195, doi:10.1002/biof.96 (2010).
194 Adli, M. & Baldwin, A. S. IKK-i/IKKepsilon controls constitutive, cancer cell-associated NF-kappaB activity via regulation of Ser-536 p65/RelA phosphorylation. *The Journal of biological chemistry* **281**, 26976-26984, doi:10.1074/jbc.M603133200 (2006).
195 Boehm, J. S. *et al.* Integrative genomic approaches identify IKBKE as a breast cancer oncogene. *Cell* **129**, 1065-1079, doi:10.1016/j.cell.2007.03.052 (2007).
196 Hahn, W. C. *et al.* Creation of human tumour cells with defined genetic elements. *Nature* **400**, 464-468, doi:10.1038/22780 (1999).
197 Hutti, J. E. *et al.* Phosphorylation of the tumor suppressor CYLD by the breast cancer oncogene IKKepsilon promotes cell transformation. *Molecular cell* **34**, 461-472, doi:10.1016/j.molcel.2009.04.031 (2009).
198 Li, J. *et al.* Selective TBK1/IKKi dual inhibitors with anticancer potency. *International journal of cancer. Journal international du cancer* **134**, 1972-1980, doi:10.1002/ijc.28507 (2014).

199 Liu, Y. *et al.* Amlexanox, a selective inhibitor of IKBKE, generates anti-tumoral effects by disrupting the Hippo pathway in human glioblastoma cell lines. *Cell death & disease* **8**, e3022, doi:10.1038/cddis.2017.396 (2017).

200 Zhang, Y. *et al.* Amlexanox Suppresses Osteoclastogenesis and Prevents Ovariectomy-Induced Bone Loss. *Scientific reports* **5**, 13575, doi:10.1038/srep13575 (2015).

201 Greten, F. R. *et al.* NF-kappaB is a negative regulator of IL-1beta secretion as revealed by genetic and pharmacological inhibition of IKKbeta. *Cell* **130**, 918-931, doi:10.1016/j.cell.2007.07.009 (2007).

202 Zhong, Z. *et al.* NF-kappaB Restricts Inflammasome Activation via Elimination of Damaged Mitochondria. *Cell* **164**, 896-910, doi:10.1016/j.cell.2015.12.057 (2016).

203 Seitz, C. S., Lin, Q., Deng, H. & Khavari, P. A. Alterations in NF-kappaB function in transgenic epithelial tissue demonstrate a growth inhibitory role for NF-kappaB. *Proceedings of the National Academy of Sciences of the United States of America* **95**, 2307-2312 (1998).

204 Kisseleva, T. *et al.* NF-kappaB regulation of endothelial cell function during LPS-induced toxemia and cancer. *The Journal of clinical investigation* **116**, 2955-2963, doi:10.1172/JCI27392 (2006).

205 Luedde, T. *et al.* Deletion of NEMO/IKKgamma in liver parenchymal cells causes steatohepatitis and hepatocellular carcinoma. *Cancer cell* **11**, 119-132, doi:10.1016/j.ccr.2006.12.016 (2007).

206 Tan, C. & Waldmann, T. A. Proteasome inhibitor PS-341, a potential therapeutic agent for adult T-cell leukemia. *Cancer research* **62**, 1083-1086 (2002).

207 Kane, R. C., Farrell, A. T., Sridhara, R. & Pazdur, R. United States Food and Drug Administration approval summary: bortezomib for the treatment of progressive multiple myeloma after one prior therapy. *Clinical cancer research : an official journal of the American Association for Cancer Research* **12**, 2955-2960, doi:10.1158/1078-0432.CCR-06-0170 (2006).

208 Godwin, P. *et al.* Targeting nuclear factor-kappa B to overcome resistance to chemotherapy. *Frontiers in oncology* **3**, 120, doi:10.3389/fonc.2013.00120 (2013).

209 Aggarwal, S., Takada, Y., Singh, S., Myers, J. N. & Aggarwal, B. B. Inhibition of growth and survival of human head and neck squamous cell carcinoma cells by curcumin via modulation of nuclear factor-kappaB signaling. *International journal of cancer. Journal international du cancer* **111**, 679-692, doi:10.1002/ijc.20333 (2004).

210 Ianaro, A. *et al.* NEMO-binding domain peptide inhibits proliferation of human melanoma cells. *Cancer letters* **274**, 331-336, doi:10.1016/j.canlet.2008.09.038 (2009).

211 Wang, Z. *et al.* A variant of estrogen receptor-{alpha}, hER-{alpha}36: transduction of estrogen- and antiestrogen-dependent membrane-initiated mitogenic signaling. *Proceedings of the National Academy of Sciences of the United States of America* **103**, 9063-9068, doi:10.1073/pnas.0603339103 (2006).

212 Li, Q. *et al.* Increased expression of estrogen receptor alpha-36 by breast cancer oncogene IKKepsilon promotes growth of ER-negative breast cancer cells. *Cellular physiology and biochemistry : international journal of experimental cellular physiology, biochemistry, and pharmacology* **31**, 833-841, doi:10.1159/000350101 (2013).

213 Barbie, T. U. *et al.* Targeting an IKBKE cytokine network impairs triple-negative breast cancer growth. *The Journal of clinical investigation* **124**, 5411-5423, doi:10.1172/JCI75661 (2014).

214 Wang, X., Su, L. & Ou, Q. Yes-associated protein promotes tumour development in luminal epithelial derived breast cancer. *European journal of cancer* **48**, 1227-1234, doi:10.1016/j.ejca.2011.10.001 (2012).

215 Yuan, M. *et al.* Yes-associated protein (YAP) functions as a tumor suppressor in breast. *Cell death and differentiation* **15**, 1752-1759, doi:10.1038/cdd.2008.108 (2008).

216 Mehner, C. *et al.* Tumor cell expression of MMP3 as a prognostic factor for poor survival in pancreatic, pulmonary, and mammary carcinoma. *Genes & cancer* **6**, 480-489, doi:10.18632/genesandcancer.90 (2015).
217 Wang, G. L., Jiang, B. H., Rue, E. A. & Semenza, G. L. Hypoxia-inducible factor 1 is a basic-helix-loop-helix-PAS heterodimer regulated by cellular O2 tension. *Proceedings of the National Academy of Sciences of the United States of America* **92**, 5510-5514 (1995).
218 Huang, L. E., Arany, Z., Livingston, D. M. & Bunn, H. F. Activation of hypoxia-inducible transcription factor depends primarily upon redox-sensitive stabilization of its alpha subunit. *The Journal of biological chemistry* **271**, 32253-32259 (1996).
219 Kallio, P. J., Pongratz, I., Gradin, K., McGuire, J. & Poellinger, L. Activation of hypoxia-inducible factor 1alpha: posttranscriptional regulation and conformational change by recruitment of the Arnt transcription factor. *Proceedings of the National Academy of Sciences of the United States of America* **94**, 5667-5672 (1997).
220 Epstein, A. C. *et al.* C. elegans EGL-9 and mammalian homologs define a family of dioxygenases that regulate HIF by prolyl hydroxylation. *Cell* **107**, 43-54 (2001).
221 Wood, S. M. *et al.* Selection and analysis of a mutant cell line defective in the hypoxia-inducible factor-1 alpha-subunit (HIF-1alpha). Characterization of hif-1alpha-dependent and -independent hypoxia-inducible gene expression. *The Journal of biological chemistry* **273**, 8360-8368 (1998).
222 Hayashi, M. *et al.* Induction of glucose transporter 1 expression through hypoxia-inducible factor 1alpha under hypoxic conditions in trophoblast-derived cells. *The Journal of endocrinology* **183**, 145-154, doi:10.1677/joe.1.05599 (2004).
223 Kim, J. W., Tchernyshyov, I., Semenza, G. L. & Dang, C. V. HIF-1-mediated expression of pyruvate dehydrogenase kinase: a metabolic switch required for cellular adaptation to hypoxia. *Cell metabolism* **3**, 177-185, doi:10.1016/j.cmet.2006.02.002 (2006).
224 Papandreou, I., Cairns, R. A., Fontana, L., Lim, A. L. & Denko, N. C. HIF-1 mediates adaptation to hypoxia by actively downregulating mitochondrial oxygen consumption. *Cell metabolism* **3**, 187-197, doi:10.1016/j.cmet.2006.01.012 (2006).
225 Vander Heiden, M. G., Cantley, L. C. & Thompson, C. B. Understanding the Warburg effect: the metabolic requirements of cell proliferation. *Science* **324**, 1029-1033, doi:10.1126/science.1160809 (2009).
226 Warburg, O., Posener, K., Negelein, E. Über den Stoffwechsel der Carcinomzelle. *Biochemische Zeitschrift* **152**, 319-344 (1924).
227 DeBerardinis, R. J. *et al.* Beyond aerobic glycolysis: transformed cells can engage in glutamine metabolism that exceeds the requirement for protein and nucleotide synthesis. *Proceedings of the National Academy of Sciences of the United States of America* **104**, 19345-19350, doi:10.1073/pnas.0709747104 (2007).
228 Scott, D. A. *et al.* Comparative metabolic flux profiling of melanoma cell lines: beyond the Warburg effect. *The Journal of biological chemistry* **286**, 42626-42634, doi:10.1074/jbc.M111.282046 (2011).
229 Funes, J. M. *et al.* Transformation of human mesenchymal stem cells increases their dependency on oxidative phosphorylation for energy production. *Proceedings of the National Academy of Sciences of the United States of America* **104**, 6223-6228, doi:10.1073/pnas.0700690104 (2007).
230 Lim, H. Y., Ho, Q. S., Low, J., Choolani, M. & Wong, K. P. Respiratory competent mitochondria in human ovarian and peritoneal cancer. *Mitochondrion* **11**, 437-443, doi:10.1016/j.mito.2010.12.015 (2011).
231 Patra, K. C. & Hay, N. The pentose phosphate pathway and cancer. *Trends in biochemical sciences* **39**, 347-354, doi:10.1016/j.tibs.2014.06.005 (2014).

232 Jiang, P. *et al.* p53 regulates biosynthesis through direct inactivation of glucose-6-phosphate dehydrogenase. *Nature cell biology* **13**, 310-316, doi:10.1038/ncb2172 (2011).
233 Ying, H. *et al.* Oncogenic Kras maintains pancreatic tumors through regulation of anabolic glucose metabolism. *Cell* **149**, 656-670, doi:10.1016/j.cell.2012.01.058 (2012).
234 Yuneva, M., Zamboni, N., Oefner, P., Sachidanandam, R. & Lazebnik, Y. Deficiency in glutamine but not glucose induces MYC-dependent apoptosis in human cells. *The Journal of cell biology* **178**, 93-105, doi:10.1083/jcb.200703099 (2007).
235 Wise, D. R. *et al.* Myc regulates a transcriptional program that stimulates mitochondrial glutaminolysis and leads to glutamine addiction. *Proceedings of the National Academy of Sciences of the United States of America* **105**, 18782-18787, doi:10.1073/pnas.0810199105 (2008).
236 Ratnikov, B. *et al.* Glutamate and asparagine cataplerosis underlie glutamine addiction in melanoma. *Oncotarget* **6**, 7379-7389 (2015).
237 van Geldermalsen, M. *et al.* ASCT2/SLC1A5 controls glutamine uptake and tumour growth in triple-negative basal-like breast cancer. *Oncogene* **35**, 3201-3208, doi:10.1038/onc.2015.381 (2016).
238 Hassanein, M. *et al.* Targeting SLC1a5-mediated glutamine dependence in non-small cell lung cancer. *International journal of cancer. Journal international du cancer* **137**, 1587-1597, doi:10.1002/ijc.29535 (2015).
239 Patil, M. D., Bhaumik, J., Babykutty, S., Banerjee, U. C. & Fukumura, D. Arginine dependence of tumor cells: targeting a chink in cancer's armor. *Oncogene* **35**, 4957-4972, doi:10.1038/onc.2016.37 (2016).
240 Mullen, A. R. *et al.* Reductive carboxylation supports growth in tumour cells with defective mitochondria. *Nature* **481**, 385-388, doi:10.1038/nature10642 (2011).
241 Mullen, A. R. *et al.* Oxidation of alpha-ketoglutarate is required for reductive carboxylation in cancer cells with mitochondrial defects. *Cell reports* **7**, 1679-1690, doi:10.1016/j.celrep.2014.04.037 (2014).
242 Yang, M. & Vousden, K. H. Serine and one-carbon metabolism in cancer. *Nature reviews. Cancer* **16**, 650-662, doi:10.1038/nrc.2016.81 (2016).
243 Newman, A. C. & Maddocks, O. D. K. One-carbon metabolism in cancer. *British journal of cancer* **116**, 1499-1504, doi:10.1038/bjc.2017.118 (2017).
244 Zhong, H. *et al.* Overexpression of hypoxia-inducible factor 1alpha in common human cancers and their metastases. *Cancer research* **59**, 5830-5835 (1999).
245 Hoffmann, A. C. *et al.* High expression of HIF1a is a predictor of clinical outcome in patients with pancreatic ductal adenocarcinomas and correlated to PDGFA, VEGF, and bFGF. *Neoplasia* **10**, 674-679 (2008).
246 Baba, Y. *et al.* HIF1A overexpression is associated with poor prognosis in a cohort of 731 colorectal cancers. *The American journal of pathology* **176**, 2292-2301, doi:10.2353/ajpath.2010.090972 (2010).
247 Forsythe, J. A. *et al.* Activation of vascular endothelial growth factor gene transcription by hypoxia-inducible factor 1. *Molecular and cellular biology* **16**, 4604-4613 (1996).
248 Buchler, P. *et al.* Hypoxia-inducible factor 1 regulates vascular endothelial growth factor expression in human pancreatic cancer. *Pancreas* **26**, 56-64 (2003).
249 Liu, Y. *et al.* The expression and significance of HIF-1alpha and GLUT-3 in glioma. *Brain research* **1304**, 149-154, doi:10.1016/j.brainres.2009.09.083 (2009).
250 Bhaskar, P. T. *et al.* mTORC1 hyperactivity inhibits serum deprivation-induced apoptosis via increased hexokinase II and GLUT1 expression, sustained Mcl-1 expression, and glycogen synthase kinase 3beta inhibition. *Molecular and cellular biology* **29**, 5136-5147, doi:10.1128/MCB.01946-08 (2009).

251 Semenza, G. L., Roth, P. H., Fang, H. M. & Wang, G. L. Transcriptional regulation of genes encoding glycolytic enzymes by hypoxia-inducible factor 1. *The Journal of biological chemistry* **269**, 23757-23763 (1994).

252 Minchenko, A. *et al.* Hypoxia-inducible factor-1-mediated expression of the 6-phosphofructo-2-kinase/fructose-2,6-bisphosphatase-3 (PFKFB3) gene. Its possible role in the Warburg effect. *The Journal of biological chemistry* **277**, 6183-6187, doi:10.1074/jbc.M110978200 (2002).

253 Obach, M. *et al.* 6-Phosphofructo-2-kinase (pfkfb3) gene promoter contains hypoxia-inducible factor-1 binding sites necessary for transactivation in response to hypoxia. *The Journal of biological chemistry* **279**, 53562-53570, doi:10.1074/jbc.M406096200 (2004).

254 Kim, W. Y. & Kaelin, W. G. Role of VHL gene mutation in human cancer. *Journal of clinical oncology : official journal of the American Society of Clinical Oncology* **22**, 4991-5004, doi:10.1200/JCO.2004.05.061 (2004).

255 Laughner, E., Taghavi, P., Chiles, K., Mahon, P. C. & Semenza, G. L. HER2 (neu) signaling increases the rate of hypoxia-inducible factor 1alpha (HIF-1alpha) synthesis: novel mechanism for HIF-1-mediated vascular endothelial growth factor expression. *Molecular and cellular biology* **21**, 3995-4004, doi:10.1128/MCB.21.12.3995-4004.2001 (2001).

256 Zhong, H. *et al.* Modulation of hypoxia-inducible factor 1alpha expression by the epidermal growth factor/phosphatidylinositol 3-kinase/PTEN/AKT/FRAP pathway in human prostate cancer cells: implications for tumor angiogenesis and therapeutics. *Cancer research* **60**, 1541-1545 (2000).

257 Habano, W. *et al.* Reduced expression and loss of heterozygosity of the SDHD gene in colorectal and gastric cancer. *Oncology reports* **10**, 1375-1380 (2003).

258 Pollard, P. J., Wortham, N. C. & Tomlinson, I. P. The TCA cycle and tumorigenesis: the examples of fumarate hydratase and succinate dehydrogenase. *Ann Med* **35**, 632-639 (2003).

259 Selak, M. A. *et al.* Succinate links TCA cycle dysfunction to oncogenesis by inhibiting HIF-alpha prolyl hydroxylase. *Cancer cell* **7**, 77-85, doi:10.1016/j.ccr.2004.11.022 (2005).

260 Dalla-Favera, R. *et al.* Human c-myc onc gene is located on the region of chromosome 8 that is translocated in Burkitt lymphoma cells. *Proceedings of the National Academy of Sciences of the United States of America* **79**, 7824-7827 (1982).

261 Beroukhim, R. *et al.* The landscape of somatic copy-number alteration across human cancers. *Nature* **463**, 899-905, doi:10.1038/nature08822 (2010).

262 Zack, T. I. *et al.* Pan-cancer patterns of somatic copy number alteration. *Nature genetics* **45**, 1134-1140, doi:10.1038/ng.2760 (2013).

263 Chen, Y. *et al.* Identification of druggable cancer driver genes amplified across TCGA datasets. *PloS one* **9**, e98293, doi:10.1371/journal.pone.0098293 (2014).

264 Osthus, R. C. *et al.* Deregulation of glucose transporter 1 and glycolytic gene expression by c-Myc. *The Journal of biological chemistry* **275**, 21797-21800, doi:10.1074/jbc.C000023200 (2000).

265 Yuneva, M. O. *et al.* The metabolic profile of tumors depends on both the responsible genetic lesion and tissue type. *Cell metabolism* **15**, 157-170, doi:10.1016/j.cmet.2011.12.015 (2012).

266 Shim, H. *et al.* c-Myc transactivation of LDH-A: implications for tumor metabolism and growth. *Proceedings of the National Academy of Sciences of the United States of America* **94**, 6658-6663 (1997).

267 Aledo, J. C., Gomez-Fabre, P. M., Olalla, L. & Marquez, J. Identification of two human glutaminase loci and tissue-specific expression of the two related genes. *Mammalian*

genome : official journal of the International Mammalian Genome Society **11**, 1107-1110 (2000).

268 Martin-Rufian, M. *et al.* Mammalian glutaminase Gls2 gene encodes two functional alternative transcripts by a surrogate promoter usage mechanism. *PloS one* **7**, e38380, doi:10.1371/journal.pone.0038380 (2012).

269 Xiao, D. *et al.* Myc promotes glutaminolysis in human neuroblastoma through direct activation of glutaminase 2. *Oncotarget* **6**, 40655-40666, doi:10.18632/oncotarget.5821 (2015).

270 Noguchi, T., Yamada, K., Inoue, H., Matsuda, T. & Tanaka, T. The L- and R-type isozymes of rat pyruvate kinase are produced from a single gene by use of different promoters. *The Journal of biological chemistry* **262**, 14366-14371 (1987).

271 Christofk, H. R. *et al.* The M2 splice isoform of pyruvate kinase is important for cancer metabolism and tumour growth. *Nature* **452**, 230-233, doi:10.1038/nature06734 (2008).

272 Noguchi, T., Inoue, H. & Tanaka, T. The M1- and M2-type isozymes of rat pyruvate kinase are produced from the same gene by alternative RNA splicing. *The Journal of biological chemistry* **261**, 13807-13812 (1986).

273 David, C. J., Chen, M., Assanah, M., Canoll, P. & Manley, J. L. HnRNP proteins controlled by c-Myc deregulate pyruvate kinase mRNA splicing in cancer. *Nature* **463**, 364-368, doi:10.1038/nature08697 (2010).

274 Sun, Q. *et al.* Mammalian target of rapamycin up-regulation of pyruvate kinase isoenzyme type M2 is critical for aerobic glycolysis and tumor growth. *Proceedings of the National Academy of Sciences of the United States of America* **108**, 4129-4134, doi:10.1073/pnas.1014769108 (2011).

275 Yang, W. *et al.* EGFR-induced and PKCepsilon monoubiquitylation-dependent NF-kappaB activation upregulates PKM2 expression and promotes tumorigenesis. *Molecular cell* **48**, 771-784, doi:10.1016/j.molcel.2012.09.028 (2012).

276 Jurica, M. S. *et al.* The allosteric regulation of pyruvate kinase by fructose-1,6-bisphosphate. *Structure* **6**, 195-210 (1998).

277 Chaneton, B. *et al.* Serine is a natural ligand and allosteric activator of pyruvate kinase M2. *Nature* **491**, 458-462, doi:10.1038/nature11540 (2012).

278 Keller, K. E., Tan, I. S. & Lee, Y. S. SAICAR stimulates pyruvate kinase isoform M2 and promotes cancer cell survival in glucose-limited conditions. *Science* **338**, 1069-1072, doi:10.1126/science.1224409 (2012).

279 Miao, Y., Lu, M., Yan, Q., Li, S. & Feng, Y. Inhibition of Proliferation, Migration, and Invasion by Knockdown of Pyruvate Kinase-M2 (PKM2) in Ovarian Cancer SKOV3 and OVCAR3 Cells. *Oncology research* **24**, 463-475, doi:10.3727/096504016X14685034103671 (2016).

280 Yan, X. L., Zhang, X. B., Ao, R. & Guan, L. Effects of shRNA-Mediated Silencing of PKM2 Gene on Aerobic Glycolysis, Cell Migration, Cell Invasion, and Apoptosis in Colorectal Cancer Cells. *Journal of cellular biochemistry* **118**, 4792-4803, doi:10.1002/jcb.26148 (2017).

281 Vinuela, E., Salas, M. L. & Sols, A. End-product inhibition of yeast phosphofructokinase by ATP. *Biochemical and biophysical research communications* **12**, 140-145 (1963).

282 Vander Heiden, M. G. *et al.* Evidence for an alternative glycolytic pathway in rapidly proliferating cells. *Science* **329**, 1492-1499, doi:10.1126/science.1188015 (2010).

283 Luo, W. *et al.* Pyruvate kinase M2 is a PHD3-stimulated coactivator for hypoxia-inducible factor 1. *Cell* **145**, 732-744, doi:10.1016/j.cell.2011.03.054 (2011).

284 Palsson-McDermott, E. M. *et al.* Pyruvate kinase M2 regulates Hif-1alpha activity and IL-1beta induction and is a critical determinant of the warburg effect in LPS-activated macrophages. *Cell metabolism* **21**, 65-80, doi:10.1016/j.cmet.2014.12.005 (2015).

285 Anastasiou, D. *et al.* Pyruvate kinase M2 activators promote tetramer formation and suppress tumorigenesis. *Nature chemical biology* **8**, 839-847, doi:10.1038/nchembio.1060 (2012).

286 Metzger, E. *et al.* Phosphorylation of histone H3 at threonine 11 establishes a novel chromatin mark for transcriptional regulation. *Nature cell biology* **10**, 53-60, doi:10.1038/ncb1668 (2008).

287 Yang, W. *et al.* PKM2 phosphorylates histone H3 and promotes gene transcription and tumorigenesis. *Cell* **150**, 685-696, doi:10.1016/j.cell.2012.07.018 (2012).

288 Li, S. *et al.* Serine and SAM Responsive Complex SESAME Regulates Histone Modification Crosstalk by Sensing Cellular Metabolism. *Molecular cell* **60**, 408-421, doi:10.1016/j.molcel.2015.09.024 (2015).

289 Liang, J. *et al.* Mitochondrial PKM2 regulates oxidative stress-induced apoptosis by stabilizing Bcl2. *Cell research* **27**, 329-351, doi:10.1038/cr.2016.159 (2017).

290 Yang, P., Li, Z., Fu, R., Wu, H. & Li, Z. Pyruvate kinase M2 facilitates colon cancer cell migration via the modulation of STAT3 signalling. *Cellular signalling* **26**, 1853-1862, doi:10.1016/j.cellsig.2014.03.020 (2014).

291 Barthel, A. *et al.* Regulation of GLUT1 gene transcription by the serine/threonine kinase Akt1. *The Journal of biological chemistry* **274**, 20281-20286 (1999).

292 Pore, N. *et al.* Akt1 activation can augment hypoxia-inducible factor-1alpha expression by increasing protein translation through a mammalian target of rapamycin-independent pathway. *Molecular cancer research : MCR* **4**, 471-479, doi:10.1158/1541-7786.MCR-05-0234 (2006).

293 Schwartzenberg-Bar-Yoseph, F., Armoni, M. & Karnieli, E. The tumor suppressor p53 down-regulates glucose transporters GLUT1 and GLUT4 gene expression. *Cancer research* **64**, 2627-2633 (2004).

294 Matoba, S. *et al.* p53 regulates mitochondrial respiration. *Science* **312**, 1650-1653, doi:10.1126/science.1126863 (2006).

295 Zacharias, N. M. *et al.* Metabolic Differences in Glutamine Utilization Lead to Metabolic Vulnerabilities in Prostate Cancer. *Scientific reports* **7**, 16159, doi:10.1038/s41598-017-16327-z (2017).

296 Parsons, D. W. *et al.* An integrated genomic analysis of human glioblastoma multiforme. *Science* **321**, 1807-1812, doi:10.1126/science.1164382 (2008).

297 Yan, H. *et al.* IDH1 and IDH2 mutations in gliomas. *N Engl J Med* **360**, 765-773, doi:10.1056/NEJMoa0808710 (2009).

298 Mardis, E. R. *et al.* Recurring mutations found by sequencing an acute myeloid leukemia genome. *N Engl J Med* **361**, 1058-1066, doi:10.1056/NEJMoa0903840 (2009).

299 Dang, L. *et al.* Cancer-associated IDH1 mutations produce 2-hydroxyglutarate. *Nature* **462**, 739-744, doi:10.1038/nature08617 (2009).

300 Xu, W. *et al.* Oncometabolite 2-hydroxyglutarate is a competitive inhibitor of alpha-ketoglutarate-dependent dioxygenases. *Cancer cell* **19**, 17-30, doi:10.1016/j.ccr.2010.12.014 (2011).

301 Figueroa, M. E. *et al.* Leukemic IDH1 and IDH2 mutations result in a hypermethylation phenotype, disrupt TET2 function, and impair hematopoietic differentiation. *Cancer cell* **18**, 553-567, doi:10.1016/j.ccr.2010.11.015 (2010).

302 Turcan, S. *et al.* IDH1 mutation is sufficient to establish the glioma hypermethylator phenotype. *Nature* **483**, 479-483, doi:10.1038/nature10866 (2012).

303 Xiao, M. *et al.* Inhibition of alpha-KG-dependent histone and DNA demethylases by fumarate and succinate that are accumulated in mutations of FH and SDH tumor suppressors. *Genes & development* **26**, 1326-1338, doi:10.1101/gad.191056.112 (2012).

304 Locasale, J. W. *et al.* Phosphoglycerate dehydrogenase diverts glycolytic flux and contributes to oncogenesis. *Nature genetics* **43**, 869-874, doi:10.1038/ng.890 (2011).
305 Possemato, R. *et al.* Functional genomics reveal that the serine synthesis pathway is essential in breast cancer. *Nature* **476**, 346-350, doi:10.1038/nature10350 (2011).
306 Song, Z., Feng, C., Lu, Y., Lin, Y. & Dong, C. PHGDH is an independent prognosis marker and contributes cell proliferation, migration and invasion in human pancreatic cancer. *Gene*, doi:10.1016/j.gene.2017.11.014 (2017).
307 Zhang, B. *et al.* PHGDH Defines a Metabolic Subtype in Lung Adenocarcinomas with Poor Prognosis. *Cell reports* **19**, 2289-2303, doi:10.1016/j.celrep.2017.05.067 (2017).
308 Zaal, E. A. *et al.* Bortezomib resistance in multiple myeloma is associated with increased serine synthesis. *Cancer & metabolism* **5**, 7, doi:10.1186/s40170-017-0169-9 (2017).
309 Vie, N. *et al.* Overexpression of phosphoserine aminotransferase PSAT1 stimulates cell growth and increases chemoresistance of colon cancer cells. *Molecular cancer* **7**, 14, doi:10.1186/1476-4598-7-14 (2008).
310 Yang, Y. *et al.* PSAT1 regulates cyclin D1 degradation and sustains proliferation of non-small cell lung cancer cells. *International journal of cancer. Journal international du cancer* **136**, E39-50, doi:10.1002/ijc.29150 (2015).
311 Liu, B. *et al.* Overexpression of Phosphoserine Aminotransferase 1 (PSAT1) Predicts Poor Prognosis and Associates with Tumor Progression in Human Esophageal Squamous Cell Carcinoma. *Cellular physiology and biochemistry : international journal of experimental cellular physiology, biochemistry, and pharmacology* **39**, 395-406, doi:10.1159/000445633 (2016).
312 Liao, K. M. *et al.* Overexpression of the PSAT1 Gene in Nasopharyngeal Carcinoma Is an Indicator of Poor Prognosis. *Journal of Cancer* **7**, 1088-1094, doi:10.7150/jca.15258 (2016).
313 De Marchi, T. *et al.* Phosphoserine aminotransferase 1 is associated to poor outcome on tamoxifen therapy in recurrent breast cancer. *Scientific reports* **7**, 2099, doi:10.1038/s41598-017-02296-w (2017).
314 Pollari, S. *et al.* Enhanced serine production by bone metastatic breast cancer cells stimulates osteoclastogenesis. *Breast cancer research and treatment* **125**, 421-430, doi:10.1007/s10549-010-0848-5 (2011).
315 Sun, L. *et al.* cMyc-mediated activation of serine biosynthesis pathway is critical for cancer progression under nutrient deprivation conditions. *Cell research* **25**, 429-444, doi:10.1038/cr.2015.33 (2015).
316 Li, X., Xun, Z. & Yang, Y. Inhibition of phosphoserine phosphatase enhances the anticancer efficacy of 5-fluorouracil in colorectal cancer. *Biochemical and biophysical research communications* **477**, 633-639, doi:10.1016/j.bbrc.2016.06.112 (2016).
317 Sato, K. *et al.* Phosphoserine Phosphatase Is a Novel Prognostic Biomarker on Chromosome 7 in Colorectal Cancer. *Anticancer research* **37**, 2365-2371, doi:10.21873/anticanres.11574 (2017).
318 Gupta, R., Yang, Q., Dogra, S. K. & Wajapeyee, N. Serine hydroxymethyl transferase 1 stimulates pro-oncogenic cytokine expression through sialic acid to promote ovarian cancer tumor growth and progression. *Oncogene* **36**, 4014-4024, doi:10.1038/onc.2017.37 (2017).
319 Zhang, L. *et al.* Prognostic and therapeutic value of mitochondrial serine hydroxyl-methyltransferase 2 as a breast cancer biomarker. *Oncology reports* **36**, 2489-2500, doi:10.3892/or.2016.5112 (2016).
320 Ye, J. *et al.* Serine catabolism regulates mitochondrial redox control during hypoxia. *Cancer discovery* **4**, 1406-1417, doi:10.1158/2159-8290.CD-14-0250 (2014).

321 Maddocks, O. D., Labuschagne, C. F., Adams, P. D. & Vousden, K. H. Serine Metabolism Supports the Methionine Cycle and DNA/RNA Methylation through De Novo ATP Synthesis in Cancer Cells. *Molecular cell* **61**, 210-221, doi:10.1016/j.molcel.2015.12.014 (2016).

322 Maddocks, O. D. K. *et al.* Modulating the therapeutic response of tumours to dietary serine and glycine starvation. *Nature* **544**, 372-376, doi:10.1038/nature22056 (2017).

323 Labuschagne, C. F., van den Broek, N. J., Mackay, G. M., Vousden, K. H. & Maddocks, O. D. Serine, but not glycine, supports one-carbon metabolism and proliferation of cancer cells. *Cell reports* **7**, 1248-1258, doi:10.1016/j.celrep.2014.04.045 (2014).

324 DeNicola, G. M. *et al.* NRF2 regulates serine biosynthesis in non-small cell lung cancer. *Nature genetics* **47**, 1475-1481, doi:10.1038/ng.3421 (2015).

325 Amelio, I. *et al.* p73 regulates serine biosynthesis in cancer. *Oncogene* **33**, 5039-5046, doi:10.1038/onc.2013.456 (2014).

326 Ma, L. *et al.* Control of nutrient stress-induced metabolic reprogramming by PKCzeta in tumorigenesis. *Cell* **152**, 599-611, doi:10.1016/j.cell.2012.12.028 (2013).

327 Schneider, C. A., Rasband, W. S. & Eliceiri, K. W. NIH Image to ImageJ: 25 years of image analysis. *Nature methods* **9**, 671-675 (2012).

328 Mackay, G. M., Zheng, L., van den Broek, N. J. & Gottlieb, E. Analysis of Cell Metabolism Using LC-MS and Isotope Tracers. *Methods in enzymology* **561**, 171-196, doi:10.1016/bs.mie.2015.05.016 (2015).

329 Wilkes, E. & Cutillas, P. R. Label-Free Phosphoproteomic Approach for Kinase Signaling Analysis. *Methods in molecular biology* **1636**, 199-217, doi:10.1007/978-1-4939-7154-1_13 (2017).

330 Perkins, D. N., Pappin, D. J., Creasy, D. M. & Cottrell, J. S. Probability-based protein identification by searching sequence databases using mass spectrometry data. *Electrophoresis* **20**, 3551-3567, doi:10.1002/(SICI)1522-2683(19991201)20:18<3551::AID-ELPS3551>3.0.CO;2-2 (1999).

331 Wilkes, E. H., Casado, P., Rajeeve, V. & Cutillas, P. R. Kinase activity ranking using phosphoproteomics data (KARP) quantifies the contribution of protein kinases to the regulation of cell viability. *Molecular & cellular proteomics : MCP* **16**, 1694-1704, doi:10.1074/mcp.O116.064360 (2017).

332 R: A Language and Environment for Statistical Computing v. 3.5.1 (R Foundation for Statistical Computing, Vienna, Austria, 2018).

333 RStudio: Integrated Development for R. (RStudio, Inc., Boston, MA, 2015).

334 ggplot2: Elegant Graphics for Data Analysis (Springer-Verlag New York, 2016).

335 Huang da, W., Sherman, B. T. & Lempicki, R. A. Bioinformatics enrichment tools: paths toward the comprehensive functional analysis of large gene lists. *Nucleic acids research* **37**, 1-13, doi:10.1093/nar/gkn923 (2009).

336 Li, Y. *et al.* Identification of a novel serine phosphorylation site in human glutamine:fructose-6-phosphate amidotransferase isoform 1. *Biochemistry* **46**, 13163-13169, doi:10.1021/bi700694c (2007).

337 Eguchi, S. *et al.* AMP-activated protein kinase phosphorylates glutamine : fructose-6-phosphate amidotransferase 1 at Ser243 to modulate its enzymatic activity. *Genes to cells : devoted to molecular & cellular mechanisms* **14**, 179-189, doi:10.1111/j.1365-2443.2008.01260.x (2009).

338 Hornbeck, P. V. *et al.* PhosphoSitePlus, 2014: mutations, PTMs and recalibrations. *Nucleic acids research* **43**, D512-520, doi:10.1093/nar/gku1267 (2015).

339 Coulibaly, F., Lassalle, E., Baker, H. M. & Baker, E. N. Structure of phosphoserine aminotransferase from Mycobacterium tuberculosis. *Acta crystallographica. Section D, Biological crystallography* **68**, 553-563, doi:10.1107/S0907444912004829 (2012).

340 Duncan, K. & Coggins, J. R. The serC-aro A operon of Escherichia coli. A mixed function operon encoding enzymes from two different amino acid biosynthetic pathways. *The Biochemical journal* **234**, 49-57 (1986).
341 Hester, G. *et al.* Crystal structure of phosphoserine aminotransferase from Escherichia coli at 2.3 A resolution: comparison of the unligated enzyme and a complex with alpha-methyl-l-glutamate. *Journal of molecular biology* **286**, 829-850, doi:10.1006/jmbi.1998.2506 (1999).
342 Berman, H. M. *et al.* The Protein Data Bank. *Nucleic acids research* **28**, 235-242 (2000).
343 Berman, H., Henrick, K. & Nakamura, H. Announcing the worldwide Protein Data Bank. *Nat Struct Biol* **10**, 980, doi:10.1038/nsb1203-980 (2003).
344 Zhou, A. Y. *et al.* IKKepsilon-mediated tumorigenesis requires K63-linked polyubiquitination by a cIAP1/cIAP2/TRAF2 E3 ubiquitin ligase complex. *Cell reports* **3**, 724-733, doi:10.1016/j.celrep.2013.01.031 (2013).
345 Mertins, P. *et al.* Proteogenomics connects somatic mutations to signalling in breast cancer. *Nature* **534**, 55-62, doi:10.1038/nature18003 (2016).
346 Klammer, M. *et al.* Phosphosignature predicts dasatinib response in non-small cell lung cancer. *Molecular & cellular proteomics : MCP* **11**, 651-668, doi:10.1074/mcp.M111.016410 (2012).
347 Stuart, S. A. *et al.* A Phosphoproteomic Comparison of B-RAFV600E and MKK1/2 Inhibitors in Melanoma Cells. *Molecular & cellular proteomics : MCP* **14**, 1599-1615, doi:10.1074/mcp.M114.047233 (2015).
348 Baek, J. Y., Jun, D. Y., Taub, D. & Kim, Y. H. Characterization of human phosphoserine aminotransferase involved in the phosphorylated pathway of L-serine biosynthesis. *The Biochemical journal* **373**, 191-200, doi:10.1042/BJ20030144 (2003).
349 Zhou, H. *et al.* Toward a comprehensive characterization of a human cancer cell phosphoproteome. *Journal of proteome research* **12**, 260-271, doi:10.1021/pr300630k (2013).
350 Itkonen, H. M. *et al.* UAP1 is overexpressed in prostate cancer and is protective against inhibitors of N-linked glycosylation. *Oncogene* **34**, 3744-3750, doi:10.1038/onc.2014.307 (2015).
351 Shaul, Y. D. *et al.* Dihydropyrimidine accumulation is required for the epithelial-mesenchymal transition. *Cell* **158**, 1094-1109, doi:10.1016/j.cell.2014.07.032 (2014).
352 Kaushik, A. K. *et al.* Inhibition of the hexosamine biosynthetic pathway promotes castration-resistant prostate cancer. *Nature communications* **7**, 11612, doi:10.1038/ncomms11612 (2016).
353 Zhao, B., Li, L., Tumaneng, K., Wang, C. Y. & Guan, K. L. A coordinated phosphorylation by Lats and CK1 regulates YAP stability through SCF(beta-TRCP). *Genes & development* **24**, 72-85, doi:10.1101/gad.1843810 (2010).
354 Tsai, S. C. & Seto, E. Regulation of histone deacetylase 2 by protein kinase CK2. *The Journal of biological chemistry* **277**, 31826-31833, doi:10.1074/jbc.M204149200 (2002).
355 Muller, B. M. *et al.* Differential expression of histone deacetylases HDAC1, 2 and 3 in human breast cancer--overexpression of HDAC2 and HDAC3 is associated with clinicopathological indicators of disease progression. *BMC cancer* **13**, 215, doi:10.1186/1471-2407-13-215 (2013).
356 Shan, W. *et al.* HDAC2 overexpression correlates with aggressive clinicopathological features and DNA-damage response pathway of breast cancer. *Am J Cancer Res* **7**, 1213-1226 (2017).
357 Bernhardt, S. *et al.* Proteomic profiling of breast cancer metabolism identifies SHMT2 and ASCT2 as prognostic factors. *Breast cancer research : BCR* **19**, 112, doi:10.1186/s13058-017-0905-7 (2017).

358 Kim, D. *et al.* SHMT2 drives glioma cell survival in ischaemia but imposes a dependence on glycine clearance. *Nature* **520**, 363-367, doi:10.1038/nature14363 (2015).
359 Woo, C. C., Chen, W. C., Teo, X. Q., Radda, G. K. & Lee, P. T. Downregulating serine hydroxymethyltransferase 2 (SHMT2) suppresses tumorigenesis in human hepatocellular carcinoma. *Oncotarget* **7**, 53005-53017, doi:10.18632/oncotarget.10415 (2016).
360 Sadzak, I. *et al.* Recruitment of Stat1 to chromatin is required for interferon-induced serine phosphorylation of Stat1 transactivation domain. *Proceedings of the National Academy of Sciences of the United States of America* **105**, 8944-8949, doi:10.1073/pnas.0801794105 (2008).
361 Nigdelioglu, R. *et al.* Transforming Growth Factor (TGF)-beta Promotes de Novo Serine Synthesis for Collagen Production. *The Journal of biological chemistry* **291**, 27239-27251, doi:10.1074/jbc.M116.756247 (2016).
362 Bao, X. R. *et al.* Mitochondrial dysfunction remodels one-carbon metabolism in human cells. *eLife* **5**, doi:10.7554/eLife.10575 (2016).
363 Pacold, M. E. *et al.* A PHGDH inhibitor reveals coordination of serine synthesis and one-carbon unit fate. *Nature chemical biology* **12**, 452-458, doi:10.1038/nchembio.2070 (2016).
364 Kravchenko, V. V., Mathison, J. C., Schwamborn, K., Mercurio, F. & Ulevitch, R. J. IKKi/IKKepsilon plays a key role in integrating signals induced by pro-inflammatory stimuli. *The Journal of biological chemistry* **278**, 26612-26619, doi:10.1074/jbc.M303001200 (2003).
365 Péant, B. *et al.* IκB-Kinase-epsilon (IKKε) over-expression promotes the growth of prostate cancer through the C/EBP-β dependent activation of IL-6 gene expression. *Oncotarget*, doi:10.18632/oncotarget.11629 (2016).
366 Doyle, S. L. *et al.* Nuclear factor kappaB2 p52 protein has a role in antiviral immunity through IkappaB kinase epsilon-dependent induction of Sp1 protein and interleukin 15. *The Journal of biological chemistry* **288**, 25066-25075, doi:10.1074/jbc.M113.469122 (2013).
367 Lin, C. H. *et al.* A small domain of CBP/p300 binds diverse proteins: solution structure and functional studies. *Molecular cell* **8**, 581-590 (2001).
368 Yang, H. *et al.* Transcriptional activity of interferon regulatory factor (IRF)-3 depends on multiple protein-protein interactions. *European journal of biochemistry / FEBS* **269**, 6142-6151 (2002).
369 Vazquez, A., Markert, E. K. & Oltvai, Z. N. Serine biosynthesis with one carbon catabolism and the glycine cleavage system represents a novel pathway for ATP generation. *PloS one* **6**, e25881, doi:10.1371/journal.pone.0025881 (2011).
370 Adams, C. M. Role of the transcription factor ATF4 in the anabolic actions of insulin and the anti-anabolic actions of glucocorticoids. *The Journal of biological chemistry* **282**, 16744-16753, doi:10.1074/jbc.M610510200 (2007).
371 Seo, J. *et al.* Atf4 regulates obesity, glucose homeostasis, and energy expenditure. *Diabetes* **58**, 2565-2573, doi:10.2337/db09-0335 (2009).
372 Ye, J. *et al.* Pyruvate kinase M2 promotes de novo serine synthesis to sustain mTORC1 activity and cell proliferation. *Proceedings of the National Academy of Sciences of the United States of America* **109**, 6904-6909, doi:10.1073/pnas.1204176109 (2012).
373 Paz, S. *et al.* Ubiquitin-regulated recruitment of IkappaB kinase epsilon to the MAVS interferon signaling adapter. *Molecular and cellular biology* **29**, 3401-3412, doi:10.1128/MCB.00880-08 (2009).
374 Rosenbloom, K. R. *et al.* ENCODE data in the UCSC Genome Browser: year 5 update. *Nucleic acids research* **41**, D56-63, doi:10.1093/nar/gks1172 (2013).

375 Linn, T. C., Pettit, F. H. & Reed, L. J. Alpha-keto acid dehydrogenase complexes. X. Regulation of the activity of the pyruvate dehydrogenase complex from beef kidney mitochondria by phosphorylation and dephosphorylation. *Proceedings of the National Academy of Sciences of the United States of America* **62**, 234-241 (1969).

376 Rardin, M. J., Wiley, S. E., Naviaux, R. K., Murphy, A. N. & Dixon, J. E. Monitoring phosphorylation of the pyruvate dehydrogenase complex. *Analytical biochemistry* **389**, 157-164, doi:10.1016/j.ab.2009.03.040 (2009).

377 Korotchkina, L. G. & Patel, M. S. Site specificity of four pyruvate dehydrogenase kinase isoenzymes toward the three phosphorylation sites of human pyruvate dehydrogenase. *The Journal of biological chemistry* **276**, 37223-37229, doi:10.1074/jbc.M103069200 (2001).

378 Whitehouse, S., Cooper, R. H. & Randle, P. J. Mechanism of activation of pyruvate dehydrogenase by dichloroacetate and other halogenated carboxylic acids. *The Biochemical journal* **141**, 761-774 (1974).

379 Wang, Y. *et al.* Amino acid deprivation promotes tumor angiogenesis through the GCN2/ATF4 pathway. *Neoplasia* **15**, 989-997 (2013).

380 Kato, M., Li, J., Chuang, J. L. & Chuang, D. T. Distinct structural mechanisms for inhibition of pyruvate dehydrogenase kinase isoforms by AZD7545, dichloroacetate, and radicicol. *Structure* **15**, 992-1004, doi:10.1016/j.str.2007.07.001 (2007).

381 Li, X. *et al.* Mitochondria-Translocated PGK1 Functions as a Protein Kinase to Coordinate Glycolysis and the TCA Cycle in Tumorigenesis. *Molecular cell* **61**, 705-719, doi:10.1016/j.molcel.2016.02.009 (2016).

382 Chae, Y. C. *et al.* Mitochondrial Akt Regulation of Hypoxic Tumor Reprogramming. *Cancer cell* **30**, 257-272, doi:10.1016/j.ccell.2016.07.004 (2016).

383 Challa, S. *et al.* IKBKE Is a Substrate of EGFR and a Therapeutic Target in Non-Small Cell Lung Cancer with Activating Mutations of EGFR. *Cancer research* **76**, 4418-4429, doi:10.1158/0008-5472.CAN-16-0069 (2016).

384 Xie, X. *et al.* IkappaB kinase epsilon and TANK-binding kinase 1 activate AKT by direct phosphorylation. *Proceedings of the National Academy of Sciences of the United States of America* **108**, 6474-6479, doi:10.1073/pnas.1016132108 (2011).

385 Dickhout, J. G. *et al.* Integrated stress response modulates cellular redox state via induction of cystathionine gamma-lyase: cross-talk between integrated stress response and thiol metabolism. *The Journal of biological chemistry* **287**, 7603-7614, doi:10.1074/jbc.M111.304576 (2012).

386 Zhang, C. *et al.* ATF4 is directly recruited by TLR4 signaling and positively regulates TLR4-trigged cytokine production in human monocytes. *Cell Mol Immunol* **10**, 84-94, doi:10.1038/cmi.2012.57 (2013).

387 Gao, S. *et al.* PSAT1 is regulated by ATF4 and enhances cell proliferation via the GSK3beta/beta-catenin/cyclin D1 signaling pathway in ER-negative breast cancer. *Journal of experimental & clinical cancer research : CR* **36**, 179, doi:10.1186/s13046-017-0648-4 (2017).

388 Bensaad, K. *et al.* TIGAR, a p53-inducible regulator of glycolysis and apoptosis. *Cell* **126**, 107-120, doi:10.1016/j.cell.2006.05.036 (2006).

389 Kawauchi, K., Araki, K., Tobiume, K. & Tanaka, N. p53 regulates glucose metabolism through an IKK-NF-kappaB pathway and inhibits cell transformation. *Nature cell biology* **10**, 611-618, doi:10.1038/ncb1724 (2008).

390 Sommermann, T. G., O'Neill, K., Plas, D. R. & Cahir-McFarland, E. IKKbeta and NF-kappaB transcription govern lymphoma cell survival through AKT-induced plasma membrane trafficking of GLUT1. *Cancer research* **71**, 7291-7300, doi:10.1158/0008-5472.CAN-11-1715 (2011).

391 Reid, M. A. *et al.* IKKbeta promotes metabolic adaptation to glutamine deprivation via phosphorylation and inhibition of PFKFB3. *Genes & development* **30**, 1837-1851, doi:10.1101/gad.287235.116 (2016).
392 Bakkar, N. *et al.* IKKalpha and alternative NF-kappaB regulate PGC-1beta to promote oxidative muscle metabolism. *The Journal of cell biology* **196**, 497-511, doi:10.1083/jcb.201108118 (2012).
393 Mauro, C. *et al.* NF-kappaB controls energy homeostasis and metabolic adaptation by upregulating mitochondrial respiration. *Nature cell biology* **13**, 1272-1279, doi:10.1038/ncb2324 (2011).
394 Zhao, P. *et al.* TBK1 at the Crossroads of Inflammation and Energy Homeostasis in Adipose Tissue. *Cell* **172**, 731-743 e712, doi:10.1016/j.cell.2018.01.007 (2018).
395 Samanta, D. & Semenza, G. L. Serine Synthesis Helps Hypoxic Cancer Stem Cells Regulate Redox. *Cancer research* **76**, 6458-6462, doi:10.1158/0008-5472.CAN-16-1730 (2016).
396 Afonyushkin, T. *et al.* Oxidized phospholipids regulate expression of ATF4 and VEGF in endothelial cells via NRF2-dependent mechanism: novel point of convergence between electrophilic and unfolded protein stress pathways. *Arterioscler Thromb Vasc Biol* **30**, 1007-1013, doi:10.1161/ATVBAHA.110.204354 (2010).
397 Gwinn, D. M. *et al.* Oncogenic KRAS Regulates Amino Acid Homeostasis and Asparagine Biosynthesis via ATF4 and Alters Sensitivity to L-Asparaginase. *Cancer cell* **33**, 91-107 e106, doi:10.1016/j.ccell.2017.12.003 (2018).
398 Mertins, P. *et al.* Integrated proteomic analysis of post-translational modifications by serial enrichment. *Nature methods* **10**, 634-637, doi:10.1038/nmeth.2518 (2013).
399 Mertins, P. *et al.* Ischemia in tumors induces early and sustained phosphorylation changes in stress kinase pathways but does not affect global protein levels. *Molecular & cellular proteomics : MCP* **13**, 1690-1704, doi:10.1074/mcp.M113.036392 (2014).
400 Olsen, J. V. *et al.* Quantitative phosphoproteomics reveals widespread full phosphorylation site occupancy during mitosis. *Science signaling* **3**, ra3, doi:10.1126/scisignal.2000475 (2010).
401 Rigbolt, K. T. *et al.* System-wide temporal characterization of the proteome and phosphoproteome of human embryonic stem cell differentiation. *Science signaling* **4**, rs3, doi:10.1126/scisignal.2001570 (2011).
402 Sharma, K. *et al.* Ultradeep human phosphoproteome reveals a distinct regulatory nature of Tyr and Ser/Thr-based signaling. *Cell reports* **8**, 1583-1594, doi:10.1016/j.celrep.2014.07.036 (2014).
403 Uhlen, M. *et al.* Proteomics. Tissue-based map of the human proteome. *Science* **347**, 1260419, doi:10.1126/science.1260419 (2015).
404 *The Human Protein Atlas. at <www.proteinatlas.org>*, 2018).
405 Curtis, C. *et al.* The genomic and transcriptomic architecture of 2,000 breast tumours reveals novel subgroups. *Nature* **486**, 346-352, doi:10.1038/nature10983 (2012).
406 Cancer Genome Atlas, N. Comprehensive molecular portraits of human breast tumours. *Nature* **490**, 61-70, doi:10.1038/nature11412 (2012).
407 Ciriello, G. *et al.* Comprehensive Molecular Portraits of Invasive Lobular Breast Cancer. *Cell* **163**, 506-519, doi:10.1016/j.cell.2015.09.033 (2015).
408 Chandel, N. S. *et al.* Reactive oxygen species generated at mitochondrial complex III stabilize hypoxia-inducible factor-1alpha during hypoxia: a mechanism of O2 sensing. *The Journal of biological chemistry* **275**, 25130-25138, doi:10.1074/jbc.M001914200 (2000).
409 Xiang, Y. *et al.* Targeted inhibition of tumor-specific glutaminase diminishes cell-autonomous tumorigenesis. *The Journal of clinical investigation* **125**, 2293-2306, doi:10.1172/JCI75836 (2015).

410 Shroff, E. H. *et al.* MYC oncogene overexpression drives renal cell carcinoma in a mouse model through glutamine metabolism. *Proceedings of the National Academy of Sciences of the United States of America* **112**, 6539-6544, doi:10.1073/pnas.1507228112 (2015).
411 Hudson, C. D. *et al.* Altered glutamine metabolism in platinum resistant ovarian cancer. *Oncotarget* **7**, 41637-41649, doi:10.18632/oncotarget.9317 (2016).
412 Le, A. *et al.* Glucose-independent glutamine metabolism via TCA cycling for proliferation and survival in B cells. *Cell metabolism* **15**, 110-121, doi:10.1016/j.cmet.2011.12.009 (2012).
413 Gross, M. I. *et al.* Antitumor activity of the glutaminase inhibitor CB-839 in triple-negative breast cancer. *Molecular cancer therapeutics* **13**, 890-901, doi:10.1158/1535-7163.MCT-13-0870 (2014).
414 Huang, Q. *et al.* Characterization of the interactions of potent allosteric inhibitors with glutaminase C, a key enzyme in cancer cell glutamine metabolism. *The Journal of biological chemistry* **293**, 3535-3545, doi:10.1074/jbc.M117.810101 (2018).
415 McDermott, L. A. *et al.* Design and evaluation of novel glutaminase inhibitors. *Bioorg Med Chem* **24**, 1819-1839, doi:10.1016/j.bmc.2016.03.009 (2016).
416 Mullarky, E. *et al.* Identification of a small molecule inhibitor of 3-phosphoglycerate dehydrogenase to target serine biosynthesis in cancers. *Proceedings of the National Academy of Sciences of the United States of America* **113**, 1778-1783, doi:10.1073/pnas.1521548113 (2016).
417 Wang, Q. *et al.* Rational Design of Selective Allosteric Inhibitors of PHGDH and Serine Synthesis with Anti-tumor Activity. *Cell Chem Biol* **24**, 55-65, doi:10.1016/j.chembiol.2016.11.013 (2017).
418 Zhang, T. *et al.* Disruption of De Novo Serine Synthesis in Muller Cells Induced Mitochondrial Dysfunction and Aggravated Oxidative Damage. *Molecular neurobiology*, doi:10.1007/s12035-017-0840-8 (2018).
419 Hamanaka, R. B. *et al.* Inhibition of PHGDH Attenuates Bleomycin-induced Pulmonary Fibrosis. *American journal of respiratory cell and molecular biology*, doi:10.1165/rcmb.2017-0186OC (2017).
420 Yoshino, H. *et al.* PHGDH as a key enzyme for serine biosynthesis in HIF2alpha targeting therapy for renal cell carcinoma. *Cancer research*, doi:10.1158/0008-5472.CAN-17-1589 (2017).
421 Maddocks, O. D. *et al.* Serine starvation induces stress and p53-dependent metabolic remodelling in cancer cells. *Nature* **493**, 542-546, doi:10.1038/nature11743 (2013).
422 Gao, X. *et al.* Serine Availability Influences Mitochondrial Dynamics and Function through Lipid Metabolism. *Cell reports* **22**, 3507-3520, doi:10.1016/j.celrep.2018.03.017 (2018).
423 Ma, E. H. *et al.* Serine Is an Essential Metabolite for Effector T Cell Expansion. *Cell metabolism* **25**, 345-357, doi:10.1016/j.cmet.2016.12.011 (2017).
424 Paiardini, A. *et al.* Screening and in vitro testing of antifolate inhibitors of human cytosolic serine hydroxymethyltransferase. *ChemMedChem* **10**, 490-497, doi:10.1002/cmdc.201500028 (2015).
425 Witschel, M. C. *et al.* Inhibitors of plasmodial serine hydroxymethyltransferase (SHMT): cocrystal structures of pyrazolopyrans with potent blood- and liver-stage activities. *Journal of medicinal chemistry* **58**, 3117-3130, doi:10.1021/jm501987h (2015).
426 Ducker, G. S. *et al.* Human SHMT inhibitors reveal defective glycine import as a targetable metabolic vulnerability of diffuse large B-cell lymphoma. *Proceedings of the National Academy of Sciences of the United States of America* **114**, 11404-11409, doi:10.1073/pnas.1706617114 (2017).